

博士論文

**Development of the Crystallization Free  
Crystallographic Analysis Method Using Porous Complex**

(細孔性錯体を用いた結晶化不要の結晶構造解析法の開発)

吉岡 翔太

## Contents

<b>Chapter 1 General Introduction</b> .....	1
1.1 Guest inclusion crystal of rigid structure .....	2
1.2 Guest inclusion crystal of porous network complex .....	4
1.3 Overview of this thesis .....	11
References .....	13
<b>Chapter 2 Development of the Crystalline Sponge Method</b> .....	17
2.1 Introduction .....	18
2.2 Synthesis and solvent exchange of the crystalline sponge .....	18
2.3 Inclusion and X-ray analysis of liquid isoprene .....	24
2.4 Microgram scale inclusion and X-ray analysis of guaiazulene .....	25
2.5 Selection of the crystalline sponge .....	27
2.6 Crystalline sponge analysis of other guests.....	28
2.7 Summary .....	29
2.8 Experimental section .....	30
References .....	47
<b>Chapter 3 X-ray Analysis of Trace Amount of Sample by the Crystalline Sponge Method</b> ..	49
3.1 Introduction .....	50
3.2 Nanogram scale guest inclusion and X-ray analysis .....	51
3.3 LC-SCD: Combination of the microgram scale liquid chromatography separation and X-ray analysis.....	52
3.4 Crystalline sponge analysis of trace amount of gaseous sample.....	55
3.5 Summary .....	57
3.6 Experimental section .....	58
Reference.....	70



<b>Chapter 4 Absolute Structure Determination by the Crystalline sponge Method</b>	71
4.1 Introduction	72
4.2 Absolute structure determination of point chiral molecules	73
4.3 Absolute structure determination of axial chiral molecules	76
4.4 Summary	78
4.5 Experimental Section	80
References	92
<b>Chapter 5 X-ray Analysis of Ozonides by the Crystalline Sponge Method</b>	93
5.1 Introduction	94
5.2 Microgram scale ozonide inclusion into the crystalline sponge	95
5.3 X-ray analysis of cyclopentene ozonide by the crystalline sponge method	95
5.4 X-ray analysis of stilbene ozonide by the crystalline sponge method	97
5.5 Heating experiment of stilbene ozonide inclusion crystalline sponge	98
5.6 X-ray analysis of styrene ozonide by the crystalline sponge method	99
5.7 Summary	100
5.8 Experimental section	102
References	111
<b>Chapter 6 Application of the Crystalline Sponge Method to Synthetic Chemistry</b>	113
6.1 Introduction	114
6.2 Determination of the substituent position of C–H functionalization products	115
6.3 Determination of the stereochemistry of complex ring connected compound	117
6.4 Determination of the planar chirality constructed by ring-closing metathesis	118
6.5 Summary	119
6.6 Experimental section	120
References	130

<b>Chapter 7 Scope and Limitations of the Crystalline Sponge Method</b> .....	131
7.1 Introduction .....	132
7.2 Suitable size of the target compound .....	133
7.3 Suitable solvent for the guest inclusion .....	134
7.4 Functional group effect on the inclusion .....	135
7.5 Obtained data quality and structure by the crystalline sponge method .....	137
7.6 Missassignment due to the disorder .....	141
7.7 Summary .....	143
7.8 Experimental section .....	144
References .....	158
<b>Chapter 8 Summary and Perspective</b> .....	160
<b>List of Publications</b> .....	164
<b>Acknowledgment</b> .....	165

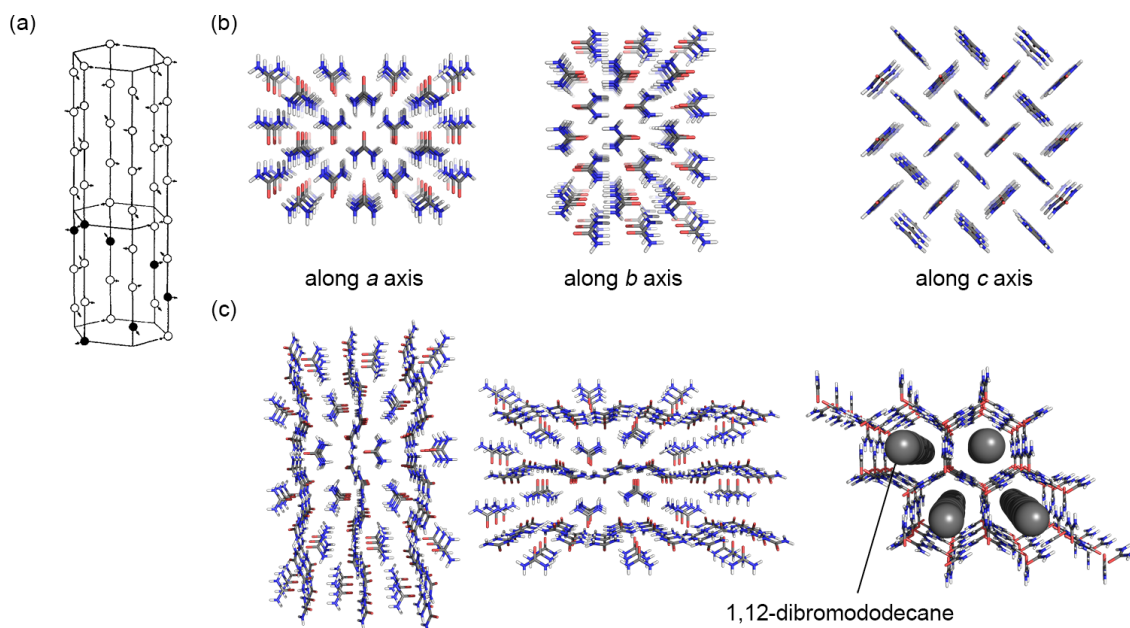


## **Chapter 1**

### **General Introduction**

## 1.1 Guest inclusion crystal of rigid structure

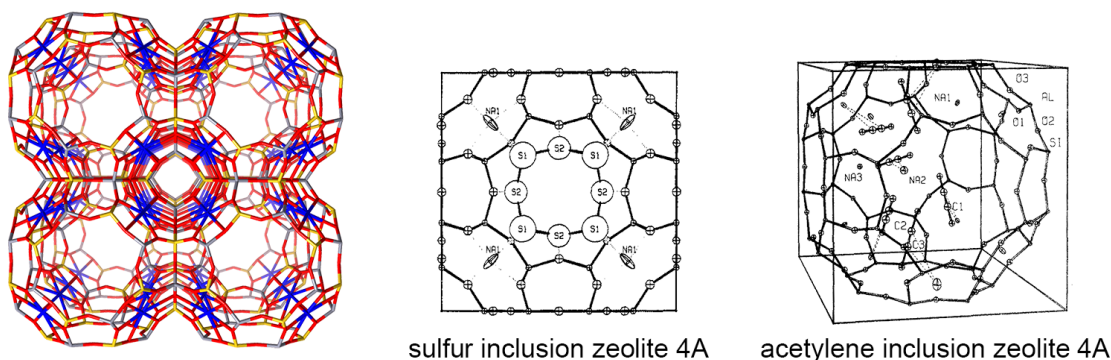
The guest inclusion crystals or clathrate crystals first appeared in 1940s by Schlenk and Powell as urea complex and hydroquinone complex.<sup>1-3</sup> Before that, Bengen described the formation of the *n*-alkane inclusion urea crystal and the guest inclusion compound, especially water inclusion compound has been well known as hydrate.<sup>4</sup> Their structural analysis of the inclusion crystal, however, had to wait the progress of the X-ray crystallographic analysis. In 1949, X-ray crystallographic analysis revealed that the inclusion structure of *n*-alkane in hexagonal columnar urea structure constructed by hydrogen bonds (Figure 1.1a). The hexagonal columnar urea crystal has the rigid 5 Å sized one dimensional pore and it is only formed with *n*-alkane derivatives.<sup>3</sup> After these reports, the guest in the host crystal has been extensively studied in terms of interaction, separation, guest exchange and so on.<sup>4-9</sup> One of the striking features of the urea crystal applied to the industry was selective inclusion of *n*-alkane derivatives, and inclusion crystal was not formed with other branched alkane or without *n*-alkane derivatives (Figure 1.1b).<sup>10,11</sup> It was enabled by the rigidity of the hexagonal columnar crystal structure, which does not fit to branched alkane structure and its small size suitable for the selective inclusion of *n*-alkane derivatives. Harris et al. also demonstrated the rigidity of the several urea inclusion crystals by the single crystal X-ray diffraction study. They prepared the urea inclusion crystal with 1,12-dibromododecane, *n*-hexadecane, 1,10-dichloro-*n*-decane, dioctanoyl peroxide and others and analyzed by X-ray diffraction (Figure 1.1c). The diffraction pattern indicated the hexagonal columnar structure of urea crystals were same among every guest compound. On the other hand, the included guest structures were depended critically upon the guest.<sup>12,13</sup> These data suggested that the periodicity of the hexagonal urea structure and rather flexible guest orientation was incommensurate due to the rigidity of the urea structure. When the periodicities of host and included guests are incommensurate, the guests are not observable. However, once the guest ordering in the host structure is achieved and the periodicities are commensurate, included guest molecules behave as a part of the single crystal, and are observable by the X-ray diffraction analysis.



**Figure 1.1.** (a) First example of hexagonal columnar urea inclusion crystal structure reported in 1949. (b) X-ray crystal structure of urea without *n*-alkane derivative. (c) X-ray crystal structure of columnar urea inclusion crystal of 1,12-dibromododecane. 1,12-dibromododecane was represented in CPK mode in the view along *c* axis (in along *a* and *b* axis views, the guest was omitted for clarity)

Other than urea, guest inclusion phenomenon was extensively studied in many host molecules.<sup>14-16</sup> In the crystalline or solid state, zeolite was also employed for the solid host due to its rigid nature of the structure.<sup>17-19</sup> Many different sized pores of zeolite were synthesized and applied to the catalyst, separation device, adsorption and so on by inclusion of the guest molecules.<sup>20,21</sup> Zeolite was synthesized from inorganic components and it shows unusual stability of the framework structure. In terms of the crystalline nature of the zeolite, Seff et al. demonstrated single crystal X-ray diffraction analyses of guest exchanged zeolite 4A.<sup>22,23</sup> They first dehydrated the crystals of zeolite 4A at 350 °C under the reduced pressure ( $10^{-5}$  Torr) for 24 h and then the resultant zeolite was treated with ammonia. X-ray analysis revealed that 32 molecules of ammonia was included in the unit cell of the crystal.<sup>24</sup> As the similar dehydration and guest uptake procedure, they also performed other guest exchange and single crystal X-ray analysis of sulfur and acetylene in the single crystalline zeolite 4A (Figure 1.2).<sup>25,26,27</sup> Furthermore, due to the rigidity of framework of zeolite, the structure of the zeolite 4A was totally maintained and intact upon the guest exchanging reduced

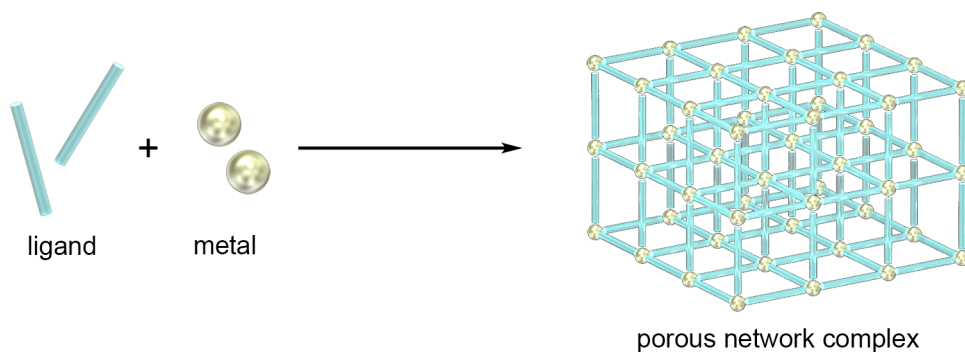
pressure conditions. Though, ammonia, sulfur and acetylene were successfully exchanged as the guest molecules and observed by the X-ray diffraction, examples of observing the exchanged guest molecules in single crystal fashion was quite rare. For the zeolite case, the similar reason to the urea inclusion crystal was considerable that the host structure is too rigid to make the periodicity of host framework and guest orientation commensurate.



**Figure 1.2.** Single crystal X-ray structures of zeolite 4A (left), sulfur inclusion zeolite 4A (center) and acetylene inclusion zeolite 4A.

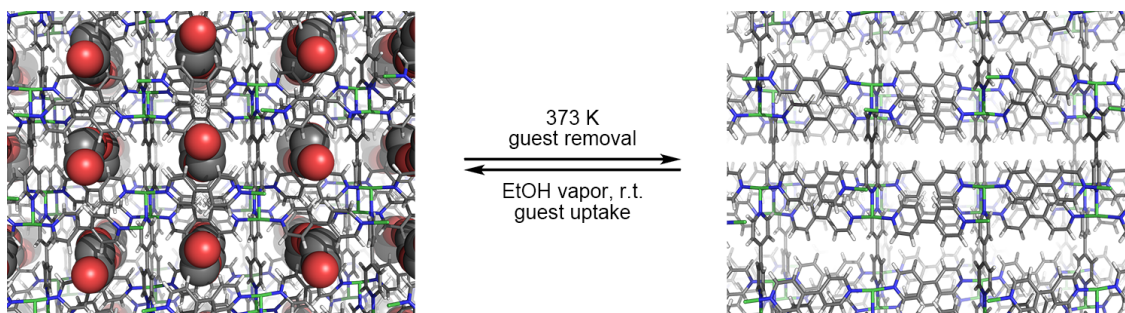
## 1.2 Guest inclusion crystal of porous network complex

To make the periodicity of framework and guest orientation commensurate, flexible host compound, which alter the host structure depending on the surrounding chemical conditions is desirable. The origin of the rigidity of urea inclusion crystals and zeolites are strong bond energy to construct the structures. Therefore, flexible structure should be constructed with much lower bond strength. The coordination bond matches the requirement for constructing the flexible porous material. By means of the coordination bond, a lot of porous complexes such as coordination networks, metal organic frameworks (MOFs) and porous coordination polymers (PCPs) have been reported (Figure 1.3).<sup>28-32</sup> Early examples were sporadically reported,<sup>33-35</sup> however the huge amount of reports about the porous complexes based on the coordination bond were published after the report by Robson et al..<sup>36,37</sup> Since the variety of metals and ligands form the coordination bond in different bond strength, designability of the framework structure is much higher than other crystalline host compounds.<sup>38</sup> Therefore, from rigid zeolite-like network complexes to the flexible porous complexes were reported.



**Figure 1.3.** Schematic representation of the synthesis and structure of a porous network complex.

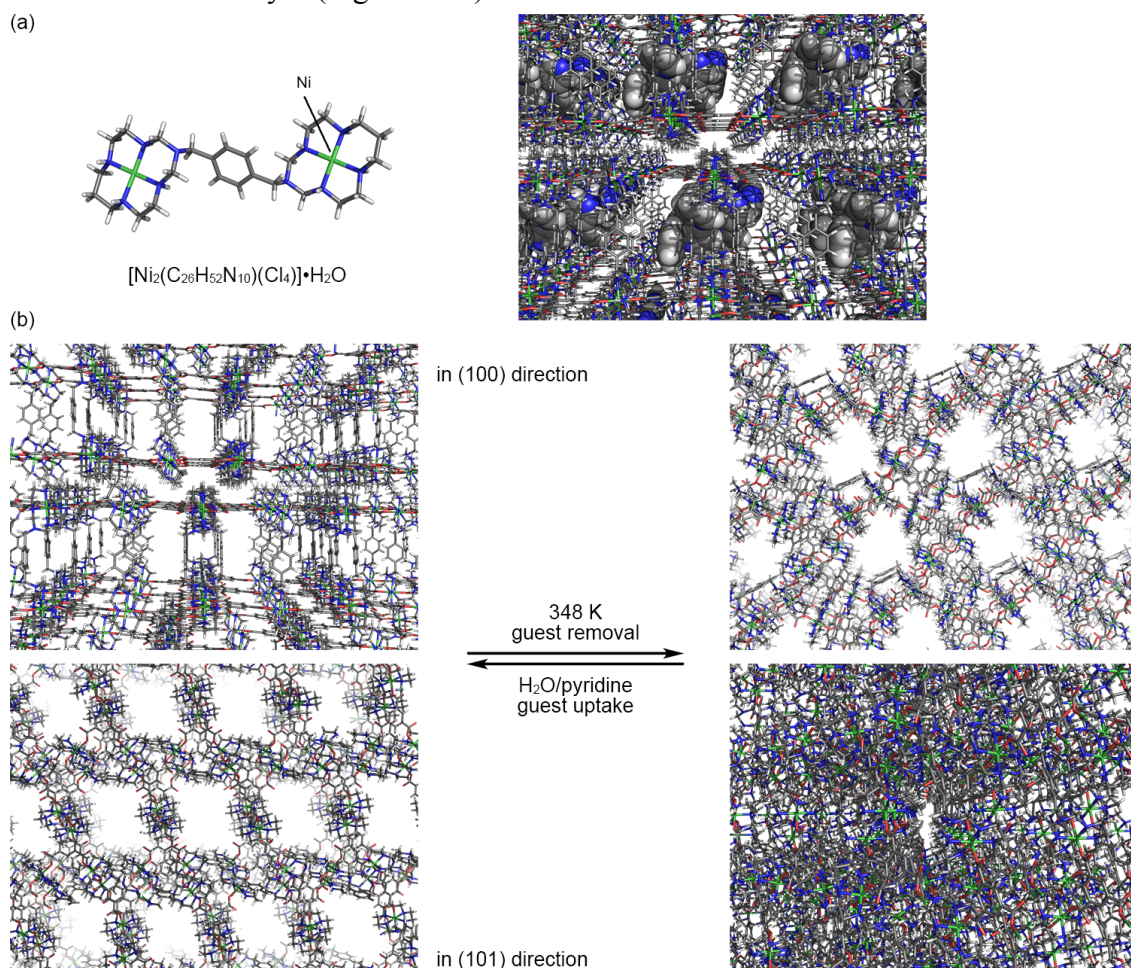
Rosseinsky et al. reported that when the porous complex was synthesized with 4,4'-bipyridine and  $\text{Ni}(\text{NO}_3)_2$ , the extremely robust porous complex was obtained.<sup>39,40</sup> This robust porous complex is stable toward the solvent removal (MeOH, EtOH or *i*-PrOH) and uptake cycle, and characterized by the single crystal X-ray analysis in both solvated and desolvated state (Figure 1.4). The rigidity of the complex was demonstrated by the small average shift ( $0.06 \text{ \AA}$ ) of the atom position of the framework before and after desolvation. Other robust coordination networks were also extensively studied.<sup>41-43</sup>



**Figure 1.4.** Single crystal X-ray structures of Rosseinsky's rigid porous network before and after guest removal. In the guest inclusion structure, guest EtOH was represented in CPK model.

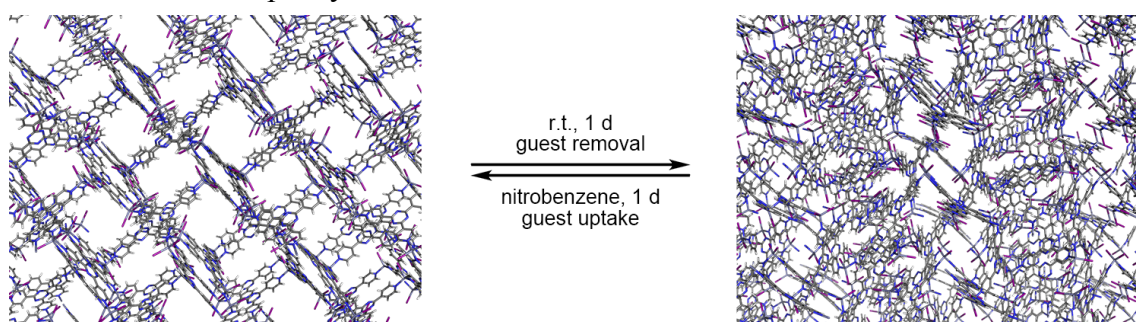


On the other hand, flexible porous network complex were also reported. In 2002, Suh et al. reported a flexible porous network complex synthesized from dinickel(II) bismacrocylic complex  $[\text{Ni}_2(\text{C}_{26}\text{H}_{52}\text{N}_{10})(\text{Cl}_4)] \cdot \text{H}_2\text{O}$  and sodium 1,3,5-benzentricarboxylate ( $\text{Na}_3\text{btc}$ ) (Figure 1.5a).<sup>44</sup> This flexible porous complex maintained the single crystallinity upon desolvation and solvation cycle. When the crystal of as synthesized flexible network  $[[\text{Ni}_2(\text{C}_{26}\text{H}_{52}\text{N}_{10})]_3[\text{btc}]_3 \cdot 6\text{C}_6\text{H}_5\text{N} \cdot 36\text{H}_2\text{O}]$  was dried at 75 °C for 1.5 h, the crystal was desolvated and single crystal of  $[[\text{Ni}_2(\text{C}_{26}\text{H}_{52}\text{N}_{10})]_3[\text{btc}]_3 \cdot 4\text{H}_2\text{O}]$  was obtained. During the desolvation process, the crystal structure was drastically changed in terms of the cell parameter, volume and thickness of the bilayer (Figure 1.5b).



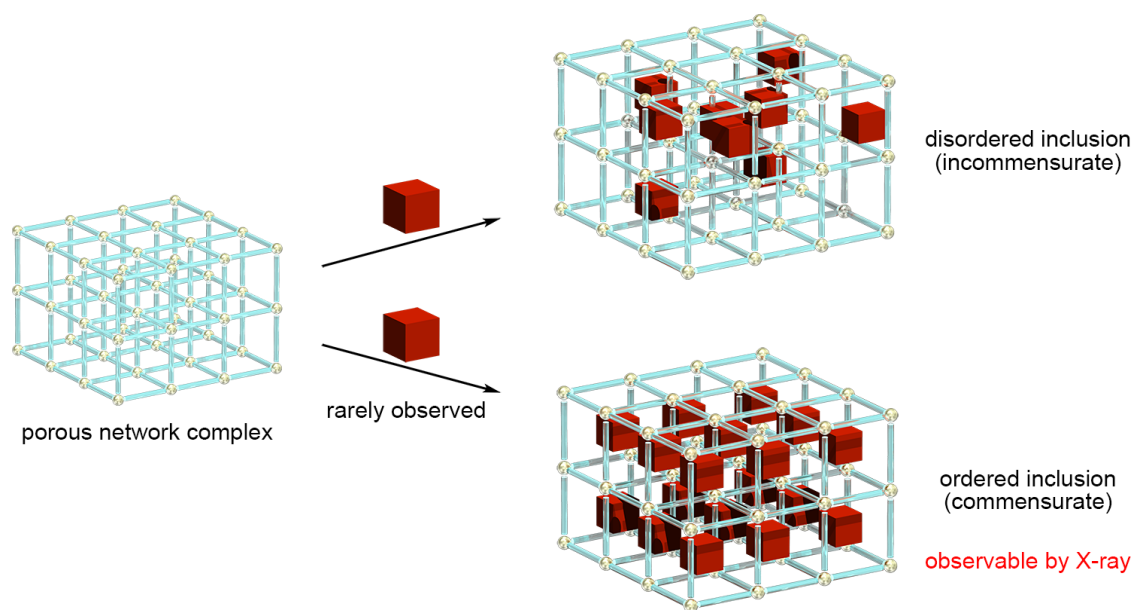
**Figure 1.5.** (a) The bismacrocylic complex ligand and single crystal X-ray structure of as synthesized complex (guest pyridine was represented in CPK model). (b) Host framework structure transformation of Suh's porous complex by guest removal and uptake. The guest structure was omitted for clarity.

Fujita et al. also reported flexible porous network complex, which exhibit solvent exchange ability from nitrobenzene to benzene or other organic solvents composed of  $ZnI_2$  and 2,4,6-tri(4-pyridyl)triazine.<sup>45</sup> This porous complex showed shrinking and swelling behavior on the framework upon solvent removal and uptake process. They also demonstrated that this flexible network showed guest inclusion ability of non-solvent molecules in a single-crystal-to-single-crystal fashion by addition of large excess amount of triphenylene.<sup>46</sup>



**Figure 1.6.** Host framework structure transformation of Fujita's porous complex by guest removal and uptake. The guest structure was omitted for clarity.

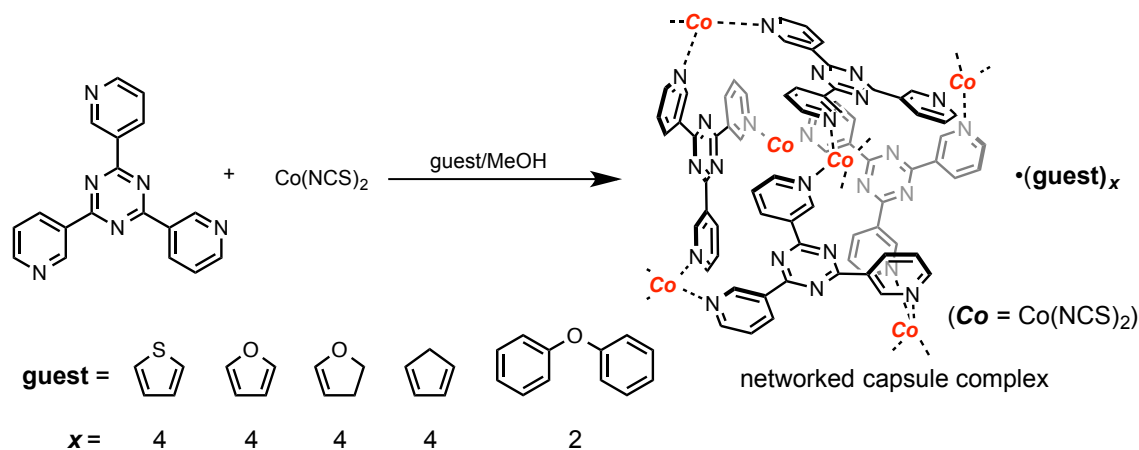
Considering the huge number of reports on guest inclusion into the porous network complex including non-single crystalline fashion, the porous complex has one of the best materials to include guest molecules into the porous structure. Furthermore, the included molecules are observable by the X-ray diffraction analysis when the single crystallinity of the porous network complexes is intact upon guest inclusion and the periodicity of the framework and guest molecules are commensurate. However, as the drawback of the flexible nature of the porous complex, the stability of the network structures upon solvent and guest exchange was lower than that of single crystalline zeolite. Due to the difficulties on maintaining the single crystallinity and realizing commensurate periodicity of framework and guests even with the porous network complex, only a limited numbers of the single crystal X-ray observations of the exchanged guest molecules were reported.<sup>47-51</sup> Most of the guest inclusion attempts into the porous network complex resulted in a deterioration of the crystallinity or random inclusion of guest molecules, which are not observable by the X-ray diffraction (Figure 1.7). Therefore, a general method to include guest molecules into the pore and to align them has not been established.



**Figure 1.7.** Disordered guest inclusion and ordered inclusion into the porous network complex. Ordered guest molecules are observable by the X-ray diffraction study.

The author and co-workers reported the synthesis and guest encapsulation properties of the networked capsule complex which was synthesized from  $\text{Co}(\text{NCS})_2$  and 2,4,6-tri(3-pyridyl)triazine (Scheme 1.1). (List of Publications 1)

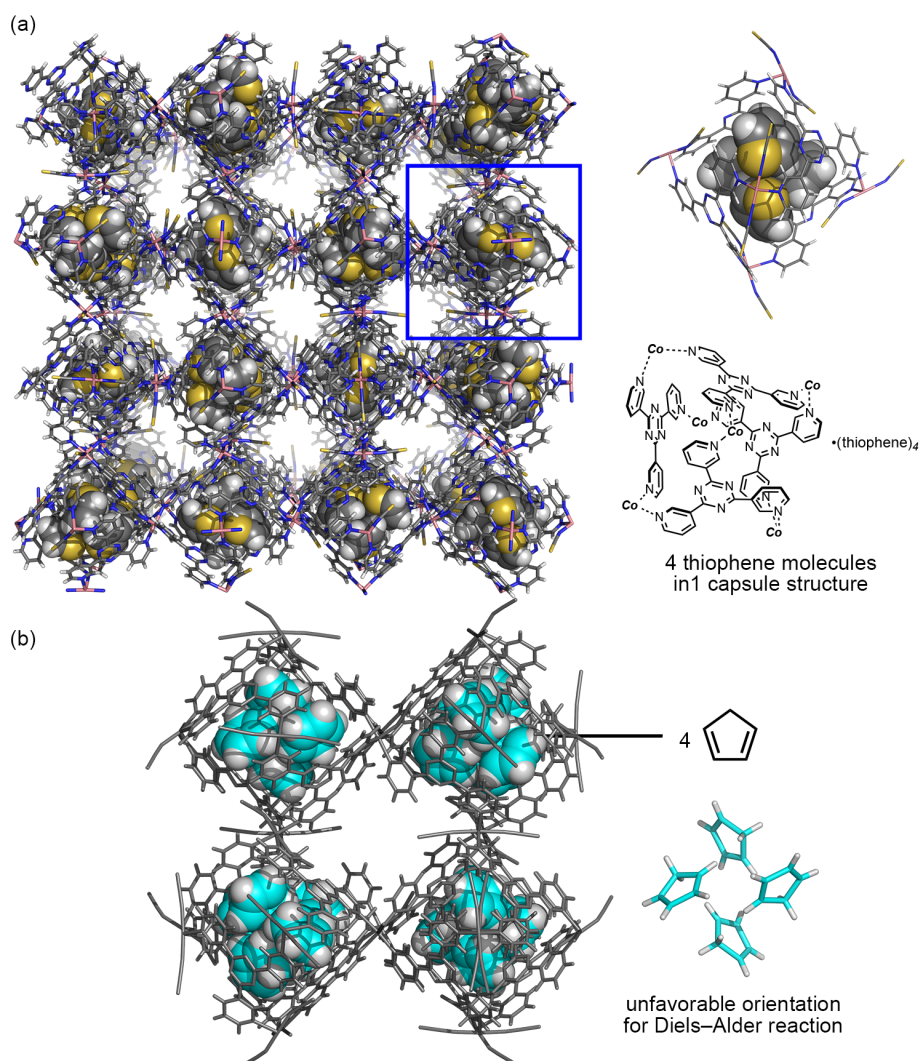
**Scheme 1.1.** A synthesis of networked capsule complex.



In this porous network complex, the small molecular sized capsule was infinitely arrayed, and the various solvents were included in the capsule structure such as thiophen, furan, diphenyl ether and cyclopentadiene. These included solvent were



tightly packed in the capsule structure and observable by the X-ray diffraction analysis (Figure 1.8a). Furthermore, in the capsule structure, highly reactive cyclopentadiene, which was easily dimerized into dicyclopentadiene at room temperature, was intact upon heating at 40 °C for 1 d because cyclopentadiene molecules were kept in a disfavored orientation for the Diels–Alder reaction. These orientation and intact cyclopentadiene after applying heat were analyzed by the single crystal X-ray diffraction study (Figure 1.8b).



**Figure 1.8.** (a) Packing structure of the networked capsule complex synthesized from thiophene. (b) X-ray structure of cyclopentadiene inclusion networked capsule complex after applying heat at 40 °C for 1 d. (In all structures, guest molecules are represented in CPK model.)

Distinguishing the guest molecules in the capsule structure from the molecules in the pore (outside of the capsule) was almost impossible by other spectroscopic method. However, the X-ray diffraction analysis clearly and easily revealed the molecular structures and conformations of guest molecules in the capsule structure. Though the encapsulated guest compounds, cyclopentadiene and thiopehen, are liquid compounds at the ambient temperature, their molecular structures were clearly observed by the X-ray diffraction analyses without crystallization of them. Since the guest compounds were highly ordered in the capsule network complex, even the liquid guest structures could be observed without crystallization processes. These results led the author to an idea of applying the guest inclusion and its single crystal X-ray analysis in the porous complex as a new analysis method of molecular structure. Though the X-ray diffraction analysis is undoubtedly the most powerful analysis method in terms of the structure determination, the difficulty on a preparation of a target single crystal limits the target scope of the X-ray analysis. If a general method to include and align guest molecules in a porous complex is established, a conventional crystallization of target molecule, which is a biggest hurdle of the current single crystal X-ray diffraction analysis, becomes unnecessary.

### 1.3 Over view of this thesis

The objective of this thesis is to establish a new X-ray analysis protocol of determining molecular structure by means of including it into the crystalline porous complex and aligning it in the pore. The developed method, “crystalline sponge method”, broke an intrinsic limitation of conventional single crystal X-ray crystallography that the measurement cannot be performed without a crystal of the target compound. The keys to realize the method were treating the porous complex with cyclohexane prior to new guest accommodations, and guest alignment procedure by the slow solvent evaporation. The treatment of the complex with cyclohexane washed out nitrobenzene, which was initially stuck on the pore strongly, and made the complex available to include new guest molecules. Slow evaporation of the solvent aligned the guest molecules in the pore and made the periodicity of the framework and guests commensurate by fitting the host structure to guests. By means of the crystalline sponge method, various guest molecules were successfully determined by just soaking the crystal of porous complex into the guest solution and various applications were demonstrated.

This thesis is composed of the following chapters.

In chapter 2, the general method to include and align the guest molecules in the porous complex was developed. Upon guest molecule inclusions, the single crystallinities of the porous complex crystals were fully maintained, and the included guest structures were clearly analyzed by the single crystal X-ray diffraction analysis without guest crystallization.

In chapter 3, the crystalline sponge method was applied for nanogram scale guest analysis and combined with chromatographic separation. The hidden potential of the X-ray crystallographic analysis for trace amount scale analysis was disclosed by the crystalline sponge method. Combination of the chromatographic separation demonstrated the possible application of the crystalline sponge method to scarce natural product mixture analysis.

In chapter 4, absolute structure determinations of chiral guest molecules were demonstrated. Due to the flexible nature of the host porous complex, chiral guest inclusion complex were chirally distorted, and their absolute structures were successfully determined. Furthermore, anomalous scattering effect was obtained from

heavy atoms in the host porous complex and an introduction of a heavy atom into the guest molecules was unnecessary.

In chapter 5, the small scale X-ray analysis by the crystalline sponge method was applied for a risk free structural analysis of dangerous ozonide compounds. Ozonides structures were safely analyzed from the reaction mixture without isolation of them. The availability of X-ray analysis of dangerous compounds by the crystalline sponge under the risk-free conditions was demonstrated.

In chapter 6, the crystalline sponge method was utilized for the quick structural analysis method of the complicated synthetic compound. Even for the compounds, which have difficulty in structural analysis by the NMR spectroscopy or mass spectrometry, the crystalline sponge method served as a quick and conclusive analysis method.

In chapter 7, the scope and limitations of the crystalline sponge method were disclosed. The current crystalline sponge has some limitations on the target compound size, solubility and obtained data quality. Understanding the scope and limitations contribute not only for using the method, but also for developing the next generation crystalline sponge.

In chapter 8, the author summarized this thesis and provided future visions.

## References

- 1 D. E. Palin, H. M. Powell, *Nature* **1945**, *156*, 334–335.
- 2 D. E. Palin, H. M. Powell, *J. Chem. Soc.* **1947**, 208–221.
- 3 W. Schlenk, *Justus Liebigs Ann. Chem.* **1949**, *565*, 204–240.
- 4 M. F. Bengen, *German Patent application OZ 123 438* **1940**.
- 5 A. E. Smith, *J. Chem. Phys.* **1950**, *18*, 150–151.
- 6 A. E. Smith, *Acta Cryst.* **1952**, *5*, 1224–235.
- 7 R. W. Schiessler, D. Flitter, *J. Am. Chem. Soc.* **1952**, *74*, 1720–1723.
- 8 K. D. M. Harris, J. M. Thomas, *J. Chem. Soc. Faraday Trans.* **1990**, *86*, 2985–2996.
- 9 A. A. Khan, S. T. Bramwell, K. D. . Harris, B. M. Kariuki, M. R. Truter, *Chem. Phys. Lett.* **1999**, *307*, 320–326.
- 10 H. Schlenk, R. T. Holman, *J. Am. Chem. Soc.* **1950**, *72*, 5001–5004.
- 11 V. Zavodnik, A. Stash, V. Tsirelson, R. de Vries, D. Feil, *Acta Crystallogr. Sect. B Struct. Sci.* **1999**, *55*, 45–54.
- 12 L. Yeo, K. D. M. Harris, *Acta Crystallogr. Sect. B Struct. Sci.* **1997**, *53*, 822–830.
- 13 W. J. Zimmerschied, R. A. Dinerstein, A. W. Weitkamp, R. F. Marschner, *Ind. Eng. Chem.* **1950**, *42*, 1300–1306.
- 14 C. D. Gutsche, *Acc. Chem. Res.* **1983**, *16*, 161–170.
- 15 C. J. Pedersen, *J. Am. Chem. Soc.* **1967**, *89*, 7017–7036.
- 16 J. Szejtli, *Chem. Rev.* **1998**, *98*, 1743–1754.
- 17 D. W. Breck, W. G. Eversole, R. M. Milton, T. B. Reed, T. L. Thomas, *J. Am. Chem. Soc.* **1956**, *78*, 5963–5972.
- 18 T. B. Reed, D. W. Breck, *J. Am. Chem. Soc.* **1956**, *78*, 5972–5977.
- 19 M. E. Davis, R. F. Lobo, *Chem. Mater.* **1992**, *4*, 756–768.
- 20 T. C. Bowen, R. D. Noble, J. L. Falconer, *J. Memb. Sci.* **2004**, *245*, 1–33.
- 21 Y. Tao, H. Kanoh, L. Abrams, K. Kaneko, *Chem. Rev.* **2006**, *106*, 896–910.
- 22 L. Broussard, D. P. Shoemaker, *J. Am. Chem. Soc.* **1960**, *82*, 1041–1051.
- 23 K. Seff, *Acc. Chem. Res.* **1976**, *9*, 121–128.
- 24 R. Y. Yanagida, K. Seff, *J. Phys. Chem.* **1972**, *76*, 2597–2601.
- 25 A. A. Amaro, K. Seff, *J. Chem. Soc. Chem. Commun.* **1972**, 1201–1202.
- 26 A. A. Amaro, K. Seff, *J. Phys. Chem.* **1973**, *77*, 906–910.



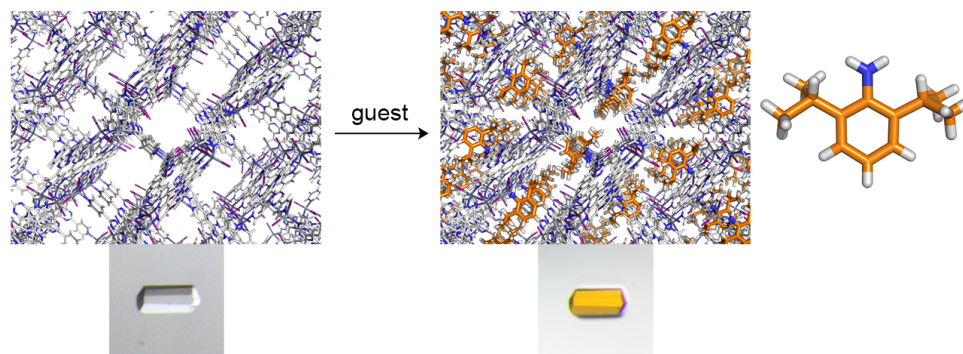
- 27 A. Depla, E. Verheyen, A. Veyfeyken, E. Gobechiya, T. Hartmann, R. Schaefer, J. A. Martens, C. E. A. Kirschhock, *Phys. Chem. Chem. Phys.* **2011**, *13*, 13730–13737.
- 28 S. R. Batten, R. Robson, *Angew. Chem. Int. Ed.* **1998**, *37*, 1460–1494.
- 29 M. Eddaoudi, D. B. Moler, H. Li, B. Chen, T. M. Reineke, M. O’Keeffe, O. M. Yaghi, *Acc. Chem. Res.* **2001**, *34*, 319–330.
- 30 S. Kitagawa, R. Kitaura, S. Noro, *Angew. Chem. Int. Ed.* **2014**, *43*, 2334–2375.
- 31 G. Férey, *Chem. Soc. Rev.* **2008**, *37*, 191–214.
- 32 H. Furukawa, K. E. Cordova, M. O’Keeffe, O. M. Yaghi, *Science* **2013**, *341*, 974.
- 33 Y. Kinoshita, I. Matsubara, Y. Saito, *Bull. Chem. Soc. Jpn.* **1959**, *32*, 741–747.
- 34 Y. Kinoshita, I. Matsubara, T. Higuchi, Y. Saito, *Bull. Chem. Soc. Jpn.* **1959**, *32*, 1221–1226.
- 35 T. Iwamoto, T. Miyoshi, T. Miyamoto, Y. Sasaki, S. Fujiwara, *Bull. Chem. Soc. Jpn.* **1967**, *40*, 1174–1178.
- 36 B. Hoskins, R. Robson, *J. Am. Chem. Soc.* **1989**, *111*, 5962–5964.
- 37 B. F. Hoskins, R. Robson, *J. Am. Chem. Soc.* **1990**, *112*, 1546–1554.
- 38 O. M. Yaghi, M. O’Keeffe, N. W. Ockwig, H. K. Chae, M. Eddaoudi, J. Kim, *Nature* **2003**, *423*, 705–714.
- 39 C. J. Kepert, M. J. Rosseinsky, *Chem. Commun.* **1999**, *536*, 375–376.
- 40 M. Kondo, T. Yoshitomi, H. Matsuzaka, S. Kitagawa, K. Seki, *Angew. Chemie Int. Ed. Engl.* **1997**, *36*, 1725–1727.
- 41 S. S. –Y. Chui, S. M. –F. Lo, J. P. H. Charmant, A. G. Orpen, I. D. Williams, *Science* **1999**, *283*, 1148–1150.
- 42 K. Biradha, Y. Hongo, M. Fujita, *Angew. Chem. Int. Ed.* **2000**, *39*, 3843–3845.
- 43 H. Li, M. Eddaoudi, M. O’Keeffe, O. M. Yaghi, *Nature* **1999**, *402*, 276–279.
- 44 M. P. Suh, J. W. Ko, H. J. Choi, *J. Am. Chem. Soc.* **2002**, *124*, 10976–10977.
- 45 K. Biradha, M. Fujita, *Angew. Chem. Int. Ed.* **2002**, *41*, 3392–3395.
- 46 O. Ohmori, M. Kawano, M. Fujita, *J. Am. Chem. Soc.* **2004**, *126*, 16292–16293.
- 47 M. Kawano, M. Fujita, *Coord. Chem. Rev.* **2007**, *251*, 2592–2605.
- 48 H. Kim, H. Chun, G.-H. Kim, H.-S. Lee, K. Kim, *Chem. Commun.* **2006**, 2759–2761.

- 49 R. Kitaura, S. Kitagawa, Y. Kubota, T. C. Kobayashi, K. Kindo, Y. Mita, A. Matsuo, M. Kobayashi, H.-C. Chang, T. C. Ozawa, M. Suzuki, M. Sakata, M. Takata, *Science* **2002**, 298, 2358–2361.
- 50 R. Matsuda, R. Kitaura, S. Kitagawa, Y. Kubota, R. V Belosludov, T. C. Kobayashi, H. Sakamoto, T. Chiba, M. Takata, Y. Kawazoe, Y. Mita, *Nature* **2005**, 436, 238–241.
- 51 Q. Li, W. Zhang, O. S. Miljanić, C.-H. Sue, Y.-L. Zhao, L. Liu, C. B. Knobler, J. F. Stoddart, O. M. Yaghi, *Science* **2009**, 325, 855–859.



## Chapter 2

### Development of the Crystalline Sponge Method



#### Abstract

A new protocol for preparing the single crystalline sample suitable to X-ray crystallographic analysis without crystallization was established as the crystalline sponge method. Soaking a piece of the crystalline sponge, a kind of porous complex, into a target compound solution afforded the target inclusion crystalline sponge. In the pore of the crystalline sponge, the target compound was trapped at the specific position and highly ordered in a periodic fashion. Therefore, the included guest molecules were observable by the X-ray diffraction analysis. This protocol provides the method for X-ray observation of the non-crystalline target compound without crystallization of it.

## 2.1 Introduction

Guest inclusion into the porous material such as zeolite, metal organic frameworks (MOFs) and porous coordination polymers (PCPs) were extensively studied in terms of the inclusion behavior, storage, separation, reactivity, conductivity and so on.<sup>1-8</sup> Most of the porous materials can be synthesized in a single crystalline form, however these single crystals are often unstable to guest exchange or immersion into other solvents and lost the single crystallinity or decomposed.<sup>9</sup> Powder crystal was sufficient to perform other than single crystal X-ray analysis such as powder X-ray analysis, differential scanning calorimetry (DSC), gas sorption study and so on. In order to achieve single crystal X-ray diffraction analysis of an included guest molecule, maintaining the single crystallinity of the host porous complex upon guest inclusion is inevitable and the first critical hurdle. In addition to maintaining the single crystallinity, aligning included guest molecules in the pore of the porous complex is the second hurdle. Due to these difficulties, relatively limited numbers of examples that achieved the guest exchange and its observation by single crystal X-ray diffraction were reported among the numerous reports on the porous complex.<sup>10-14</sup>

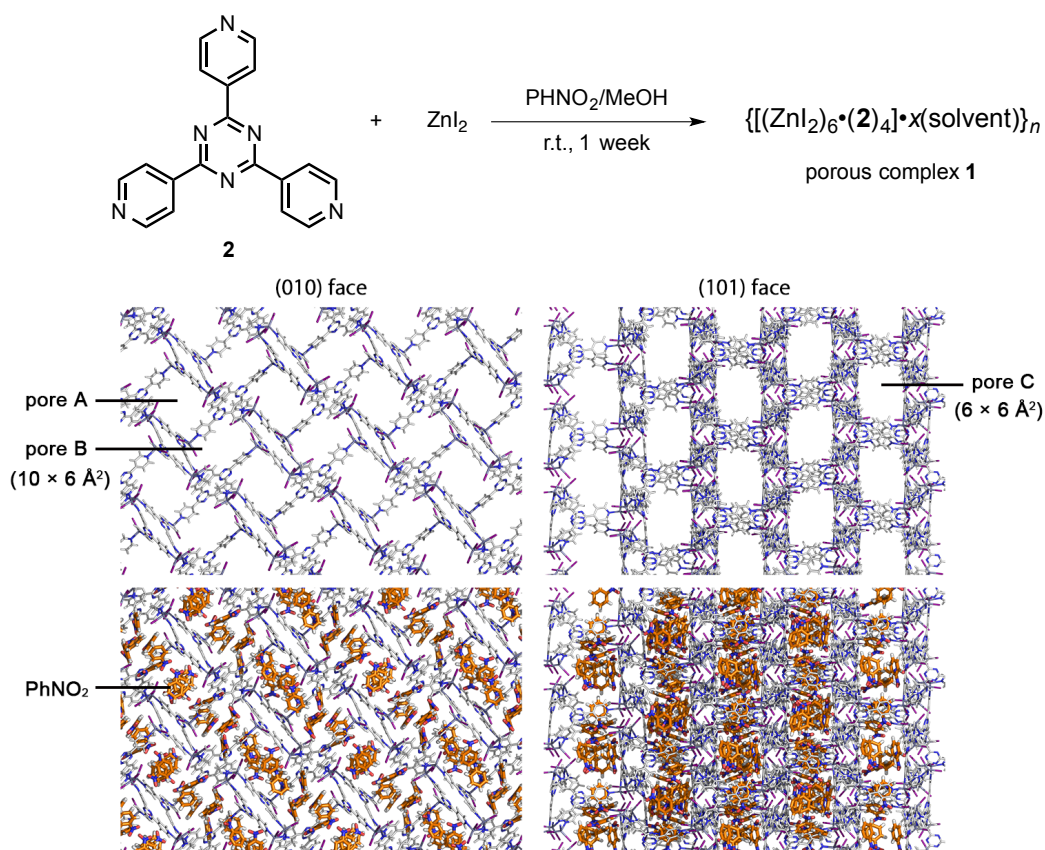
In this study, a porous complex which was constructed by the coordination bond of pyridine ligand to  $ZnI_2$  was utilized for the host porous material. Taking an advantage of single crystalline nature and flexible nature of the porous complex, it was demonstrated to include guest molecules from their solution, tightly bind and align the guest molecules in the pore, while the crystal maintained the single crystallinity. By means of the guest inclusion into the porous material, observation of the included guest molecules along the host framework by single crystal X-ray diffraction analysis without crystallization could be achieved.

## 2.2 Synthesis and solvent exchange of the crystalline sponge

As a host porous complex, a porous complex **1** was employed in the following three respects. First, the porous complex **1** was obtained in a single crystalline form and has a suitable sized pore in the structure. Second, it showed flexible nature depending on the surrounding chemical environment. Third, the reported space group of the complex **1** was monoclinic  $C2/c$ , which is relatively low symmetry among the porous complexes, MOFs, PCPs. Lower symmetry is suitable for the guest observation in the structure. Crystals of porous complex **1** were synthesized by a complexation reaction

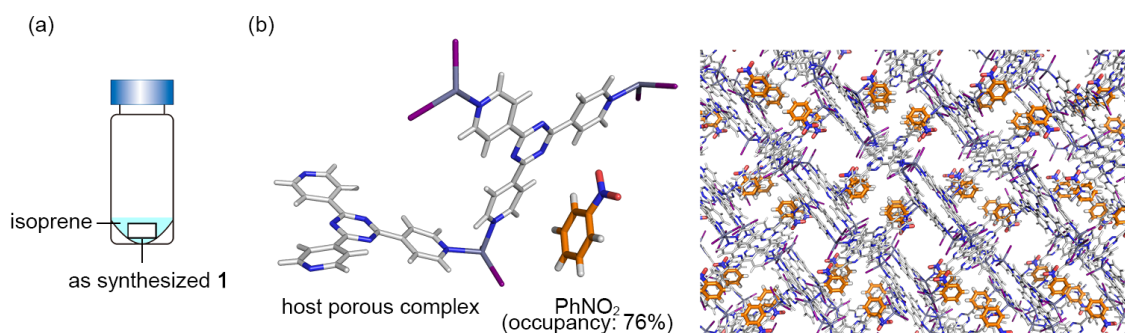
by the layer diffusion method between 2,4,6-tri(4-pyridyl)-1,3,5-triazine (**2**) in nitrobenzene (**3**) and  $\text{ZnI}_2$  in MeOH according to the previously described procedure (Scheme 2.1).<sup>15</sup> The porous complex **1** was obtained in single crystalline form suitable for the single crystal X-ray diffraction analysis. The structure of **1** was observed as  $\{[(\text{ZnI}_2)_6 \cdot (\mathbf{2})_4] \cdot x(\text{solvent})\}_n$  ( $x = 10$ , solvent =  $\text{PhNO}_2$ ) by the single crystal X-ray diffraction analysis. The space group was converged with monoclinic  $P2_1/a$  space group, which was different from that in the previous report.<sup>15</sup> The porous complex **1** has two different, but similar sized pore A and pore B in a direction perpendicular to the Miller index (010) face, and also has another pore C in a direction perpendicular to the Miller index (101) face. The size of the pore A and B were ca.  $10 \times 6 \text{ \AA}^2$  and pore C was ca.  $6 \times 6 \text{ \AA}^2$ . Pores of as synthesized **1** were fully occupied by the solvent **3** (Figure 2.1).

**Scheme 2.1.** A synthesis of porous complex **1**.



**Figure 2.1.** The crystal structure of as synthesized porous complex **1** and its pores at (010) and (101) face without solvent (top) and with solvent nitrobenzene (bottom).

To include and align the new guest compound in the porous complex **1**, a guest exchange experiment was examined by soaking crystals of **1** into a drop of liquid isoprene (**4**). The crystals of **1** were placed in a microvial with a drop of **4** (~ 5  $\mu$ L), and sealed vial was allowed to stand for 2 d at room temperature (Figure 2.2a). After 2 d, the resultant crystal with good crystallinity was subjected to the X-ray diffraction analysis. The structure was converged with monoclinic  $C2/c$  space group, which was different from the initial space group monoclinic  $P2_1$ . X-ray analysis revealed only **3** with 76% refined occupancy in the pore of the porous crystal **1**, and the residual electron density scattered over the pore could not be assigned to isoprene. However, the structure still contained a large guest accessible void, in which no strong electron density was observed, and even for the observed **3**, refined occupancy was not 100% (Figure 2.2b). This result indicated the structure contained severe disorder of **3** and **4**. Since solvent **3** was initially bound strongly in the pore of as synthesized **1** by  $\pi$ - $\pi$  interaction, hydrogen bond and multiple CH- $\pi$  interaction, the inclusion of **4** resulted in a partial and disordered inclusion.



**Figure 2.2.** (a) Schematic representation of the inclusion of isoprene into as synthesized **1**. (b) The X-ray structure of the resultant crystal. Observed nitrobenzene was shown in orange color. The asymmetric unit (left) and the packing structure (right).

Thus, solvent exchange from nitrobenzene to other solvent with weaker interaction to **1** prior to the new guest inclusion was examined. First, exchanging solvent was optimized. The crystals were washed with and soaked in various solvents. During the solvent exchange process, the crystal of **1** was damaged by or dissolved in most of the solvent, and diffraction pattern of the solvent exchanged crystal was terribly bad or impossible to observe. Among the extensive screening of the exchanging solvent, cyclohexane gave the best result in terms of the crystallinity (Table 2.1).

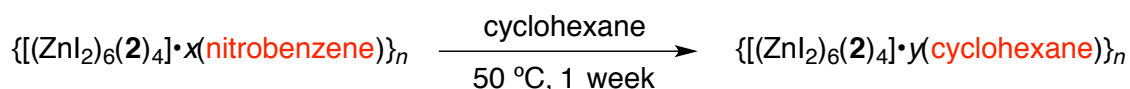
**Table 2.1.** The result of the exchanging solvent screening.

exchanged solvent	H <sub>2</sub> O	MeOH	EtOH	CH <sub>3</sub> CN	DMSO	Et <sub>2</sub> O	THF	1,2-dimethoxyethane	toluene	methylcyclohexane	CH <sub>2</sub> Cl <sub>2</sub>	CHCl <sub>3</sub>	AcOEt	hexane	cyclohexane
crystallinity	dissolved					completely lost <sup>a</sup>					partially lost <sup>b</sup>			maintained <sup>c</sup>	

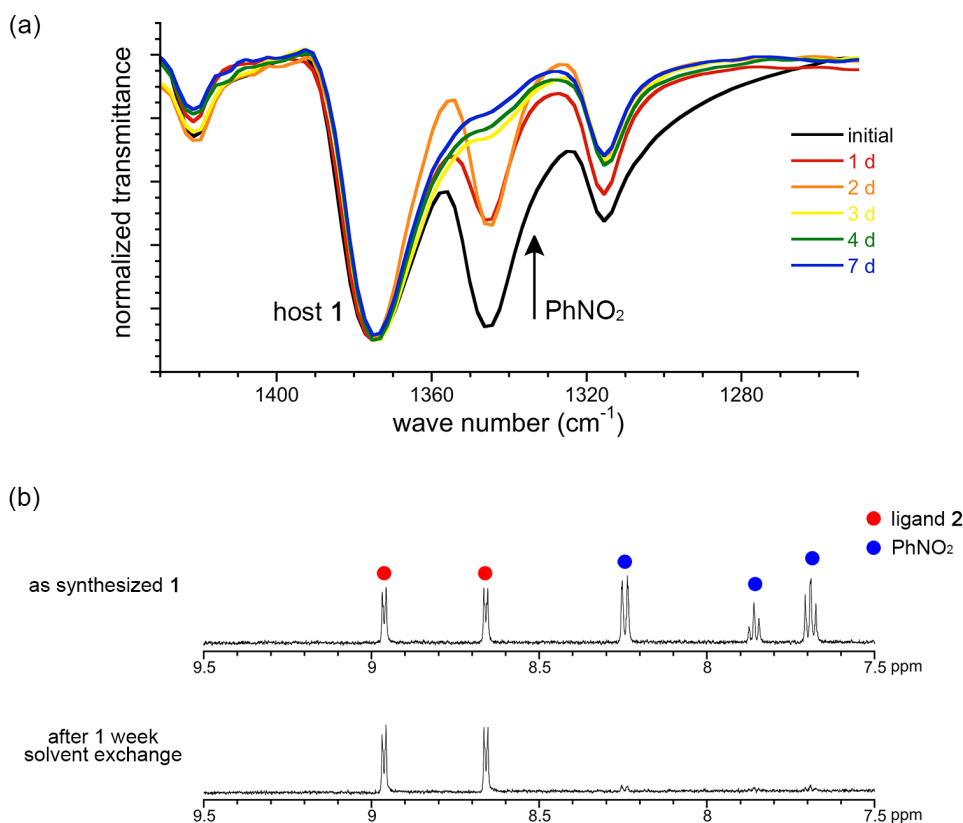
<sup>a</sup>Crystals were turned to be dark color and X-ray diffraction was not observed. <sup>b</sup>Although crystals were severely cracked, they still maintain the crystallinity partially and the diffraction could be observed at low resolution. When solvent exchange was performed with mixed solvent CH<sub>2</sub>Cl<sub>2</sub>/cyclohexane=1:9 (v/v), the crystallinity was maintained. <sup>c</sup>The cracks were observed on the large sized crystal.

Second, solvent exchanging time with the cyclohexane was also optimized. In a test tube, ca. 20 mg of as synthesized crystal **1** was placed, and washed with fresh nitrobenzene (10 mL × 2) to remove uncoordinated ligand **2** remained on the surface of **1**. Then, 10 mL of cyclohexane was put into the test tube, and the test tube was allowed to stand in an incubator at 50 °C for various incubation time. During the exchanging process, supernatant was replaced with 10 mL of fresh cyclohexane once a day. In order to check the ratio of the solvent exchange to cyclohexane, the process was monitored by the microscopic IR spectroscopy. Microscopic IR measurement of as synthesized complex **1** showed sharp absorptions at 1344 cm<sup>-1</sup> and 1375 cm<sup>-1</sup> attributable to the absorption of included **3** and ligand **2**, respectively. The ratio of the absorption at 1344 cm<sup>-1</sup> to 1375 cm<sup>-1</sup> was decreased with increasing the solvent exchanging time (Figure 2.3a). From the IR spectra, solvent exchange to cyclohexane was almost completed at 1 week. The completion of the exchange was also confirmed by the NMR measurement of an extract from the crystal of **1** after a week solvent exchange (Figure 2.3b).

**Scheme 2.2.** A solvent exchange of porous complex **1**.





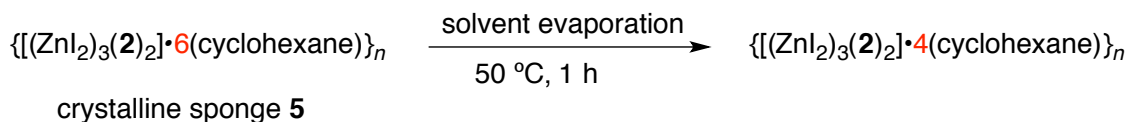


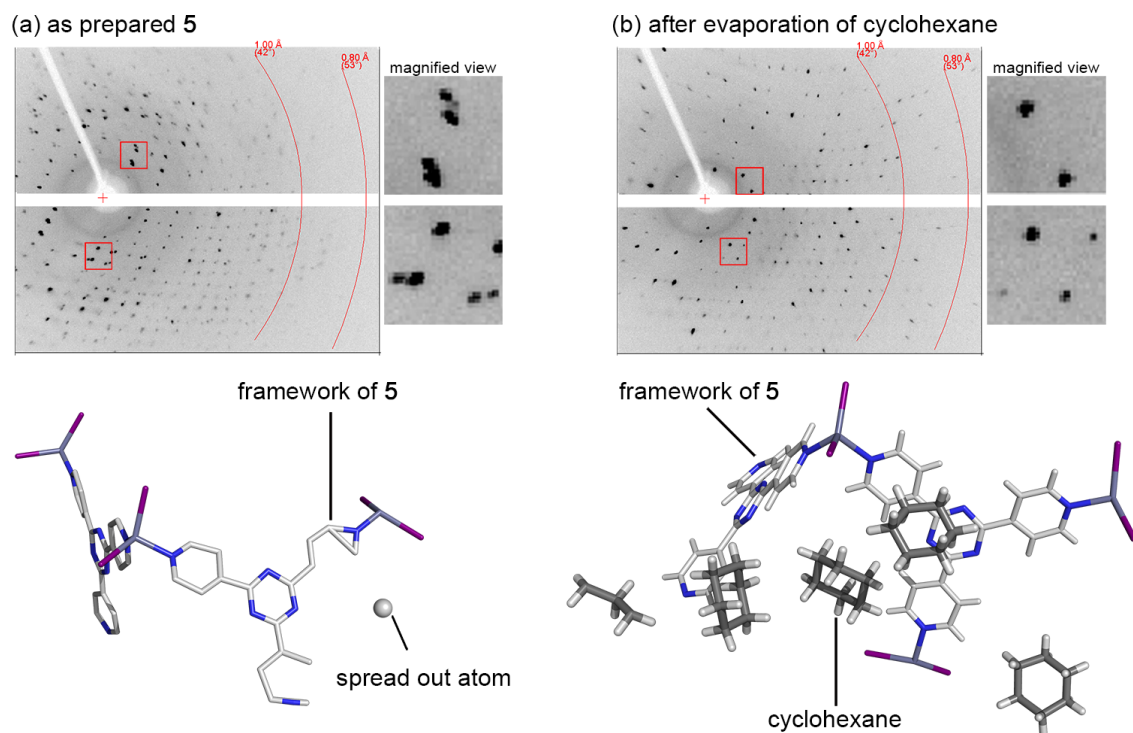
**Figure 2.3.** (a) Microscopic IR spectra of porous complex **1** during the solvent exchange to cyclohexane. (b)  $^1\text{H}$  NMR spectra of extracts from as synthesized **1** (top) and **1** after 1 week solvent exchange (500 MHz,  $\text{DMSO-}d_6$ , 300 K).

Hereafter, cyclohexane exchanged porous complex **1** was defined as crystalline sponge **5**. The structural characterization of **5** was performed with X-ray diffraction analysis and elemental analysis. The diffraction pattern of as prepared **5** gave the split diffraction spot and the structural analysis did not converge and the atom assigned to the host framework of **5** was spread out (Figure 2.4a). However, when the crystal **5** was placed in a microvial with 5  $\mu\text{L}$  of cyclohexane followed by gradual solvent cyclohexane evaporation over 1 h at 50  $^\circ\text{C}$ , the diffraction pattern of the resultant crystal **5** was drastically improved. The structure was converged and included solvent cyclohexane molecules were clearly observed (Figure 2.4b). Elemental analyses of both as prepared **5** and **5** after cyclohexane evaporation gave the formula as  $\{[(\text{ZnI}_2)_3 \cdot (\mathbf{2})_2] \cdot (\text{cyclohexane})_6\}_n$  and  $\{[(\text{ZnI}_2)_3 \cdot (\mathbf{2})_2] \cdot (\text{cyclohexane})_4\}_n$ , respectively (Scheme 2.3). These data indicated the framework structure and cyclohexane in the pore of as prepared **5** was swellheaded and highly disordered due to the excess inclusion

of cyclohexane. Therefore, removal of the excess cyclohexane from as prepared **5** might induce the structural ordering of host framework and guest cyclohexane all over the crystal. Furthermore, the structural flexibility of the host framework, which was reported for the nitrobenzene inclusion porous complex **1** was also maintained after solvent exchange to cyclohexane.<sup>15</sup> Since a rapid cyclohexane evaporation within 1 minute at higher temperature (90 °C) deteriorated the crystallinity, gradual structural change of **5** by gradual evaporation was important to induce the ordered structure in single-crystal-to-single-crystal fashion (Figure S2.4). The X-ray analysis of **5** was finally converged with monoclinic *C2/c* space group and characterized as  $\{[(\text{ZnI}_2)_3 \cdot (\mathbf{2})_2] \cdot x(\text{solvent})\}_n$  ( $x = 4$ , solvent = cyclohexane). When further drying was applied for the crystalline sponge **5** under the reduced pressure,  $\{[(\text{ZnI}_2)_3 \cdot (\mathbf{2})_2] \cdot 4(\text{cyclohexane})\}_n$  structure lost further 2.5 cyclohexane molecules and changed to  $\{[(\text{ZnI}_2)_3 \cdot (\mathbf{2})_2] \cdot 1.5(\text{cyclohexane})\}_n$ , which was confirmed by the elemental analysis (supporting information). These data indicated that the initial crystalline sponge **5** included 6 cyclohexane molecules, which categorized into three types by the difference of strengths of interaction with the crystalline sponge framework. Two of the 6 cyclohexane molecules were least strongly bound and quickly evaporated. Second category has 2.5 cyclohexane molecules, which were weakly trapped in the structure, however they evaporated below the boiling point of cyclohexane. The last 1.5 molecules of cyclohexane were strongly trapped in the crystalline sponge **5** even under the reduced pressure (0.1 Torr, for 30 min). A thermogravimetric analysis also showed that least volatile 1.5 molecules of cyclohexane were most strongly bound in the structure (Figure S2.3).

**Scheme 2.3.** Solvent evaporation from swellheaded crystalline sponge **5**.

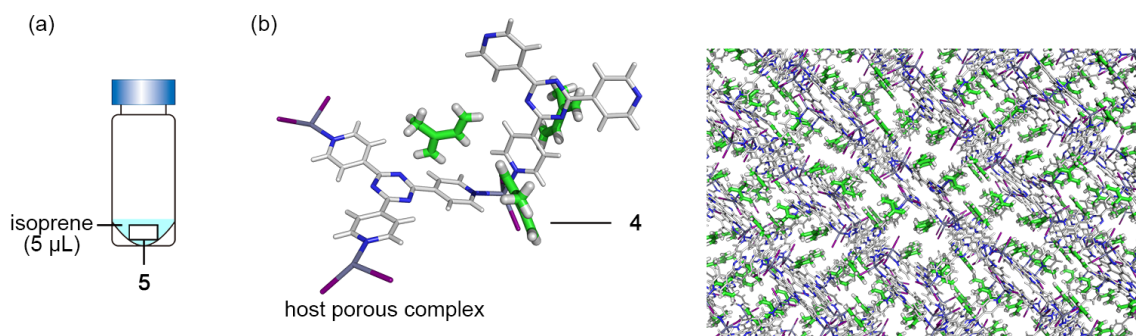




**Figure 2.4.** The X-ray diffraction patterns and magnified view of the red square (top) and X-ray structure of asymmetric unit (bottom) of (a) as prepared **5** and (b) **5** after cyclohexane evaporation

### 2.3 Inclusion and X-ray analysis of liquid isoprene

With cyclohexane exchanged crystalline sponge **5**, inclusion of **4** was reexamined. A piece of the crystalline sponge **5** was placed in a microvial with a drop of **4** ( $\sim 5 \mu\text{L}$ ). The vial was tightly capped and allowed to stand for 2 d at room temperature as previous experiment (Figure 2.5a). After 2 d the resultant colorless crystal was subjected to the single crystal X-ray diffraction study. The result of the X-ray analysis was in sharp contrast to that of as synthesized porous complex **1**, and showed the structure of **4** included in the pore of the crystalline sponge **5** (Figure 2.5b). These data indicated that the replacement of the nitrobenzene by cyclohexane that had the weaker interaction with the framework is essential to accommodate new guest molecules. By including into the crystalline sponge **5**, even a liquid compound whose boiling point is around r.t. could be observed by the X-ray diffraction analysis. Furthermore, the success of the X-ray analysis of liquid **4** without crystallization showed large potential to apply this X-ray analysis method to other targets.



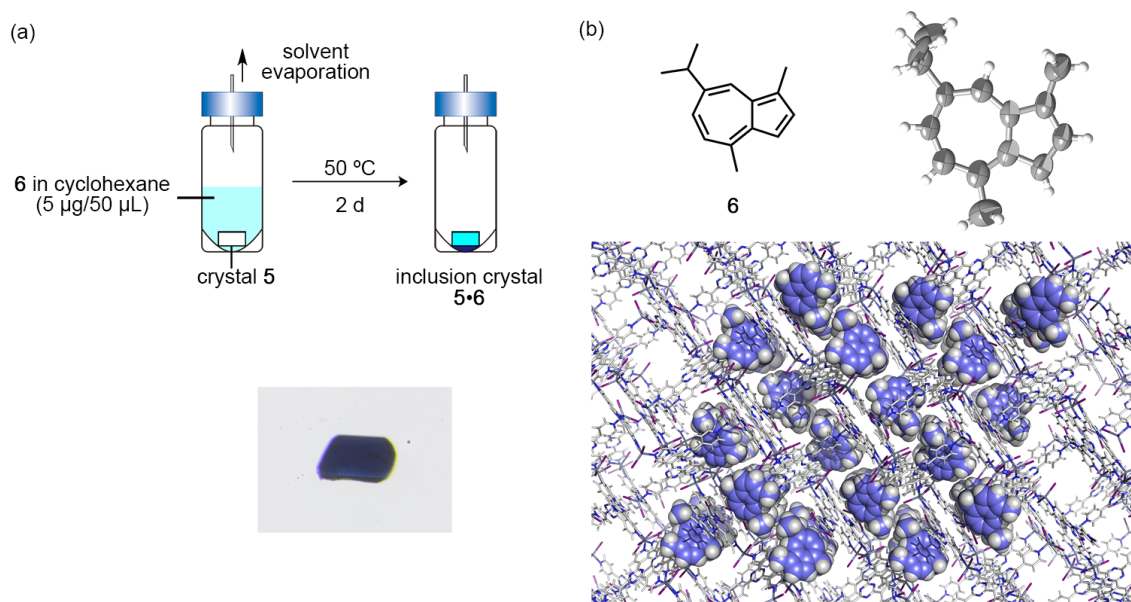
**Figure 2.5.** (a) Schematic representation of the inclusion of isoprene into **5**. (b) The X-ray structure of the resultant crystal. Observed **4** structures were shown in green color. The asymmetric unit (left) and the packing structure (right).

#### 2.4 Microgram scale inclusion and X-ray analysis of guaiazulene

Encouraged by the success of the X-ray analysis of the liquid compound without crystallization, next, inclusion and X-ray analysis with microgram scale of solid guaiazulene (**6**) were examined. Theoretically, X-ray diffraction analysis can be performed with only a piece of the target crystal. Calculation based on the size of the crystalline sponge ( $100 \times 100 \times 100 \mu\text{m}^3$ ), porosity of the crystal (50%) and density of the organic molecules (ca.  $1 \text{ g/cm}^3$ ) suggested that requisite sample amount to fulfill the whole pore of the crystalline sponge **5** was ca.  $0.5 \mu\text{g}$  of sample. Thus, microgram scale guest inclusion experiment was examined with a piece of crystalline sponge **1** and  $0.5 \mu\text{g}$  of blue color solid **6**.

Since inclusion by neat conditions of **6** was not available unlike liquid **4**, diluted cyclohexane solution ( $0.5 \mu\text{g}/50 \mu\text{L}$ ) of **6** was added to the crystalline sponge **5** to include **6**. Inclusion was performed for 2 d with the same procedure as the inclusion of **4**, however **6** was not observed in the crystalline sponge by the X-ray diffraction analysis. Instead of **6**, cyclohexane molecules were observed in the pore. These data suggested that though the interaction between cyclohexane and framework was weak, large excess amount of cyclohexane was almost exclusively included into the pore. Thus, the removal of large amount of solvent cyclohexane from the system by the slow evaporation was carried out. By evaporating the cyclohexane from the system, an equilibrium between concentration of **6** in supernatant and in crystalline sponge was pushed to the included state.

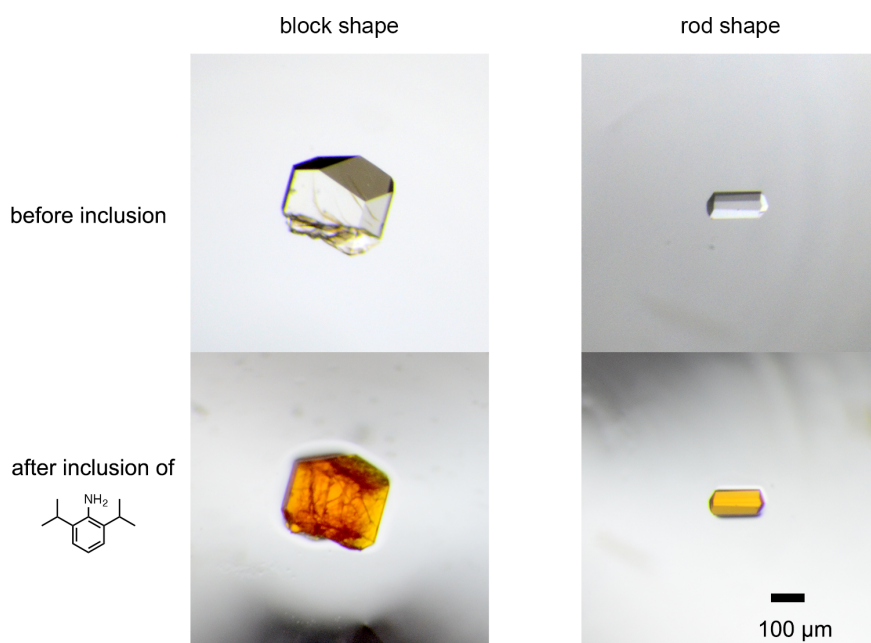
With the optimized conditions as described above, inclusion of 0.5  $\mu\text{g}$  of **6** was performed. After the complete evaporation of cyclohexane at 50  $^{\circ}\text{C}$  over 2 d (Figure 2.6a), the resultant crystalline sponge **5** was turned to be dark blue, and it suggested that **6** was included into the crystalline sponge **5**. Single crystal X-ray diffraction study gave an excellent diffraction pattern even in the higher resolution area ( $\sim 0.8 \text{ \AA}$ ). The crystal structure clearly revealed the molecular structure of **6** trapped in a pore of the crystalline sponge **5** (Figure 2.6b). It is noteworthy that substituent methyl and isopropyl groups on the azulene core were easily assigned without any disorder.



**Figure 2.6.** (a) Schematic representation of the inclusion of **6** by gradual solvent evaporation (top) and photograph of the resultant crystal **5•6** (bottom). (b) The X-ray structure of the inclusion crystal **5•6**. The thermal factor of included **6** at the 50% probability (top right). In the packing structure, observed **6** structures were represented in blue colored CPK model.

## 2.5 Selection of the crystal of the crystalline sponge

Inclusion of 0.5  $\mu\text{g}$  of **6** by soaking and solvent evaporation process gave another important insight about stability of the crystalline sponge **5**. The crystalline sponge **5** mainly contained two types of the crystal shape that were categorized as block and rod type, respectively.<sup>16</sup> The crystallinities of each type of crystal **5** were sufficiently maintained upon solvent exchange to cyclohexane and X-ray diffraction study of the two types of the crystal showed same structure. However, these two different shaped crystals showed different stability toward the guest inclusion process. The difference of the stability was clearly demonstrated by the inclusion of 2,6-diisopropylaniline from cyclohexane solution (5  $\mu\text{g}$ / 50  $\mu\text{L}$ ). The single crystallinity of the block shaped crystal was deteriorated and a lot of cracks on the crystal appeared after the soaking and evaporation process, while the crystallinity of the rod shaped crystal was completely maintained and the X-ray diffraction pattern was excellent, even after the complete solvent evaporation over 2 d at 50  $^{\circ}\text{C}$  (Figure 2.7). Additionally, the solvent evaporation rate was also critical to maintain the crystallinity. Quick evaporation of cyclohexane within 1 h at higher temperature (90  $^{\circ}\text{C}$ ) gave the deterioration of the crystallinity, while the slow evaporation over 2 d gave a crystal with good crystallinity.

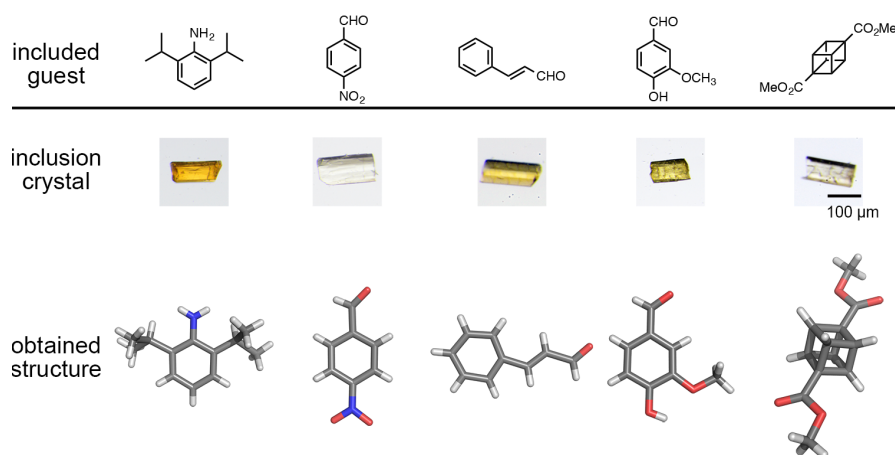


**Figure 2.7.** Photographs of block and rod shaped crystal **5** before and after inclusion of 2,6-diisopropylaniline.



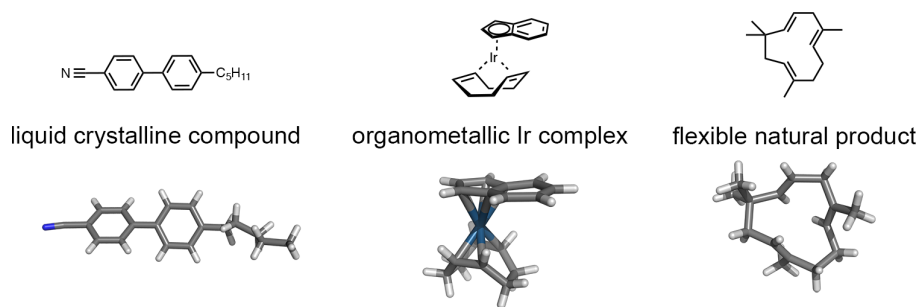
## 2.6 Crystalline sponge analysis of other guests

The success of the crystalline sponge analysis of **4** and **6** motivated the crystalline sponge analysis of other target compound with 5  $\mu\text{g}$  scale. Variety of compounds listed (Figure 2.8) were also analyzed with the crystalline sponge method. During the inclusion over 2 d, some compounds caused the crystal damage and slightly deteriorated the crystallinity of **5**, however all the X-ray diffraction analysis of the resultant crystals showed included target compounds in the pore of **5**, respectively.



**Figure 2.8.** Various guest compounds analyzed by the crystalline sponge method.

When the target compounds were insoluble to cyclohexane, 5  $\mu\text{L}$  of  $\text{CH}_2\text{Cl}_2$  solution (1 mg/1 mL) of the target compound was added to the microvial containing crystalline sponge **5** and 45  $\mu\text{L}$  of cyclohexane. Interestingly, the crystalline sponge analysis was also applicable to a liquid crystalline 4-cyano-4'-pentylbiphenyl, an organometallic compound, (1,5-cyclooctadiene)-( $\eta^5$ -indenyl)iridium(I) and a flexible macrocyclic natural product,  $\alpha$ -humulene. Usually the single crystal X-ray guest observation in the porous complex was limited to a few specific guest molecules,<sup>17-19</sup> however these X-ray analyses listed above performed with 5  $\mu\text{g}$  of sample and one crystal of **5** showed a large generality of the crystalline sponge method.



**Figure 2.9.** X-ray structures of liquid crystalline, organometallic, and natural compound determined by the crystalline sponge method.

## 2.7 Summary

In this chapter, the experimental procedure of the inclusion and aligning the target molecules in the crystalline sponge was developed. Solvent exchange from nitrobenzene to cyclohexane gave the suitable crystalline sponge for guest inclusion while the crystal maintains its single crystallinity. It was also important to use the rod shaped crystalline sponge for guest inclusion. X-ray analyses of various target inclusion crystalline sponges clearly revealed the included target structures even with the liquid target compound. This procedure enabled X-ray single crystallographic analysis of target compound without crystallization and established as the crystalline sponge method. The applicability of the crystalline sponge method to many types of compounds was also demonstrated.



## 2.7 Experimental Section

Materials and Methods	31-36
Elemental analysis of the crystalline sponge <b>5</b>	34
Thermogravimetric analysis of the crystalline sponge <b>5</b>	35
Crystallographic data	37-41
<b>Figure S2.1.</b> Schematic illustration of the synthesis and photograph of <b>1</b>	33
<b>Figure S2.2.</b> Photograph of crystals <b>1</b> after solvent exchange	34
<b>Figure S2.3.</b> TG spectrum of <b>5</b>	35
<b>Figure S2.4.</b> Photograph of rapidly solvent evaporated <b>1</b>	35
<b>Figure S2.5-S2.12.</b> X-ray crystallographic data	37-41

## Materials and method

### Reagents and equipment

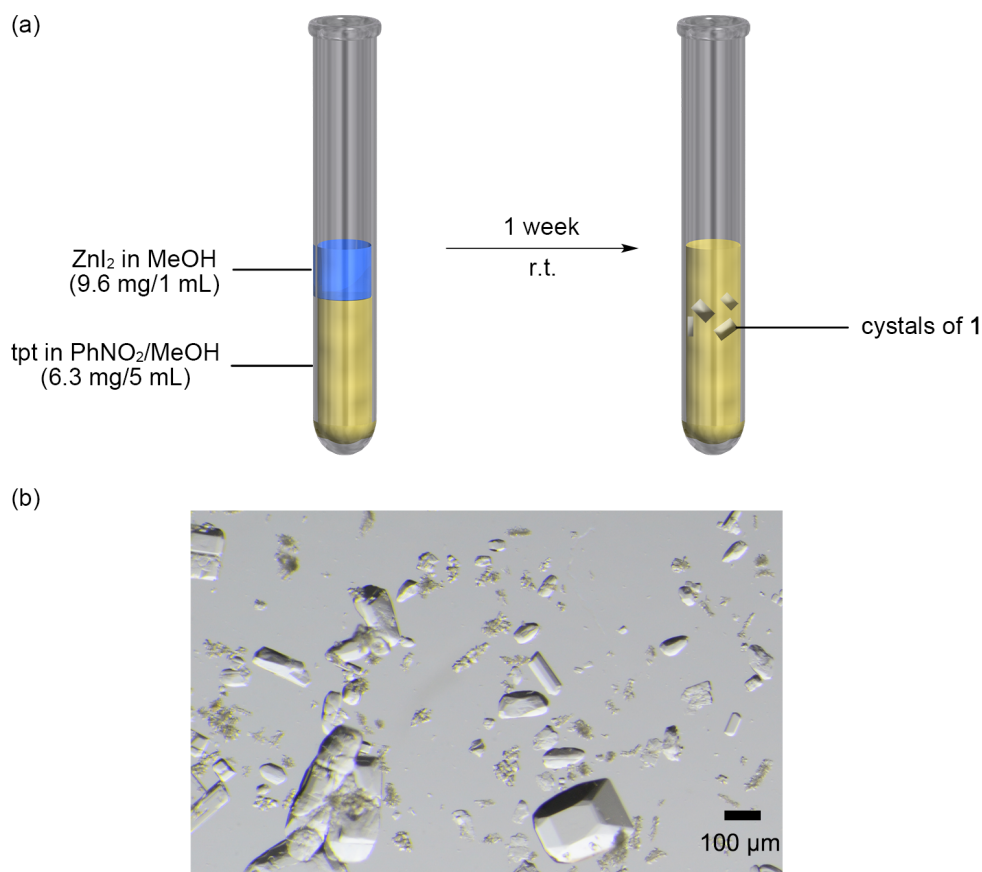
Solvents and reagents were purchased from TCI Co., Ltd., WAKO Pure Chemical Industries Ltd., and Sigma-Aldrich Corporation and used without further purification.  $^1\text{H}$  NMR spectra were recorded on a Bruker AVANCE III HD 500 MHz spectrometer equipped with 5 mm BBO gradient probe and a Bruker AVANCE 500 MHz spectrometer equipped with TCI gradient CryoProbe. All NMR spectra data were recorded at 300 K and chemical shift values are reported in parts per million (ppm) relative to an internal standard tetramethylsilane. Microscopic FT-IR spectra were recorded on a Varian DIGILAB Scimitar instrument and are reported in frequency of absorption ( $\text{cm}^{-1}$ ). Single crystal X-ray diffraction data were collected on a BRUKER APEX-II CCD diffractometer equipped with a focusing mirror ( $\text{MoK}_\alpha$  radiation  $\lambda = 0.71073 \text{ \AA}$ ) and a  $\text{N}_2$  generator (Japan Thermal Eng. Co., Ltd.) or Rigaku XtaLAB P200 diffractometer equipped with a PILATUS-200K detector with multi-layer mirror monochromater ( $\text{MoK}_\alpha$  radiation  $\lambda = 0.71073 \text{ \AA}$ ). For single crystal X-ray diffraction analysis and microscopic IR measurement, fluorolube® and mineral oil were used as a protectant for the single crystals. Thermogravimetric analyses were carried out with a NETZSCH STA 409 PG/T Luxx equipped with a QMS 403C/T under  $\text{N}_2$  gas flow (30 ml/min) at a heating rate 5 K/min.

### X-ray crystallographic analysis

Single crystal X-ray diffraction data were processed with Bruker APEX2 software and CrystalClear program.<sup>20,21</sup> For Bruker data, absorption correction was performed by multi-scan method in SADABS and space groups were determined by XPREP program.<sup>1</sup> The structures were solved by direct methods and refined by full-matrix least-squares calculations on  $F^2$  using SHELXL-97 program.<sup>22</sup> In the determination of space group, the XPREP program suggested space group was employed for analyzing the structure.

When vanillin and dimethyl cubane-1,4-dicarboxylic acid dimethyl ester were included into the crystalline sponge **5**, initial space group  $C2/c$  was changed to the triclinic  $P\bar{1}$ . After the initial phase determination, all the atoms for the host framework (*i.e.*  $ZnI_2$  and tpt ligands) were assigned and the structure was refined anisotropically except for hydrogen atoms. Since the host framework was in some cases highly disordered, atoms were partially restrained with DFIX, FLAT, SIMU and ISOR commands. Atoms for the guest molecules (including solvent molecules) were then assigned to the residual Q-peaks. The guest structures were first refined isotropically with a suitable occupancy that was estimated by refinement using FVAR. If available, the guest structures were subsequently refined anisotropically. The final crystal structures leave large solvent-accessible voids where only weak Q-peaks were observed because that solvent or guest molecules were highly disordered. Such Q-peaks have been treated with PLATON SQUEEZE program, resulting in reasonable  $R_1$  and  $wR_2$  values as compared with  $R_{int}$ .<sup>23</sup> Note that due to the minor disorder with solvent molecules, the X-ray data quality of crystalline sponge method was rather lower than conventional single crystal X-ray analysis for small molecules using their pure single crystals.

### Synthesis of the porous complex **1**



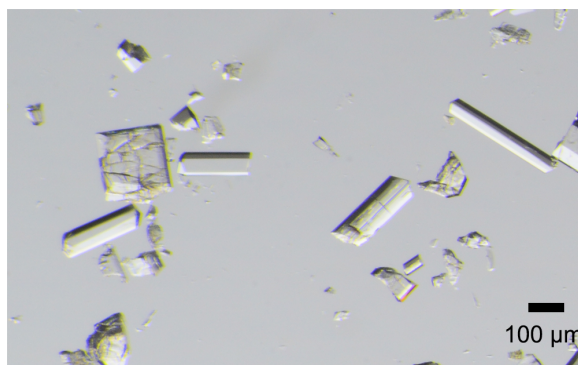
**Figure S2.1.** (a) A schematic illustration of the synthesis of porous complex **1** by layer diffusion method. (b) A photograph of as synthesized porous complex **1**.

Onto a solution of 2,4,6-tri(4-pyridyl)-1,3,5-triazine (**2**) (6.3 mg, 0.02 mmol) in nitrobenzene (4.0 mL) and methanol (1.0 mL), was slowly layered a  $\text{ZnI}_2$  (9.6 mg, 0.03 mmol) solution in methanol (1.0 mL). The solution was allowed to stand for 1 week at ambient temperature. After 1 week, colorless crystals were furnished on the wall of the test tube. Resulting colorless crystals were collected by scratching off from the wall of test tube by spatula. Elemental analysis (%); Found: C 36.85, H 2.49, N 10.63; Calcd: C 36.68, H 2.30, N 10.85 for  $\{[(\text{ZnI}_2)_6(\mathbf{2})_4] \cdot (\text{C}_6\text{H}_5\text{NO}_2)_{11}\}_n$

#### Solvent exchange of the porous complex **1** by cyclohexane

As synthesized crystals **1** (~50 mg) were washed with fresh nitrobenzene (5 mL  $\times$  3 times) and cyclohexane (10 mL  $\times$  3 times). The crystals were immersed in

cyclohexane (10 mL) and incubated at 50 °C for 1 week. During the incubation, solvent cyclohexane was replaced to the fresh cyclohexane every day.



**Figure S2.2.** A photograph of porous complex **1** after solvent exchange to cyclohexane.

#### Elemental analysis of solvent exchanged crystalline sponge **5**

- Crystalline sponge **5** swellheaded by cyclohexane

The crystalline sponge **5** stored in cyclohexane was collected by filtration. The collected crystals were immediately subjected to the elemental analysis within 1 min.

Elemental analysis (%); Found: C 41.34, H 4.62, N 7.97; Calcd: C 41.43, H 4.64, N 8.05 for  $\{[(\text{ZnI}_2)_3(\mathbf{2})_2] \cdot (\text{C}_6\text{H}_{12})_6\}_n$

- Crystalline sponge **5** after removing the excess cyclohexane

The crystalline sponge **5** stored in cyclohexane was collected by filtration. The collected crystals were placed in a microvial with pinhole and stored for 30 min at room temperature. After 30 min, resultant crystals were subjected to the elemental analysis.

Elemental analysis (%); Found: C 37.67, H 3.53, N 8.75; Calcd: C 37.56, H 3.78, N 8.76 for  $\{[(\text{ZnI}_2)_3(\mathbf{2})_2] \cdot (\text{C}_6\text{H}_{12})_4\}_n$

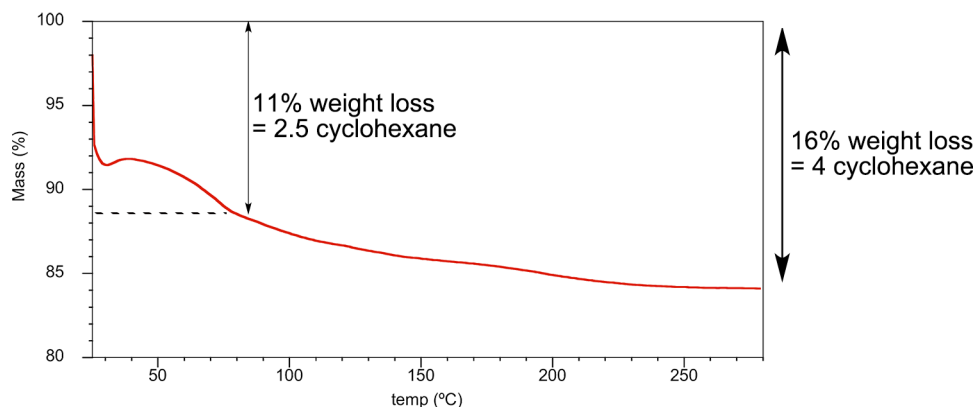
- Crystalline sponge **5** after drying in vacuo

The crystalline sponge **5** stored in cyclohexane was collected by filtration. The collected crystals were placed in a round bottom flask and dried in vacuo (0.1 Torr) for 30 min at room temperature. After 30 min, resultant crystals were subjected to the elemental analysis.

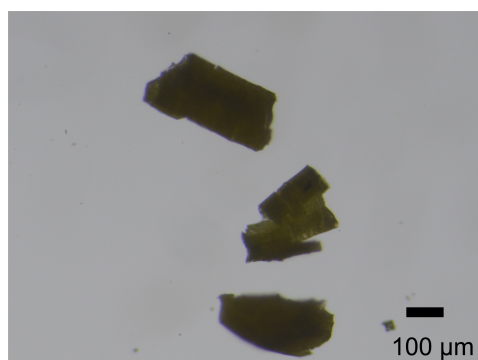
Elemental analysis (%); Found: C 31.48, H 2.23, N 9.90; Calcd: C 31.64, H 2.48, N 9.84 for  $\{[(\text{ZnI}_2)_3(\mathbf{2})_2] \cdot (\text{C}_6\text{H}_{12})_{1.5}\}_n$

**Thermogravimetric (TG) analysis of crystalline sponge 5**

The crystalline sponge **5** stored in cyclohexane was collected by filtration and immediately subjected to the TG analysis. The TG spectrum showed 11% weight loss below 80 °C, which is a boiling point of cyclohexane and totally 16% weight loss until 300 °C. The 11% weight loss was equal to the loss of 2.5 molecules of cyclohexane from  $\{[(\text{ZnI}_2)_3(\mathbf{2})_2] \cdot 4(\text{C}_6\text{H}_{12})\}_n$  and the 16% weight loss was equal to the loss of 4 molecules of cyclohexane. The 5% weight loss during 80-300 °C corresponded to the loss of 1.5 cyclohexane molecules. This data was also corresponded to the elemental analysis result that the crystalline sponge **5** still included 1.5 cyclohexane molecules even after drying in vacuo. Despite the several attempts, TG analysis didn't afford the weight loss corresponded to the  $\{[(\text{ZnI}_2)_3(\mathbf{2})_2] \cdot 6(\text{C}_6\text{H}_{12})\}_n$  structure *i.e.* the loss of the 6 cyclohexane molecules (24 wt%). Since the preparation of the measurement was performed under the nitrogen flow, the excess 2 cyclohexane molecules, which were most weakly bound in swellheaded  $\{[(\text{ZnI}_2)_3(\mathbf{2})_2] \cdot 6(\text{C}_6\text{H}_{12})\}_n$  structure might be evaporated before running the TG measurement.



**Figure S2.3.** TG spectrum of the crystalline sponge **5**.



**Figure S2.4.** A photo of the solvent evaporated crystalline sponges at 90°C. The transparency and crystallinity were totally deteriorated.

### **Guest inclusion into porous complex 1 and crystalline sponge 5**

#### **Inclusion of isoprene into as synthesized crystalline sponge 1**

To a micro vial containing a piece of as synthesized crystalline sponge **1**, was added a drop of isoprene (a few  $\mu\text{L}$ ). The vial was tightly capped with a screw cap and allowed to stand for 2 d at room temperature.

#### **General procedure for inclusion of guest molecules into crystalline sponge 5**

To a micro vial containing a cyclohexane exchanged single crystal of  $[(\text{ZnI}_2)_3(\text{tpt})_2]_n$  (**5**; tpt = tri(4-pyridyl)-1,3,5-triazine) and cyclohexane (45  $\mu\text{L}$ ), 5  $\mu\text{L}$  of dichloromethane solution of target compounds (1 mg/1 mL) was added. Then, the crystal containing microvial was allowed to stand at 45 °C and the solvent was gradually evaporated over 2 d.

**Crystallographic data****As synthesized complex 1**

Crystallographic data:  $C_{72}H_{48}N_{24}Zn_6I_{12} \cdot 10(C_6H_5NO_2)$ ,  $M = 4395.46$ , colorless rod,  $0.2 \times 0.2 \times 0.2 \text{ mm}^3$ , monoclinic, space group  $P2_1/a$ ,  $a = 30.177(2)$ ,  $b = 15.0724(10)$ ,  $c = 35.112(2) \text{ \AA}$ ,  $\beta = 101.952(3)^\circ$ ,  $V = 15624.1(17) \text{ \AA}^3$ ,  $Z = 4$ ,  $D_c = 1.869 \text{ g/cm}^3$ ,  $F000 = 8416$ ,  $\mu = 3.349 \text{ mm}^{-1}$ ,  $T = 93(2) \text{ K}$ ,  $1.380 < \theta < 25.342^\circ$ , 22657 unique reflections out of 28270 with  $I > 2\sigma(I)$ ,  $R_{\text{int}} = 0.1055$ , 1837 parameters, 0 restraints, GoF = 1.248, final  $R$  factors  $R_1 = 0.0681$  and  $wR_2 = 0.2001$  for all data. CCDC deposit number: unpublished result.

IR (single crystal, fluorolube): 1616, 1576, 1519, 1421, 1373, 1344, 1314, 1057, 1022  $\text{cm}^{-1}$ .

**As synthesized complex 1 soaked in 4**

Crystallographic data:  $C_{36}H_{24}N_{12}Zn_3I_6 \cdot 0.76(C_6H_5NO_2)$ ,  $M = 1675.74$ , colorless rod,  $0.1 \times 0.08 \times 0.08 \text{ mm}^3$ , monoclinic, space group  $C2/c$ ,  $a = 35.054(2)$ ,  $b = 15.0141(10)$ ,  $c = 30.458(2) \text{ \AA}$ ,  $\beta = 102.169(3)^\circ$ ,  $V = 15670.0(17) \text{ \AA}^3$ ,  $Z = 8$ ,  $D_c = 1.421 \text{ g/cm}^3$ ,  $F000 = 6245$ ,  $\mu = 3.305 \text{ mm}^{-1}$ ,  $T = 93(2) \text{ K}$ ,  $1.189 < \theta < 25.368^\circ$ , 7243 unique reflections out of 14330 with  $I > 2\sigma(I)$ ,  $R_{\text{int}} = 0.1118$ , 558 parameters, 6 restraints, GoF = 1.032, final  $R$  factors  $R_1 = 0.0989$  and  $wR_2 = 0.3305$  for all data. CCDC deposit number: unpublished result.

**Inclusion complex 5•4**

Crystallographic data (before the SQUEEZE treatment):  $C_{36}H_{24}N_{12}Zn_3I_6 \cdot 1.97(C_5H_8)$ ,  $M = 1715.64$ , colorless rod,  $0.08 \times 0.05 \times 0.05 \text{ mm}^3$ , monoclinic space group  $C2/c$ ,  $a = 35.060(4)$ ,  $b = 14.7672(16)$ ,  $c = 30.527(3) \text{ \AA}$ ,  $\beta = 101.0880(10)^\circ$ ,  $V = 15510(3) \text{ \AA}^3$ ,  $Z = 8$ ,  $D_c = 1.390 \text{ g/cm}^3$ ,  $F000 = 6035$ ,  $\mu = 3.335 \text{ mm}^{-1}$ ,  $T = 90(2) \text{ K}$ ,  $1.36 < \theta < 26.53^\circ$ , 10929 unique reflections out of 16083 with  $I > 2\sigma(I)$ ,  $R_{\text{int}} = 0.0449$ , 628 parameters, 19 restraints, GoF = 1.085, final  $R$  factors  $R_1 = 0.0661$  and  $wR_2 = 0.2402$  for all data. CCDC deposit number: unpublished result.

IR (single crystal, fluorolube): 3084, 3055, 2970, 2926, 2851, 1595, 1510, 1424  $\text{cm}^{-1}$ .



**Inclusion complex 5•6 (500 ng scale inclusion)**

Crystallographic data (before the SQUEEZE treatment):  $C_{36}H_{24}N_{12}Zn_3I_6 \cdot 0.6(C_{15}H_{18})$ ,  $M = 1701.16$ , colorless rod,  $0.07 \times 0.06 \times 0.06 \text{ mm}^3$ , monoclinic, space group  $C2/c$ ,  $a = 34.644(4)$ ,  $b = 14.879(3)$ ,  $c = 30.836(6) \text{ \AA}$ ,  $\beta = 101.787(2)^\circ$ ,  $V = 15560(5) \text{ \AA}^3$ ,  $Z = 8$ ,  $D_c = 1.452 \text{ g/cm}^3$ ,  $F000 = 6418$ ,  $\mu = 3.329 \text{ mm}^{-1}$ ,  $T = 90(2) \text{ K}$ ,  $1.20 < \theta < 26.39^\circ$ , 8293 unique reflections out of 15819 with  $I > 2\sigma(I)$ ,  $R_{\text{int}} = 0.0524$ , 649 parameters, 72 restraints,  $\text{GoF} = 1.468$ , final  $R$  factors  $R_1 = 0.1236$  and  $wR_2 = 0.4323$  for all data. CCDC deposit number: unpublished result.

Crystallographic data (after the SQUEEZE treatment):  $C_{36}H_{24}N_{12}Zn_3I_6 \cdot 0.6(C_{15}H_{18})$ ,  $M = 1701.16$ , colorless rod,  $0.07 \times 0.06 \times 0.06 \text{ mm}^3$ , monoclinic, space group  $C2/c$ ,  $a = 34.644(4)$ ,  $b = 14.879(3)$ ,  $c = 30.836(6) \text{ \AA}$ ,  $\beta = 101.787(2)^\circ$ ,  $V = 15560(5) \text{ \AA}^3$ ,  $Z = 8$ ,  $D_c = 1.452 \text{ g/cm}^3$ ,  $F000 = 6374$ ,  $\mu = 3.328 \text{ mm}^{-1}$ ,  $T = 90(2) \text{ K}$ ,  $1.20 < \theta < 26.39^\circ$ , 7948 unique reflections out of 15819 with  $I > 2\sigma(I)$ ,  $R_{\text{int}} = 0.0424$ , 649 parameters, 75 restraints,  $\text{GoF} = 1.097$ , final  $R$  factors  $R_1 = 0.0859$  and  $wR_2 = 0.3021$  for all data. CCDC deposit number: 910382.

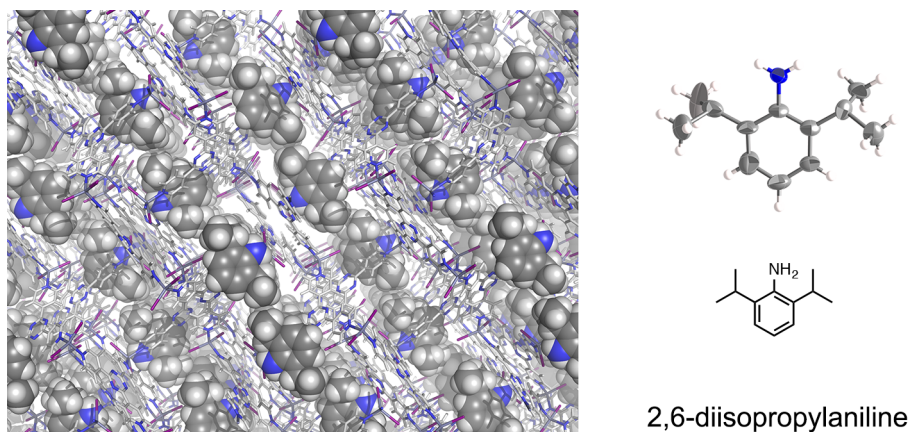
IR (single crystal, fluorolube): 3098, 3054, 2924, 2856, 1514, 1464, 1425, 1369  $\text{cm}^{-1}$ .

**2,6-diisopropylaniline inclusion crystalline sponge 5**

Crystallographic data (before the SQUEEZE treatment):  $C_{36}H_{24}N_{12}Zn_3I_6 \cdot 0.76(C_{12}H_{19}N)$ ,  $M = 1716.27$ , brown rod,  $0.06 \times 0.05 \times 0.04 \text{ mm}^3$ , monoclinic, space group  $C2/c$ ,  $a = 35.752(9)$ ,  $b = 14.774(4)$ ,  $c = 30.594(10) \text{ \AA}$ ,  $\beta = 101.647^\circ$ ,  $V = 15828(7) \text{ \AA}^3$ ,  $Z = 8$ ,  $D_c = 1.441 \text{ g/cm}^3$ ,  $F000 = 6317$ ,  $\mu = 3.273 \text{ mm}^{-1}$ ,  $T = 90(2) \text{ K}$ ,  $2.22 < \theta < 26.37^\circ$ , 12305 unique reflections out of 16106 with  $I > 2\sigma(I)$ ,  $R_{\text{int}} = 0.0422$ , 632 parameters, 182 restraints,  $\text{GoF} = 1.410$ , final  $R$  factors  $R_1 = 0.1550$  and  $wR_2 = 0.5006$  for all data. CCDC deposit number: unpublished data.

Crystallographic data (after the SQUEEZE treatment):  $C_{36}H_{24}N_{12}Zn_3I_6 \cdot 0.76(C_{12}H_{19}N)$ ,  $M = 1716.27$ , brown rod,  $0.06 \times 0.05 \times 0.04 \text{ mm}^3$ , monoclinic, space group  $C2/c$ ,  $a = 35.752(9)$ ,  $b = 14.774(4)$ ,  $c = 30.594(10) \text{ \AA}$ ,  $\beta = 101.647^\circ$ ,  $V = 15828(7) \text{ \AA}^3$ ,  $Z = 8$ ,  $D_c = 1.441 \text{ g/cm}^3$ ,  $F000 = 6452$ ,  $\mu = 3.273 \text{ mm}^{-1}$ ,  $T = 90(2) \text{ K}$ ,  $2.22 < \theta < 26.37^\circ$ , 11927 unique reflections out of 16106 with  $I > 2\sigma(I)$ ,  $R_{\text{int}} = 0.0459$ , 632 parameters, 182 restraints,  $\text{GoF} = 1.410$ , final  $R$  factors  $R_1 = 0.1182$  and  $wR_2 = 0.3520$  for all data. CCDC deposit number: 910385.

IR (single crystal, fluorolube): 3091, 3051, 2955, 2867, 1617, 1513, 1457, 1440, 1377  $\text{cm}^{-1}$ .



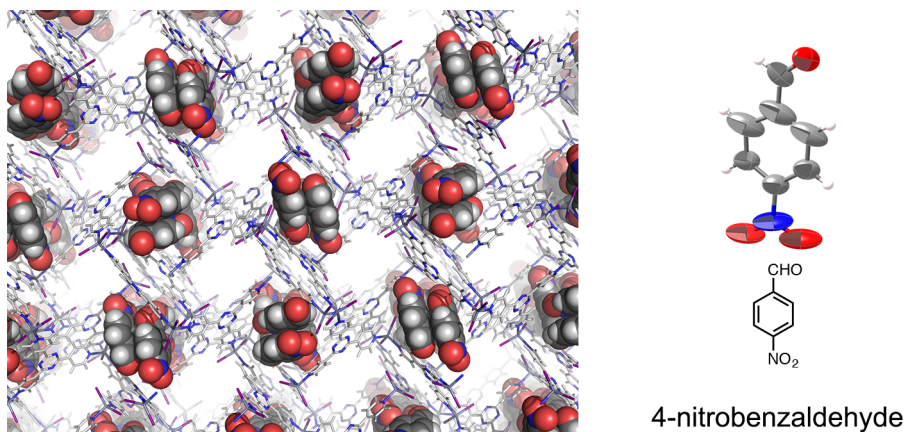
**Figure S2.5.** The X-ray crystal structure of 2,6-diisopropylaniline inclusion crystalline sponge 5. Guest molecules were drawn in CPK model in the packing structure and the thermal ellipsoid of the guest molecule was drawn at the 50% probability level.

**4-Nitrobenzaldehyde inclusion crystalline sponge 5**

Crystallographic data (before the SQUEEZE treatment):  $C_{36}H_{24}N_{12}Zn_3I_6 \cdot (C_7H_5NO_3)$ ,  $M = 1733.30$ , colorless rod,  $0.07 \times 0.06 \times 0.05 \text{ mm}^3$ , monoclinic, space group  $C2/c$ ,  $a = 35.602(11)$ ,  $b = 14.879(5)$ ,  $c = 30.538(10) \text{ \AA}$ ,  $\beta = 103.153^\circ$ ,  $V = 15752 \text{ \AA}^3$ ,  $Z = 8$ ,  $D_c = 1.462 \text{ g/cm}^3$ ,  $F000 = 6480$ ,  $\mu = 3.292 \text{ mm}^{-1}$ ,  $T = 90(2) \text{ K}$ ,  $2.21 < \theta < 23.25^\circ$ , 8514 unique reflections out of 13831 with  $I > 2\sigma(I)$ ,  $R_{\text{int}} = 0.0700$ , 713 parameters, 104 restraints,  $\text{GoF} = 1.217$ , final  $R$  factors  $R_1 = 0.1363$  and  $wR_2 = 0.4717$  for all data. CCDC deposit number: unpublished data.

Crystallographic data (after the SQUEEZE treatment):  $C_{36}H_{24}N_{12}Zn_3I_6 \cdot (C_7H_5NO_3)$ ,  $M = 1733.30$ , colorless rod,  $0.07 \times 0.06 \times 0.05 \text{ mm}^3$ , monoclinic, space group  $C2/c$ ,  $a = 35.602(11)$ ,  $b = 14.879(5)$ ,  $c = 30.538(10) \text{ \AA}$ ,  $\beta = 103.153^\circ$ ,  $V = 15752 \text{ \AA}^3$ ,  $Z = 8$ ,  $D_c = 1.462 \text{ g/cm}^3$ ,  $F000 = 6480$ ,  $\mu = 3.292 \text{ mm}^{-1}$ ,  $T = 90(2) \text{ K}$ ,  $2.21 < \theta < 23.25^\circ$ , 8514 unique reflections out of 13831 with  $I > 2\sigma(I)$ ,  $R_{\text{int}} = 0.0700$ , 713 parameters, 104 restraints,  $\text{GoF} = 1.217$ , final  $R$  factors  $R_1 = 0.1130$  and  $wR_2 = 0.3380$  for all data. CCDC deposit number: 910384.

IR (single crystal, fluorolube): 3101, 3068, 3056, 2923, 2851, 1703, 1524, 1377, 1340  $\text{cm}^{-1}$ .



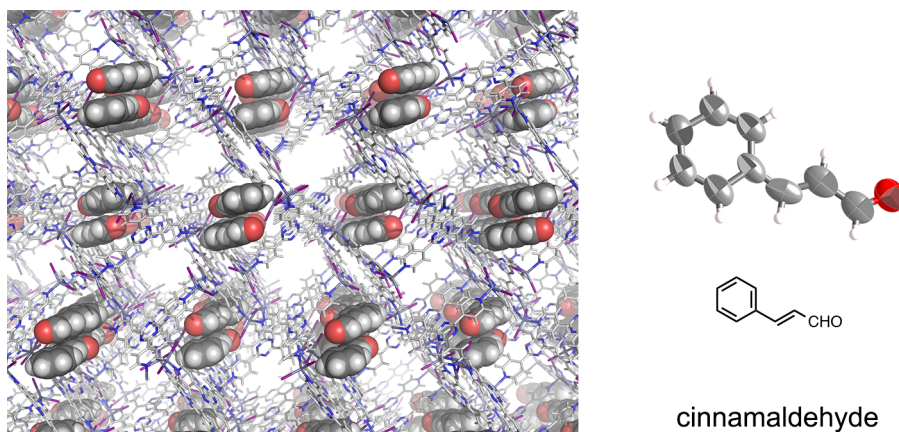
**Figure S2.6.** The X-ray crystal structure of 4-nitrobenzaldehyde inclusion crystalline sponge 5. Guest molecules were drawn in CPK model in the packing structure and the thermal ellipsoid of the guest molecule was drawn at the 50% probability level.

**Cinnamaldehyde inclusion crystalline sponge 5**

Crystallographic data (before the SQUEEZE treatment):  $C_{36}H_{24}N_{12}Zn_3I_6 \cdot 0.5(C_9H_8O)$ ,  $M = 1648.26$ , colorless rod,  $0.17 \times 0.07 \times 0.05 \text{ mm}^3$ , monoclinic, space group  $C2/c$ ,  $a = 34.847(4)$ ,  $b = 14.7560(16)$ ,  $c = 30.740(4) \text{ \AA}$ ,  $\beta = 102.007(2)^\circ$ ,  $V = 15461(3) \text{ \AA}^3$ ,  $Z = 8$ ,  $D_c = 1.416 \text{ g/cm}^3$ ,  $F000 = 6175$ ,  $\mu = 3.347 \text{ mm}^{-1}$ ,  $T = 90(2) \text{ K}$ ,  $1.19 < \theta < 26.00^\circ$ , 10942 unique reflections out of 15196 with  $I > 2\sigma(I)$ ,  $R_{\text{int}} = 0.0602$ , 604 parameters, 95 restraints,  $\text{GoF} = 1.052$ , final  $R$  factors  $R_1 = 0.0954$  and  $wR_2 = 0.3255$  for all data. CCDC deposit number: unpublished data.

Crystallographic data (after the SQUEEZE treatment):  $C_{36}H_{24}N_{12}Zn_3I_6 \cdot 0.5(C_9H_8O)$ ,  $M = 1648.26$ , colorless rod,  $0.17 \times 0.07 \times 0.05 \text{ mm}^3$ , monoclinic, space group  $C2/c$ ,  $a = 34.847(4)$ ,  $b = 14.7560(16)$ ,  $c = 30.740(4) \text{ \AA}$ ,  $\beta = 102.007(2)^\circ$ ,  $V = 15461(3) \text{ \AA}^3$ ,  $Z = 8$ ,  $D_c = 1.416 \text{ g/cm}^3$ ,  $F000 = 6136$ ,  $\mu = 3.347 \text{ mm}^{-1}$ ,  $T = 90(2) \text{ K}$ ,  $1.19 < \theta < 26.00^\circ$ , 10901 unique reflections out of 15196 with  $I > 2\sigma(I)$ ,  $R_{\text{int}} = 0.0558$ , 604 parameters, 45 restraints,  $\text{GoF} = 1.173$ , final  $R$  factors  $R_1 = 0.0750$  and  $wR_2 = 0.2631$  for all data. CCDC deposit number: 910386.

IR (single crystal, fluorolube): 3091, 3051, 2955, 2867, 1617, 1513, 1457, 1440, 1377  $\text{cm}^{-1}$ .



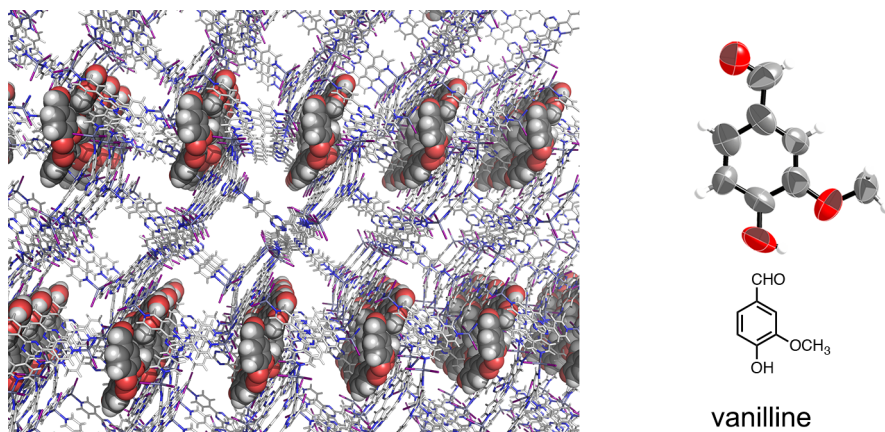
**Figure S2.7.** The X-ray crystal structure of cinnamaldehyde inclusion crystalline sponge 5. Guest molecules were drawn in CPK model in the packing structure and the thermal ellipsoid of the guest molecule was drawn at the 50% probability level.

**Vanillin inclusion crystalline sponge 5**

Crystallographic data (before the SQUEEZE treatment):  $C_{72}H_{48}N_{24}Zn_6I_{12} \cdot 2(C_8H_8O_3)$ ,  $M = 3468.65$ , yellow rod,  $0.10 \times 0.08 \times 0.05 \text{ mm}^3$ , triclinic, space group  $P\bar{1}$ ,  $a = 14.907(5)$ ,  $b = 18.608(6)$ ,  $c = 32.920(11) \text{ \AA}$ ,  $\alpha = 103.269(4)^\circ$ ,  $\beta = 93.089(4)^\circ$ ,  $\gamma = 108.970(4)^\circ$ ,  $V = 8323(5) \text{ \AA}^3$ ,  $Z = 2$ ,  $D_c = 1.384 \text{ g/cm}^3$ ,  $F000 = 3248$ ,  $\mu = 3.115 \text{ mm}^{-1}$ ,  $T = 90(2) \text{ K}$ ,  $0.64 < \theta < 25.00^\circ$ , 16584 unique reflections out of 28540 with  $I > 2\sigma(I)$ ,  $R_{\text{int}} = 0.0555$ , 1227 parameters, 171 restraints,  $\text{GoF} = 2.017$ , final  $R$  factors  $R_1 = 0.1654$  and  $wR_2 = 0.5334$  for all data. CCDC deposit number: unpublished data.

Crystallographic data (after the SQUEEZE treatment):  $C_{72}H_{48}N_{24}Zn_6I_{12} \cdot 2(C_8H_8O_3)$ ,  $M = 3468.65$  yellow rod,  $0.10 \times 0.08 \times 0.05 \text{ mm}^3$ , triclinic, space group  $P\bar{1}$ ,  $a = 14.907(5)$ ,  $b = 18.608(6)$ ,  $c = 32.920(11) \text{ \AA}$ ,  $\alpha = 103.269(4)^\circ$ ,  $\beta = 93.089(4)^\circ$ ,  $\gamma = 108.970(4)^\circ$ ,  $V = 8323(5) \text{ \AA}^3$ ,  $Z = 2$ ,  $D_c = 1.384 \text{ g/cm}^3$ ,  $F000 = 3248$ ,  $\mu = 3.115 \text{ mm}^{-1}$ ,  $T = 90(2) \text{ K}$ ,  $0.64 < \theta < 25.00^\circ$ , 16584 unique reflections out of 28540 with  $I > 2\sigma(I)$ ,  $R_{\text{int}} = 0.0555$ , 1227 parameters, 171 restraints,  $\text{GoF} = 1.158$ , final  $R$  factors  $R_1 = 0.1103$  and  $wR_2 = 0.3402$  for all data. CCDC deposit number: 910387.

IR (single crystal, fluorolube): 3410, 3099, 3058, 1686, 1613, 1590, 1518, 1428, 1376  $\text{cm}^{-1}$ .



**Figure S2.8.** The X-ray crystal structure of vanilline inclusion crystalline sponge 5. Guest molecules were drawn in CPK model in the packing structure and the thermal ellipsoid of the guest molecule was drawn at the 50% probability level.

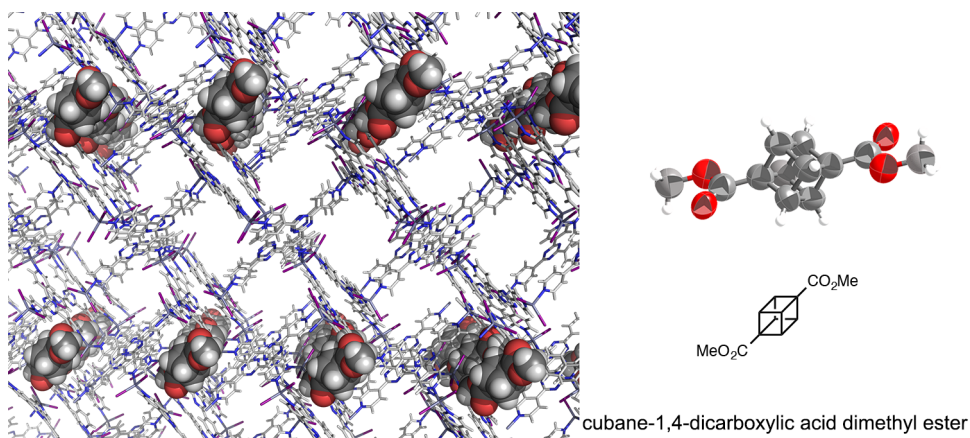


**Cubane-1,4-dicarboxylic acid dimethyl ester inclusion crystalline sponge 5**

Crystallographic data (before the SQUEEZE treatment):  $C_{72}H_{48}N_{24}Zn_6I_{12} \cdot 0.7(C_6H_6O_2)$ ,  $M = 3241.44$ , colorless rod,  $0.14 \times 0.04 \times 0.04 \text{ mm}^3$ , triclinic, space group  $P\bar{1}$ ,  $a = 14.952(9)$ ,  $b = 18.584(11)$ ,  $c = 32.756(19) \text{ \AA}$ ,  $\alpha = 104.933(8)^\circ$ ,  $\beta = 102.349(7)^\circ$ ,  $\gamma = 111.615(8)^\circ$ ,  $V = 7678(8) \text{ \AA}^3$ ,  $Z = 2$ ,  $D_c = 1.402 \text{ g/cm}^3$ ,  $F_{000} = 2975$ ,  $\mu = 3.369 \text{ mm}^{-1}$ ,  $T = 90(2) \text{ K}$ ,  $0.69 < \theta < 25.00^\circ$ , 8761 unique reflections out of 26911 with  $I > 2\sigma(I)$ ,  $R_{\text{int}} = 0.1690$ , 1099 parameters, 826 restraints,  $\text{GoF} = 1.588$ , final  $R$  factors  $R_1 = 0.2042$  and  $wR_2 = 0.5784$  for all data. CCDC deposit number: unpublished data.

Crystallographic data (after the SQUEEZE treatment):  $C_{72}H_{48}N_{24}Zn_6I_{12} \cdot 0.7(C_6H_6O_2)$ ,  $M = 3241.44$ , colorless rod,  $0.14 \times 0.04 \times 0.04 \text{ mm}^3$ , triclinic, space group  $P\bar{1}$ ,  $a = 14.952(9)$ ,  $b = 18.584(11)$ ,  $c = 32.756(19) \text{ \AA}$ ,  $\alpha = 104.933(8)^\circ$ ,  $\beta = 102.349(7)^\circ$ ,  $\gamma = 111.615(8)^\circ$ ,  $V = 7678(8) \text{ \AA}^3$ ,  $Z = 2$ ,  $D_c = 1.402 \text{ g/cm}^3$ ,  $F_{000} = 3009$ ,  $\mu = 3.369 \text{ mm}^{-1}$ ,  $T = 90(2) \text{ K}$ ,  $0.69 < \theta < 25.00^\circ$ , 8761 unique reflections out of 26911 with  $I > 2\sigma(I)$ ,  $R_{\text{int}} = 0.1216$ , 1099 parameters, 295 restraints,  $\text{GoF} = 0.940$ , final  $R$  factors  $R_1 = 0.1345$  and  $wR_2 = 0.3775$  for all data. CCDC deposit number: 910389.

IR (single crystal, fluorolube): 3099, 3052, 2929, 2850, 1710, 1516, 1376  $\text{cm}^{-1}$ .



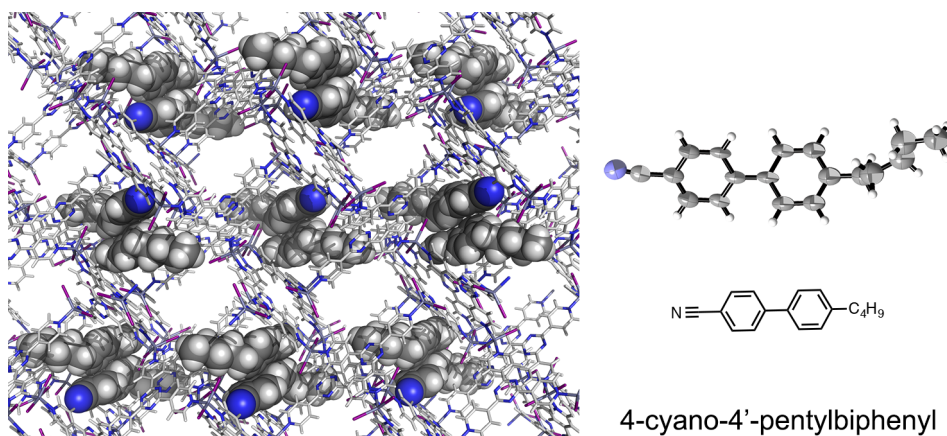
**Figure S2.9.** The X-ray crystal structure of cubane-1,4-dicarboxylic acid dimethyl ester inclusion crystalline sponge **5**. Guest molecules were drawn in CPK model in the packing structure and the thermal ellipsoid of the guest molecule was drawn at the 50% probability level.

**4-Cyano-4'-pentylbiphenyl inclusion crystalline sponge 5**

Crystallographic data (before the SQUEEZE treatment):  $C_{36}H_{24}N_{12}Zn_3I_6 \cdot 0.53(C_{18}H_{19}N) \cdot 0.47(C_6H_{12})$ ,  $M = 1754.49$ , colorless rod,  $0.15 \times 0.05 \times 0.04 \text{ mm}^3$ , monoclinic, space group  $C2/c$ ,  $a = 35.80(5)$ ,  $b = 14.64(2)$ ,  $c = 31.25(4) \text{ \AA}$ ,  $\beta = 103.064(12)^\circ$ ,  $V = 15958(40) \text{ \AA}^3$ ,  $Z = 8$ ,  $D_c = 1.461 \text{ g/cm}^3$ ,  $F000 = 6607$ ,  $\mu = 3.248 \text{ mm}^{-1}$ ,  $T = 90(2) \text{ K}$ ,  $1.168 < \theta < 26.407^\circ$ , 13293 unique reflections out of 16343 with  $I > 2\sigma(I)$ ,  $R_{\text{int}} = 0.0315$ , 705 parameters, 294 restraints,  $\text{GoF} = 1.113$ , final  $R$  factors  $R_1 = 0.0658$  and  $wR_2 = 0.2218$  for all data. CCDC deposit number: unpublished data.

Crystallographic data (after the SQUEEZE treatment):  $C_{36}H_{24}N_{12}Zn_3I_6 \cdot 0.53(C_{18}H_{19}N) \cdot 0.47(C_6H_{12})$ ,  $M = 1754.49$ , colorless rod,  $0.15 \times 0.05 \times 0.04 \text{ mm}^3$ , monoclinic, space group  $C2/c$ ,  $a = 35.80(5)$ ,  $b = 14.64(2)$ ,  $c = 31.25(4) \text{ \AA}$ ,  $\beta = 103.064(12)^\circ$ ,  $V = 15958(40) \text{ \AA}^3$ ,  $Z = 8$ ,  $D_c = 1.461 \text{ g/cm}^3$ ,  $F000 = 6607$ ,  $\mu = 3.248 \text{ mm}^{-1}$ ,  $T = 90(2) \text{ K}$ ,  $1.168 < \theta < 26.407^\circ$ , 13168 unique reflections out of 16343 with  $I > 2\sigma(I)$ ,  $R_{\text{int}} = 0.0315$ , 705 parameters, 294 restraints,  $\text{GoF} = 1.062$ , final  $R$  factors  $R_1 = 0.0486$  and  $wR_2 = 0.1510$  for all data. CCDC deposit number: unpublished data.

IR (single crystal, fluorolube): 3097, 3053, 2923, 2846, 1515, 1448, 1378  $\text{cm}^{-1}$ .



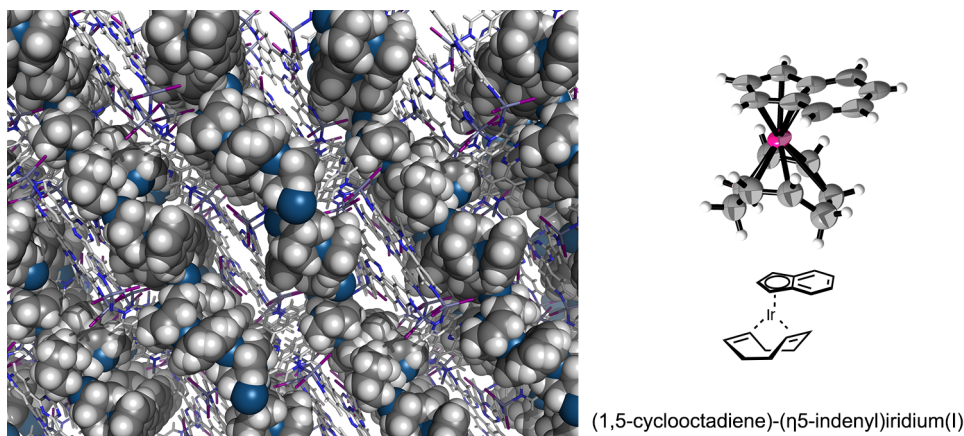
**Figure S2.10.** The X-ray crystal structure of 4-cyano-4'-pentylbiphenyl inclusion crystalline sponge **5**. Guest molecules were drawn in CPK model in the packing structure and the thermal ellipsoid of the guest molecule was drawn at the 30% probability level.

**(1,5-Cyclooctadiene)-(η<sup>5</sup>-indenyl)iridium(I) inclusion crystalline sponge 5**

Crystallographic data (before the SQUEEZE treatment): C<sub>123.46</sub>H<sub>109.68</sub>N<sub>24</sub>Zn<sub>6</sub>I<sub>12</sub>Ir<sub>3.76</sub>, *M* = 4567.11, red, 0.14 × 0.09 × 0.06 mm<sup>3</sup>, triclinic, space group *P* $\bar{1}$ , *a* = 14.734(4), *b* = 19.318(6), *c* = 30.550(9) Å, α = 101.017(4)°, β = 90.059(4)°, γ = 112.370(3)°, *V* = 7867(4) Å<sup>3</sup>, *Z* = 2, *D*<sub>c</sub> = 1.928 g/cm<sup>3</sup>, *F*<sub>000</sub> = 4248, μ = 6.465 mm<sup>-1</sup>, *T* = 90(2) K, 0.681 < θ < 26.796°, 25600 unique reflections out of 32720 with *I* > 2σ(*I*), *R*<sub>int</sub> = 0.0587, 1700 parameters, 1395 restraints, GoF = 1.089, final *R* factors *R*<sub>1</sub> = 0.2013 and *wR*<sub>2</sub> = 0.4720 for all data. CCDC deposit number: unpublished data.

Crystallographic data (after the SQUEEZE treatment): C<sub>123.46</sub>H<sub>109.68</sub>N<sub>24</sub>Zn<sub>6</sub>I<sub>12</sub>Ir<sub>3.76</sub>, *M* = 4567.11, red, 0.14 × 0.09 × 0.06 mm<sup>3</sup>, triclinic, space group *P* $\bar{1}$ , *a* = 14.734(4), *b* = 19.318(6), *c* = 30.550(9) Å, α = 101.017(4)°, β = 90.059(4)°, γ = 112.370(3)°, *V* = 7867(4) Å<sup>3</sup>, *Z* = 2, *D*<sub>c</sub> = 1.928 g/cm<sup>3</sup>, *F*<sub>000</sub> = 4248, μ = 6.465 mm<sup>-1</sup>, *T* = 90(2) K, 0.681 < θ < 26.796°, 25420 unique reflections out of 32720 with *I* > 2σ(*I*), *R*<sub>int</sub> = 0.0572, 1700 parameters, 1395 restraints, GoF = 1.083, final *R* factors *R*<sub>1</sub> = 0.1790 and *wR*<sub>2</sub> = 0.4577 for all data. CCDC deposit number: unpublished data.

IR (single crystal, fluorolube): 3099, 3052, 2929, 2850, 1710, 1516, 1376 cm<sup>-1</sup>.



**Figure S2.11.** The X-ray crystal structure of (1,5-Cyclooctadiene)-(η<sup>5</sup>-indenyl)iridium(I) inclusion crystalline sponge **5**. Guest molecules were drawn in CPK model in the packing structure and the thermal ellipsoid of the guest molecule was drawn at the 50% probability level.

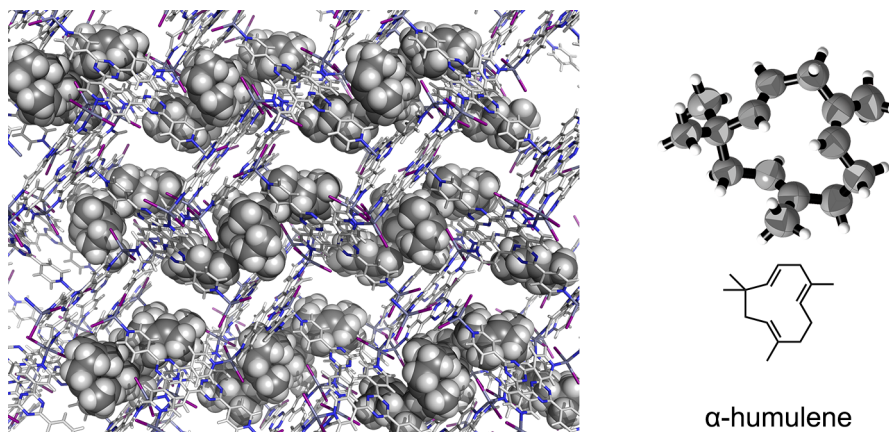


**$\alpha$ -Humulene inclusion crystalline sponge 5**

Crystallographic data (before the SQUEEZE treatment):  $C_{72}H_{48}N_{24}Zn_6I_{12} \cdot 2(C_{15}H_{24}) \cdot 0.5(C_6H_{12})$ ,  $M = 3615.12$ , colorless rod,  $0.15 \times 0.06 \times 0.05$  mm<sup>3</sup>, monoclinic, space group  $Cc$ ,  $a = 34.646(3)$ ,  $b = 14.8889(13)$ ,  $c = 30.571(3)$  Å,  $\beta = 100.9010(10)^\circ$ ,  $V = 15486(2)$  Å<sup>3</sup>,  $Z = 4$ ,  $D_c = 1.551$  g/cm<sup>3</sup>,  $F_{000} = 6864$ ,  $\mu = 3.349$  mm<sup>-1</sup>,  $T = 90(2)$  K,  $1.197 < \theta < 26.516^\circ$ , 22878 unique reflections out of 32052 with  $I > 2\sigma(I)$ ,  $R_{int} = 0.0240$ , 1528 parameters, 1571 restraints, GoF = 1.038, final  $R$  factors  $R_1 = 0.0671$  and  $wR_2 = 0.2379$  for all data. CCDC deposit number: unpublished data.

Crystallographic data (after the SQUEEZE treatment):  $C_{72}H_{48}N_{24}Zn_6I_{12} \cdot 2(C_{15}H_{24}) \cdot 0.5(C_6H_{12})$ ,  $M = 3615.12$ , colorless rod,  $0.15 \times 0.06 \times 0.05$  mm<sup>3</sup>, monoclinic, space group  $Cc$ ,  $a = 34.646(3)$ ,  $b = 14.8889(13)$ ,  $c = 30.571(3)$  Å,  $\beta = 100.9010(10)^\circ$ ,  $V = 15486(2)$  Å<sup>3</sup>,  $Z = 4$ ,  $D_c = 1.551$  g/cm<sup>3</sup>,  $F_{000} = 6864$ ,  $\mu = 3.349$  mm<sup>-1</sup>,  $T = 90(2)$  K,  $1.197 < \theta < 26.516^\circ$ , 22838 unique reflections out of 32052 with  $I > 2\sigma(I)$ ,  $R_{int} = 0.0240$ , 1528 parameters, 1571 restraints, GoF = 1.100, final  $R$  factors  $R_1 = 0.0613$  and  $wR_2 = 0.2102$  for all data. CCDC deposit number: unpublished data.

IR (single crystal, fluorolube): 3097, 3053, 2923, 2846, 1515, 1448, 1378 cm<sup>-1</sup>.



**Figure S2.12.** The X-ray crystal structure of  $\alpha$ -humulene inclusion crystalline sponge 5. Guest molecules were drawn in CPK model in the packing structure and the thermal ellipsoid of the guest molecule was drawn at the 50% probability level.

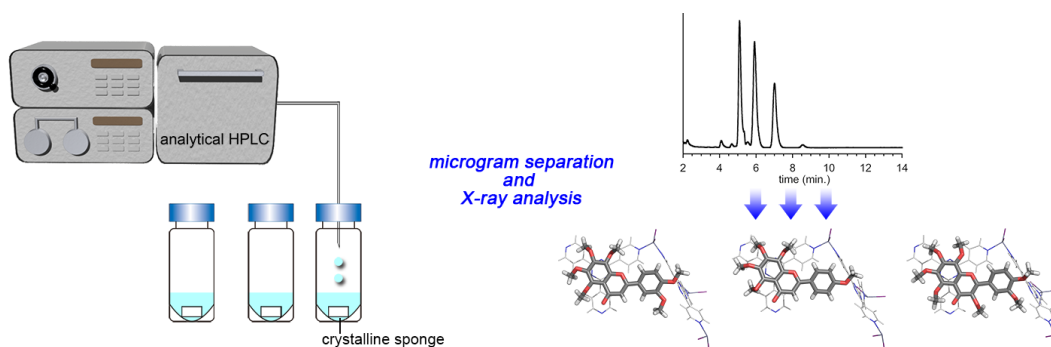
## References

- 1 S. R. Batten, R. Robson, *Angew. Chem. Int. Ed.* **1998**, *37*, 1460–1494.
- 2 O. M. Yaghi, M. O’Keeffe, N. W. Ockwig, H. K. Chae, M. Eddaoudi, J. Kim, *Nature* **2003**, *423*, 705–714.
- 3 S. Kitagawa, R. Kitaura, S. Noro, *Angew. Chem. Int. Ed.*, **2014**, *43*, 2334–2375.
- 4 G. Férey, *Chem. Soc. Rev.* **2008**, *37*, 191–214.
- 5 H. Furukawa, K. E. Cordova, M. O’Keeffe, O. M. Yaghi, *Science* **2013**, *341*, 974.
- 6 Y. Inokuma, M. Kawano, M. Fujita, *Nat. Chem.* **2011**, *3*, 349–358.
- 7 Z. Wang, S. M. Cohen, *Chem. Soc. Rev.* **2009**, *38*, 1315–1329.
- 8 M. E. Davis, *Nature* **2002**, *417*, 813–821.
- 9 K. A. Cychoz, A. J. Matzger, *Langmuir* **2010**, *26*, 17198–202.
- 10 C. J. Kepert, M. J. Rosseinsky, *Chem. Commun.* **1999**, *536*, 375–376.
- 11 H. Li, M. Eddaoudi, M. O’Keeffe, O. M. Yaghi, *Nature* **1999**, *402*, 276–279.
- 12 E. Deiters, V. Bulach, M. W. Hosseini, *Chem. Commun.* **2005**, 3906–3098.
- 13 O. Ohmori, M. Kawano, M. Fujita, *J. Am. Chem. Soc.* **2004**, *126*, 16292–16293.
- 14 M. P. Suh, J. W. Ko, H. J. Choi, *J. Am. Chem. Soc.* **2002**, *124*, 10976–10977.
- 15 K. Biradha, M. Fujita, *Angew. Chem. Int. Ed.* **2002**, *41*, 3392–3395.
- 16 A cluster of small crystals, which were apparently not suitable for the single crystal X-ray analysis, was also observed other than the block and rod shaped crystals.
- 17 H. Kim, H. Chun, G.-H. Kim, H.-S. Lee, K. Kim, *Chem. Commun.* **2006**, 2759–2761.
- 18 R. Kitaura, S. Kitagawa, Y. Kubota, T. C. Kobayashi, K. Kindo, Y. Mita, A. Matsuo, M. Kobayashi, H.-C. Chang, T. C. Ozawa, M. Suzuki, M. Sakata, M. Takata, *Science*. **2002**, *298*, 2358–2361.
- 19 R. Matsuda, R. Kitaura, S. Kitagawa, Y. Kubota, R. V Belosludov, T. C. Kobayashi, H. Sakamoto, T. Chiba, M. Takata, Y. Kawazoe, Y. Mita, *Nature* **2005**, *436*, 238–241.
- 20 *APEX2*, *SADABS* and *XPREP*, Bruker AXS Inc., Madison, Wisconsin, USA, 2007.
- 21 *CrystalClear-SM Expert 2.1 b32*, Rigaku Corporation, Tokyo, Japan, 2013.
- 22 G. M. Sheldrick, *Acta Cryst.* **2008**, *A64*, 112–122.

- 23 P. van der Sluis, A. L. Spek, *Acta Cryst.* **1990**, **A46**, 194–201.

## Chapter 3

### Crystalline Sponge Analysis of Trace Amount Sample



#### Abstract

The guest inclusion scale of the crystalline sponge method was further downscaled to the nanogram order. The obtained guest structure from 50 ng of the guest molecules showed similar quality to the data obtained from 0.5  $\mu\text{g}$  scale guest inclusion. Furthermore, the combination of the crystalline sponge method and analytical HPLC enabled the X-ray analysis of the mixture extracted from *C. Unshiu*. The great potential for the trace amount mixture analysis with combination of the crystalline sponge method and HPLC as LC-SCD analysis was demonstrated. For the future application to the GC-SCD analysis, a trace amount of gaseous samples were also successfully analyzed by the crystalline sponge method.

### 3.1 Introduction

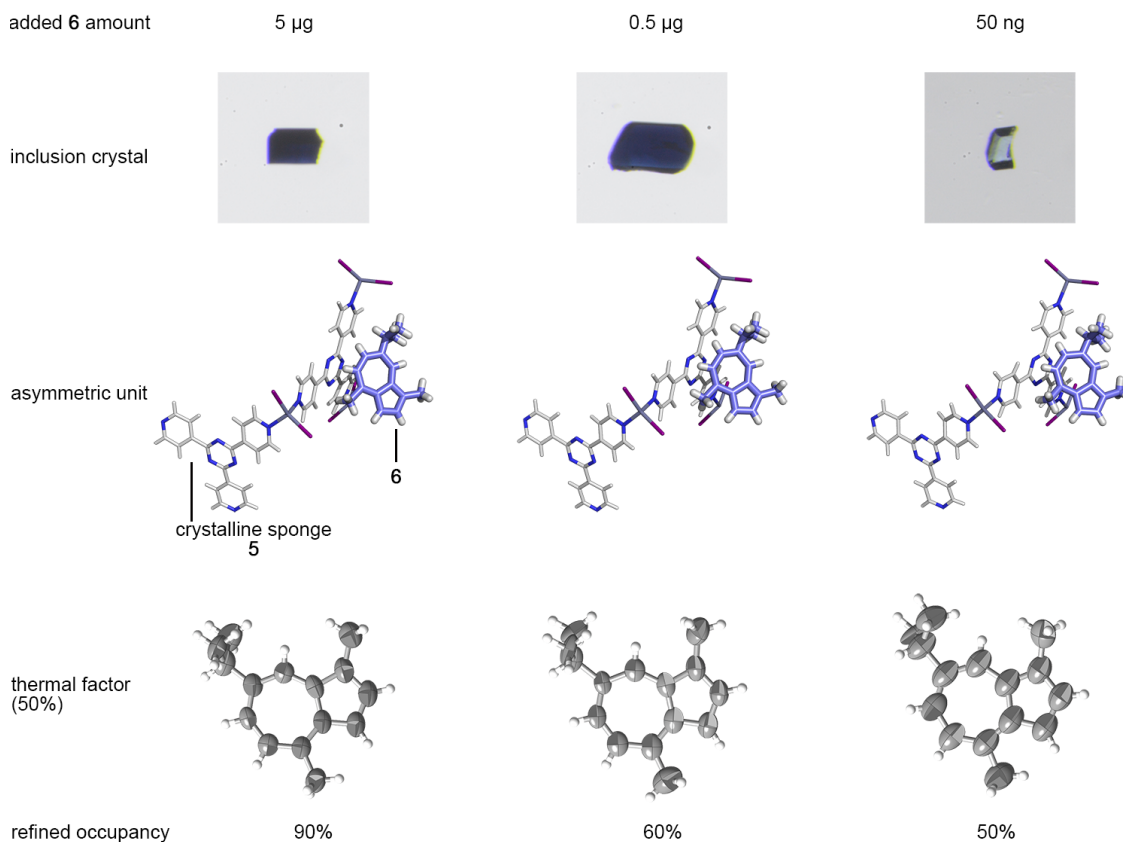
Available sample amount always limits the available analysis method due to the sensitivity of the method or applicable sample conditions.<sup>1</sup> The nanogram to microgram sample scale analysis is highly required in the field of the natural product chemistry, medicinal chemistry and so on. This scale is a suitable range of separation by an analytical high performance liquid chromatography (HPLC) or gas chromatography (GC) and usually the analysis was performed with the combination of the chromatography.<sup>4-6</sup> However, for the conventional X-ray crystallographic analysis, at least a few mg of sample are required to prepare a single crystal of target compound suitable for the diffraction study. Due to this scale limitation, the compound only available in nanogram to microgram was out of the target scope of the X-ray diffraction analysis. Therefore, in contrast to NMR or MS, single crystal X-ray diffraction analysis (SCD) was never combined with HPLC or GC as LC-SCD or GC-SCD.

Here, it was demonstrated that the crystalline sponge method could analyze and determine structure from the nanogram order amount sample and even from the gaseous sample. Furthermore, the HPLC separated microgram scale fractions were successfully analyzed by combining HPLC and SCD as LC-SCD analysis.

### 3.2 Nanogram scale guest inclusion and X-ray analysis

In the crystal structure of guaiazulene inclusion crystalline sponge (**5•6**) prepared from 0.5  $\mu\text{g}$  of **6**, actually observed amount of **6** by the X-ray analysis was calculated to be only 26 ng out of whole added 0.5  $\mu\text{g}$  of **6**. This calculation motivated a further downscaling of the inclusion guest scale, then added amount of **6** was reduced to 50 ng, and nanogram scale crystalline sponge analysis was examined.

A piece of crystal ( $50 \times 50 \times 30 \mu\text{m}^3$  size) **5**, which was smaller than that of 0.5  $\mu\text{g}$  scale inclusion, was soaked in 50 ng of **6** containing cyclohexane solution (50 ng/50  $\mu\text{L}$ ), and incubated at 50  $^\circ\text{C}$  for 2 d to evaporate the solvent. After 2 d, the resultant crystalline sponge turned to be pale blue. A color change of the crystalline sponge **5** was smaller than that of the 0.5  $\mu\text{g}$  scale inclusion case. However, X-ray analysis also clearly revealed the molecular structure of **6** along with the crystalline sponge framework. Included **6** was trapped at the same position to the 0.5  $\mu\text{g}$  inclusion case. Comparing the color change among the 50 ng, 0.5  $\mu\text{g}$  and 5  $\mu\text{g}$  scale inclusion results showed that the degree of color change decreased as the decreasing the added amount of **6**, and indicated that the included amount also decreased in the same order. This microscopic observation tendency corresponded to the tendency of the refined occupancy and the size of the thermal ellipsoid of the X-ray structure of **6** *i.e.* the occupancy decreased and the size of the thermal ellipsoid increased. However, the structures of **6** were clearly observed and refined without any disorder of the substituent group and azulene core even in the case of 50 ng scale inclusion (Figure 3.1).



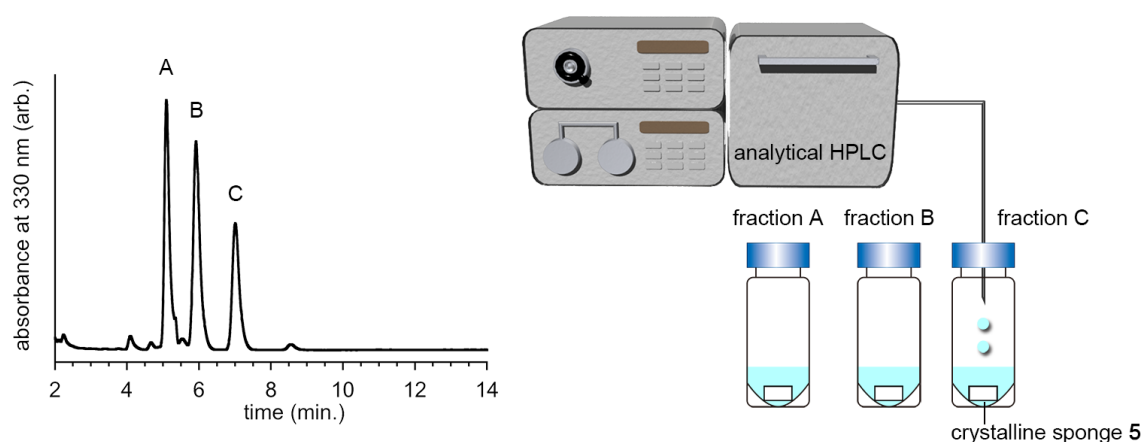
**Figure 3.1.** Relationship between added guest **6** amount and obtained data. Photographs of the inclusion crystals **5•6**, asymmetric units, thermal factors of included **6** and refined occupancies of **6**.

### 3.3 LC-SCD: Combination of the microgram scale chromatographic separation and X-ray analysis

The advantage of the trace amount scale single crystal X-ray diffraction analysis by the crystalline sponge method was made the most of when the method was combined with microgram scale chromatographic separation. To demonstrate the combination of chromatographic separation and crystalline sponge analysis, HPLC was employed as the separation method and was combined with the crystalline sponge method as LC-SCD analysis.

A series of polymethoxyflavones (PMFs) were extracted from finely ground air dried *C. Unshiu* peel (20 g) by  $\text{CHCl}_3$  (100 mL  $\times$  2 times) at room temperature.<sup>7,8</sup> After filtration, solution was concentrated to give an orange oil. The resulting oil was purified with short silica gel column chromatography first with  $\text{CH}_2\text{Cl}_2$  as an eluent, and

then with  $\text{CH}_2\text{Cl}_2/\text{AcOEt}$  (9:1) to give 20 mg of crude PMFs mixture. The crude mixture of PMFs (30  $\mu\text{g}$ ) dissolved in THF (5  $\mu\text{L}$ ) was analyzed with an analytical HPLC (eluent:  $\text{CH}_3\text{CN}/\text{H}_2\text{O}$  = 52:48, flow rate: 1 mL/min, column: Develosil ODS-5). An obtained chromatogram showed the mixture contained three different PMFs (fraction A, fraction B and fraction C) in 6  $\mu\text{g}$ , 7  $\mu\text{g}$  and 5  $\mu\text{g}$ , respectively. Three main fractions were collected into different micro vials, and analyzed with the crystalline sponge method with previously optimized conditions *i.e.* soaking a crystalline sponge in the target solution for 2 d at 50  $^\circ\text{C}$  (Figure 3.2).



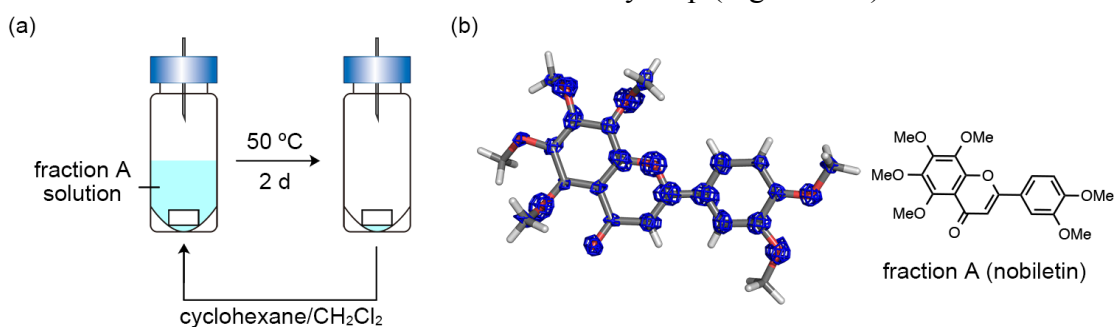
**Figure 3.2.** HPLC chromatogram of PMFs mixture (left) and schematic representation of LC-SCD analysis (right).

After complete solvent evaporation over 2 d, the crystalline sponge **5** soaked to the fraction A solution turned to be pale yellow. This color change indicated that inclusion of the fraction A into the crystalline sponge. However, the detailed structure could not be analyzed due to the weak observed electron density derived from the included guest. This was because of low inclusion amount of PMFs into the crystalline sponge.

In order to increase the included PMFs amount, inclusion time was elongated. During the inclusion process, the target compound was included into the crystalline sponge from the supernatant solution *i.e.* inclusion did not occur after complete evaporation of the solvent. Thus, in order to keep the PMFs as solution, 50  $\mu\text{L}$  of cyclohexane/ $\text{CH}_2\text{Cl}_2$  (9:1) mixed solvent was added again to the crystalline sponge and incubated at 50  $^\circ\text{C}$ . This solvent evaporation and addition cycle was repeated (Figure 3.3a). During this inclusion cycle by solvent addition and evaporation, gradual

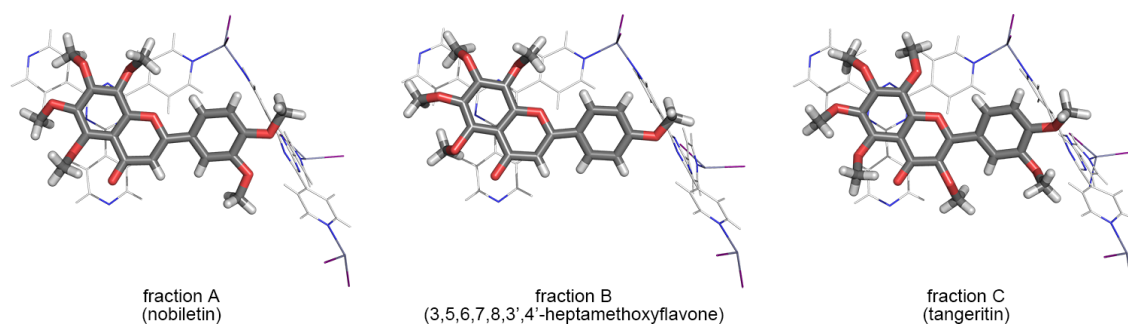


deterioration of the crystallinity of the crystalline sponge was observed. The best result was obtained after the 4th cycle. The X-ray analysis of fraction A inclusion crystalline sponge after 4th cycle revealed the detailed structure of included fraction A as nobiletin. The methoxy group substituted positions and number were easily determined based on the observed electron density map (Figure 3.3b).



**Figure 3.3.** (a) Solvent evaporation and addition cycle for increasing the included guest amount. (b) The observed electron density map ( $F_o$ , contour:  $0.6\sigma$ ) superimposed on the refined structure of the fraction A obtained by the LC-SCD analysis.

X-ray analyses of a series of PMFs inclusion crystalline sponge prepared by the similar fashion as fraction A revealed each included PMF structures. Methoxy substituted positions and numbers were also easily determined, and fractions A, B and C were assigned as nobiletin, 3,5,6,7,8,3',4'-heptamethoxyflavone and tangeritin (Figure 3.4). These results also corresponded to that of high-resolution mass spectrometry of each fraction. Analyzing the compounds with similar structure like PMFs by NMR or MS has still difficulty even combining with HPLC separation.<sup>9</sup> However combining HPLC separation and X-ray analysis by the crystalline sponge method provides the quick and easy structure determination of the mixture of similar structure compounds. The success of LC-SCD analysis showed large potential of application to many fields and potential of combining the crystalline sponge method with other techniques.



**Figure 3.4.** X-ray crystal structures of all the fractions of *C. Unshiu* extracted PMFs analyzed by the LC-SCD method.

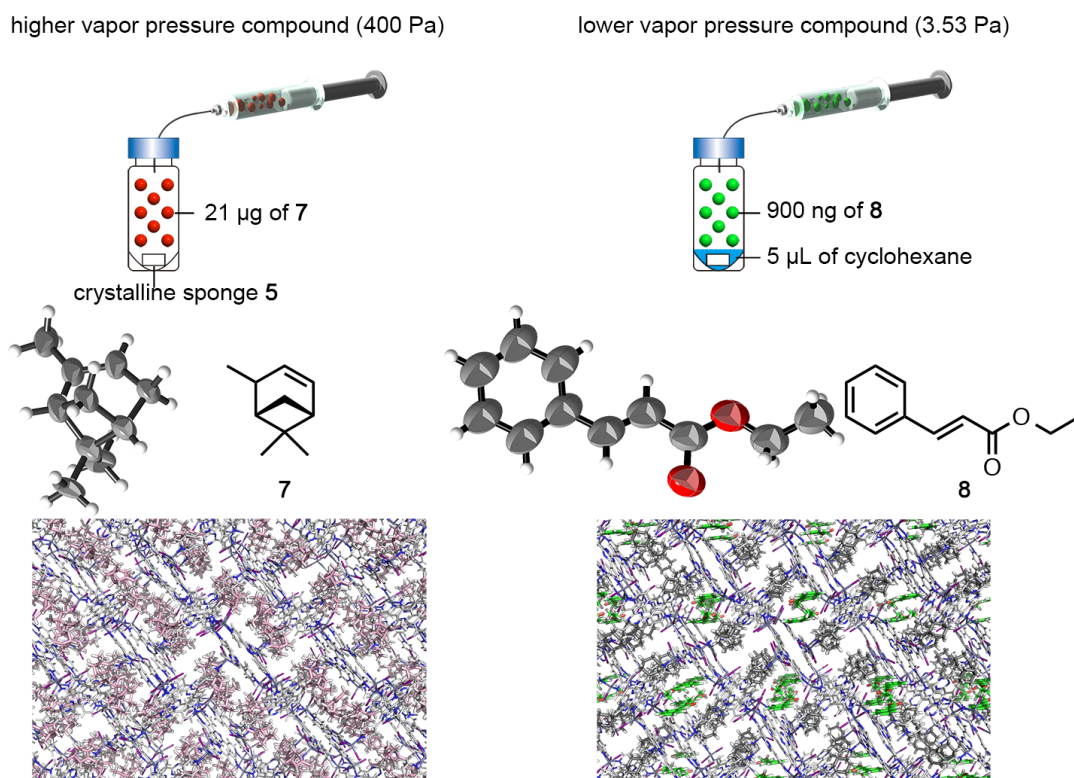
### 3.4 Crystalline sponge analysis of trace amount of gaseous sample

The importance of the trace amount sample analysis is not limited to the liquid or solid compounds, but the analysis of trace amount of gaseous compounds are also of the great interest particularly in the flavor chemistry.<sup>10,11</sup> Then, the inclusions and crystalline sponge analysis of some flavor compounds from their vapor were examined.

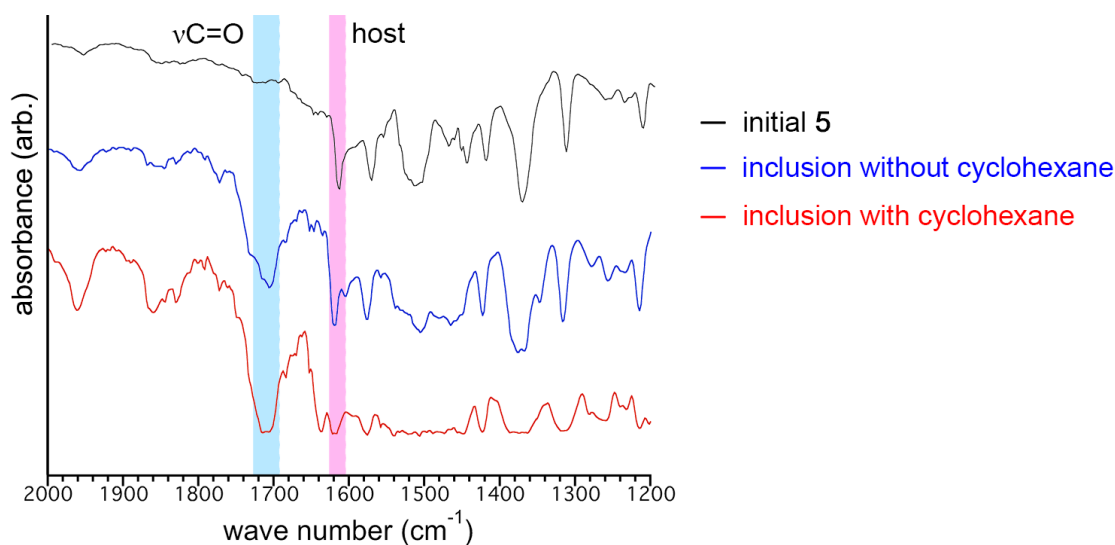
The experiment started with (1*S*)-(-)- $\alpha$ -pinene (**7**), a fruity flavor compound, which has relatively higher saturated vapor pressure (400 Pa). A saturated vapor of **7** (1 mL), prepared in the similar fashion to the head space analysis was poured in a septum capped micro vial containing a piece of crystal **5** without any solvent.<sup>11</sup> Calculation based on the ideal gas law showed 1 mL of saturated vapor of **7** contained ca. 21  $\mu$ g of **7**. The vial was tightly covered with the parafilm and allowed to stand for 8 d. After 8 d, the X-ray diffraction study of the resultant crystal **5** showed included structure of **7** along with the host framework. The obtained thermal factor was converged with reasonably small value (Figure 3.5). Interestingly, the crystalline sponge analysis of **7** by the standard protocol did not work and structure of **7** was not observed in the pore *i.e.* inclusion by soaking the crystalline sponge **5** into a solution of **7**, and gradual solvent evaporation protocol did not afford the inclusion crystal **5**•**7**. GC analysis showed an evaporation of dissolved **7** from the cyclohexane solution during the incubation process (Figure S3.1). The interaction between **7** and the crystalline sponge was too weak to trap **7** in the pore before complete evaporation of **7** and the solvent.

Further downscaling of vapor inclusion was attempted with ethyl cinnamate (**8**), the saturated vapor pressure of which is 3.53 Pa. A saturated vapor of **8** (10 mL, 900 ng) was poured into a crystalline sponge **5** containing sealed 10 mL round bottom flask and placed at room temperature for 5 d. Though the structure of **8** was not observed by the

X-ray diffraction analysis of the resultant crystal, microscopic IR measurement showed a peak at  $1696\text{ cm}^{-1}$  which is attributable to C=O stretching of **8**. Then inclusion procedure was slightly modified as performing inclusion from 10 mL of saturated vapor **8** under the coexistence of 5  $\mu\text{L}$  of cyclohexane. With the coexistence of cyclohexane, the ratio of the absorbance at  $1696\text{ cm}^{-1}$  to absorbance at  $1620\text{ cm}^{-1}$ , which is derived from the host framework increased and it was suggested that the amount of included **8** increased (Figure 3.6). In fact, the included **8** was observed in the pore of the resultant crystal prepared under the coexistence of cyclohexane (Figure 3.5). When cyclohexane remained at the bottom of the microvial with the crystalline sponge **5**, vapor **8** might be dissolved into cyclohexane, and then was included into the crystalline sponge.



**Figure 3.5.** Schematic representations for guest inclusion from their vapors and X-ray crystal structures of included **7** and **8** in crystalline sponge **5**. Thermal factor was drawn at the 50% probability level for **7** and 30% for **8**. In the packing structure, the included **7**, **8** and solvent cyclohexane were represented in pink, green and gray color, respectively.



**Figure 3.6.** Microscopic IR spectra of inclusion complex **5•8** without cyclohexane and with cyclohexane.

The success of inclusion and X-ray analysis of gaseous compound by the crystalline sponge method would open the door for combining the separation by GC and X-ray analysis as GC-SCD analysis.

### 3.5 Summary

In this chapter, the inclusion guest scale into the crystalline sponge was decreased to 50 ng scale, and the large potential of the crystalline sponge method for the trace amount sample analysis was demonstrated. Furthermore, the crystalline sponge method and HPLC separation was combined as LC-SCD analysis. In addition to the combination with the HPLC, the success of the gaseous compound inclusion and X-ray analysis by the crystalline sponge method showed the potential of combination with GC separation.

### 3.5 Experimental Section

Materials and Methods	59-61
GC-MS analysis of the crystalline sponge soaked solution of <b>7</b>	62
Crystallographic data	63-69
<b>Figure S3.1.</b> GC-MS spectra of crystalline sponge soaked solution of <b>7</b>	62
<b>Figure S3.2-S3.6.</b> X-ray crystallographic data	63-69

## Materials and method

### Reagents and equipment

Solvents and reagents were purchased from TCI Co., Ltd., WAKO Pure Chemical Industries Ltd., and Sigma-Aldrich Corporation and used without further purification. *C. Unshiu* was cultivated in Nishi-Uwajima, Ehime prefecture, Japan in 2011. Silica gel column chromatography was performed on Silica gel 60N, spherical neutral (Kanto Reagents). <sup>1</sup>H NMR spectra were recorded on a Bruker AVANCE III HD 500 MHz spectrometer equipped with 5 mm BBO gradient probe and a Bruker AVANCE 500 MHz spectrometer equipped with TCI gradient CryoProbe. All NMR spectra data were recorded at 300 K and chemical shift values are reported in parts per million (ppm) relative to an internal standard tetramethylsilane. High-resolution mass spectra were recorded on a Bruker MAXIS spectrometer. GC-MS analysis was performed on Agilent Technologies 6890N. HPLC separation was carried out using JASCO UV-970 spectrometer equipped with a JASCO PU-980 pump and a reverse phase column Develosil ODS-5 (Nomura Chemical Co., LTD.). Microscopic FT-IR spectra were recorded on a Varian DIGILAB Scimitar instrument and are reported in frequency of absorption (cm<sup>-1</sup>). Single crystal X-ray diffraction data were collected on a BRUKER APEX-II CCD diffractometer equipped with a focusing mirror (MoK<sub>α</sub> radiation  $\lambda = 0.71073 \text{ \AA}$ ) and a N<sub>2</sub> generator (Japan Thermal Eng. Co., Ltd.) or Rigaku XtaLAB P200 diffractometer equipped with a PILATUS-200K detector with multi-layer mirror monochromater (CuK<sub>α</sub> radiation  $\lambda = 1.54187 \text{ \AA}$ ). For single crystal X-ray diffraction analysis and microscopic IR measurement, fluorolube® and mineral oil were used as a protectant for the single crystals.

### X-ray crystallographic analysis

Single crystal X-ray diffraction data were processed with Bruker APEX2 software and CrystalClear program.<sup>12,13</sup> For Bruker data, absorption correction was performed by multi-scan method in SADABS and space groups were determined by XPREP program.<sup>1</sup> The structures were solved by direct methods and refined by full-matrix least-squares calculations on  $F^2$  using SHELXL-97 and SHELXL-2014 program.<sup>14</sup> In the determination of space group, the XPREP program suggested space group was employed for analyzing the structure.

After the initial phase determination, all the atoms for the host framework (*i.e.* ZnI<sub>2</sub> and tpt ligands) were assigned and the structure was refined anisotropically except for hydrogen atoms. Since the host framework was in some cases highly disordered, atoms were partially restrained with DFIX, FLAT, SIMU and ISOR commands. Atoms for the guest molecules (including solvent molecules) were then assigned to the residual Q-peaks. The guest structures were first refined isotropically with a suitable occupancy that is estimated by refinement using FVAR. If available, the guest structures were subsequently refined anisotropically. The final crystal structures leave large solvent-accessible voids where only weak Q-peaks were observed because that solvent or guest molecules are highly disordered. Such Q-peaks have been treated with PLATON SQUEEZE program, resulting in reasonable  $R_1$  and  $wR_2$  values as compared with  $R_{int}$ .<sup>15</sup> Note that due to the minor disorder with solvent molecules, the X-ray data quality of crystalline sponge method is rather lower than conventional single crystal X-ray analysis for small molecules using their pure single crystals.

## Nanogram and microgram scale guest inclusion into a crystalline sponge **5**

### General procedure

To a micro vial containing a cyclohexane exchanged single crystal of  $[(\text{ZnI}_2)_3(\text{tpt})_2]_n$  (**5**; tpt = tri(4-pyridyl)-1,3,5-triazine) and cyclohexane (45  $\mu\text{L}$ ), 5  $\mu\text{L}$  of cyclohexane solution of target compounds (1 mg/1 mL) was added. Then, the crystal containing microvial was allowed to stand at 45 °C and the solvent was gradually evaporated over 2 d.

### Extraction of PMFs from *C. Unshiu*

Finely ground dried *C. Unshiu* peel (20 g) was extracted with  $\text{CHCl}_3$  (100 mL  $\times$  2 times) at room temperature. After filtration, solution was concentrated to give an orange oil. The resulting oil was purified with short silica gel column chromatography first with  $\text{CH}_2\text{Cl}_2$  as an eluent, and then with  $\text{CH}_2\text{Cl}_2/\text{AcOEt}$  (9:1) to give 20 mg of crude PMFs mixture.

### LC-SCD analysis of PMFs

The crude mixture of PMFs (30  $\mu\text{g}$ ) was dissolved in THF (5  $\mu\text{L}$ ) and was analyzed with an analytical HPLC (eluent:  $\text{CH}_3\text{CN}/\text{H}_2\text{O}$  = 52:48, flow rate: 1 mL/min, column: Develosil ODS-5). Three main fractions were collected into micro vials, respectively. After the solvent evaporation, to each fraction containing micro vial, were added a piece of crystalline sponge **5**, 45  $\mu\text{L}$  of cyclohexane and 5  $\mu\text{L}$  of  $\text{CH}_2\text{Cl}_2$ . The inclusion was performed with the procedure described in the main context.

### Characterization of PMFs by high-resolution mass spectrometry

Fraction A: nobiletin

HRMS (ESI-MS) for  $\text{C}_{21}\text{H}_{23}\text{O}_9$  calcd for  $[M+H]^+$   $m/z$  403.1393. found 403.1403

Fraction B: 3,5,6,7,8,3',4'-heptamethoxyflavone

HRMS (ESI-MS) for  $\text{C}_{22}\text{H}_{25}\text{O}_9$  calcd for  $[M+H]^+$   $m/z$  433.1499. found 433.1482

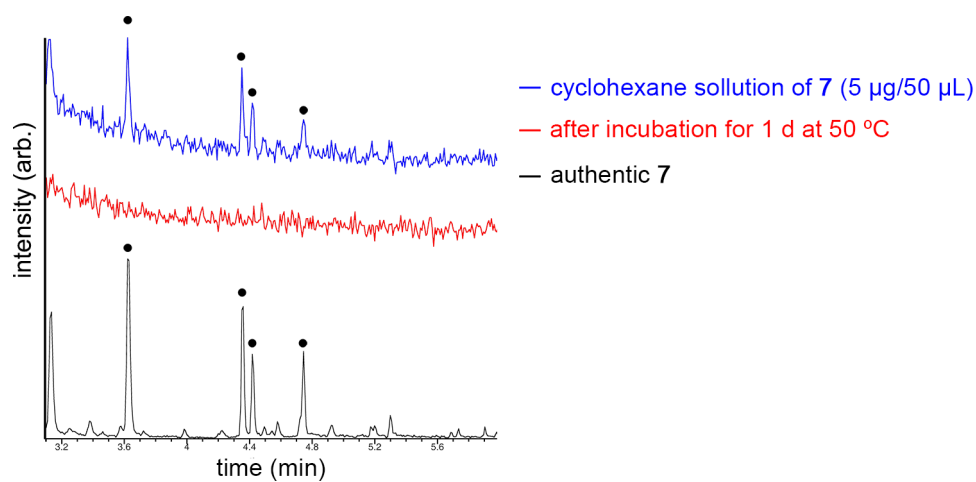
Fraction C: tangeritin

HRMS (ESI-MS) for  $\text{C}_{20}\text{H}_{21}\text{O}_7$  calcd for  $[M+H]^+$   $m/z$  373.1289. found 373.1283

After the isolation on a large scale (~5 mg),  $^1\text{H}$  NMR spectrum of each fraction was identical to the previously reported spectrum<sup>16</sup>.



### GC analysis of the crystalline sponge soaked solution of **7**

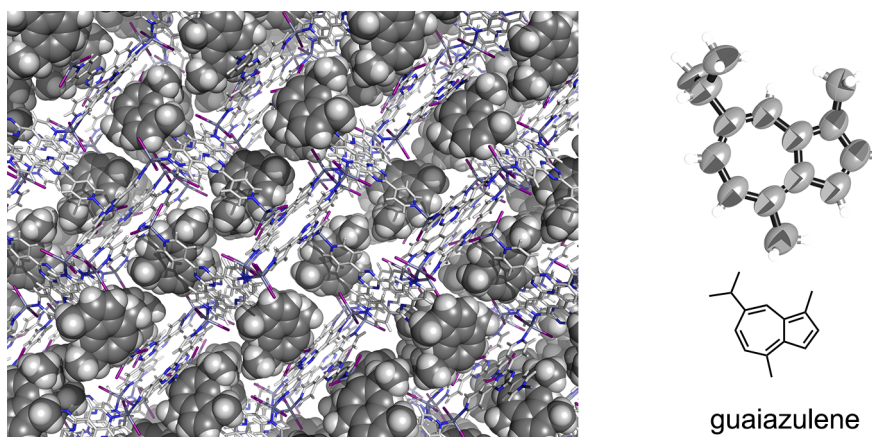


**Figure S3.1.** GC spectra of initial **7** solution (blue), **7** solution after incubation for 1 d at 50 °C (red) and authentic **7** (black).

**Crystallographic data****Inclusion complex 5•6 (50 ng scale inclusion)**

Crystallographic data (before the SQUEEZE treatment):  $C_{36}H_{24}N_{12}Zn_3I_6 \cdot 0.5(C_{15}H_{18})$ ,  $M = 1681.33$ , colorless cubic,  $0.05 \times 0.05 \times 0.03 \text{ mm}^3$ , monoclinic, space group  $C2/c$ ,  $a = 35.069(2)$ ,  $b = 14.8561(9)$ ,  $c = 31.093(2) \text{ \AA}$ ,  $\beta = 102.504(7)^\circ$ ,  $V = 15814.7(18) \text{ \AA}^3$ ,  $Z = 8$ ,  $D_c = 1.412 \text{ g/cm}^3$ ,  $F000 = 6288$ ,  $\mu = 19.682 \text{ mm}^{-1}$ ,  $T = 90(2) \text{ K}$ ,  $3.24 < \theta < 68.25^\circ$ , 5107 unique reflections out of 14251 with  $I > 2\sigma(I)$ ,  $R_{\text{int}} = 0.1005$ , 650 parameters, 634 restraints,  $\text{GoF} = 1.520$ , final  $R$  factors  $R_1 = 0.1856$  and  $wR_2 = 0.5597$  for all data. CCDC deposit number: unpublished data.

Crystallographic data (after the SQUEEZE treatment):  $C_{36}H_{24}N_{12}Zn_3I_6 \cdot 0.5(C_{15}H_{18})$ ,  $M = 1681.33$ , colorless cubic,  $0.05 \times 0.05 \times 0.03 \text{ mm}^3$ , monoclinic, space group  $C2/c$ ,  $a = 35.069(2)$ ,  $b = 14.8561(9)$ ,  $c = 31.093(2) \text{ \AA}$ ,  $\beta = 102.504(7)^\circ$ ,  $V = 15814.7(18) \text{ \AA}^3$ ,  $Z = 8$ ,  $D_c = 1.412 \text{ g/cm}^3$ ,  $F000 = 6288$ ,  $\mu = 19.682 \text{ mm}^{-1}$ ,  $T = 90(2) \text{ K}$ ,  $2.98 < \theta < 68.22^\circ$ , 4827 unique reflections out of 14251 with  $I > 2\sigma(I)$ ,  $R_{\text{int}} = 0.0963$ , 650 parameters, 634 restraints,  $\text{GoF} = 0.993$ , final  $R$  factors  $R_1 = 0.1210$  and  $wR_2 = 0.1920$  for all data. CCDC deposit number: unpublished data.

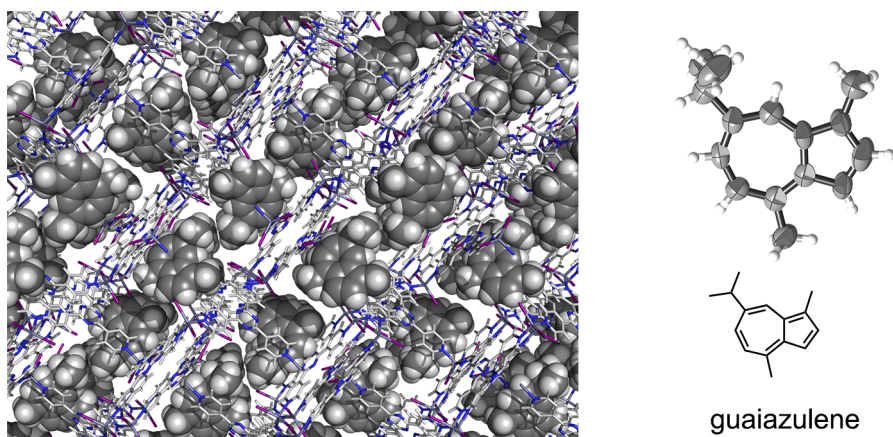


**Figure S3.2.** The X-ray crystal structure obtained 50 ng scale crystalline sponge analysis of **6**. Guest molecules were drawn in CPK model in the packing structure and the thermal ellipsoid of the guest molecule was drawn at the 50% probability level.

**Inclusion complex 5•6 (5 µg scale inclusion)**

Crystallographic data (before the SQUEEZE treatment):  $C_{36}H_{24}N_{12}Zn_3I_6 \cdot 0.8(C_6H_{18}) \cdot 0.75(C_{15}H_{18})$ ,  $M = 1832.74$ , dark blue block,  $0.10 \times 0.10 \times 0.06 \text{ mm}^3$ , monoclinic, space group  $C2/c$ ,  $a = 34.942(4)$ ,  $b = 14.8462(19)$ ,  $c = 30.976(4) \text{ \AA}$ ,  $\beta = 102.149(2)^\circ$ ,  $V = 15709(3) \text{ \AA}^3$ ,  $Z = 8$ ,  $D_c = 1.550 \text{ g/cm}^3$ ,  $F000 = 6962$ ,  $\mu = 3.303 \text{ mm}^{-1}$ ,  $T = 90(2) \text{ K}$ ,  $1.19 < \theta < 25.00^\circ$ , 11136 unique reflections out of 13841 with  $I > 2\sigma(I)$ ,  $R_{\text{int}} = 0.0318$ , 675 parameters, 65 restraints, GoF = 1.103, final  $R$  factors  $R_1 = 0.1006$  and  $wR_2 = 0.3319$  for all data. CCDC deposit number: unpublished data.

Crystallographic data (after the SQUEEZE treatment):  $C_{36}H_{24}N_{12}Zn_3I_6 \cdot 0.91(C_6H_{18}) \cdot 0.91(C_{15}H_{18})$ ,  $M = 1832.74$ , dark blue block,  $0.10 \times 0.10 \times 0.06 \text{ mm}^3$ , monoclinic, space group  $C2/c$ ,  $a = 34.942(4)$ ,  $b = 14.8462(19)$ ,  $c = 30.976(4) \text{ \AA}$ ,  $\beta = 102.149(2)^\circ$ ,  $V = 15709(3) \text{ \AA}^3$ ,  $Z = 8$ ,  $D_c = 1.550 \text{ g/cm}^3$ ,  $F000 = 6983$ ,  $\mu = 3.303 \text{ mm}^{-1}$ ,  $T = 90(2) \text{ K}$ ,  $1.19 < \theta < 25.00^\circ$ , 10975 unique reflections out of 13841 with  $I > 2\sigma(I)$ ,  $R_{\text{int}} = 0.0305$ , 675 parameters, 65 restraints, GoF = 1.138, final  $R$  factors  $R_1 = 0.0766$  and  $wR_2 = 0.2281$  for all data. CCDC deposit number: unpublished data.



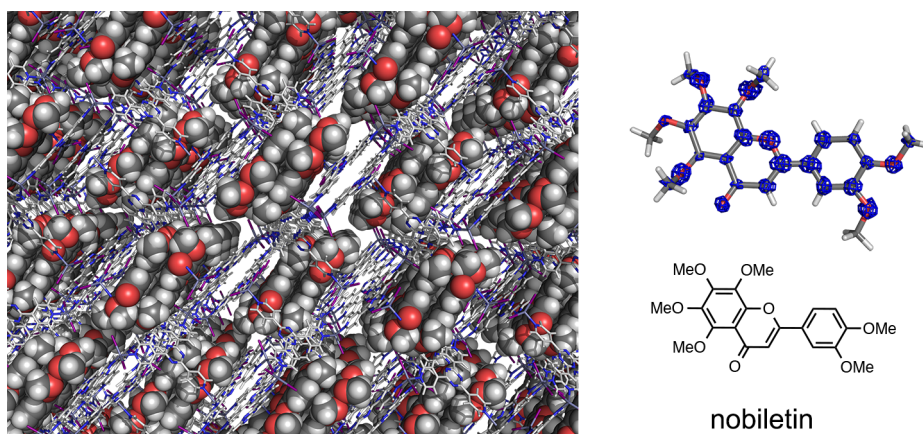
**Figure S3.3.** The X-ray crystal structure obtained 5 µg scale crystalline sponge analysis of **6**. Guest molecules were drawn in CPK model in the packing structure and the thermal ellipsoid of the guest molecule was drawn at the 50% probability level.

**Nobiletin inclusion crystalline sponge 5 (LC-SCD for fraction A)**

Crystallographic data (before the SQUEEZE treatment):  $C_{36}H_{24}N_{12}Zn_3I_6 \cdot 0.5(C_{21}H_{22}O_8)$ ,  $M_r = 1783.38$ , pale yellow rod,  $0.12 \times 0.1 \times 0.07 \text{ mm}^3$ , monoclinic, space group  $C2/c$ ,  $a = 34.562(8)$ ,  $b = 14.950(4)$ ,  $c = 30.348(7) \text{ \AA}$ ,  $\beta = 100.119(3)^\circ$ ,  $V = 15437(6) \text{ \AA}^3$   $Z = 8$ ,  $D_c = 1.535 \text{ g/cm}^3$ ,  $F_{000} = 6704$ ,  $\mu = 3.362 \text{ mm}^{-1}$ ,  $T = 93(2) \text{ K}$ ,  $1.20 < \theta < 25.00^\circ$ , 10470 unique reflections out of 13534 with  $I > 2\sigma(I)$ ,  $R_{\text{int}} = 0.0491$ , 780 parameters, 248 restraints,  $\text{GoF} = 1.153$ , final  $R$  factors  $R_1 = 0.1310$  and  $wR_2 = 0.3498$  for all data. CCDC deposit number: unpublished data.

Crystallographic data (after the SQUEEZE treatment):  $C_{36}H_{24}N_{12}Zn_3I_6 \cdot 0.5(C_{21}H_{22}O_8)$ ,  $M_r = 1783.38$ , pale yellow rod,  $0.12 \times 0.1 \times 0.07 \text{ mm}^3$ , monoclinic, space group  $C2/c$ ,  $a = 34.562(8)$ ,  $b = 14.950(4)$ ,  $c = 30.348(7) \text{ \AA}$ ,  $\beta = 100.119(3)^\circ$ ,  $V = 15437(6) \text{ \AA}^3$   $Z = 8$ ,  $D_c = 1.535 \text{ g/cm}^3$ ,  $F_{000} = 6704$ ,  $\mu = 3.362 \text{ mm}^{-1}$ ,  $T = 93(2) \text{ K}$ ,  $1.20 < \theta < 25.00^\circ$ , 10259 unique reflections out of 13534 with  $I > 2\sigma(I)$ ,  $R_{\text{int}} = 0.0491$ , 780 parameters, 248 restraints,  $\text{GoF} = 1.052$ , final  $R$  factors  $R_1 = 0.1065$  and  $wR_2 = 0.2915$  for all data. CCDC deposit number: 910391.

IR (single crystal, fluorolube): 3075, 3052, 2925, 2852, 1618, 1577, 1529, 1513, 1371  $\text{cm}^{-1}$ .



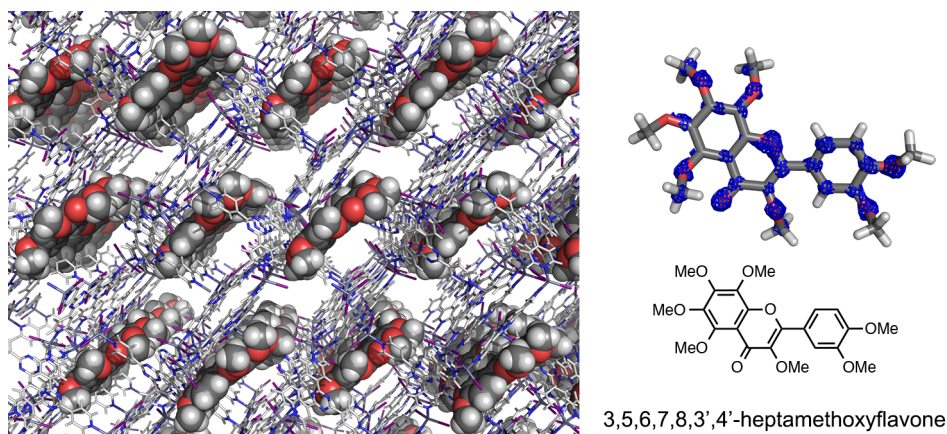
**Figure S3.4.** The X-ray crystal structure of nobiletin inclusion crystalline sponge **5**. Guest molecules were drawn in CPK model in the packing structure and the observed electron density map ( $F_o$ , contour:  $0.6\sigma$ ) superimposed on the refined structure.

**3,5,6,7,8,3',4'-Heptamethoxyflavone inclusion crystalline sponge 5**

Crystallographic data (before the SQUEEZE treatment):  $C_{72}H_{48}N_{24}Zn_6I_{12} \cdot 0.5(C_{22}H_{24}O_9)$ ,  $M = 3380.57$ , pale yellow rod,  $0.12 \times 0.1 \times 0.07 \text{ mm}^3$ , monoclinic, space group  $Cc$ ,  $a = 34.534(6)$ ,  $b = 15.028(3)$ ,  $c = 31.197(6) \text{ \AA}$ ,  $\beta = 101.215(3)^\circ$ ,  $V = 15881(5) \text{ \AA}^3$ ,  $Z = 4$ ,  $D_c = 1.414 \text{ g/cm}^3$ ,  $F_{000} = 6264$ ,  $\mu = 3.262 \text{ mm}^{-1}$ ,  $T = 90(2) \text{ K}$ ,  $1.20 < \theta < 26.00^\circ$ , 10405 unique reflections out of 31029 with  $I > 2\sigma(I)$ ,  $R_{\text{int}} = 0.1081$ , 1151 parameters, 938 restraints,  $\text{GoF} = 1.357$ , final  $R$  factors  $R_1 = 0.1076$  and  $wR_2 = 0.3260$  for all data. CCDC deposit number: unpublished data.

Crystallographic data (after the SQUEEZE treatment):  $C_{72}H_{48}N_{24}Zn_6I_{12} \cdot 0.5(C_{22}H_{24}O_9)$ ,  $M = 3380.57$ , pale yellow rod,  $0.12 \times 0.1 \times 0.07 \text{ mm}^3$ , monoclinic, space group  $Cc$ ,  $a = 34.534(6)$ ,  $b = 15.028(3)$ ,  $c = 31.197(6) \text{ \AA}$ ,  $\beta = 101.215(3)^\circ$ ,  $V = 15881(5) \text{ \AA}^3$ ,  $Z = 4$ ,  $D_c = 1.414 \text{ g/cm}^3$ ,  $F_{000} = 6312$ ,  $\mu = 3.262 \text{ mm}^{-1}$ ,  $T = 90(2) \text{ K}$ ,  $1.20 < \theta < 26.00^\circ$ , 10274 unique reflections out of 31029 with  $I > 2\sigma(I)$ ,  $R_{\text{int}} = 0.0730$ , 1151 parameters, 944 restraints,  $\text{GoF} = 0.893$ , final  $R$  factors  $R_1 = 0.0730$  and  $wR_2 = 0.2184$  for all data. CCDC deposit number: 910392.

IR (single crystal, fluorolube): 3076, 3053, 2924, 2851, 1616, 1578, 1525, 1514, 1371  $\text{cm}^{-1}$ .



**Figure S3.5.** The X-ray crystal structure of 3,5,6,7,8,3',4'-heptamethoxyflavone inclusion crystalline sponge **5**. Guest molecules were drawn in CPK model in the packing structure and the observed electron density map ( $F_o$ , contour:  $0.5\sigma$ ) superimposed on the refined structure.

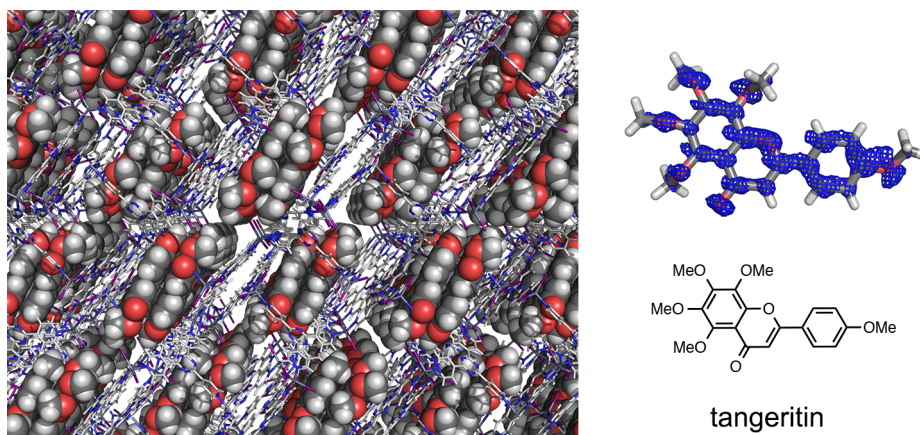


**Tangeritin inclusion crystalline sponge 5**

Crystallographic data (before the SQUEEZE treatment):  $C_{72}H_{48}N_{24}Zn_6I_{12} \cdot 0.94(C_{20}H_{20}O_7)$ ,  $M = 1930.40$ , pale yellow rod,  $0.15 \times 0.05 \times 0.05$  mm<sup>3</sup>, monoclinic, space group  $C2/c$ ,  $a = 34.103(6)$ ,  $b = 14.767(3)$ ,  $c = 30.700(6)$  Å,  $\beta = 99.802(2)^\circ$ ,  $V = 15234(5)$  Å<sup>3</sup>,  $Z = 8$ ,  $D_c = 1.683$  g/cm<sup>3</sup>,  $F_{000} = 7066$ ,  $\mu = 3.417$  mm<sup>-1</sup>,  $T = 93(2)$  K,  $1.21 < \theta < 24.71^\circ$ , 9313 unique reflections out of 12914 with  $I > 2\sigma(I)$ ,  $R_{int} = 0.0438$ , 758 parameters, 342 restraints, GoF = 1.043, final  $R$  factors  $R_1 = 0.0952$  and  $wR_2 = 0.3171$  for all data. CCDC deposit number: unpublished data.

Crystallographic data (after the SQUEEZE treatment):  $C_{72}H_{48}N_{24}Zn_6I_{12} \cdot 0.94(C_{20}H_{20}O_7)$ ,  $M = 1930.40$ , pale yellow rod,  $0.15 \times 0.05 \times 0.05$  mm<sup>3</sup>, monoclinic, space group  $C2/c$ ,  $a = 34.103(6)$ ,  $b = 14.767(3)$ ,  $c = 30.700(6)$  Å,  $\beta = 99.802(2)^\circ$ ,  $V = 15234(5)$  Å<sup>3</sup>,  $Z = 8$ ,  $D_c = 1.683$  g/cm<sup>3</sup>,  $F_{000} = 7323$ ,  $\mu = 3.417$  mm<sup>-1</sup>,  $T = 93(2)$  K,  $1.21 < \theta < 24.71^\circ$ , 9422 unique reflections out of 12914 with  $I > 2\sigma(I)$ ,  $R_{int} = 0.0823$ , 758 parameters, 342 restraints, GoF = 1.043, final  $R$  factors  $R_1 = 0.0823$  and  $wR_2 = 0.2283$  for all data. CCDC deposit number: 910393.

IR (single crystal, fluorolube): 3080, 3055, 2929, 2854, 1620, 1576, 1525, 1375 cm<sup>-1</sup>.



**Figure S3.6.** The X-ray crystal structure of tangeritin inclusion crystalline sponge 5. Guest molecules were drawn in CPK model in the packing structure and the observed electron density map ( $F_o$ , contour:  $0.6\sigma$ ) superimposed on the refined structure.

**Inclusion complex 5•7**

Crystallographic data (before the SQUEEZE treatment):  $C_{72}H_{48}N_{24}Zn_6I_{12} \cdot 4.08(C_{10}H_{16})$ ,  $M = 3719.94$ , colorless rod,  $0.08 \times 0.08 \times 0.07 \text{ mm}^3$ , monoclinic, space group  $C2$ ,  $a = 35.388(4)$ ,  $b = 14.7503(17)$ ,  $c = 30.459(4) \text{ \AA}$ ,  $\beta = 101.0740(10)^\circ$ ,  $V = 15603(3) \text{ \AA}^3$ ,  $Z = 4$ ,  $D_c = 1.584 \text{ g/cm}^3$ ,  $F000 = 7096$ ,  $\mu = 3.326 \text{ mm}^{-1}$ ,  $T = 90(2) \text{ K}$ ,  $1.173 < \theta < 26.475^\circ$ , 25494 unique reflections out of 32122 with  $I > 2\sigma(I)$ ,  $R_{\text{int}} = 0.0360$ , 1251 parameters, 207 restraints,  $\text{GoF} = 1.038$ , final  $R$  factors  $R_1 = 0.0670$  and  $wR_2 = 0.2339$  for all data. CCDC deposit number: unpublished data.

Crystallographic data (after the SQUEEZE treatment):  $C_{72}H_{48}N_{24}Zn_6I_{12} \cdot 4.08(C_{10}H_{16})$ ,  $M = 3719.94$ , colorless rod,  $0.08 \times 0.08 \times 0.07 \text{ mm}^3$ , monoclinic, space group  $C2$ ,  $a = 35.388(4)$ ,  $b = 14.7503(17)$ ,  $c = 30.459(4) \text{ \AA}$ ,  $\beta = 101.0740(10)^\circ$ ,  $V = 15603(3) \text{ \AA}^3$ ,  $Z = 4$ ,  $D_c = 1.584 \text{ g/cm}^3$ ,  $F000 = 7096$ ,  $\mu = 3.326 \text{ mm}^{-1}$ ,  $T = 90(2) \text{ K}$ ,  $1.173 < \theta < 26.475^\circ$ , 25376 unique reflections out of 32122 with  $I > 2\sigma(I)$ ,  $R_{\text{int}} = 0.0355$ , 1251 parameters, 213 restraints,  $\text{GoF} = 1.132$ , final  $R$  factors  $R_1 = 0.0568$  and  $wR_2 = 0.1911$  for all data. CCDC deposit number: unpublished data.

IR (single crystal, fluorolube): 2981, 2873, 1618, 1577, 1528, 1446, 1373, 1316, 1215  $\text{cm}^{-1}$ .

**Inclusion complex 5•8**

Crystallographic data (before the SQUEEZE treatment):  $C_{36}H_{24}N_{12}Zn_3I_6 \cdot 0.49(C_{11}H_{12}O_2) \cdot 1.77(C_6H_{12})$ ,  $M = 1816.62$ , colorless rod,  $0.10 \times 0.08 \times 0.07 \text{ mm}^3$ , monoclinic, space group  $C2/c$ ,  $a = 34.039(3)$ ,  $b = 15.0742(15)$ ,  $c = 30.064(3) \text{ \AA}$ ,  $\beta = 101.7420(10)^\circ$ ,  $V = 15104(3) \text{ \AA}^3$ ,  $Z = 8$ ,  $D_c = 1.598 \text{ g/cm}^3$ ,  $F000 = 6900$ ,  $\mu = 3.435 \text{ mm}^{-1}$ ,  $T = 90(2) \text{ K}$ ,  $1.222 < \theta < 26.505^\circ$ , 11692 unique reflections out of 15655 with  $I > 2\sigma(I)$ ,  $R_{\text{int}} = 0.0244$ , 707 parameters, 409 restraints,  $\text{GoF} = 1.054$ , final  $R$  factors  $R_1 = 0.0971$  and  $wR_2 = 0.3207$  for all data. CCDC deposit number: unpublished data.

Crystallographic data (after the SQUEEZE treatment):  $C_{36}H_{24}N_{12}Zn_3I_6 \cdot 0.49(C_{11}H_{12}O_2) \cdot 1.77(C_6H_{12})$ ,  $M = 1816.62$ , colorless rod,  $0.10 \times 0.08 \times 0.07 \text{ mm}^3$ , monoclinic, space group  $C2/c$ ,  $a = 34.039(3)$ ,  $b = 15.0742(15)$ ,  $c = 30.064(3) \text{ \AA}$ ,  $\beta = 101.7420(10)^\circ$ ,  $V = 15104(3) \text{ \AA}^3$ ,  $Z = 8$ ,  $D_c = 1.598 \text{ g/cm}^3$ ,  $F000 = 6900$ ,  $\mu = 3.435 \text{ mm}^{-1}$ ,  $T = 90(2) \text{ K}$ ,  $1.222 < \theta < 26.505^\circ$ , 11629 unique reflections out of 15655 with  $I > 2\sigma(I)$ ,  $R_{\text{int}} = 0.0233$ , 707 parameters, 409 restraints,  $\text{GoF} = 1.090$ , final  $R$  factors  $R_1 = 0.0779$  and  $wR_2 = 0.2527$  for all data. CCDC deposit number: unpublished data.

IR (single crystal, fluorolube): 3053, 1691, 1618, 1578, 1421  $\text{cm}^{-1}$ .

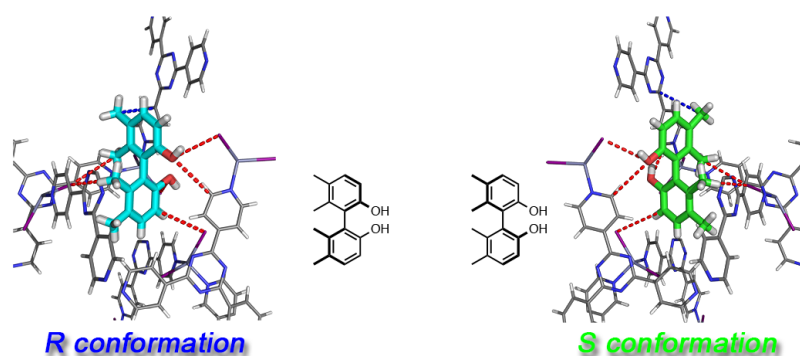


## References

- 1 G. D. Christian, *Analytical Chemistry 6th edition*. Wiley, New York, **2004**.
- 2 D. A. Sampietro, C. A. N. Catalan, M. A. Vattuone, *Isolation, Identification, and Characterization of Allelochemicals/Natural Products*, Science Publishers, **2009**.
- 3 S. Ahuja, K. Alsante, *Handbook of Isolation and Characterization of Impurities in Pharmaceuticals*, Academic Press, London, **2003**.
- 4 V. Exarchou, M. Krucker, T. A. van Beek, J. Vervoort, I. P. Gerothanassis, K. Albert, *Magn. Reson. Chem.* **2005**, *43*, 681–687.
- 5 M. Spraul, M. Hofmann, P. Dvortsak, J. K. Nicholson, I. D. Wilson, *Anal. Chem.* **1993**, *65*, 327–330.
- 6 C. O. Green, A. O. Wheatley, A. U. Osagie, E. Y. S. A. Morrison, H. N. Asemota, *Biomed. Chromatorgr.* **2007**, *21*, 48–54.
- 7 S. Han, H. M. Kim, J. M. Lee, S.-Y. Mok, S. Lee, *J. Agric. Food Chem.* **2010**, *58*, 9488–9491.
- 8 T. L. Suyama, W. H. Gerwick, K. L. McPhail, *Bioorg. Med. Chem.* **2011**, *19*, 6675–6701.
- 9 W. Jennings, T. Shibamonot *Qualitative analysis of flavor and fragrance volatiles by glass capillary gas chromatography*, Academic Press, Inc., New York, **1980**.
- 10 S. B. Hawthorne, M. S. Krieger, D. J. Miller, *Anal. Chem.* **1988**, *60*, 472–477.
- 11 *APEX2, SADABS and XPREP*, Bruker AXS Inc., Madison, Wisconsin, USA, 2007.
- 12 *CrystalClear-SM Expert 2.1 b32*, Rigaku Corporation, Tokyo, Japan, 2013.
- 13 G. M. Sheldrick, *Acta Cryst.* **2008**, *A64*, 112–122.
- 14 P. van der Sluis, A. L. Spek, *Acta Cryst.* **1990**, *A46*, 194–201.
- 15 S. Han, H. M. Kim, J. M. Lee, S. Mok, S. Lee. *J. Agric. Food Chem.* **2010**, *58*, 9488–9491.

## Chapter 4

### Absolute Structure Determination by the Crystalline Sponge Method



#### Abstract

Absolute structure determinations of various chiral molecules were performed by the crystalline sponge method. The crystalline sponge has heavy Zn and I atoms in the structure, therefore the introduction of the heavy atom into the target compound was not required to use anomalous scattering effect for the absolute structure determination. Furthermore, axial chirality was also successfully determined. The strong molecular interactions between target molecules and host crystalline sponge play an important role for the absolute structure determination by the crystalline sponge method.

## 4.1 Introduction

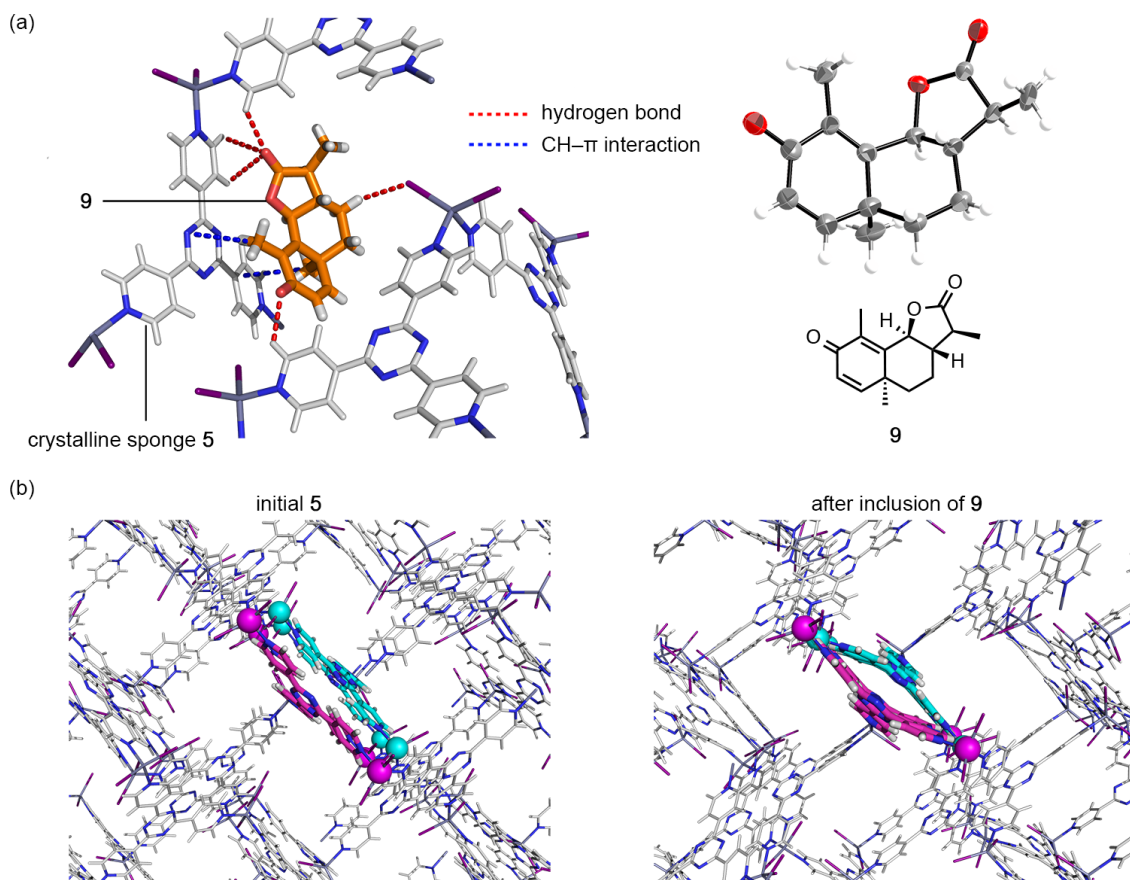
Synthesizing chiral molecules and determining the absolute structure of them are undoubtedly of great interest, but meanwhile, are still challenging.<sup>1</sup> For the synthesis and preparation of chiral molecules, the recent enantioselective synthesis method and chiral HPLC separation has been improved dramatically.<sup>2,3</sup> However, for the determination of the absolute structure, the analysis method is rather in the developing stage. X-ray crystallographic analysis based on the Bijvoet method is well established and widely used method as non-empirical determination of the absolute structure of the crystalline target.<sup>4</sup> For the non-crystalline material, some other spectroscopic methods such as the Mosher's method, the circular dichroism (CD) exciton chirality method, vibrational circular dichroism (VCD) method and others were developed.<sup>5-11</sup>

The absolute structure determination by the X-ray diffraction relies on an anomalous scattering effect of a heavy atom in the single crystal. When the target compound consists of only light C and H atoms, another few steps are required for installing a heavy atom to the target compound. In addition to that, unfortunately the crystallization attempts sometimes give no single crystal due to the intrinsic oily nature of the target compound even after derivatization. These disadvantages of the conventional X-ray crystallography for absolute structure determination are overcome by the crystalline sponge analysis using heavy atom incorporated porous complex **5**.

Here, it was demonstrated that the crystalline sponge method was applicable to the determination of the absolute structure of varieties of chiral molecules without installing heavy atom into the target compound.

## 4.2 Absolute structure determination of point chiral molecules

An absolute structure determination of point chiral molecule, santonin (**9**), was examined by the crystalline sponge method. The absolute structure of **9** was already determined 50 years ago, and **9** was widely recognized as a pharmaceutical compound.<sup>12</sup> A soaking experiment was carried out with cyclohexane solution of **9** (5  $\mu\text{g}/50 \mu\text{L}$ ) and a piece of crystal **5** by the method established in chapter 2. The resultant crystal was subjected to the X-ray diffraction analysis. The chiral **9** soaked crystalline sponge structure was solved in a chiral monoclinic  $P2_1$  space group, which was automatically determined by the XPREP program. In the crystal structure, included **9** structures were clearly observed along with the framework of **5** and its absolute structure was successfully assigned. The determined absolute structure was supported by the Flack parameter converged with reasonably small value, 0.092(18).<sup>13</sup> The change of the space group of the crystalline sponge from initial achiral monoclinic  $C2/c$  to chiral monoclinic  $P2_1$  was driven by the inclusion of **9**. The strong host-guest interactions such as hydrogen bonds between C–H $\cdots$ I, C–H $\cdots$ O and multiple CH– $\pi$  interaction were observed between **9** and framework of **5** (Figure 4.1a). The host crystalline sponge framework was chirally distorted by the molecular interactions and dense packing effects of the guest molecules. The positions of Zn and I atoms were slightly moved from the initial positions due to the rotation of pyridine moiety of ligand **1** (Figure 4.1b). The chiral distortion of the framework was propagated all over the crystal and also the chiral information was transferred. The strong interaction contributed not only for the chiral distortion of the host structure but also for small thermal factor of **9** by binding strongly to the framework.

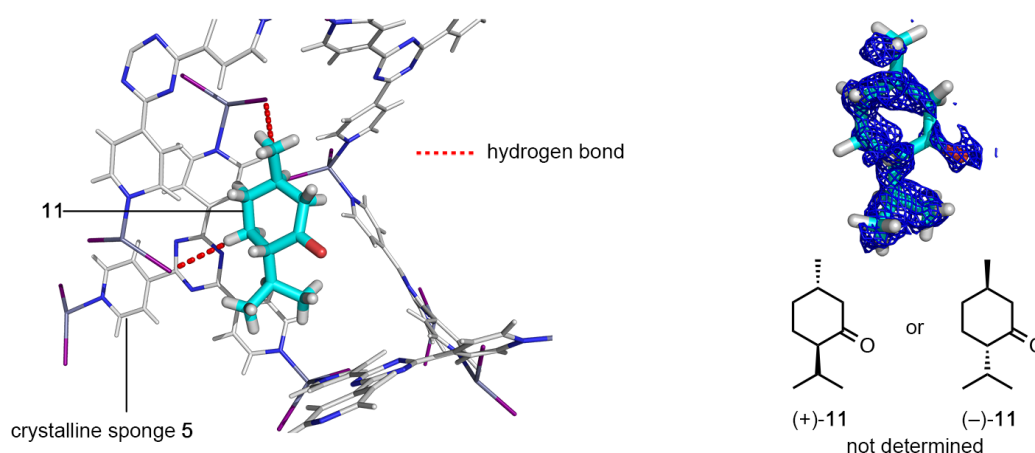


**Figure 4.1.** (a) Observed molecular interactions between **9** and crystalline sponge framework in the crystal structure of **5·9** and thermal factor of the included **9** drawn at the 50% probability level. (b) The distortion of the crystalline sponge framework after inclusion of **9**. Zn atoms and ligand **2** were represented in ball and stick model, respectively (included solvent and guest **9** were omitted for clarity).

In addition to **9**, the absolute structure of  $5\alpha$ -androstane (**10**), which consists of only light C and H atoms, was also determined by the crystalline sponge method. A cyclohexane solution of **10** ( $5\ \mu\text{g}/5\ \mu\text{L}$ ) was added to the crystalline sponge **5** and included into it. An X-ray analysis of resultant crystal **5·10** converged with monoclinic  $C2$  space group and revealed the correct absolute structure of included **10** along with the host framework (Figure S4.3). The Flack parameter was also converged with acceptable range, 0.02(3), for absolute structure determination.<sup>14</sup>

Surprisingly low Flack parameters for inclusion structures **5·9** and **5·10** were obtained even with the Mo  $K\alpha$  radiation X-ray source ( $\lambda = 0.71073\ \text{\AA}$ ) for the guest compounds **9** and **10**, which contain only light atoms. This was because of the

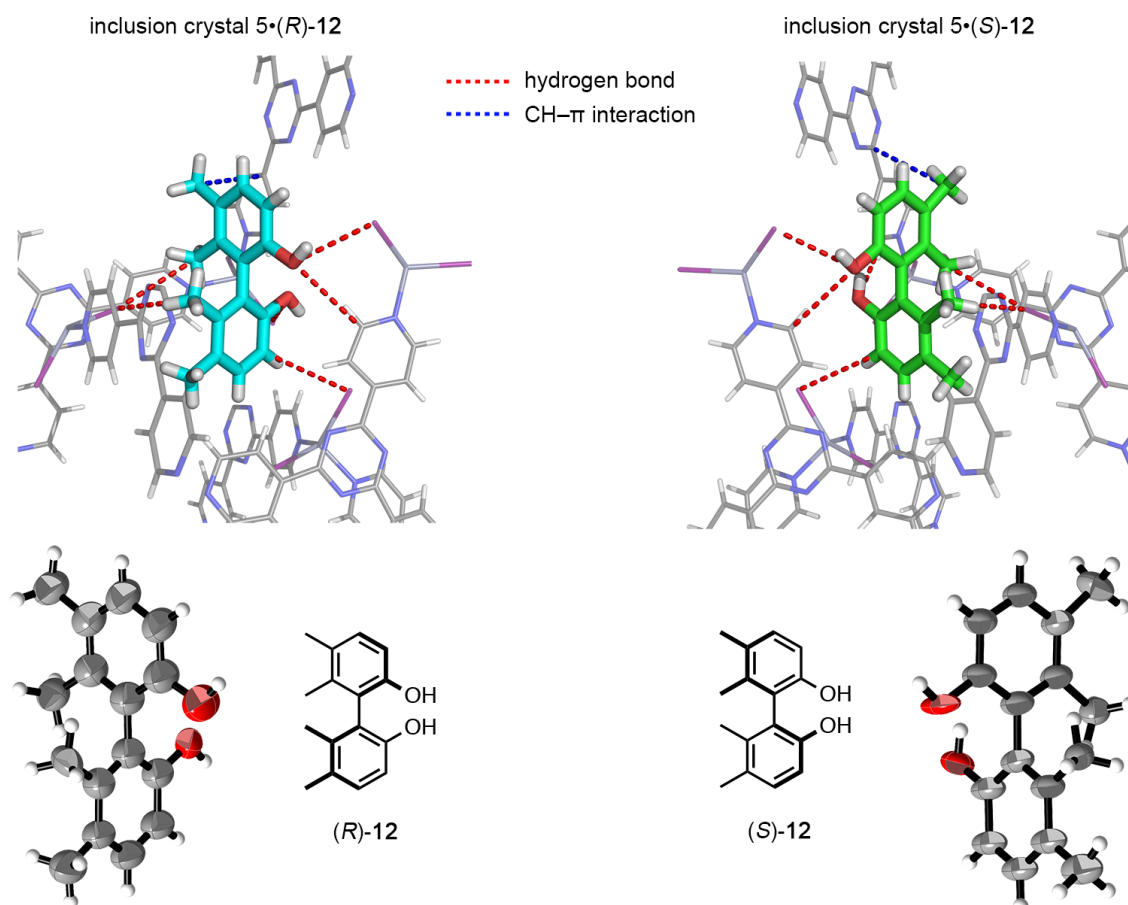
anomalous scattering effect of heavy Zn and I atoms in the host crystalline sponge **5**. However, when (–)-menthone (**11**) was analyzed by the crystalline sponge method, the Flack parameter converged with 0.46(6) and did not decrease below 0.3, *i.e.* the absolute structure could not be determined. The observed electron density around the guest structure was too weak and blurred to determine the structure (Figure 4.2). Though hydrogen bond was observed in the crystal structure of **5**•**11**, the numbers of observed interactions of **5**•**11** were relatively less than those of **5**•**9** and **5**•**10**. Moreover, the large void filled with the disordered solvent and guest molecules remained in the crystal structure even after the full assignment of the strong residual electron density. The loose packing of the structure also made the transfer of chiral information to the framework inefficient. These data gave an important insight about determining absolute structures by the crystalline sponge method based on the anomalous scattering effect of the host framework. The strong host-guest interactions are inevitable to induce the chirality of the whole inclusion crystal and also to use anomalous scattering effect of the host framework. If the target compound has less interaction or only weak interaction with the framework, chiral information of the guest molecules was not transferred, and the absolute structure of target molecules could not be determined by the crystalline sponge method.



**Figure 4.2.** Observed molecular interactions between **11** and crystalline sponge framework and observed electron density map ( $F_o$ , contour:  $0.4\sigma$ ) around **11**.

### 4.3 Absolute structure determination of axially chiral molecules

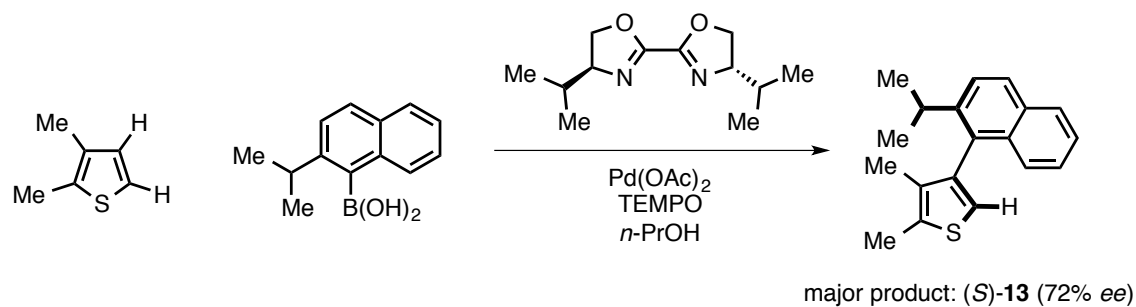
Encouraged by the success of absolute structure determination of **9** and **10**, crystalline sponge analysis of an axially chiral molecules was examined. Axially chiral compounds are often utilized as chiral ligands or auxiliaries. Due to their wide application, the synthetic method and chiral separation of axially chiral compounds are well studied and established. However, determining the absolute structure is rather less well-established.<sup>15,16</sup> Axially chiral compounds (*R*)- and (*S*)-5,5',6,6'-tetramethyl-1,1'-biphenyl-2,2'-diol (**12**) were analyzed by the crystalline sponge method. After inclusion of (*R*)-**12**, the resultant crystalline sponge showed good crystallinity and gave a good diffraction pattern. The structure was solved in a chiral monoclinic *C*2 space group, which was determined by the XPREP program. The X-ray analysis revealed included (*R*)-**12** molecule in the pore of the crystalline sponge **5** with a correct (*R*) stereochemistry. The Flack parameter of **5**•(*R*)-**12** was converged with a slightly high value, 0.187(8), however it was still in the range below 0.3. The enantiomer (*S*)-**12** also afforded inclusion complex **5**•(*S*)-**12**, and the crystal structure of **5**•(*S*)-**12** was also solved in monoclinic *C*2 space group. The included biphenyl structure was converged with (*S*) configuration with the Flack parameter 0.225(12). In the obtained structures, (*R*)-**12** and (*S*)-**12** were trapped by the same interaction with the host crystalline sponge. The proximal orientation of -OH groups of (*R*)-**12** and (*S*)-**12** and the iodine atom of the crystalline sponge in the obtained structure indicated the existence of O–H•••I hydrogen bond. Also, CH– $\pi$  interaction with the pyridine ligand was observed. Both inclusion structures **5**•(*R*)-**12** and **5**•(*S*)-**12** were observed in a relationship of the mirror image including trapped positions and observed interactions between **5** and **12** by reflecting the chirality of (*R*)-**12** and (*S*)-**12**. Though the refined occupancy of included (*R*)-**12** and (*S*)-**12** were moderate (~50%), the observed electron density maps were well superimposed on the each refined structures (Figure S4.6 and Figure S4.7). Thus, the obtained data quality was sufficient to determine the stereochemistry of the target (*R*)-**12** and (*S*)-**12**.



**Figure 4.3.** Observed mirror symmetry molecular interactions between **12** and crystalline sponge **5** and thermal factor of *(R)*-**12** and *(S)*-**12** drawn at 50% probability level.

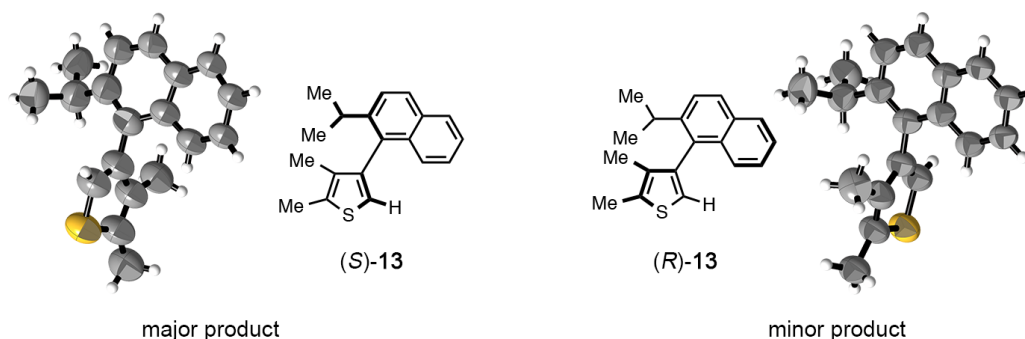
The absolute structure determination of axially chiral molecules by the crystalline sponge method was also applied to the biaryl compound 4-(2-isopropyl-naphthalen-1-yl)-2,3-dimethylthiophene (**13**). An enantioselective synthesis and chiral HPLC separation **13** were reported recently (Scheme 4.1).<sup>17</sup>

**Scheme 4.1.** An enantioselective synthesis of biaryl **13**.





Due to the oily nature of **13**, it was difficult to determine an absolute configuration of major product by conventional crystallization and X-ray analysis protocol. Therefore, a troublesome multistep derivatization and separation of diastereomers by a recrystallization process were required to determine the absolute structure. Considering the advantage of the crystalline sponge method, a few  $\mu\text{g}$  of chiral HPLC separated oily samples were enough to carry out the LC-SCD analysis. Therefore, chiral HPLC separated 1st fraction was dissolved in the 1,2-dichloroethane (1 mg/1 mL) and included into the crystalline sponge **5** for 2 d at 50 °C. After 2 d, the obtained crystal was subjected to the X-ray analysis. The X-ray crystal structural refinement was converged in a triclinic  $P1$  space group and showed included (*S*)-**13** along with the crystalline sponge framework. Though a positional disorder was observed for included (*S*)-**13**, the disordered model refinement was reasonably converged and fit on the observed electron density, and gave the small Flack parameter value, 0.198(10). As expected, the X-ray diffraction study of the 2nd fraction inclusion crystalline sponge showed included (*R*)-**13** molecule in the pore with the Flack parameter 0.153(8).



**Figure 4.4.** Obtained thermal factors of (*S*)-**13** and (*R*)-**13** by the crystalline sponge method (drawn at 50% probability level).

#### 4.4 Summary

In this chapter, the crystalline sponge method was applied to absolute structure determination of various molecules and was effective not only for the point chirality, but also for the axially chiral molecules. The important insight about the crystalline sponge method that strong molecular interaction is crucial for determining the absolute structure of guest molecules was also obtained. Though the careful structural analysis

was required, it is a great advantage of the crystalline sponge method that it does not require introduction of the heavy atom into the target compound.

## 4.5 Experimental section

Materials and Methods	81-84
Crystallographic data	85-91
<b>Scheme S4.1.</b> A synthesis of enantiomerically pure ( <i>R</i> )- <b>12</b> and ( <i>S</i> )- <b>12</b>	83
<b>Figure S4.2.</b> <sup>31</sup> P NMR spectra of ( <i>R</i> )- <b>12</b> precursor and ( <i>S</i> )- <b>12</b> precursor	83
<b>Figure S4.2-S4.8.</b> X-ray crystallographic data	85-91

## Materials and method

### Reagents and equipment

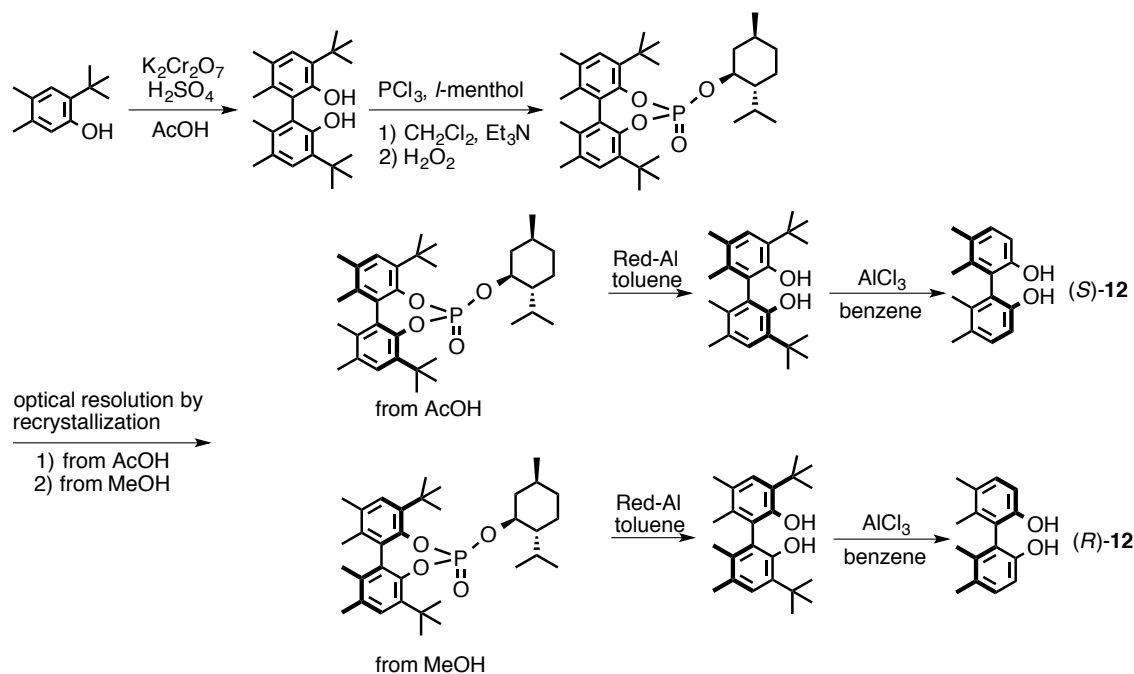
Solvents and reagents were purchased from TCI Co., Ltd., WAKO Pure Chemical Industries Ltd., and Sigma-Aldrich Corporation and used without further purification.

4-(2-isopropyl-naphthalen-1-yl)-2,3-dimethylthiophene was provided by the courtesy of Profs. Itami and Yamaguchi (Nagoya University).  $^1\text{H}$  NMR spectra and  $^{31}\text{P}$  NMR spectra were measured on a Bruker AVANCE III HD 500 MHz spectrometer equipped with 5 mm BBO gradient probe and a Bruker AVANCE 500 MHz spectrometer equipped with TCI gradient CryoProbe. All NMR spectra data were recorded at 300 K and chemical shift values are reported in parts per million (ppm) relative to an internal standard tetramethylsilane (for  $^1\text{H}$  NMR) or 85% phosphoric acid (for  $^{31}\text{P}$  NMR). Microscopic FT-IR spectra were recorded on a Varian DIGILAB Scimitar instrument and are reported in frequency of absorption ( $\text{cm}^{-1}$ ). Single crystal X-ray diffraction data were collected on a BRUKER APEX-II CCD diffractometer equipped with a focusing mirror ( $\text{MoK}_\alpha$  radiation  $\lambda = 0.71073 \text{ \AA}$ ) and a  $\text{N}_2$  generator (Japan Thermal Eng. Co., Ltd.) or Rigaku XtaLAB P200 diffractometer equipped with a PILATUS-200K detector with multi-layer mirror monochromator ( $\text{MoK}_\alpha$  radiation  $\lambda = 0.71073 \text{ \AA}$ ). For single crystal X-ray diffraction analysis and microscopic IR measurement, fluorolube® and mineral oil were used as a protectant for the single crystals.

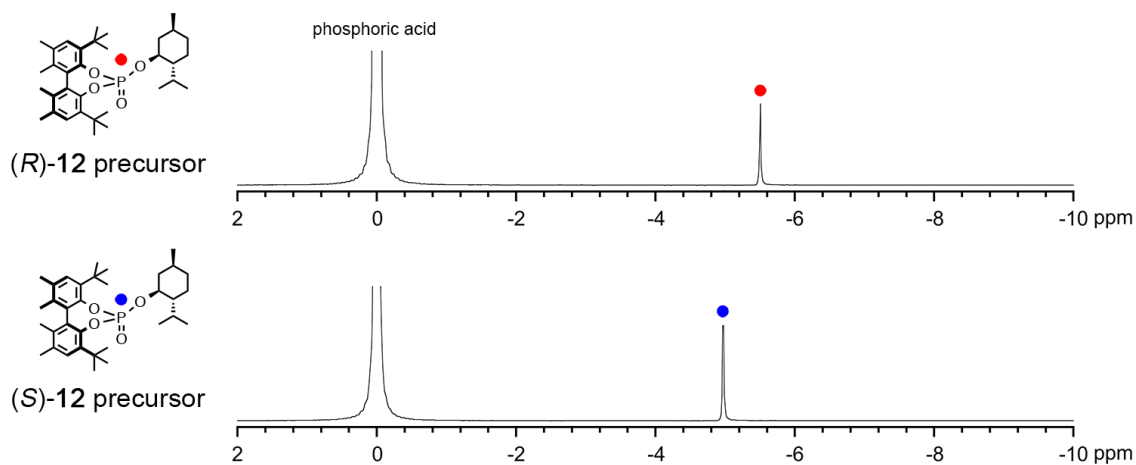
### X-ray crystallographic analysis

Single crystal X-ray diffraction data were processed with Bruker APEX2 software and CrystalClear program.<sup>18,19</sup> For Bruker data, absorption correction was performed by multi-scan method in SADABS and space groups were determined by XPREP program.<sup>1</sup> The structures were solved by direct methods and refined by full-matrix least-squares calculations on  $F^2$  using SHELXL-97 program.<sup>20</sup> In the determination of space group, the XPREP program suggested space group was employed for analyzing the structure.

After the initial phase determination, all the atoms for the host framework (*i.e.* ZnI<sub>2</sub> and tpt ligands) were assigned and the structure was refined anisotropically except for hydrogen atoms. Since the host framework was in some cases highly disordered, atoms were partially restrained with DFIX, FLAT, SIMU and ISOR commands. Atoms for the guest molecules (including solvent molecules) were then assigned to the residual Q-peaks. The guest structures were first refined isotropically with a suitable occupancy that is estimated by refinement using FVAR. If available, the guest structures were subsequently refined anisotropically. The final crystal structures leave large solvent-accessible voids where only weak Q-peaks were observed because that solvent or guest molecules are highly disordered. Such Q-peaks have been treated with PLATON SQUEEZE program, resulting in reasonable  $R_1$  and  $wR_2$  values as compared with  $R_{\text{int}}$ .<sup>21</sup> Note that due to the minor disorder with solvent molecules, the X-ray data quality of crystalline sponge method is rather lower than conventional single crystal X-ray analysis for small molecules using their pure single crystals.

**Synthesis and optical resolution of 5,5',6,6'-tetramethyl-1,1'-biphenyl-2,2'-diol (**12**)**Scheme S4.1. A synthesis of the enantiomerically pure (*R*)-**12** and (*S*)-**12**

According to the previously reported procedure, **12** was synthesized by oxidative homocoupling of 2-*tert*-butyl-4,5-dimethylphenol followed by an optical resolution and removal of *tert*-butyl group.<sup>22</sup> An optical resolution of **12** was performed by recrystallization from refluxing acetic acid and MeOH after derivatization of the oxidative coupling product with (–)-menthoxy dichlorophosphite. Enantiomerically pure (*R*)-**12** and (*S*)-**12** were obtained by removal of the phosphite and *tert*-butyl group from recrystallized pure diastereomers (> 99% *de*) in 7% overall yield at first recrystallization.



**Figure S4.1.** <sup>31</sup>P NMR spectra of obtained pure diastereomers by recrystallization (202 MHz, 300 K, CDCl<sub>3</sub>).

### **Inclusion of chiral guest molecules into crystalline sponge 5**

#### **General procedure for inclusion of guest molecules into crystalline sponge 5**

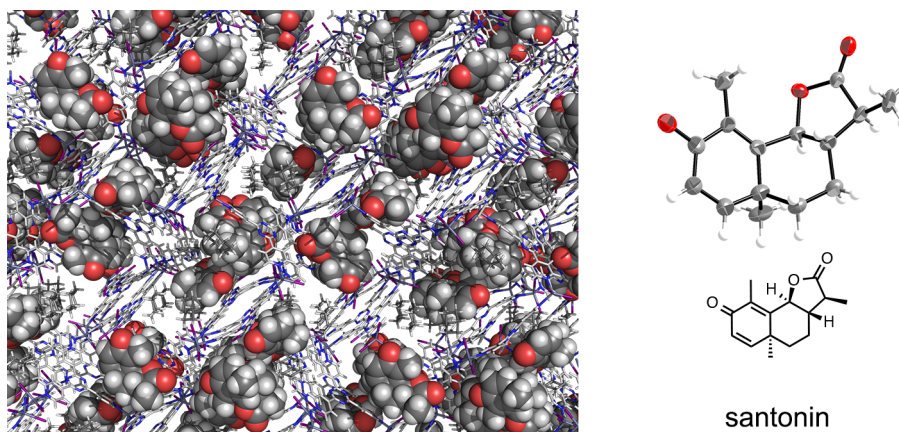
To a micro vial containing a cyclohexane exchanged single crystal of  $[(\text{ZnI}_2)_3(\text{tpt})_2]_n$  (**5**; tpt = tri(4-pyridyl)-1,3,5-triazine) and cyclohexane (75  $\mu\text{L}$ ), 5  $\mu\text{L}$  of 1,2-dichloroethane solution of target compounds (1 mg/1 mL) was added. Then, the crystal containing microvial was allowed to stand at 50 °C and the solvent was gradually evaporated over 2 d.

**Crystallographic data****Inclusion complex 5•9**

Crystallographic data (before the SQUEEZE treatment):  $C_{144}H_{96}N_{48}Zn_{12}I_{24} \cdot 5(C_{15}H_{16}O_3) \cdot 6(C_6H_{12})$ ,  $M = 8065.13$ , colorless rod,  $0.15 \times 0.05 \times 0.04 \text{ mm}^3$ , monoclinic, space group  $P2_1$ ,  $a = 32.866(5)$ ,  $b = 14.853(2)$ ,  $c = 34.850(6) \text{ \AA}$ ,  $\beta = 105.848(2)^\circ$ ,  $V = 16366(5) \text{ \AA}^3$ ,  $Z = 2$ ,  $D_c = 1.637 \text{ g/cm}^3$ ,  $F000 = 7752$ ,  $\mu = 3.182 \text{ mm}^{-1}$ ,  $T = 90(2) \text{ K}$ ,  $0.75 < \theta < 25.50^\circ$ , 48750 unique reflections out of 60731 with  $I > 2\sigma(I)$ ,  $R_{\text{int}} = 0.0825$ , 3187 parameters, 2149 restraints, GoF = 1.153, final  $R$  factors  $R_1 = 0.0933$  and  $wR_2 = 0.2215$  for all data, Flack parameter = 0.10(2). CCDC deposit number: unpublished result.

Crystallographic data (after the SQUEEZE treatment):  $C_{144}H_{96}N_{48}Zn_{12}I_{24} \cdot 5(C_{15}H_{16}O_3) \cdot 6(C_6H_{12})$ ,  $M = 8065.13$ , colorless rod,  $0.15 \times 0.05 \times 0.04 \text{ mm}^3$ , monoclinic, space group  $P2_1$ ,  $a = 32.866(5)$ ,  $b = 14.853(2)$ ,  $c = 34.850(6) \text{ \AA}$ ,  $\beta = 105.848(2)^\circ$ ,  $V = 16366(5) \text{ \AA}^3$ ,  $Z = 2$ ,  $D_c = 1.637 \text{ g/cm}^3$ ,  $F000 = 7752$ ,  $\mu = 3.182 \text{ mm}^{-1}$ ,  $T = 90(2) \text{ K}$ ,  $0.75 < \theta < 25.50^\circ$ , 48049 unique reflections out of 60731 with  $I > 2\sigma(I)$ ,  $R_{\text{int}} = 0.0818$ , 3187 parameters, 2227 restraints, GoF = 1.101, final  $R$  factors  $R_1 = 0.0827$  and  $wR_2 = 0.1813$  for all data, Flack parameter = 0.092(818). CCDC deposit number: 910390.

IR (single crystal, fluorolube): 3081, 3061, 2926, 2854, 1780, 1630, 1514, 1370  $\text{cm}^{-1}$ .



**Figure S4.2.** The X-ray crystal structure of **5•9**. Guest molecules were drawn in CPK model in the packing structure and the thermal ellipsoid of the guest molecule was drawn at the 50% probability level.

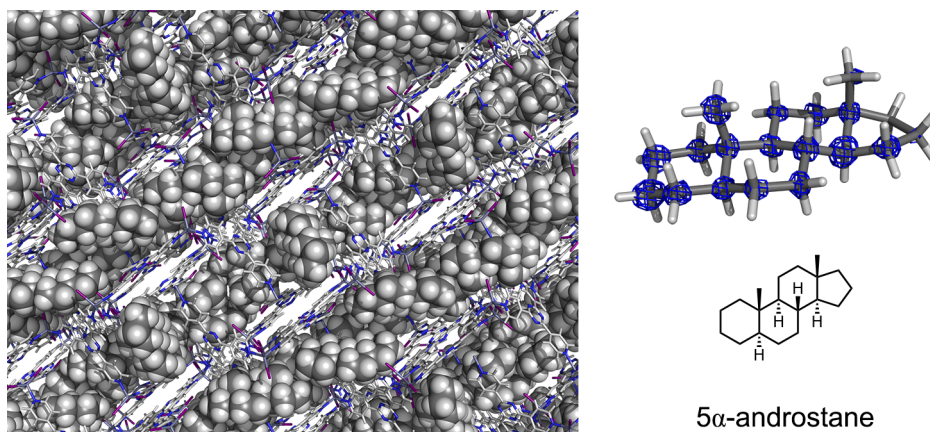


**Inclusion complex 5•10**

Crystallographic data (before the SQUEEZE treatment):  $C_{72}H_{48}N_{24}Zn_6I_{12} \cdot 2.43(C_{19}H_{32}) \cdot 1.37(C_6H_{12})$ ,  $M = 3912.58$ , colorless rod,  $0.23 \times 0.07 \times 0.06 \text{ mm}^3$ , monoclinic, space group  $C2$ ,  $a = 35.191(3)$ ,  $b = 14.9332(10)$ ,  $c = 30.983(2) \text{ \AA}$ ,  $\beta = 102.740(3)^\circ$ ,  $V = 15881(2) \text{ \AA}^3$ ,  $Z = 4$ ,  $D_c = 1.636 \text{ g/cm}^3$ ,  $F000 = 7538$ ,  $\mu = 3.273 \text{ mm}^{-1}$ ,  $T = 93(2) \text{ K}$ ,  $1.228 < \theta < 25.355^\circ$ , 22164 unique reflections out of 28131 with  $I > 2\sigma(I)$ ,  $R_{\text{int}} = 0.0477$ , 1335 parameters, 255 restraints,  $\text{GoF} = 1.016$ , final  $R$  factors  $R_1 = 0.0573$  and  $wR_2 = 0.1865$  for all data, Flack parameter =  $0.02(3)$ . CCDC deposit number: unpublished result.

Crystallographic data (after the SQUEEZE treatment):  $C_{72}H_{48}N_{24}Zn_6I_{12} \cdot 2.43(C_{19}H_{32}) \cdot 1.37(C_6H_{12})$ ,  $M = 3912.58$ , colorless rod,  $0.23 \times 0.07 \times 0.06 \text{ mm}^3$ , monoclinic, space group  $C2$ ,  $a = 35.191(3)$ ,  $b = 14.9332(10)$ ,  $c = 30.983(2) \text{ \AA}$ ,  $\beta = 102.740(3)^\circ$ ,  $V = 15881(2) \text{ \AA}^3$ ,  $Z = 4$ ,  $D_c = 1.636 \text{ g/cm}^3$ ,  $F000 = 7538$ ,  $\mu = 3.273 \text{ mm}^{-1}$ ,  $T = 93(2) \text{ K}$ ,  $1.228 < \theta < 25.355^\circ$ , 22168 unique reflections out of 28131 with  $I > 2\sigma(I)$ ,  $R_{\text{int}} = 0.0477$ , 1335 parameters, 255 restraints,  $\text{GoF} = 1.016$ , final  $R$  factors  $R_1 = 0.0556$  and  $wR_2 = 0.1708$  for all data, Flack parameter =  $0.03(3)$ . CCDC deposit number: unpublished result.

IR (single crystal, fluorolube): 3055, 2926, 2852, 1618, 1577, 1519, 1450, 1377  $\text{cm}^{-1}$ .



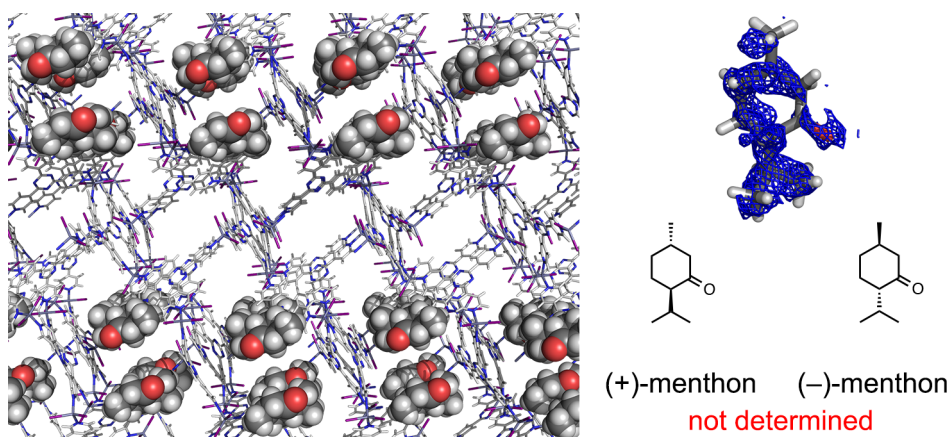
**Figure S4.3.** The X-ray crystal structure of **5•10** and the observed electron density map ( $F_o$ , contour:  $0.6\sigma$ ). Guest molecules were drawn in CPK model in the packing structure.

**Inclusion complex 5•11**

Crystallographic data (before the SQUEEZE treatment):  $C_{72}H_{48}N_{24}Zn_6I_{12} \cdot 0.69(C_{10}H_{18}O)$ ,  $M = 3271.14$ , colorless rod,  $0.09 \times 0.07 \times 0.07 \text{ mm}^3$ , monoclinic, space group  $C2$ ,  $a = 35.0669(10)$ ,  $b = 14.590(3)$ ,  $c = 33.9869(10) \text{ \AA}$ ,  $\beta = 107.758(3)^\circ$ ,  $V = 16560(3) \text{ \AA}^3$ ,  $Z = 4$ ,  $D_c = 1.312 \text{ g/cm}^3$ ,  $F000 = 6094$ ,  $\mu = 3.125 \text{ mm}^{-1}$ ,  $T = 93(2) \text{ K}$ ,  $1.190 < \theta < 26.212^\circ$ , 10676 unique reflections out of 29637 with  $I > 2\sigma(I)$ ,  $R_{\text{int}} = 0.1229$ , 1073 parameters, 678 restraints, GoF = 1.110 final  $R$  factors  $R_1 = 0.1087$  and  $wR_2 = 0.3332$  for all data, Flack parameter = 0.46(6). CCDC deposit number: unpublished result.

Crystallographic data (after the SQUEEZE treatment):  $C_{72}H_{48}N_{24}Zn_6I_{12} \cdot 0.69(C_{10}H_{18}O)$ ,  $M = 3271.14$ , colorless rod,  $0.09 \times 0.07 \times 0.07 \text{ mm}^3$ , monoclinic, space group  $C2$ ,  $a = 35.0669(10)$ ,  $b = 14.590(3)$ ,  $c = 33.9869(10) \text{ \AA}$ ,  $\beta = 107.758(3)^\circ$ ,  $V = 16560(3) \text{ \AA}^3$ ,  $Z = 4$ ,  $D_c = 1.312 \text{ g/cm}^3$ ,  $F000 = 6094$ ,  $\mu = 3.125 \text{ mm}^{-1}$ ,  $T = 93(2) \text{ K}$ ,  $1.190 < \theta < 26.212^\circ$ , 10550 unique reflections out of 29637 with  $I > 2\sigma(I)$ ,  $R_{\text{int}} = 0.1229$ , 1073 parameters, 678 restraints, GoF = 0.770 final  $R$  factors  $R_1 = 0.736$  and  $wR_2 = 0.2128$  for all data, Flack parameter = 0.52(4). CCDC deposit number: unpublished result.

IR (single crystal, fluorolube): 2926, 1740, 1599, 1560, 1482, 1420, 1366  $\text{cm}^{-1}$ .



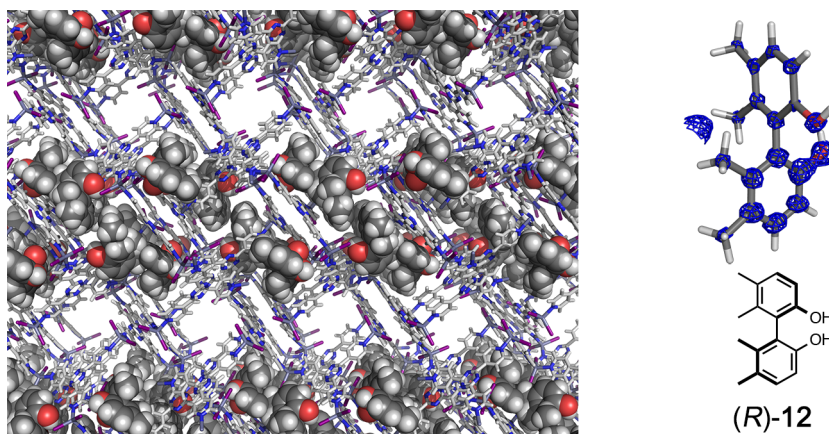
**Figure S4.4.** The X-ray crystal structure of **5•11** and the observed electron density map ( $F_o$ , contour:  $0.3\sigma$ ). Guest molecules were drawn in CPK model in the packing structure.

**Inclusion complex 5•(R)-12**

Crystallographic data (before the SQUEEZE treatment):  $C_{72}H_{48}N_{24}Zn_6I_{12} \cdot 0.92(C_{16}H_{16}O_2)$   $M = 3388.49$ , colorless block,  $0.12 \times 0.08 \times 0.08 \text{ mm}^3$ , monoclinic, space group  $C2$ ,  $a = 34.200(3) \text{ \AA}$ ,  $b = 15.1265(13) \text{ \AA}$ ,  $c = 31.003(3) \text{ \AA}$ ,  $\beta = 102.3850(10)^\circ$ ,  $V = 15665(2) \text{ \AA}^3$ ,  $Z = 4$ ,  $D_c = 1.437 \text{ g/cm}^3$ ,  $F000 = 6337$ ,  $\mu = 3.306 \text{ mm}^{-1}$ ,  $T = 90(2) \text{ K}$ ,  $1.219 < \theta < 26.437^\circ$ , 21133 unique reflections out of 32155 with  $I > 2\sigma(I)$ ,  $R_{\text{int}} = 0.0315$ , 1542 parameters, 1823 restraints,  $\text{GoF} = 1.045$ , final  $R$  factors  $R_1 = 0.1009$ , and  $wR_2 = 0.3214$  for all data, Flack parameter = 0.187(8). CCDC deposit number: unpublished result.

Crystallographic data (after the SQUEEZE treatment):  $C_{72}H_{48}N_{24}Zn_6I_{12} \cdot 0.92(C_{16}H_{16}O_2)$   $M = 3388.49$ , colorless block,  $0.12 \times 0.08 \times 0.08 \text{ mm}^3$ , Monoclinic, space group  $C2$ ,  $a = 34.200(3) \text{ \AA}$ ,  $b = 15.1265(13) \text{ \AA}$ ,  $c = 31.003(3) \text{ \AA}$ ,  $\beta = 102.3850(10)^\circ$ ,  $V = 15665(2) \text{ \AA}^3$ ,  $Z = 4$ ,  $D_c = 1.437 \text{ g/cm}^3$ ,  $F000 = 6337$ ,  $\mu = 3.306 \text{ mm}^{-1}$ ,  $T = 90(2) \text{ K}$ ,  $1.219 < \theta < 26.437^\circ$ , 20500 unique reflections out of 32155 with  $I > 2\sigma(I)$ ,  $R_{\text{int}} = 0.0289$ , 1542 parameters, 1829 restraints,  $\text{GoF} = 1.125$ , final  $R$  factors  $R_1 = 0.0693$ , and  $wR_2 = 0.2201$  for all data, Flack parameter = 0.156(8). CCDC deposit number: unpublished result.

IR (single crystal, fluorolube): 3495, 3053, 2918, 2851, 1616, 1576, 1529, 1466, 1423, 1375,  $1316 \text{ cm}^{-1}$ .



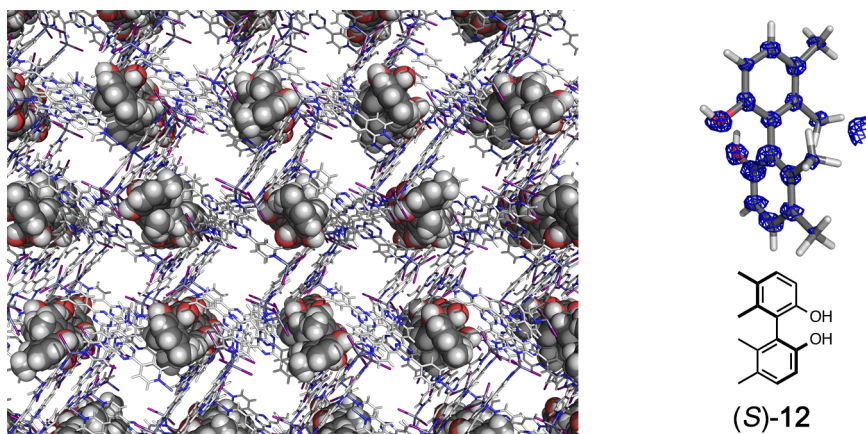
**Figure S4.5.** The X-ray crystal structure of **5•(R)-12** and the observed electron density map ( $F_o$ , contour:  $0.7\sigma$ ). Guest molecules were drawn in CPK model in the packing structure.

**Inclusion complex 5•(S)-12**

Crystallographic data (before the SQUEEZE treatment):  $C_{72}H_{48}N_{24}Zn_6I_{12} \cdot 0.91(C_{16}H_{18}O_2)$ ,  $M = 3385.17$ , colorless rod,  $0.06 \times 0.05 \times 0.03 \text{ mm}^3$ , monoclinic, space group  $C2$ ,  $a = 34.237(3)$ ,  $b = 15.1451(3)$ ,  $c = 30.952(3) \text{ \AA}$ ,  $\beta = 102.7340(3)^\circ$ ,  $V = 15655(2) \text{ \AA}^3$ ,  $Z = 4$ ,  $D_c = 1.436 \text{ g/cm}^3$ ,  $F000 = 6330$ ,  $\mu = 3.309 \text{ mm}^{-1}$ ,  $T = 90(2) \text{ K}$ ,  $1.219 < \theta < 24.692^\circ$ , 17303 unique reflections out of 26051 with  $I > 2\sigma(I)$ ,  $R_{\text{int}} = 0.0511$ , 1521 parameters, 1536 restraints,  $\text{GoF} = 1.048$ , final  $R$  factors  $R_1 = 0.1071$  and  $wR_2 = 0.3238$  for all data, Flack parameter =  $0.225(12)$ . CCDC deposit number: unpublished result.

Crystallographic data (after the SQUEEZE treatment):  $C_{72}H_{48}N_{24}Zn_6I_{12} \cdot 0.91(C_{16}H_{18}O_2)$ ,  $M = 3385.17$ , colorless rod,  $0.06 \times 0.05 \times 0.03 \text{ mm}^3$ , monoclinic, space group  $C2$ ,  $a = 34.237(3)$ ,  $b = 15.1451(3)$ ,  $c = 30.952(3) \text{ \AA}$ ,  $\beta = 102.7340(3)^\circ$ ,  $V = 15655(2) \text{ \AA}^3$ ,  $Z = 4$ ,  $D_c = 1.436 \text{ g/cm}^3$ ,  $F000 = 6330$ ,  $\mu = 3.309 \text{ mm}^{-1}$ ,  $T = 90(2) \text{ K}$ ,  $1.219 < \theta < 24.692^\circ$ , 16662 unique reflections out of 26051 with  $I > 2\sigma(I)$ ,  $R_{\text{int}} = 0.0511$ , 1521 parameters, 1536 restraints,  $\text{GoF} = 1.091$ , final  $R$  factors  $R_1 = 0.0731$  and  $wR_2 = 0.2199$  for all data, Flack parameter =  $0.195(13)$ . CCDC deposit number: unpublished result.

IR (single crystal, fluorolube): 3528, 3053, 2924, 2850, 1616, 1578, 1514, 1468, 1422, 1377,  $1316 \text{ cm}^{-1}$ .



**Figure S4.6.** The X-ray crystal structure of **5•(S)-12** and the observed electron density map ( $F_o$ , contour:  $0.7\sigma$ ). Guest molecules were drawn in CPK model in the packing structure.

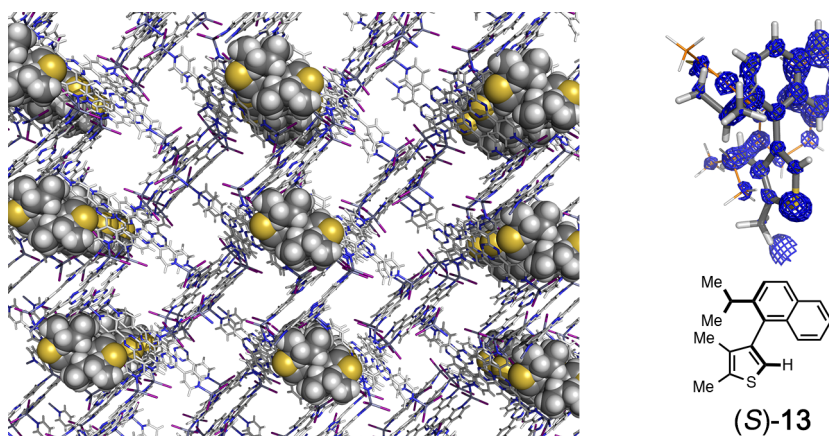


**Inclusion complex 1•(S)-13 (first fraction)**

Crystallographic data (before the SQUEEZE treatment):  $C_{144}H_{96}N_{48}Zn_{12}I_{24} \cdot C_{19}H_{20}S$ ,  $M = 6609.13$ , colorless block,  $0.1 \times 0.08 \times 0.05 \text{ mm}^3$ , triclinic, space group  $P1$ ,  $a = 15.0996(13) \text{ \AA}$ ,  $b = 18.7767(16) \text{ \AA}$ ,  $c = 29.882(3) \text{ \AA}$ ,  $\alpha = 79.6740(10)^\circ$ ,  $\beta = 102.3850(10)^\circ$ ,  $\gamma = 66.2770(10)^\circ$ ,  $V = 7606.5(11) \text{ \AA}^3$ ,  $Z = 1$ ,  $D_c = 1.443 \text{ g/cm}^3$ ,  $F000 = 3078$ ,  $\mu = 3.408 \text{ mm}^{-1}$ ,  $T = 90(2) \text{ K}$ ,  $1.208 < \theta < 26.392^\circ$ , 32754 unique reflections out of 60654 with  $I > 2\sigma(I)$ ,  $R_{\text{int}} = 0.0176$ , 2576 parameters, 2282 restraints,  $\text{GoF} = 1.034$ , final  $R$  factors  $R_1 = 0.0880$ , and  $wR_2 = 0.3208$  for all data, Flack parameter =  $0.266(10)$ . CCDC deposit number: unpublished result.

Crystallographic data (after the SQUEEZE treatment):  $C_{144}H_{96}N_{48}Zn_{12}I_{24} \cdot C_{19}H_{20}S$ ,  $M = 6609.13$ , colorless block,  $0.1 \times 0.08 \times 0.05 \text{ mm}^3$ , triclinic, space group  $P1$ ,  $a = 15.0996(13) \text{ \AA}$ ,  $b = 18.7767(16) \text{ \AA}$ ,  $c = 29.882(3) \text{ \AA}$ ,  $\alpha = 79.6740(10)^\circ$ ,  $\beta = 102.3850(10)^\circ$ ,  $\gamma = 66.2770(10)^\circ$ ,  $V = 7606.5(11) \text{ \AA}^3$ ,  $Z = 1$ ,  $D_c = 1.443 \text{ g/cm}^3$ ,  $F000 = 3078$ ,  $\mu = 3.408 \text{ mm}^{-1}$ ,  $T = 90(2) \text{ K}$ ,  $1.208 < \theta < 26.392^\circ$ , 31612 unique reflections out of 60654 with  $I > 2\sigma(I)$ ,  $R_{\text{int}} = 0.0167$ , 2576 parameters, 2294 restraints,  $\text{GoF} = 1.156$ , final  $R$  factors  $R_1 = 0.0487$ , and  $wR_2 = 0.1281$  for all data, Flack parameter =  $0.198(10)$ . CCDC deposit number: unpublished result.

IR (single crystal, mineral oil): 3358, 3054, 2953, 2855, 1672, 1618, 1576, 1523, 1423, 1374,  $1316 \text{ cm}^{-1}$ .



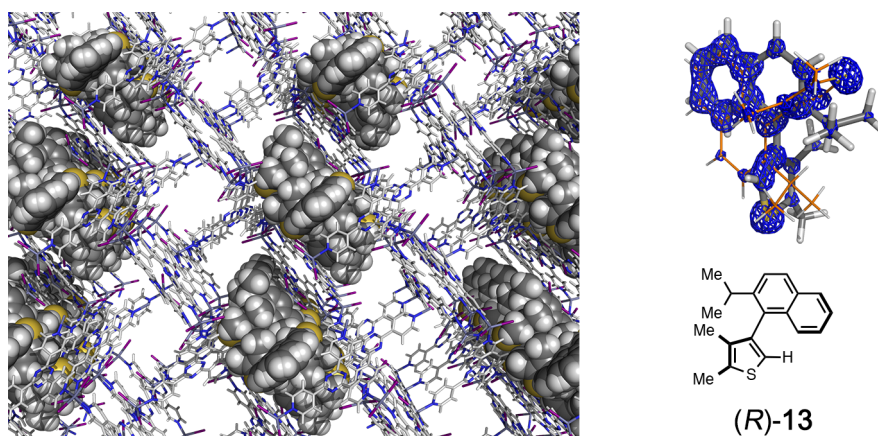
**Figure S4.7.** The X-ray crystal structure of **5•(S)-13** and the observed electron density map ( $F_o$ , contour:  $0.5\sigma$ ). Guest molecules were drawn in CPK model in the packing structure. Disordered guest counter part was shown in narrow orange stick in the density map.

**Inclusion complex 1•(R)-13 (second fraction)**

Crystallographic data (before the SQUEEZE treatment):  $C_{144}H_{96}N_{48}Zn_{12}I_{24} \cdot 2(C_{19}H_{20}S)$ ,  $M = 6889.54$ , colorless block,  $0.07 \times 0.07 \times 0.05 \text{ mm}^3$ , triclinic, space group  $P1$ ,  $a = 14.9240(14) \text{ \AA}$ ,  $b = 18.8308(19) \text{ \AA}$ ,  $c = 31.302(3) \text{ \AA}$ ,  $\alpha = 78.7840(10)^\circ$ ,  $\beta = 89.8980(10)^\circ$ ,  $\gamma = 66.6710(10)^\circ$ ,  $V = 7894.5(13) \text{ \AA}^3$ ,  $Z = 1$ ,  $D_c = 1.449 \text{ g/cm}^3$ ,  $F000 = 3228$ ,  $\mu = 3.294 \text{ mm}^{-1}$ ,  $T = 90(2) \text{ K}$ ,  $0.666 < \theta < 25.701^\circ$ , 39457 unique reflections out of 59075 with  $I > 2\sigma(I)$ ,  $R_{\text{int}} = 0.0258$ , 2990 parameters, 2850 restraints,  $\text{GoF} = 1.072$ , final  $R$  factors  $R_1 = 0.0682$ , and  $wR_2 = 0.2391$  for all data, Flack parameter = 0.218(7). CCDC deposit number: unpublished result.

Crystallographic data (after the SQUEEZE treatment):  $C_{144}H_{96}N_{48}Zn_{12}I_{24} \cdot 2(C_{19}H_{20}S)$ ,  $M = 6889.54$ , colorless block,  $0.07 \times 0.07 \times 0.05 \text{ mm}^3$ , triclinic, space group  $P1$ ,  $a = 14.9240(14) \text{ \AA}$ ,  $b = 18.8308(19) \text{ \AA}$ ,  $c = 31.302(3) \text{ \AA}$ ,  $\alpha = 78.7840(10)^\circ$ ,  $\beta = 89.8980(10)^\circ$ ,  $\gamma = 66.6710(10)^\circ$ ,  $V = 7894.5(13) \text{ \AA}^3$ ,  $Z = 1$ ,  $D_c = 1.449 \text{ g/cm}^3$ ,  $F000 = 3228$ ,  $\mu = 3.294 \text{ mm}^{-1}$ ,  $T = 90(2) \text{ K}$ ,  $0.666 < \theta < 25.701^\circ$ , 38886 unique reflections out of 59075 with  $I > 2\sigma(I)$ ,  $R_{\text{int}} = 0.0242$ , 2990 parameters, 2856 restraints,  $\text{GoF} = 1.103$ , final  $R$  factors  $R_1 = 0.0440$ , and  $wR_2 = 0.1296$  for all data, Flack parameter = 0.153(8). CCDC deposit number: unpublished result.

IR (single crystal, mineral oil): 3356, 3054, 2930, 2852, 1672, 1618, 1578, 1530, 1423, 1378, 1316  $\text{cm}^{-1}$ .



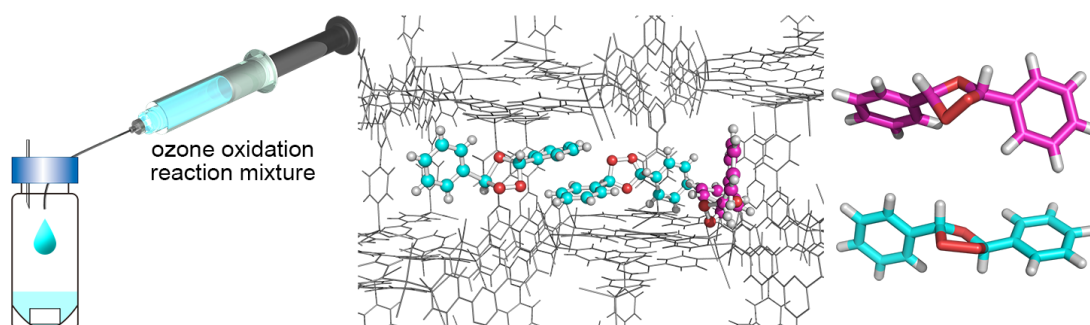
**Figure S4.8.** The X-ray crystal structure of **5•(R)-13** and the observed electron density map ( $F_o$ , contour:  $0.7\sigma$ ). Guest molecules were drawn in CPK model in the packing structure. Disorderd guest counter part was shown in narrow orange stick in the density map.

## References

- 1 H. D. Flack, G. Bernardinelli, *Chirality* **2008**, *20*, 681–690.
- 2 T. J. Ward, K. D. Ward, *Anal. Chem.* **2010**, *82*, 4712–4722.
- 3 Y. Okamoto, T. Ikai, *Chem. Soc. Rev.* **2008**, *37*, 2593–2608.
- 4 J. M. Bijvoet, A. F. Peerdeman, A. J. van Bommel, *Nature* **1951**, *168*, 271–272.
- 5 J. A. Dale, H. S. Mosher, *J. Am. Chem. Soc.* **1973**, *95*, 512–519.
- 6 I. Ohtani, T. Kusumi, Y. Kashman, H. Kakisawa, *J. Am. Chem. Soc.* **1991**, *113*, 4092–4096.
- 7 P. J. Stephens, *J. Phys. Chem.* **1985**, *89*, 748–752.
- 8 T. B. Freedman, X. Cao, R. K. Dukor, L. A. Nafie, *Chirality* **2003**, *15*, 743–758.
- 9 P. J. Stephens, F. J. Devlin, J.-J. Pan, *Chirality* **2008**, *20*, 643–663.
- 10 L. D. Barron, M. P. Bogaard, A. D. Buckingham, *J. Am. Chem. Soc.* **1973**, *95*, 603–605.
- 11 P. Herwig, K. Zawatzky, M. Grieser, O. Heber, B. Jordon-Thaden, C. Krantz, O. Novotný, R. Repnow, V. Schurig, D. Schwalm, Z. Vager, A. Wolf, O. Trapp, H. Kreckel, *Science* **2013**, *342*, 1084–1086.
- 12 E. J. Corey, *J. Am. Chem. Soc.* **1955**, *77*, 1044–1045.
- 13 H. D. Flack, G. Bernardinelli, *Acta Cryst.* **1999**, *A55*, 908–915.
- 14 H. D. Flack, G. Bernardinelli, *J. Appl. Crystallogr.* **2000**, *33*, 1143–1148.
- 15 O. Baudoin, *Eur. J. Org. Chem.* **2005**, *20*, 4223–4229.
- 16 G. Bringmann, A. J. Price Mortimer, P. A. Keller, M. J. Gresser, J. Garner, M. Breuning, *Angew. Chem. Int. Ed.* **2005**, *44*, 5384–5427.
- 17 K. Yamaguchi, J. Yamaguchi, A. Studer, K. Itami, *Chem. Sci.* **2012**, *3*, 2165–2169.
- 18 *APEX2*, *SADABS* and *XPREP*, Bruker AXS Inc., Madison, Wisconsin, USA, 2007.
- 19 *CrystalClear-SM Expert 2.1 b32*, Rigaku Corporation, Tokyo, Japan, 2013.
- 20 G. M. Sheldrick, *Acta Cryst.* **2008**, *A64*, 112–122.
- 21 P. van der Sluis, A. L. Spek, *Acta Cryst.* **1990**, *A46*, 194–201.
- 22 J. B. Alexander, R. R. Schrock, W. M. Davis, K. C. Hultsch, A. H. Hoveyda, J. H. Houser, *Organometallics* **2000**, *19*, 3700–3715.

## Chapter 5

### X-ray Analysis of Ozonides by the Crystalline Sponge Method



#### Abstract

Risk free X-ray crystallographic analyses of potentially explosive secondary ozonides were performed by the crystalline sponge method. Varieties of the secondary ozonide structures were successfully determined directly from 5  $\mu\text{L}$  of the ozone oxidation reaction mixture without isolation. Furthermore, when the reaction mixture contained two diastereomers, both isomers were included together into one crystalline sponge and observed at different positions in the pore. The huge potential of the crystalline sponge for the safe scale X-ray analysis of dangerous compounds was demonstrated.



## 5.1 Introduction

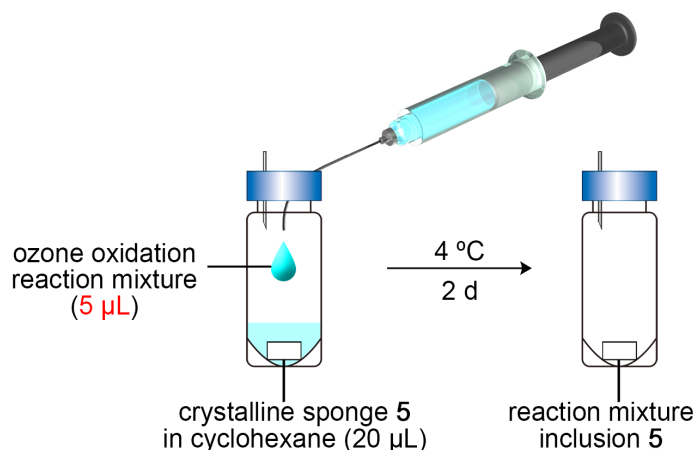
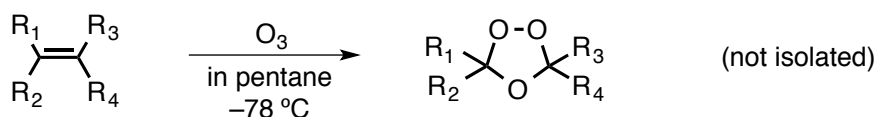
Analysis of a dangerous compound such as explosive, toxic and pyrophoric molecules has difficulty due to the limitation on the experimental or analytical equipment and limitation on the handling scale of dangerous compounds especially for the laboratory experiment.<sup>1</sup> Considering a typical potentially explosive compound, ozonide, an experiment should be carried out under the low temperature, and an experimental scale should be milligram order in diluted conditions.<sup>2-4</sup> Furthermore, the generated ozonides are normally used for the successive reaction without isolation or purification. Due to these limitations, the number of reported X-ray crystal structures of potentially explosive ozonides are quite limited, and most of the reported structures are ozonides stabilized with bulky substituents.<sup>5</sup>

One of the biggest advantages of the crystalline sponge method is its extremely small experimental scale. The crystalline sponge absorbs and aligns the target compound in its pore even from a diluted solution of the microgram scale of analyte. This ultra small experimental scale matches well for the requirement of the treatment of the dangerous compounds. In this chapter, the X-ray diffraction analyses of the potentially explosive ozonides were safely carried out and successfully determined some ozonide structures by the crystalline sponge method. In addition to the treating of the ozonide in microgram scale, the crystalline sponge analyses of ozonides were carried out without isolation or purification of the reaction mixture.

## 5.2 Microgram scale ozonide inclusion into the crystalline sponge

Secondary ozonides used in this chapter were synthesized by ozone oxidation of corresponding olefins in 5 mg scale at  $-78\text{ }^{\circ}\text{C}$  in 5 mL of *n*-pentane (Scheme 5.1). From the crude reaction mixture, only 5  $\mu\text{L}$  of solution was directly used for inclusion without isolation or purification so that potentially explosive ozonides were treated safely in microgram scale. Furthermore, ozonides inclusion into the crystalline sponge was carried out at lower temperature of  $4\text{ }^{\circ}\text{C}$  in order to suppress the thermal decomposition of the ozonides (Figure 5.1).<sup>6</sup>

**Scheme 5.1.** A synthesis of the secondary ozonide.

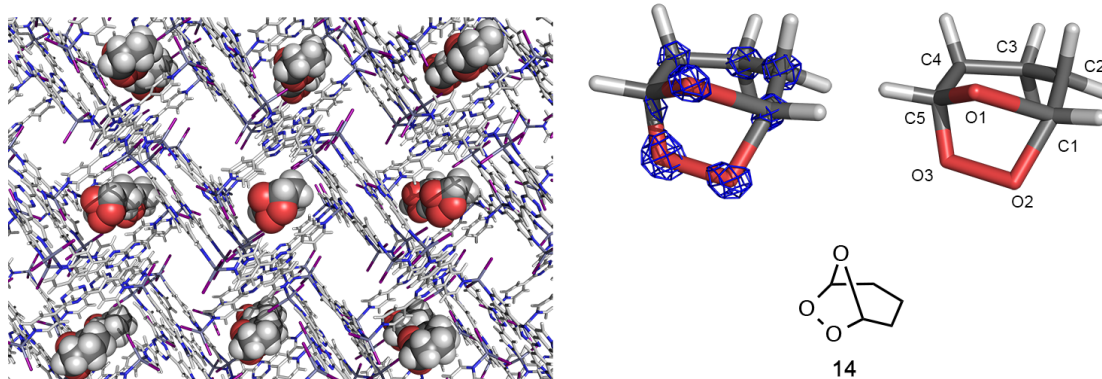


**Figure 5.1.** A schematic illustration of the microgram scale safe inclusion procedure of ozone oxidation reaction mixture into the crystalline sponge.

## 5.3 X-ray analysis of cyclopentene ozonide by the crystalline sponge method

An *n*-pentane solution of cyclopentene (5 mg/5 mL) was oxidized by an ozone gas (0.4 L/min, 400 ppm) at  $-78\text{ }^{\circ}\text{C}$  for 1 h. The completion of the ozone oxidation was monitored by an NMR spectroscopy. Since the molecular weight of cyclopentene ozonide (**14**) is quite low, its oxygen atom content is 41% and volatility is also high.<sup>7</sup> Therefore, preparing a single crystal of **14** by recrystallization is difficult. After the complete conversion of the starting cyclopentene, 5  $\mu\text{L}$  of the crude reaction mixture

was poured into crystalline sponge **5**, and inclusion was performed at 4°C for 2 d. The X-ray diffraction study of the resultant crystal revealed stably included cyclopentene ozonide (**14**) structure in the pore of the crystalline sponge. The refined structure was converged without any restraints or constraints on **14** and well superimposed on the observed electron density map (Figure 5.2). In the crystal structure **5**•**14**, solvent cyclohexane was also observed and was densely packed interacting with **14**, while the structure still contained a large solvent accessible void after an assignment of the strong residual electron density. This large solvent accessible void was derived from highly disordered structure with guest **14** and/or solvent cyclohexane, which could not be modeled. For this case, the PLATON SQUEEZE program was applied to treat the residual electron density.



**Figure 5.2.** X-ray crystal structure of inclusion crystal **5**•**14**. Included **14** was represented in CPK model in the packing structure (left), and observed electron density map ( $F_o$ , contour:  $0.9\sigma$ ) superimposed on the refined structure of **14**.

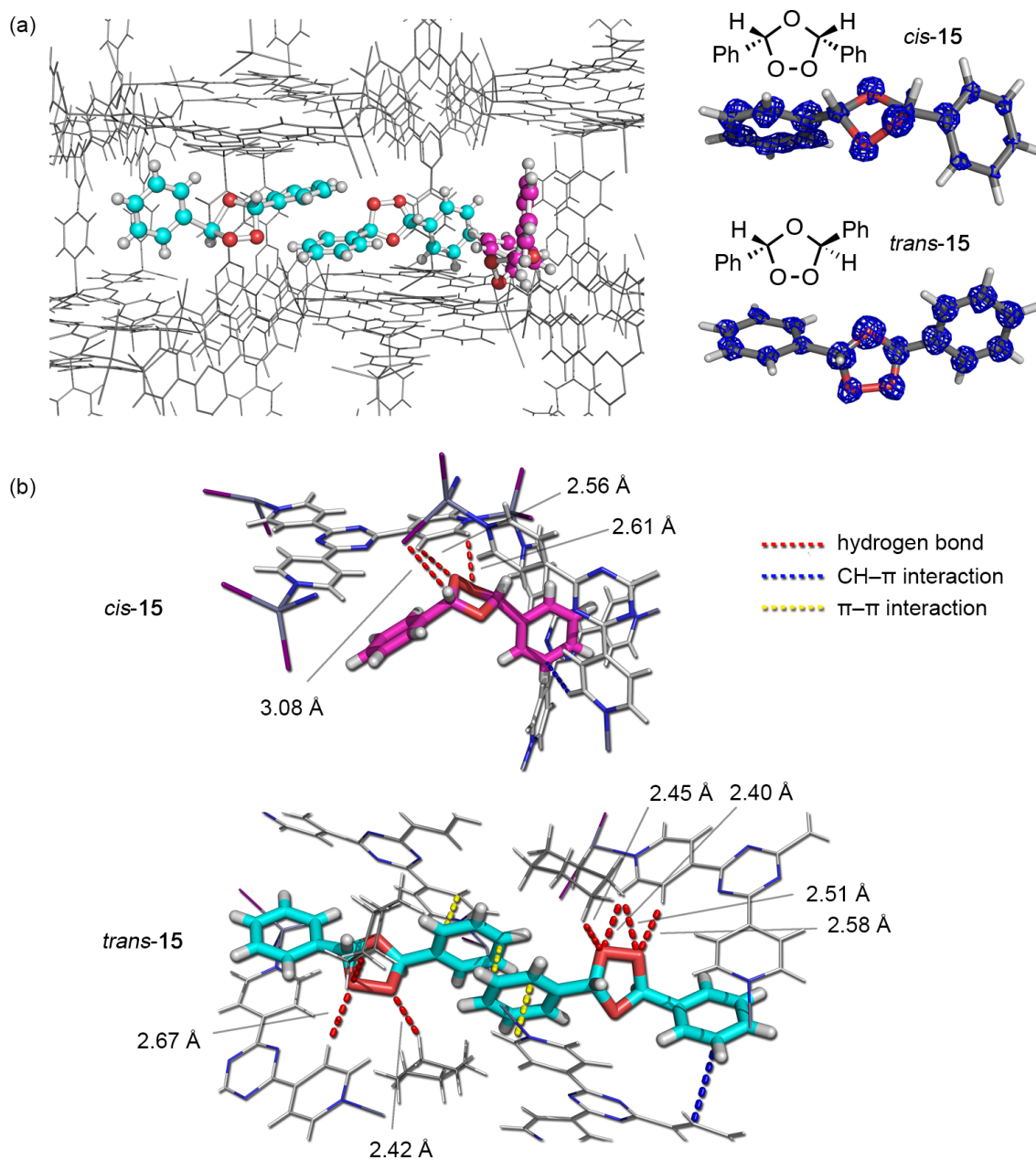
Though the refined bond length contained large error bar, the structural refinement was converged without any restraints and constraints on **14**. The C–C bond lengths of C1–C2, C2–C3, C3–C4 and C4–C5 were 1.24(7), 1.18(7), 1.34(6) and 1.62(7) Å, respectively. The C–O bond lengths of C1–O1, C1–O2, C5–O1 and C5–O3 were 1.78(6), 1.40(6), 1.56(7) and 1.23(6) Å, respectively. The O–O bond length of O2–O3 was 1.39(6) Å. Though the precise bond length and bond angle could not be discussed in 0.01 Å order, the data quality was still sufficient to analyze the bond connectivity and conformation of the guest molecules. Thus, the position of oxygen atom and peroxide bond structure of **14** could also be reasonably assigned based on the observed envelope

conformation of ozonide ring that is typical for a bicyclic ozonide.<sup>8,9</sup>

#### 5.4 X-ray analysis of stilbene ozonide by the crystalline sponge method

Another olefin, *cis*-stilbene, was also subjected to the ozone gas in *n*-pentane, and the crude reaction mixture containing *cis*- and *trans*-stilbene ozonides (*cis*-**15** and *trans*-**15**) in a 6:4 ratio calculated by the NMR analysis was obtained. The formation of two diastereomers and chemical shifts for each isomers were previously reported.<sup>10-12</sup> The reaction mixture was directly subjected to the crystalline sponge analysis without isolation using 5  $\mu$ L of the mixture and one crystalline sponge **5**. The X-ray analysis of the reaction mixture soaked crystal prepared at 4 °C for 2 d showed included **15** structures in the pore. Two isomers, *cis*-**15** and *trans*-**15**, were included both together and observed as crystallographically inequivalent molecules in one crystal structure. In the crystal structure, one *cis*-**15** and two *trans*-**15** were observed with 60, 78 and 50% of refined occupancy, and solvent cyclohexane molecules were also observed as the disorder counterpart. As in the case of **14**, *cis*-**15** and *trans*-**15** structures were converged without any restraints or constraints except AFIX 66 commands for fixing phenyl ring, which did not change the conformation or stereochemistry of ozonide rings.

The two isomers were trapped at the different site in the pore by different interactions, respectively (Figure 5.3a, Figure S5.3). For *cis*-**15**, hydrogen bond and CH- $\pi$  interaction were observed. The distance between the oxygen atoms in the peroxide bond and ligand pyridine  $\alpha$  or  $\beta$  protons were 2.56 and 2.61 Å, which were shorter than the sum of van der Waals radii of oxygen and hydrogen atoms (2.72 Å).<sup>13</sup> In addition to that, another C-H...I hydrogen bond was observed. On the other hand, C-H...O hydrogen bond, CH- $\pi$  and  $\pi$ - $\pi$  interactions were observed between the *trans*-**15** and host framework (Figure 5.3b). These differences on interactions and trapped positions indicated that the crystalline sponge **5** recognized the subtle difference of the target compounds structure and bound to the compounds at the most favored positions.

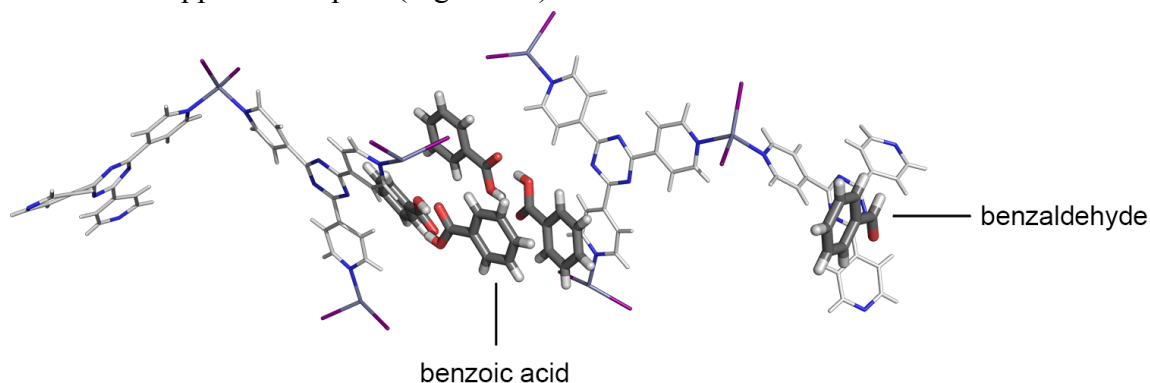


**Figure 5.3.** (a) X-ray crystal structure of inclusion crystal **5•15** and observed electron density maps ( $F_o$ , contour:  $0.7\sigma$ ). Included *cis*-**15** and *trans*-**15** were represented in ball and stick model in magenta and cyan, respectively. (b) Observed molecular interactions between **15** and host framework.

### 5.5 Heating experiment of stilbene ozonide inclusion crystalline sponge

When the inclusion of **15** into crystalline sponge **5** was performed at 50 °C instead of the inclusion at 4 °C, decomposition of **15** occurred in the crystalline sponge **5** and the structure of **15** was not observed by the X-ray diffraction analysis. Instead of **15**,

benzoic acid and benzaldehyde, which are decomposed products of **15** were observed.<sup>6</sup> NMR analysis also confirmed that ozonide **15** gradually decomposed into benzoic acid and benzaldehyde at 50 °C. This decomposition process of **15** also proceeded after inclusion into the crystalline sponge **5**. First, inclusion of the ozone oxidation mixture of *cis*-stilbene was performed at 4 °C in a micro vial and gave inclusion complex **5•15**. Then the inclusion crystal **5•15** was picked from the vial and heated at 50 °C for 2 d. After applying heat for 2 d, a microscopic IR analysis showed that the sharp absorption at 1695 cm<sup>-1</sup>, which was attributable to the C=O stretching, and broad absorption around 3462 cm<sup>-1</sup>, attributable to the O–H stretching increased (Figure S5.2). The IR spectra indicated the thermal decomposition of **15** to benzoic acid and benzaldehyde proceeded in the pore of the crystalline sponge. Furthermore, the X-ray diffraction analysis of the resultant crystalline sponge revealed benzoic acid and benzaldehyde molecules trapped in the pore (Figure 5.4).

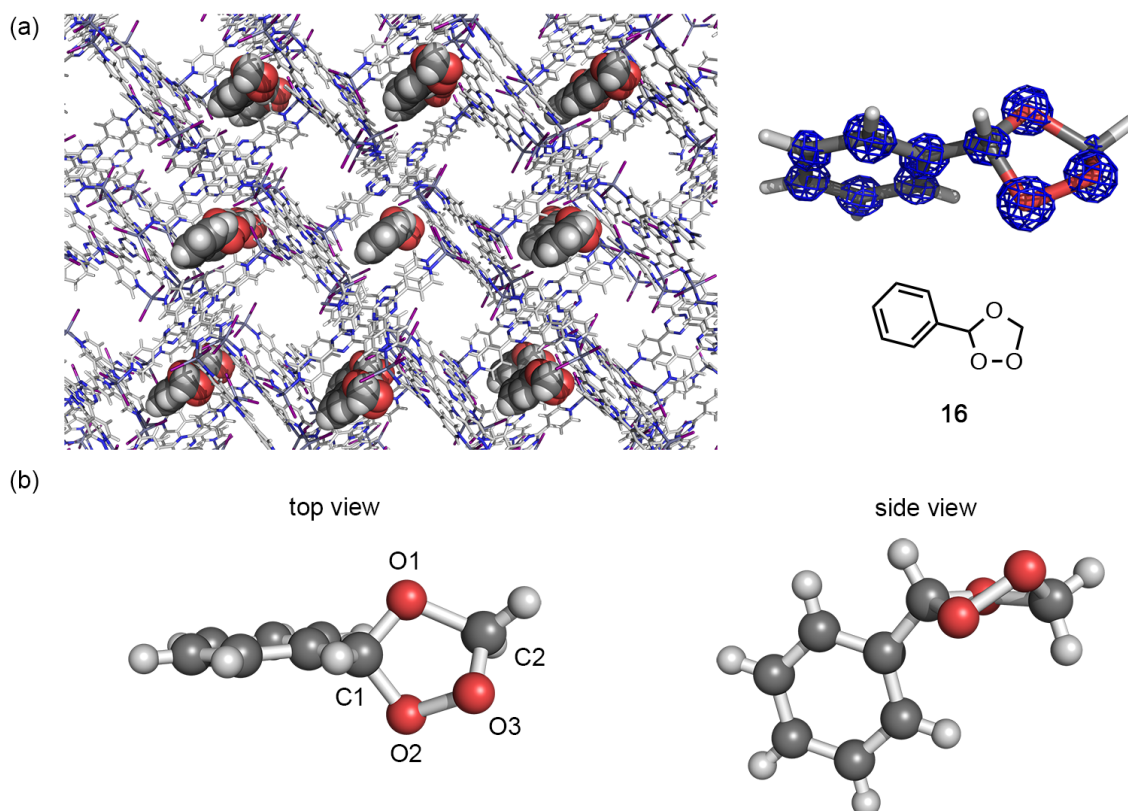


**Figure 5.4.** X-ray crystal structure of asymmetric unit of crystal **5•15** after applying heat.

### 5.6 X-ray analysis of styrene ozonide by the crystalline sponge method

The crystalline sponge analysis of styrene ozonide (**16**) was carried out with the reaction mixture prepared by an ozone oxidation of styrene in *n*-pentane. The inclusion crystalline sponge **5•16** was prepared with 5 μL of the reaction mixture and one crystalline sponge **5** at 4 °C for 2 d. As is the case in **14** and **15**, X-ray analysis revealed included **16** structure in the pore without any restraints and constraints on the ozonide ring, and observed electron density map was well superimposed on the refined structure (Figure 5.5a). However refined bond lengths of O1–C2 and O2–O3 were 1.58(7) and 1.46(4) Å, respectively, and determining the oxygen atom positions in the ozonide ring based on the C–O or O–O bond length was difficult due to the large error

bar on the bond lengths. Therefore the positions of the oxygen atoms were determined from the conformation of the five membered ozonide ring. The large dihedral angle,  $61.24^\circ$ , derived from the lone pair–lone pair repulsion of peroxide bond was observed for C1–O2–O3–C2 bond. The observed twisted conformation on the **16** is typical for the five membered ozonide ring (Figure 5.5b).<sup>14,15</sup>



**Figure 5.5.** (a) X-ray crystal structure of inclusion crystal **5•16** and observed electron density maps ( $F_o$ , contour:  $0.8\sigma$ ). Included **16** were represented in CPK model in the packing structure. (b) Observed large dihedral angle on C1–O2–O3–C2 bond.

### 5.7 Summary

In this chapter, crystallographic analyses of potentially explosive secondary ozonides were performed within the safe microgram scale by the crystalline sponge method. Furthermore, since the crystalline sponge analysis can be performed with the solution of the target compound, the inclusion of ozonides were performed from the reaction mixture without isolation. The application to the structural analysis of dangerous compounds by the crystalline sponge method is not limited to the ozonide,

but it would have a huge potential to serve as the safe analysis method of harmful compounds.



## 5.8 Experimental Section

Materials and methods	103-106
Crystallographic data	107-110
<b>Figure S5.1.</b> $^1\text{H}$ NMR spectra of ozone oxidation reaction mixture	105
<b>Figure S5.2.</b> Microscopic IR spectra of inclusion complex <b>5•15</b>	106
<b>Figure S5.3-S5.4.</b> X-ray crystallographic data	107-110

## Materials and method

### Reagents and equipment

Solvents and reagents were purchased from TCI Co., Ltd., WAKO Pure Chemical Industries Ltd., and Sigma-Aldrich Co and used without further purification.  $^1\text{H}$  NMR spectra were recorded on a Bruker AVANCE III HD 500 MHz spectrometer equipped with 5 mm BBO gradient probe and a Bruker AVANCE 500 MHz spectrometer equipped with TCI gradient CryoProbe. All NMR spectra data were recorded at 300 K and chemical shift values are reported in parts per million (ppm) relative to an internal standard tetramethylsilane. Ozone gas was generated by a SIBATA ozone generator. The concentration of ozone was measured by GASTEC GV-100 sampling device equipped with No. 18M detector tube. Microscopic IR spectra were recorded on a Varian DIGILAB Scimitar instrument and are reported in frequency of absorption ( $\text{cm}^{-1}$ ). Single crystal X-ray diffraction data were collected on a BRUKER APEX-II CCD diffractometer equipped with a focusing mirror ( $\text{MoK}_\alpha$  radiation  $\lambda = 0.71073 \text{ \AA}$ ) and a  $\text{N}_2$  generator (Japan Thermal Eng. Co., Ltd.). For single crystal X-ray diffraction analysis and microscopic IR measurement, fluorolube<sup>®</sup> and mineral oil were used as a protectant for the single crystals.

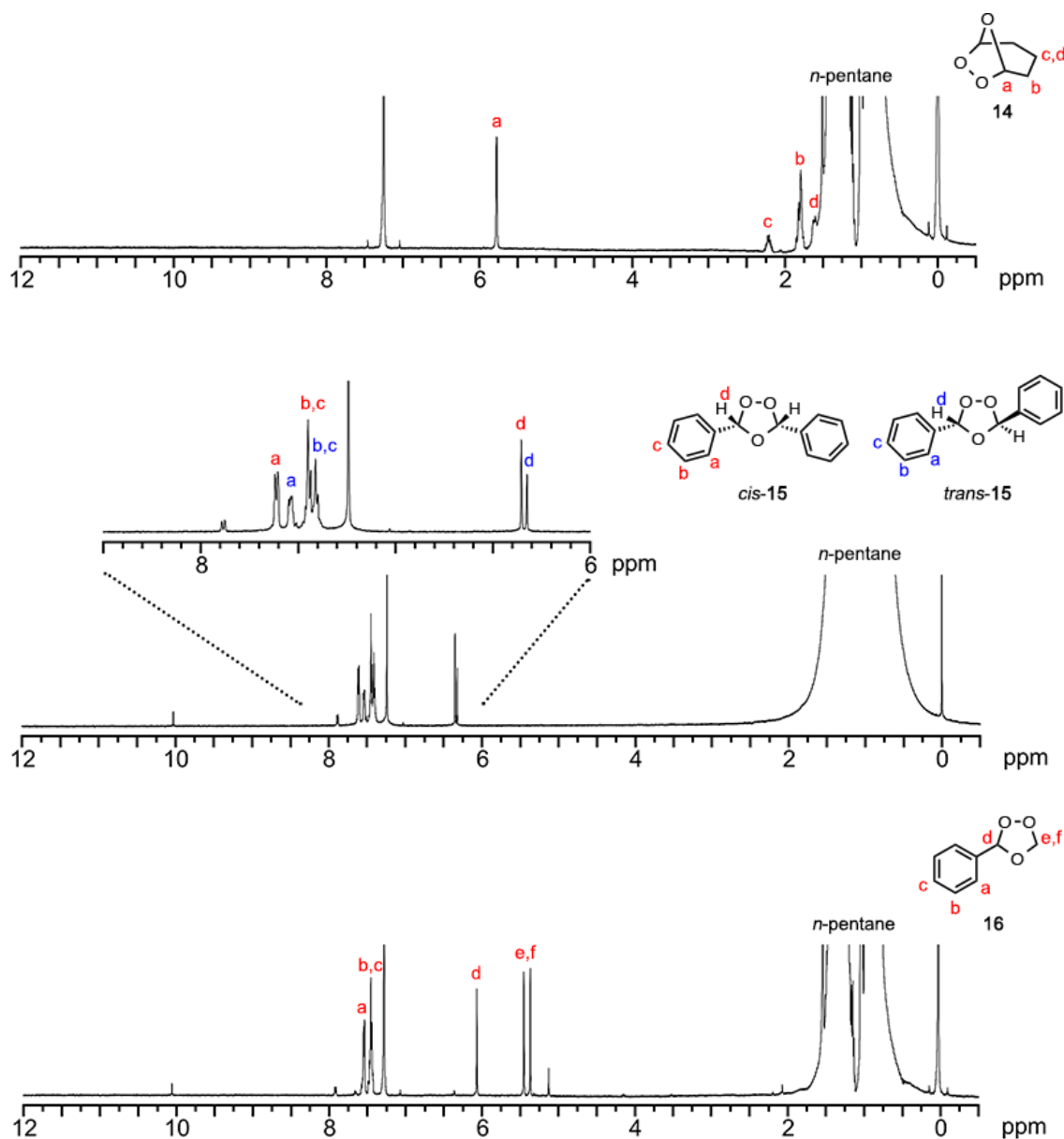
**X-ray crystallographic analysis**

Single crystal X-ray diffraction data were processed with Bruker APEX2 software.<sup>16</sup> Absorption correction was performed by multi-scan method with SADABS.<sup>1</sup> Space groups were determined by XPREP program.<sup>16</sup> The structures were solved by direct methods and refined by full-matrix least-squares calculations on  $F^2$  using SHELXL-2013 program.<sup>17</sup>

In the determination of space group, the XPREP program suggested both monoclinic  $C2/c$  and  $Cc$  space groups as possible candidates for each case reported here. When the space group  $C2/c$  was applied for the structural analysis, guest molecules were found on a symmetry plane, rendering it difficult to assign and refine for all the atoms of whole guest molecules even using PART  $-n$  command. Thus, the structures were solved in monoclinic  $Cc$  space group. Since the host framework was in some cases highly disordered, atoms were partially restrained with DFIX, FLAT, SIMU and ISOR commands. Atoms for the guest molecules (including solvent molecules) were then assigned to the residual Q-peaks. Included guest structures were first isotropically refined with an appropriate occupancy calculated by refining FVAR value followed by an anisotropic refinement, if possible. In a case where the stereochemistries of ozonides were discussed, the structures were carefully analyzed without any restraints or constraints on the atoms that constitute ozonide rings. The final crystal structures leave large solvent-accessible voids where only weak Q-peaks were observed because that solvent or guest molecules are highly disordered. Such Q-peaks have been treated with PLATON SQUEEZE program, resulting in reasonable  $R_1$  and  $wR_2$  values as compared with  $R_{\text{int}}$ .<sup>18</sup>

**Inclusion of ozone oxidation reaction mixture into crystalline sponge****General procedure for preparation of ozone oxidation reaction mixture**

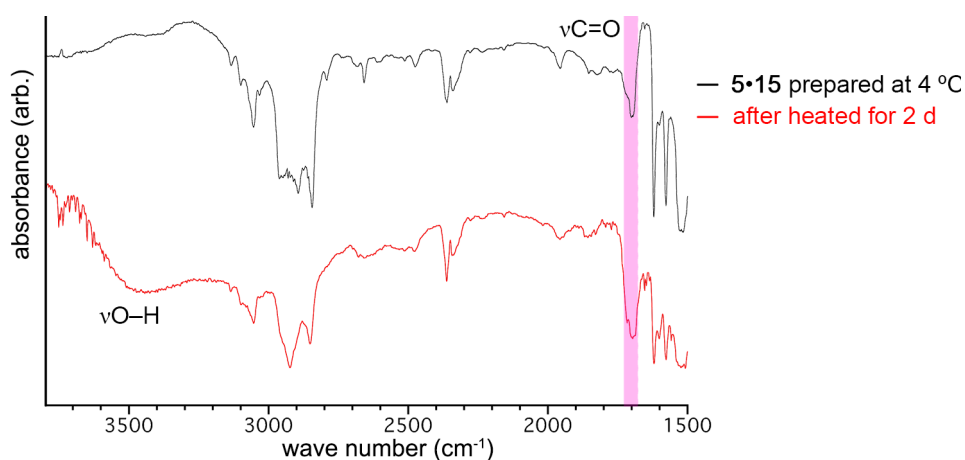
To a solution of the olefine in *n*-pentane (10 mg/4 mL), was passed ozone gas (0.4 L/min, 400 ppm) at  $-78\text{ }^{\circ}\text{C}$  for 1 h. Removing dissolved ozone from the reaction solution by Ar bubbling and 5  $\mu\text{L}$  of the resultant reaction mixture was directly subjected to the inclusion into the crystalline sponge.



**Figure S5.1.**  $^1\text{H}$  NMR spectra of reaction solution of ozone oxidation of cyclopentene, *cis*-stilbene and styrene (500 MHz,  $\text{CDCl}_3$ , 300 K).

**General procedure for inclusion of ozone oxidation reaction mixture**

To a micro vial containing a single crystal of  $[(ZnI_2)_3(\text{tpt})_2]_n$  (**5**; tpt = tri(4-pyridyl)-1,3,5-triazine) and cyclohexane (20  $\mu\text{L}$ ), 5  $\mu\text{L}$  of ozone oxidation reaction solution was added. Then, the crystal was allowed to stand at 4  $^\circ\text{C}$  and the solvent was gradually evaporated over 2 d.

**Heating experiment of 15 inclusion crystalline sponge**

**Figure S5.2.** Microscopic IR spectra of inclusion complex **5•15** prepared at 4  $^\circ\text{C}$  before and after applying heat at 50  $^\circ\text{C}$ .

**Crystallographic data****Inclusion complex 5•14**

Crystallographic data (before the SQUEEZE treatment):  $C_{72}H_{48}N_{24}Zn_6I_{12} \cdot 0.69(C_5H_8O_3) \cdot 4.02(C_6H_{12})$ ,  $M = 3588.52$ , colorless block,  $0.13 \times 0.13 \times 0.1 \text{ mm}^3$ , monoclinic, space group  $Cc$ ,  $a = 34.203(3) \text{ \AA}$ ,  $b = 15.1150(12) \text{ \AA}$ ,  $c = 29.565(2) \text{ \AA}$ ,  $\beta = 100.1070(10)^\circ$ ,  $V = 15048(2) \text{ \AA}^3$ ,  $Z = 4$ ,  $D_c = 1.581 \text{ g/cm}^3$ ,  $F000 = 6799$ ,  $\mu = 3.447 \text{ mm}^{-1}$ ,  $T = 90.0(1) \text{ K}$ ,  $1.209 < \theta < 26.376^\circ$ , 21423 unique reflections out of 30706 with  $I > 2\sigma(I)$ ,  $R_{\text{int}} = 0.0263$ , 1266 parameters, 568 restraints,  $\text{GoF} = 1.077$ , final  $R$  factors  $R_1 = 0.0656$ , and  $wR_2 = 0.2158$  for all data. CCDC deposit number: unpublished result.

Crystallographic data (after the SQUEEZE treatment):  $C_{72}H_{48}N_{24}Zn_6I_{12} \cdot 0.69(C_5H_8O_3) \cdot 4.02(C_6H_{12})$ ,  $M = 3582.57$ , colorless block,  $0.13 \times 0.13 \times 0.1 \text{ mm}^3$ , monoclinic, space group  $Cc$ ,  $a = 34.203(3) \text{ \AA}$ ,  $b = 15.1150(12) \text{ \AA}$ ,  $c = 29.565(2) \text{ \AA}$ ,  $\beta = 100.1070(10)^\circ$ ,  $V = 15048(2) \text{ \AA}^3$ ,  $Z = 4$ ,  $D_c = 1.581 \text{ g/cm}^3$ ,  $F000 = 6799$ ,  $\mu = 3.447 \text{ mm}^{-1}$ ,  $T = 90.0(1) \text{ K}$ ,  $1.209 < \theta < 26.376^\circ$ , 21259 unique reflections out of 30706 with  $I > 2\sigma(I)$ ,  $R_{\text{int}} = 0.0247$ , 1266 parameters, 568 restraints,  $\text{GoF} = 1.104$ , final  $R$  factors  $R_1 = 0.0548$ , and  $wR_2 = 0.1700$  for all data.

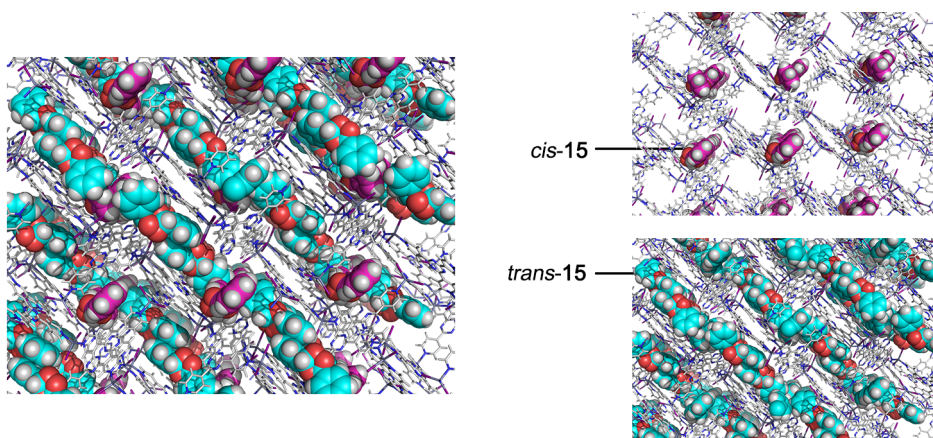
IR (single crystal, mineral oil): 3442, 3053, 2929, 2850, 1618, 1576, 1526, 1448, 1371  $1316 \text{ cm}^{-1}$ .

**Inclusion complex 5•15 (prepared at 4 °C)**

Crystallographic data (before the SQUEEZE treatment):  $C_{72}H_{48}N_{24}Zn_6I_{12} \cdot 2.28(C_{14}H_{12}O_3) \cdot 2.3(C_{14}H_{12}O_3)$ ,  $M = 3963.01$ , colorless block,  $0.1 \times 0.1 \times 0.05 \text{ mm}^3$ , monoclinic, space group  $Cc$ ,  $a = 35.46(3) \text{ \AA}$ ,  $b = 15.011(11) \text{ \AA}$ ,  $c = 30.45(2) \text{ \AA}$ ,  $\beta = 101.344(9)^\circ$ ,  $V = 15891(20) \text{ \AA}^3$ ,  $Z = 4$ ,  $D_c = 1.697 \text{ g/cm}^3$ ,  $F000 = 7820$ ,  $\mu = 3.283 \text{ mm}^{-1}$ ,  $T = 90.0(1) \text{ K}$ ,  $1.171 < \theta < 27.016^\circ$ , 19887 unique reflections out of 30131 with  $I > 2\sigma(I)$ ,  $R_{\text{int}} = 0.0441$ , 1433 parameters, 1117 restraints, GoF = 1.045, final  $R$  factors  $R_1 = 0.0487$ , and  $wR_2 = 0.1438$  for all data. CCDC deposit number: unpublished result.

Crystallographic data (after the SQUEEZE treatment):  $C_{72}H_{48}N_{24}Zn_6I_{12} \cdot 2.28(C_{14}H_{12}O_3) \cdot 2.3(C_{14}H_{12}O_3)$ ,  $M = 3963.01$ , colorless block,  $0.1 \times 0.1 \times 0.05 \text{ mm}^3$ , monoclinic, space group  $Cc$ ,  $a = 35.46(3) \text{ \AA}$ ,  $b = 15.011(11) \text{ \AA}$ ,  $c = 30.45(2) \text{ \AA}$ ,  $\beta = 101.344(9)^\circ$ ,  $V = 15891(20) \text{ \AA}^3$ ,  $Z = 4$ ,  $D_c = 1.697 \text{ g/cm}^3$ ,  $F000 = 7820$ ,  $\mu = 3.283 \text{ mm}^{-1}$ ,  $T = 90.0(1) \text{ K}$ ,  $1.171 < \theta < 27.016^\circ$ , 19947 unique reflections out of 30131 with  $I > 2\sigma(I)$ ,  $R_{\text{int}} = 0.0441$ , 1433 parameters, 1117 restraints, GoF = 1.052, final  $R$  factors  $R_1 = 0.0496$ , and  $wR_2 = 0.1468$  for all data. CCDC deposit number: unpublished result.

IR (single crystal, mineral oil): 3053, 2947, 2893, 2844, 1616, 1577, 1514, 1449, 1372,  $1316 \text{ cm}^{-1}$ .



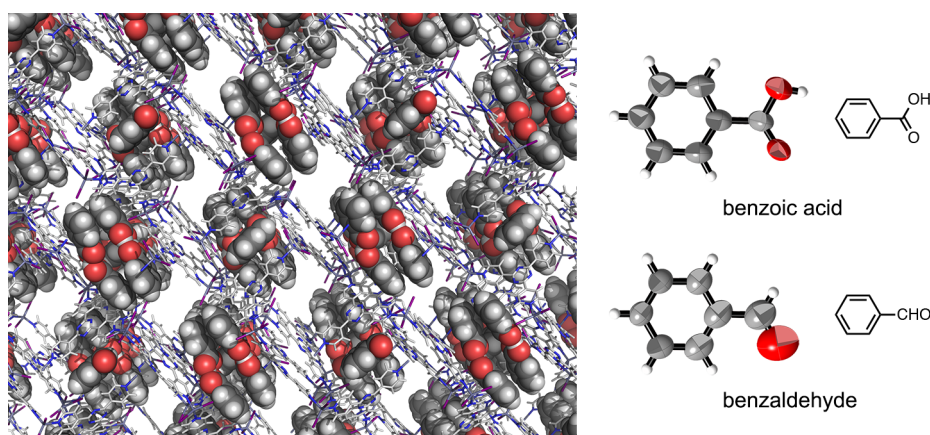
**Figure S5.3.** The X-ray crystal structure of **5•15**. Included *trans*-**15** (magenta) and *cis*-**15** (cyan) were drawn in CPK model in the packing structure.

**After applying heat at 50 °C for 2 d on inclusion complex 5•15**

Crystallographic data (before the SQUEEZE treatment):  $C_{72}H_{48}N_{24}Zn_6I_{12} \cdot 2.33(C_7H_6O_2) \cdot 0.5(C_7H_{16}O_2)$ ,  $M = 3501.95$ , colorless block,  $0.05 \times 0.05 \times 0.03 \text{ mm}^3$ , Monoclinic, space group  $Cc$ ,  $a = 35.286(4) \text{ \AA}$ ,  $b = 14.8475(16) \text{ \AA}$ ,  $c = 31.547(3) \text{ \AA}$ ,  $\beta = 102.9750(10)^\circ$ ,  $V = 16106(3) \text{ \AA}^3$ ,  $Z = 4$ ,  $D_c = 1.444 \text{ g/cm}^3$ ,  $F000 = 6564$ ,  $\mu = 3.220 \text{ mm}^{-1}$ ,  $T = 90(2) \text{ K}$ ,  $1.184 < \theta < 26.500^\circ$ , 17721 unique reflections out of 33024 with  $I > 2\sigma(I)$ ,  $R_{\text{int}} = 0.0517$ , 1364 parameters, 1234 restraints,  $\text{GoF} = 1.150$ , final  $R$  factors  $R_1 = 0.0989$ , and  $wR_2 = 0.3517$  for all data. CCDC deposit number: unpublished result.

Crystallographic data (after the SQUEEZE treatment):  $C_{72}H_{48}N_{24}Zn_6I_{12} \cdot 2.33(C_7H_6O_2) \cdot 0.5(C_7H_{16}O_2)$ ,  $M = 3501.95$ , colorless block,  $0.05 \times 0.05 \times 0.03 \text{ mm}^3$ , Monoclinic, space group  $Cc$ ,  $a = 35.286(4) \text{ \AA}$ ,  $b = 14.8475(16) \text{ \AA}$ ,  $c = 31.547(3) \text{ \AA}$ ,  $\beta = 102.9750(10)^\circ$ ,  $V = 16106(3) \text{ \AA}^3$ ,  $Z = 4$ ,  $D_c = 1.444 \text{ g/cm}^3$ ,  $F000 = 6564$ ,  $\mu = 3.220 \text{ mm}^{-1}$ ,  $T = 90(2) \text{ K}$ ,  $1.184 < \theta < 26.500^\circ$ , 17449 unique reflections out of 33024 with  $I > 2\sigma(I)$ ,  $R_{\text{int}} = 0.0441$ , 1364 parameters, 1240 restraints,  $\text{GoF} = 10.943$ , final  $R$  factors  $R_1 = 0.0768$ , and  $wR_2 = 0.2471$  for all data. CCDC deposit number: unpublished result.

IR (single crystal, mineral oil): 3056, 2923, 2851, 1692, 1618, 1577, 1523, 1451, 1417, 1374,  $1315 \text{ cm}^{-1}$ .



**Figure S5.4.** The X-ray crystal structure of **5•15** after applying heat at 50 °C for 2 d. Observed benzoic acid and benzaldehyde were drawn in CPK mode in the packing structure and the thermal ellipsoids were drawn at the 50% probability level.



**Inclusion complex 5•16**

Crystallographic data (before the SQUEEZE treatment):  $C_{72}H_{48}N_{24}Zn_6I_{12} \cdot 0.72(C_8H_8O_3)$ ,  $M = 3274.35$ , colorless rod,  $0.16 \times 0.7 \times 0.05 \text{ mm}^3$ , Monoclinic, space group  $Cc$ ,  $a = 35.567(3) \text{ \AA}$ ,  $b = 14.9030(12) \text{ \AA}$ ,  $c = 30.939(3) \text{ \AA}$ ,  $\beta = 102.1810(10)^\circ$ ,  $V = 16030(2) \text{ \AA}^3$ ,  $Z = 4$ ,  $D_c = 1.357 \text{ g/cm}^3$ ,  $F000 = 6087$ ,  $\mu = 3.229 \text{ mm}^{-1}$ ,  $T = 90(2) \text{ K}$ ,  $1.171 < \theta < 26.356^\circ$ , 23876 unique reflections out of 32671 with  $I > 2\sigma(I)$ ,  $R_{\text{int}} = 0.0278$ , 1060 parameters, 190 restraints,  $\text{GoF} = 1.063$ , final  $R$  factors  $R_1 = 0.0812$ , and  $wR_2 = 0.2886$  for all data. CCDC deposit number: unpublished result.

Crystallographic data (after the SQUEEZE treatment):  $C_{72}H_{48}N_{24}Zn_6I_{12} \cdot 0.72(C_8H_8O_3)$ ,  $M = 3274.35$ , colorless rod,  $0.16 \times 0.7 \times 0.05 \text{ mm}^3$ , Monoclinic, space group  $Cc$ ,  $a = 35.567(3) \text{ \AA}$ ,  $b = 14.9030(12) \text{ \AA}$ ,  $c = 30.939(3) \text{ \AA}$ ,  $\beta = 102.1810(10)^\circ$ ,  $V = 16030(2) \text{ \AA}^3$ ,  $Z = 4$ ,  $D_c = 1.357 \text{ g/cm}^3$ ,  $F000 = 6087$ ,  $\mu = 3.229 \text{ mm}^{-1}$ ,  $T = 90(2) \text{ K}$ ,  $1.171 < \theta < 26.356^\circ$ , 23849 unique reflections out of 32671 with  $I > 2\sigma(I)$ ,  $R_{\text{int}} = 0.0262$ , 1060 parameters, 220 restraints,  $\text{GoF} = 1.117$ , final  $R$  factors  $R_1 = 0.0463$ , and  $wR_2 = 0.1353$  for all data. CCDC deposit number: unpublished result.

IR (single crystal, mineral oil): 3056, 2962, 2888, 1618, 1577, 1528, 1456, 1375, 1313  $\text{cm}^{-1}$ .

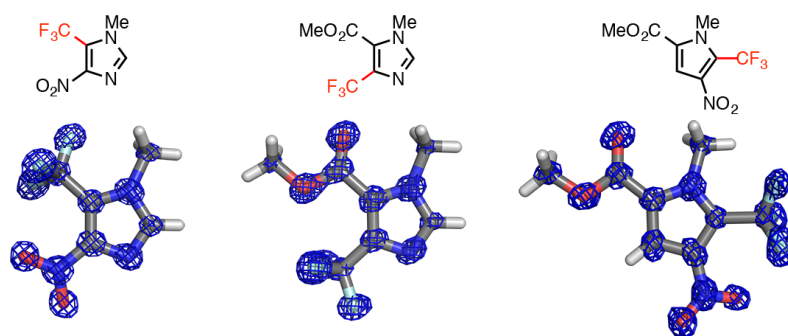
## References

- 1 A. K. Furr, *CRC Handbook of Laboratory Safety, 5th Edition*, CRC Press, Boca Raton, **2000**.
- 2 P. S. Bailey, *Chem. Rev.* **1958**, *58*, 925–1010.
- 3 R. Criegee, *Angew. Chem. Int. Ed.* **1975**, *14*, 745–752.
- 4 L. Louis, Jr., *Chem. Rev.* **1940**, *27*, 437–493.
- 5 Only 61 crystal structures of secondary ozonide were reported in the Cambridge Structural Database (CSD). Most of the structures are contained bulky substituent groups for stabilizing the ozonide.
- 6 P. R. Story, T. K. Hall, W. H. Morrison, III, J.-C. Farine, *Tetrahedron Lett.* **1968**, 5397–5400.
- 7 R. Criegee, *Justus Liebigs Ann. Chem.* **1953**, *583*, 1–36.
- 8 R. L. Kuczkowski, *Acc. Chem. Res.* **1983**, *16*, 42–47.
- 9 D. G. Borseth, R. L. Kuczkowski, *J. Phys. Chem.* **1983**, *87*, 5381–5386.
- 10 R. Criegee, A. Kerckow, H. Zinke, *Chem. Ber.* **1955**, 1878–1888.
- 11 R. Criegee, H. Korber, *Chem. Ber.* **1971**, 1807–1811.
- 12 A. P. Schaap, S. Siddiqui, S. D. Gagnon, *J. Am. Chem. Soc.* **1983**, *105*, 5149–5150.
- 13 A. Bondi, *J. Phys. Chem.* **1964**, *68*, 441–451.
- 14 D. Cremer, *Chem. Phys.* **1979**, *70*, 1898–1910
- 15 D. Cremer, *J. Am. Chem. Soc.* **1981**, *103*, 3619–3626.
- 16 *APEX2, SADABS and XPREP*, Bruker AXS Inc., Madison, Wisconsin, USA, 2007.
- 17 G. M. Sheldrick, *Acta Cryst.* **2008**, *A64*, 112–122.
- 18 P. van der Sluis, A. L. Spek, *Acta Cryst.* **1990**, *A46*, 194–201.



## Chapter 6

### Application of the Crystalline Sponge Method to Synthetic Chemistry



#### Abstract

It is difficult to determine the structure of highly functionalized molecules. To analyze their structure, a lot of time-consuming analyses such as 2D NMR, MS/MS and others are required. The crystalline sponge method provides a quick preparation method of the inclusion crystal of the target compound and a structural analysis method of the target compound. Here, the crystalline sponge method was applied for structural analyses of highly complicated compounds synthesized by the recent synthetic method. Substituted positions of the heteroarenes and atom connectivity of the complicated structure compound were easily determined. Furthermore, the absolute structures of planar, axially and helically chiral molecules were also determined. The crystalline sponge method could serve as a quick and easy method for structural analysis of complicated molecule.

## 6.1 Introduction

Recent advancement of synthetic methods enables efficient and quick construction of the target compound or fast screening of the reaction conditions.<sup>1-5</sup> Even an inert C–H bond can be easily activated by the highly active catalyst, and a new methodology was developed rapidly.<sup>6,7</sup> These developments improve the number of reaction steps and afford the target compound in a short time. Under these circumstances, the analysis of the product can be the bottleneck of the synthesis. Even if you combine a time consuming 2D NMR and MS, sometimes the conclusive spectra cannot be obtained for complicated molecules. Sometimes a structural analysis results in a misassignment of the target structure.<sup>8</sup> In terms of the structural analysis, though X-ray analysis gives conclusive information, it does not seem to be common to determine the structure of synthetic compounds by the X-ray diffraction analysis among synthetic chemists. Due to the uncertainty on the availability of a single crystal of the target molecule, single crystal X-ray analysis tends to be neglected as an analysis method. The crystalline sponge analysis provides the target inclusion crystal by a quick and reproducible manner. A single crystal X-ray analysis by the crystalline sponge method serves as a fast and easy structural analysis method especially for a regio selectivity, connectivity and stereochemistry of synthetic compounds.<sup>9</sup>

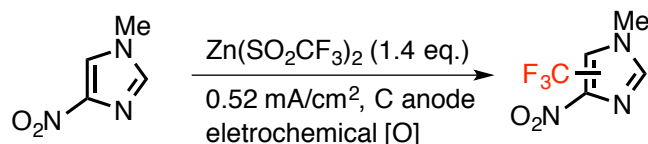
In this chapter, compounds whose structure could not be determined by other spectroscopic analyses were analyzed by the crystalline sponge method. Quick and easy structural analyses of highly functionalized heteroarenes, the compound with complicated connectivity and the compound with unknown stereochemistry by the crystalline sponge method were demonstrated.

## 6.2 Determination of the substituent position of C–H functionalization products

Highly functionalized heteroarenes are important target or subunit in the medicinal chemistry. There are a lot of methods to construct or functionalize variety of heteroarenes. However, it is often difficult to characterize the structure of highly functionalized heteroarenes especially about the substituent positions by  $^1\text{H}$  NMR or MS due to their small H atom numbers and the same  $m/z$  values among the isomers. In sharp contrast to the NMR or MS, X-ray analysis by the crystalline sponge method can give crucial information for undetermined substituent position with the small amount of non-crystalline sample or even with a residue of NMR measured sample.

The radical C–H functionalization of heteroarenes with  $\text{CF}_3$  group was reported recently. The electrochemically initiated radical C–H functionalization by zinc trifluoromethanesulfinate ( $\text{ZnTFMS}$ ) on imidazole and pyrrole derivatives afforded  $\text{CF}_3$  group introduced heteroarenes.<sup>10</sup>

**Scheme 6.1.** Electrochemically initiated radical C–H functionalization of heteroarene **17**.

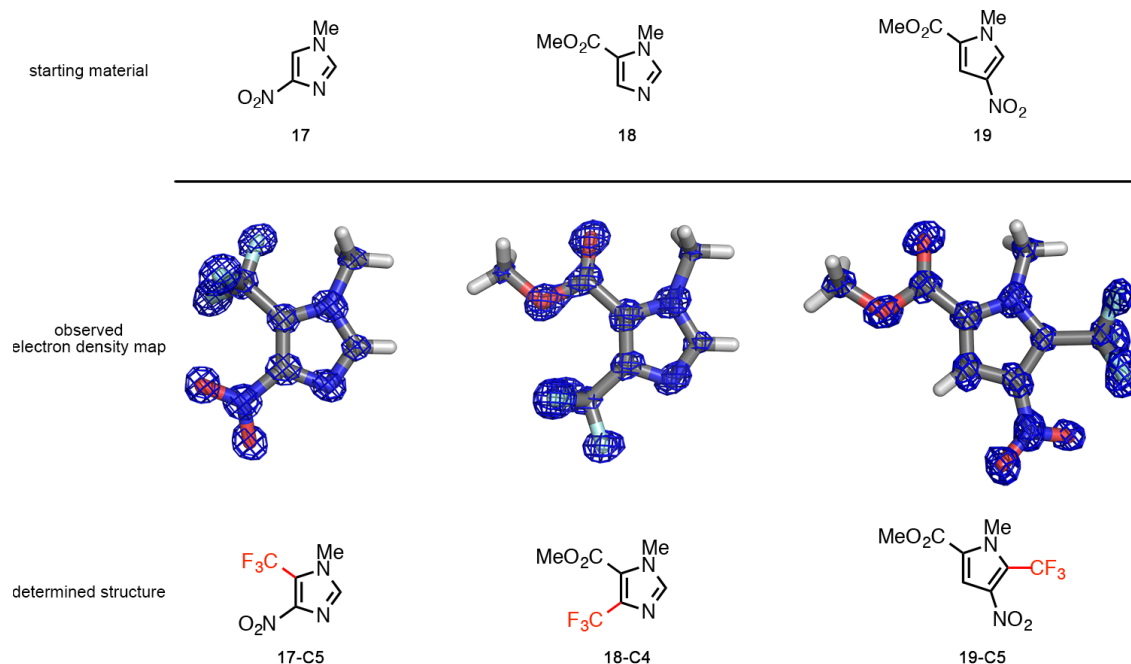


When the starting material has two or more possible substituent positions, such as 1-methyl-4-nitro-1*H*-imidazole (**17**), analyzing the  $\text{CF}_3$  introduced positions is the key to characterize the products. The possible products from **17** are C2 or C5 substituted compound (Scheme 6.1).<sup>10</sup> Though, isomers could be separated and obtained as amorphous solids by a column chromatography, characterizations of the substituent position was difficult by NMR and MS. Therefore, the crystalline sponge analysis of the second fraction (main isomer) was carried out at 50 °C for 2 d. After 2 d, the X-ray analysis of the resultant crystalline sponge clearly showed C5 position substituted **17** (**17-C5**) in the pore. After the complete structure assignment of the crystalline sponge framework, the strong residual electron density peaks attributable to **17-C5** were observed. The position of  $\text{CF}_3$ ,  $\text{NO}_2$  and  $\text{CH}_3$  groups on the imidazole core were clearly distinguishable based on the observed electron density map.

Other heteroarenes, methyl 1-methyl-1*H*-imidazole-5-carboxylate (**18**) and methyl

1-methyl-4-nitro-1*H*-pyrrole-2-carboxylate (**19**), were also functionalized by the same reaction, and main products were analyzed by the crystalline sponge method. During the targets inclusion processes, gradual deterioration of the crystallinity and some cracks on a crystal **5** were observed (Figure S6.1). Therefore, in order to maintain the crystallinity as suitable for the diffraction analysis, the inclusions of **18** derivative and **19** derivative were performed at 4 °C for 2 d and at 50 °C for 6 h, respectively. The X-ray analyses of the resultant crystals showed C4 position substituted **18** (**18-C4**) and C5 position substituted **19** (**19-C5**), respectively.

In terms of the intensity of the observed electron density, data qualities of these three examples were good enough to determine the substituted positions (electron density map could be drawn at higher than 1.0 sigma level). By combining other information about substituted groups, the crystalline sponge analysis would be an easy and quick way to determine the functionalized position.

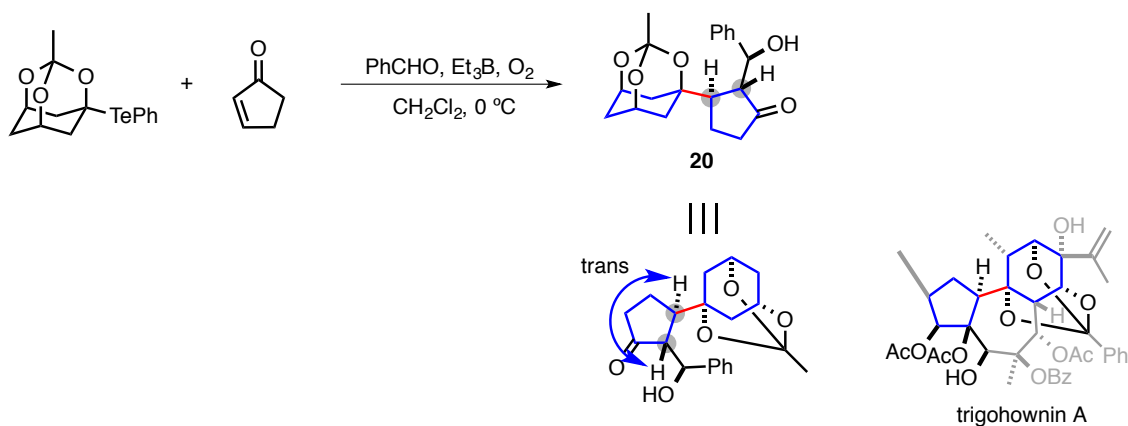


**Figure 6.1.** X-ray crystal structures of **17**, **18** and **19** obtained by the crystalline sponge analysis. The observed electron density maps ( $F_o$ , contour:  $1.0\sigma$ ) were superimposed on the each refined structure.

### 6.3 Determination of the stereochemistry of complex ring connected compound

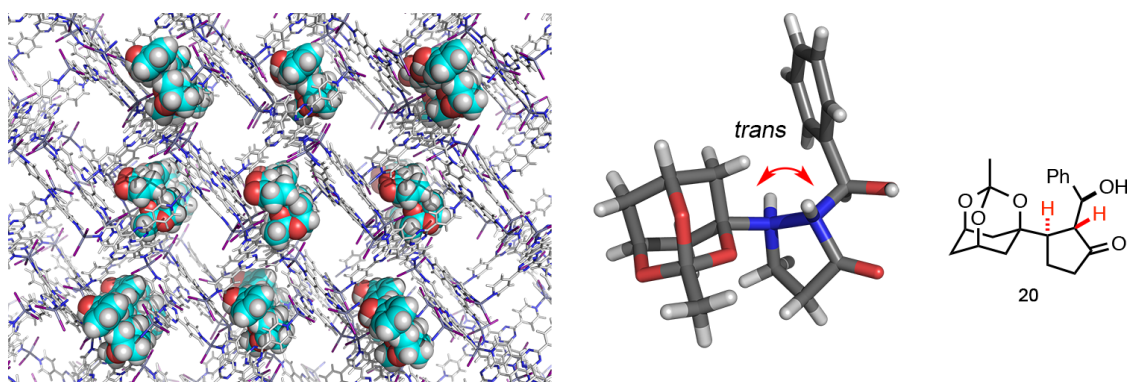
A synthesis of complicated ring connected compound **20**, which is a ring connection motif of trigohownin A, was reported by a single step three component coupling by a radical-polar crossover reaction (Scheme 6.2).<sup>11</sup> In this reaction, **20** was obtained in 80% yield by a single step coupling of radical donor, acceptor and electrophile under the air conditions mediated by Et<sub>3</sub>B for 15 min.

**Scheme 6.2.** A synthesis of **20** by the three component radical-polar crossover coupling reaction.



The stereochemistry of **20** especially *trans* connectivity of the two rings was established by NOE experiment after additional two steps deirvatization. Therefore, the crystalline sponge analysis of **20** without derivatization was examined for quick analysis of stereochemistry. The product **20** was dissolved into 1,2-dichloroethane (5 μg/5 μL) and was included into the crystalline sponge **5** at 50 °C for 2 d. The X-ray analysis of resultant crystal revealed that *trans* structure of 5 membered ring in **20** (Figure 6.2). Though the refined structure contained some restraints on bond lengths, the stereochemistry was not affected by these restratints. Derivatization free structural analysis was the apparent advantage of the crystalline sponge method not only for **20**, but also for other complicated structure compounds or NOE inactive species.



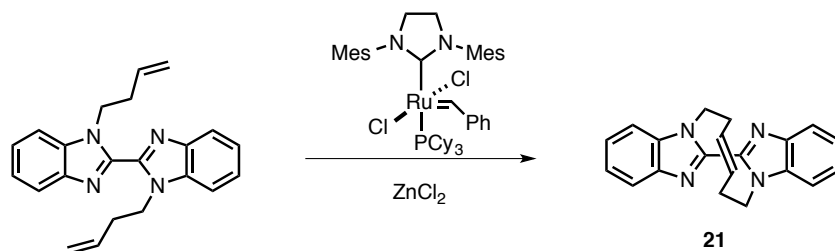


**Figure 6.2.** The *trans* structure of 5 membered ring in **20** observed by X-ray analysis with the crystalline sponge method. In the packing structure, **20** was represented in CPK model.

#### 6.4 Determination of the planar chirality constructed by ring-closing metathesis

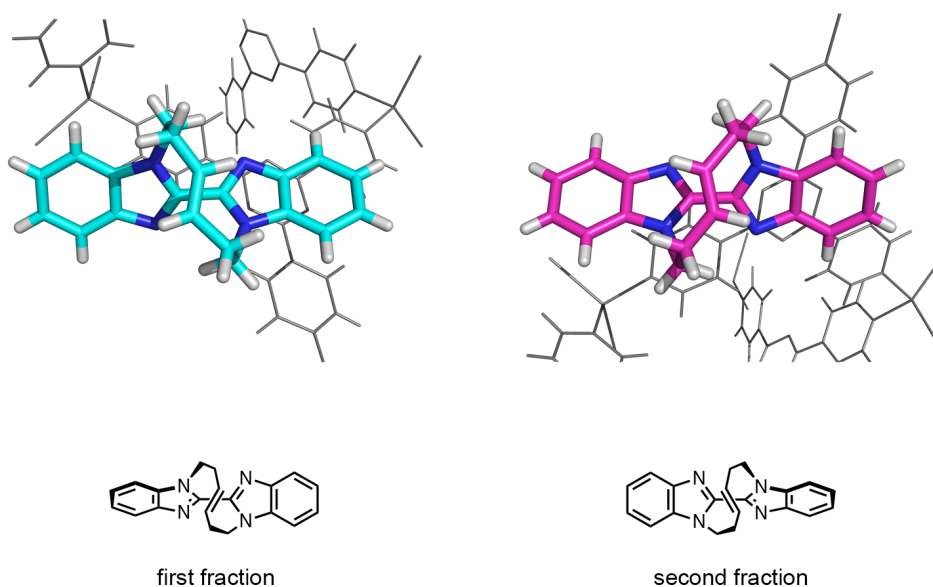
A synthesis and chiral separation of enantiomers by chiral HPLC of macrocyclic bisbenzimidazole derivative (**21**) was reported.<sup>12</sup> CD spectrum indicated the two separated fractions were in a relationship of enantiomers. However, the absolute structures of planer chirality for each fraction have remained unclear due to the difficulty on derivatization or crystallization. Then, the crystalline sponge analysis of chiral HPLC separated first fraction of **21** was carried out.

**Scheme 6.3.** A synthesis of **21** by the ring-closing methathesis.



The inclusion into crystalline sponge **5** was performed with 5  $\mu\text{g}$  of the first fraction in 1,2-dichloroethane (5  $\mu\text{L}$ ) at 50  $^{\circ}\text{C}$  for 2 d. The X-ray analysis showed included compound as *S* configuration for the planer chirality on the central *trans*-diazacycloalkene structure. This compound also has *S* axial chirality along the rigid bisbenzimidazole axis and *P* helical chirality. Due to the large steric restriction, diastereomers does not exist. The structure of first fraction was converged in a monoclinic *C2* space group with the Flack parameter 0.070(15). Then, the second

fraction analyzed by the crystalline sponge method gave the *R* configuration for planer chirality, *R* axial chirality along the rigid bisbenzimidazole axis and *M* helical chirality, which was the enantiomer of the first fraction. The refined Flack parameter was converged with 0.123(13), and these two Flack parameters indicated both stereochemistry of first and second fractions were correctly determined (Figure 6.3).



**Figure 6.3.** The refined X-ray structure of each fractions determined by the crystalline sponge analysis.

### 6.5 Summary

In this chapter, the crystalline sponge analysis was applied to the compound synthesized with the recently established synthetic method. These compounds were impossible or difficult to be determined in terms of their structures by NMR or MS. The crystalline sponge method, however, easily elucidated their structure by the X-ray diffraction analysis. The analysis time and effort to determine the synthesized molecule's structure undoubtedly became short by the crystalline sponge method.

## 6.6 Experimental Section

Materials and Methods	121-123
Crystallographic data	124-69

<b>Figure S6.1.</b> Photographs of <b>5•17</b> , <b>5•18</b> and <b>5•19</b>	123
--	-----

<b>Figure S6.2-S6.7.</b> X-ray crystallographic data	124-129
--	---------

## Materials and method

### Reagents and equipment

Solvents and reagents were purchased from TCI Co., Ltd., WAKO Pure Chemical Industries Ltd., and Sigma-Aldrich Corporation and used without further purification. Compounds **17**, **18**, and **19** were provided by Prof. Baran (The Scripps Research Institute) and **20** was provided by Profs. Inoue and Lecturer Urabe (The University of Tokyo) and **21** was provided by Profs. Mori (Kobe University) and Ogasawara (Hokkaido University). Microscopic FT-IR spectra were recorded on a Varian DIGILAB Scimitar instrument and are reported in frequency of absorption ( $\text{cm}^{-1}$ ). Single crystal X-ray diffraction data were collected on a BRUKER APEX-II CCD diffractometer equipped with a focusing mirror ( $\text{MoK}_\alpha$  radiation  $\lambda = 0.71073 \text{ \AA}$ ) and a  $\text{N}_2$  generator (Japan Thermal Eng. Co., Ltd.) or Rigaku XtaLAB P200 diffractometer equipped with a PILATUS-200K detector with multi-layer mirror monochromater ( $\text{MoK}_\alpha$  radiation  $\lambda = 0.71073 \text{ \AA}$ ). For single crystal X-ray diffraction analysis and microscopic IR measurement, fluorolube® and mineral oil were used as a protectant for the single crystals.

### X-ray crystallographic analysis

Single crystal X-ray diffraction data were processed with Bruker APEX2 software and CrystalClear program.<sup>13,14</sup> For Bruker data, absorption correction was performed by multi-scan method in SADABS and space groups were determined by XPREP program.<sup>1</sup> The structures were solved by direct methods and refined by full-matrix least-squares calculations on  $F^2$  using SHELXL-97 and SHELXL-2013 program.<sup>15</sup> In the determination of space group, the XPREP program suggested space group was employed for analyzing the structure.

After the initial phase determination, all the atoms for the host framework (*i.e.* ZnI<sub>2</sub> and tpt ligands) were assigned and the structure was refined anisotropically except for hydrogen atoms. Since the host framework was in some cases highly disordered, atoms were partially restrained with DFIX, FLAT, SIMU and ISOR commands. Atoms for the guest molecules (including solvent molecules) were then assigned to the residual Q-peaks. The guest structures were first refined isotropically with a suitable occupancy that is estimated by refinement using FVAR. If available, the guest structures were subsequently refined anisotropically. The final crystal structures leave large solvent-accessible voids where only weak Q-peaks were observed because that solvent or guest molecules are highly disordered. Such Q-peaks have been treated with PLATON SQUEEZE program, resulting in reasonable  $R_1$  and  $wR_2$  values as compared with  $R_{\text{int}}$ .<sup>16</sup>

**Inclusion of guest molecules into crystalline sponge 5****General procedure for inclusion of guest molecules into crystalline sponge 5**

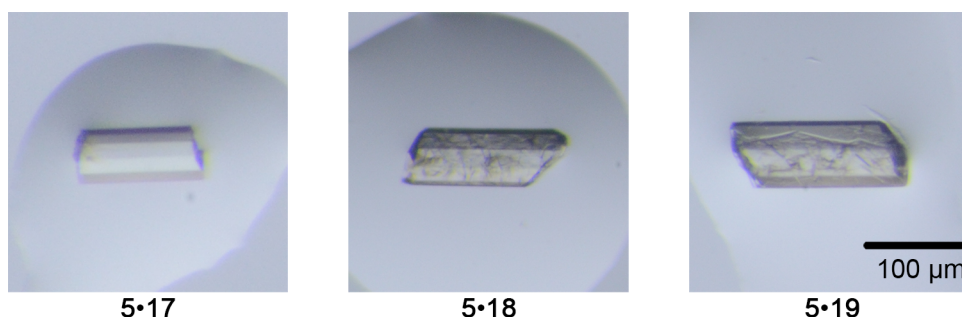
To a micro vial containing a cyclohexane exchanged single crystal of  $[(\text{ZnI}_2)_3(\text{tpt})_2]_n$  (**5**; tpt = tri(4-pyridyl)-1,3,5-triazine) and cyclohexane (75  $\mu\text{L}$ ), 5  $\mu\text{L}$  of 1,2-dichloroethane solution of target compounds (1 mg/1 mL) was added. Then, the crystal containing microvial was allowed to stand at 50  $^\circ\text{C}$  and the solvent was gradually evaporated over 2 d.

**Inclusion of 18 into crystalline sponge 5**

To a micro vial containing a cyclohexane exchanged single crystal of  $[(\text{ZnI}_2)_3(\text{tpt})_2]_n$  (**5**; tpt = tri(4-pyridyl)-1,3,5-triazine) and cyclohexane (75  $\mu\text{L}$ ), 5  $\mu\text{L}$  of 1,2-dichloroethane solution of target compounds (1 mg/1 mL) was added. The crystal containing microvial was incubated at 50  $^\circ\text{C}$  for 30 h and then, cooled at 4  $^\circ\text{C}$  for 18 h.

**Inclusion of 19 into crystalline sponge 5**

To a micro vial containing a cyclohexane exchanged single crystal of  $[(\text{ZnI}_2)_3(\text{tpt})_2]_n$  (**5**; tpt = tri(4-pyridyl)-1,3,5-triazine) and cyclohexane (75  $\mu\text{L}$ ), 5  $\mu\text{L}$  of 1,2-dichloroethane solution of target compounds (1 mg/1 mL) was added. The crystal containing microvial was incubated at 50  $^\circ\text{C}$  for 6 h. Though the target solution was not completely evaporated, the resultant crystal was subjected to the X-ray diffraction analysis. Note that complete evaporation of the solvent and contacting neat **19** with a crystal of **5** damaged on the crystallinity of **5**.

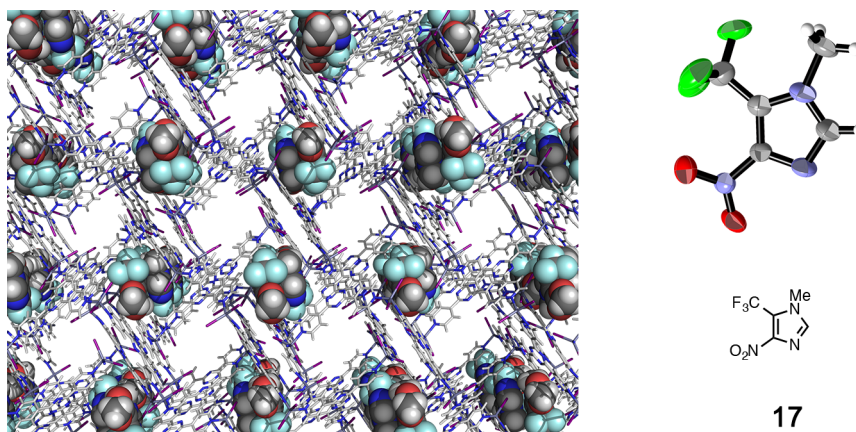


**Figure S6.1.** Photographs of the guest inclusion crystal of **5•17**, **5•18** and **5•19**. Some cracks were observed on the surface of the inclusion crystal **5•18** and **5•19**.

**Crystallographic data****Inclusion complex 5•17**

Crystallographic data (before the SQUEEZE treatment):  $C_{36}H_{24}N_{12}Zn_3I_6 \cdot C_7H_7O_2N_2F_3$ ,  $M = 1790.33$ , colorless rod,  $0.12 \times 0.04 \times 0.04 \text{ mm}^3$ , monoclinic, space group  $C2/c$ ,  $a = 32.983(3)$ ,  $b = 14.9969(13)$ ,  $c = 31.033(3) \text{ \AA}$ ,  $\beta = 100.5530(10)^\circ$ ,  $V = 15091(2) \text{ \AA}^3$ ,  $Z = 8$ ,  $D_c = 1.576 \text{ g/cm}^3$ ,  $F_{000} = 6704$ ,  $\mu = 3.444 \text{ mm}^{-1}$ ,  $T = 90(2) \text{ K}$ ,  $1.256 < \theta < 26.435^\circ$ , 12630 unique reflections out of 15511 with  $I > 2\sigma(I)$ ,  $R_{\text{int}} = 0.0248$ , 686 parameters, 0 restraints,  $\text{GoF} = 1.119$ , final  $R$  factors  $R_1 = 0.0752$  and  $wR_2 = 0.2528$  for all data.

Crystallographic data (after the SQUEEZE treatment):  $C_{36}H_{24}N_{12}Zn_3I_6 \cdot C_7H_7O_2N_2F_3$ ,  $M = 1790.33$ , colorless rod,  $0.12 \times 0.04 \times 0.04 \text{ mm}^3$ , monoclinic, space group  $C2/c$ ,  $a = 32.983(3)$ ,  $b = 14.9969(13)$ ,  $c = 31.033(3) \text{ \AA}$ ,  $\beta = 100.5530(10)^\circ$ ,  $V = 15091(2) \text{ \AA}^3$ ,  $Z = 8$ ,  $D_c = 1.576 \text{ g/cm}^3$ ,  $F_{000} = 6704$ ,  $\mu = 3.444 \text{ mm}^{-1}$ ,  $T = 90(2) \text{ K}$ ,  $1.256 < \theta < 26.435^\circ$ , 12462 unique reflections out of 15511 with  $I > 2\sigma(I)$ ,  $R_{\text{int}} = 0.0236$ , 686 parameters, 0 restraints,  $\text{GoF} = 1.119$ , final  $R$  factors  $R_1 = 0.0513$  and  $wR_2 = 0.1516$  for all data.

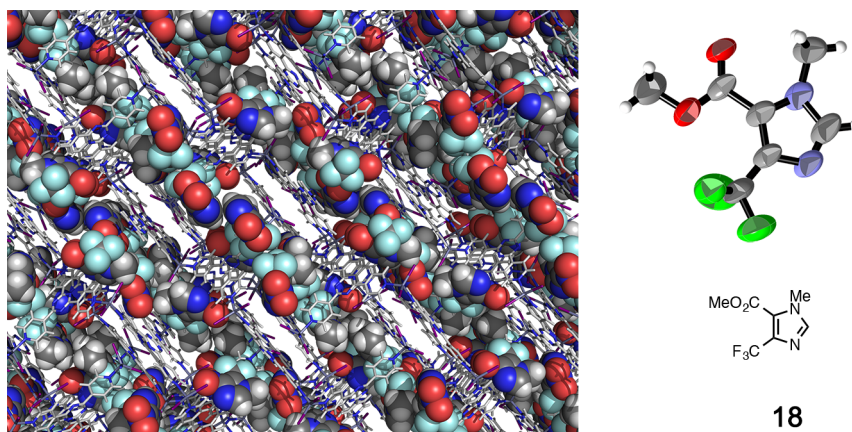


**Figure S6.2.** The X-ray crystal structure of inclusion crystal **5•17**. Guest molecules were drawn in CPK model in the packing structure and the thermal ellipsoid of the guest molecule was drawn at the 50% probability level.

**Inclusion complex 5•18**

Crystallographic data (before the SQUEEZE treatment):  $C_{36}H_{24}N_{12}Zn_3I_6 \cdot 1.92(C_5H_4O_2N_3F_3)$ ,  $M = 2151.20$ , colorless rod,  $0.12 \times 0.04 \times 0.04 \text{ mm}^3$ , monoclinic, space group  $C2/c$ ,  $a = 31.895(4)$ ,  $b = 15.133(2)$ ,  $c = 31.168(4) \text{ \AA}$ ,  $\beta = 98.082(2)^\circ$ ,  $V = 14895(3) \text{ \AA}^3$ ,  $Z = 8$ ,  $D_c = 1.919 \text{ g/cm}^3$ ,  $F_{000} = 8142$ ,  $\mu = 3.524 \text{ mm}^{-1}$ ,  $T = 90(2) \text{ K}$ ,  $1.290 < \theta < 26.357^\circ$ , 11392 unique reflections out of 14994 with  $I > 2\sigma(I)$ ,  $R_{\text{int}} = 0.0447$ , 886 parameters, 16 restraints,  $\text{GoF} = 1.081$ , final  $R$  factors  $R_1 = 0.0851$  and  $wR_2 = 0.2667$  for all data.

Crystallographic data (after the SQUEEZE treatment):  $C_{36}H_{24}N_{12}Zn_3I_6 \cdot 1.92(C_5H_4O_2N_3F_3)$ ,  $M = 2151.20$ , colorless rod,  $0.05 \times 0.03 \times 0.02 \text{ mm}^3$ , monoclinic, space group  $C2/c$ ,  $a = 31.895(4)$ ,  $b = 15.133(2)$ ,  $c = 31.168(4) \text{ \AA}$ ,  $\beta = 98.082(2)^\circ$ ,  $V = 14895(3) \text{ \AA}^3$ ,  $Z = 8$ ,  $D_c = 1.919 \text{ g/cm}^3$ ,  $F_{000} = 8142$ ,  $\mu = 3.524 \text{ mm}^{-1}$ ,  $T = 90(2) \text{ K}$ ,  $1.290 < \theta < 26.357^\circ$ , 11392 unique reflections out of 14994 with  $I > 2\sigma(I)$ ,  $R_{\text{int}} = 0.0447$ , 886 parameters, 16 restraints,  $\text{GoF} = 1.081$ , final  $R$  factors  $R_1 = 0.0851$  and  $wR_2 = 0.2667$  for all data.



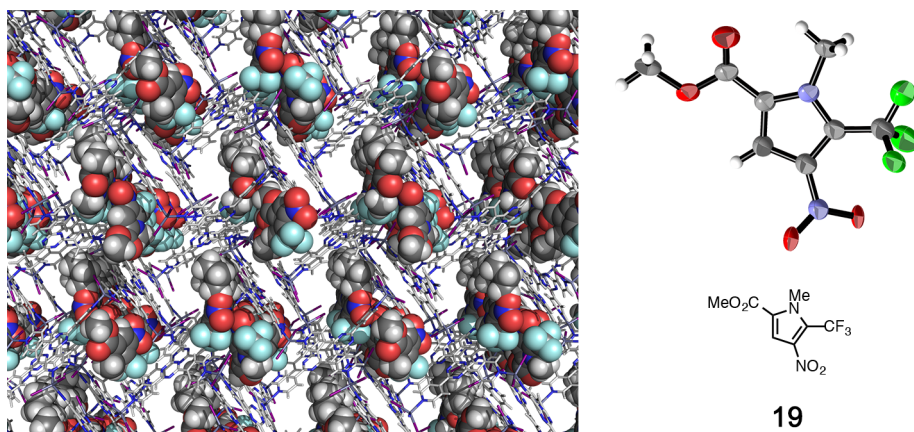
**Figure S6.3.** The X-ray crystal structure of inclusion crystal **5•18**. Guest molecules were drawn in CPK model in the packing structure and the thermal ellipsoid of the guest molecule was drawn at the 50% probability level.



**Inclusion complex 5•19**

Crystallographic data (before the SQUEEZE treatment):  $C_{72}H_{48}N_{24}Zn_6I_{12} \cdot 1.92(C_5H_4O_2N_3F_3)$ ,  $M = 3771.90$ , colorless rod,  $0.16 \times 0.06 \times 0.06$  mm<sup>3</sup>, monoclinic, space group  $Cc$ ,  $a = 33.914(18)$ ,  $b = 15.135(8)$ ,  $c = 30.963(16)$  Å,  $\beta = 100.727(6)^\circ$ ,  $V = 15616(14)$  Å<sup>3</sup>,  $Z = 4$ ,  $D_c = 1.604$  g/cm<sup>3</sup>,  $F000 = 7097$ ,  $\mu = 3.336$  mm<sup>-1</sup>,  $T = 90(2)$  K,  $1.222 < \theta < 26.389^\circ$ , 19059 unique reflections out of 28333 with  $I > 2\sigma(I)$ ,  $R_{int} = 0.0630$ , 1476 parameters, 1278 restraints,  $GoF = 1.031$ , final  $R$  factors  $R_1 = 0.1589$  and  $wR_2 = 0.4273$  for all data.

Crystallographic data (after the SQUEEZE treatment):  $C_{72}H_{48}N_{24}Zn_6I_{12} \cdot 1.92(C_5H_4O_2N_3F_3)$ ,  $M = 3771.90$ , colorless rod,  $0.16 \times 0.06 \times 0.06$  mm<sup>3</sup>, monoclinic, space group  $Cc$ ,  $a = 33.914(18)$ ,  $b = 15.135(8)$ ,  $c = 30.963(16)$  Å,  $\beta = 100.727(6)^\circ$ ,  $V = 15616(14)$  Å<sup>3</sup>,  $Z = 4$ ,  $D_c = 1.604$  g/cm<sup>3</sup>,  $F000 = 7097$ ,  $\mu = 3.336$  mm<sup>-1</sup>,  $T = 90(2)$  K,  $1.222 < \theta < 26.389^\circ$ , 19059 unique reflections out of 28333 with  $I > 2\sigma(I)$ ,  $R_{int} = 0.0630$ , 1544 parameters, 1284 restraints,  $GoF = 1.351$ , final  $R$  factors  $R_1 = 0.1309$  and  $wR_2 = 0.3821$  for all data.

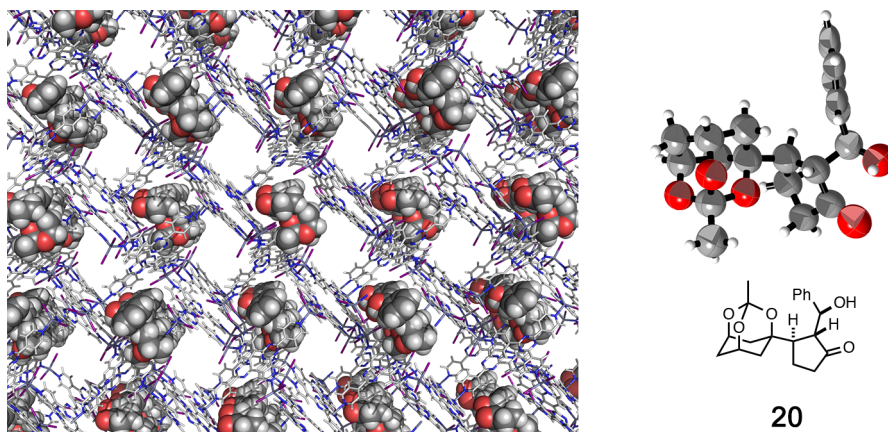


**Figure S6.4.** The X-ray crystal structure of inclusion crystal **5•19**. Guest molecules were drawn in CPK model in the packing structure and the thermal ellipsoid of the guest molecule was drawn at the 50% probability level.

**Inclusion complex 5•20**

Crystallographic data (before the SQUEEZE treatment):  $C_{72}H_{48}N_{24}Zn_6I_{12} \cdot 0.6(C_{20}H_{24}O_5)$ ,  $M = 3371.00$ , colorless rod,  $0.27 \times 0.07 \times 0.04 \text{ mm}^3$ , monoclinic, space group  $Cc$ ,  $a = 35.209(18)$ ,  $b = 14.870(2)$ ,  $c = 30.659(15) \text{ \AA}$ ,  $\beta = 100.402(2)^\circ$ ,  $V = 15735(4) \text{ \AA}^3$ ,  $Z = 4$ ,  $D_c = 1.423 \text{ g/cm}^3$ ,  $F000 = 6298$ ,  $\mu = 3.292 \text{ mm}^{-1}$ ,  $T = 90(2) \text{ K}$ ,  $1.180 < \theta < 25.242^\circ$ , 15421 unique reflections out of 27708 with  $I > 2\sigma(I)$ ,  $R_{\text{int}} = 0.0354$ , 1253 parameters, 1078 restraints,  $\text{GoF} = 1.329$ , final  $R$  factors  $R_1 = 0.1048$  and  $wR_2 = 0.3845$  for all data.

Crystallographic data (after the SQUEEZE treatment):  $C_{72}H_{48}N_{24}Zn_6I_{12} \cdot 0.6(C_{20}H_{24}O_5)$ ,  $M = 3371.00$ , colorless rod,  $0.27 \times 0.07 \times 0.04 \text{ mm}^3$ , monoclinic, space group  $Cc$ ,  $a = 35.209(18)$ ,  $b = 14.870(2)$ ,  $c = 30.659(15) \text{ \AA}$ ,  $\beta = 100.402(2)^\circ$ ,  $V = 15735(4) \text{ \AA}^3$ ,  $Z = 4$ ,  $D_c = 1.423 \text{ g/cm}^3$ ,  $F000 = 6298$ ,  $\mu = 3.292 \text{ mm}^{-1}$ ,  $T = 90(2) \text{ K}$ ,  $1.18 < \theta < 25.00^\circ$ , 15227 unique reflections out of 27708 with  $I > 2\sigma(I)$ ,  $R_{\text{int}} = 0.0468$ , 1253 parameters, 1051 restraints,  $\text{GoF} = 1.068$ , final  $R$  factors  $R_1 = 0.0772$  and  $wR_2 = 0.2577$  for all data.

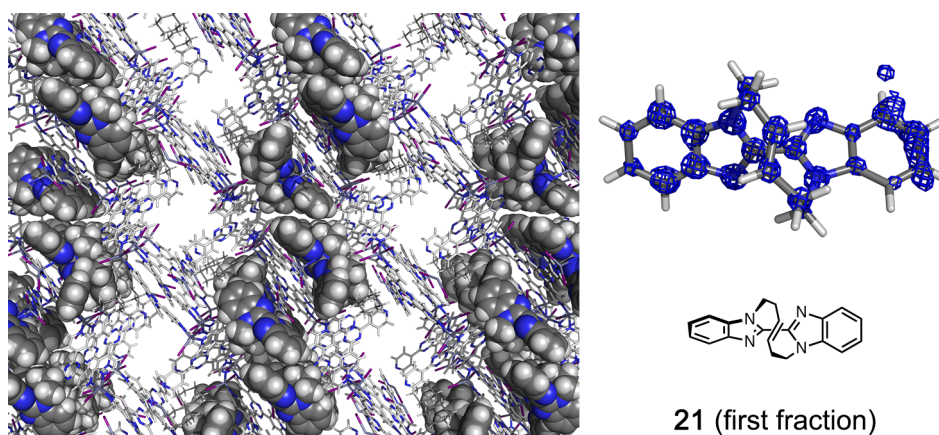


**Figure S6.5.** The X-ray crystal structure of inclusion crystal **5•20**. Guest molecules were drawn in CPK model in the packing structure and the thermal ellipsoid of the guest molecule was drawn at the 50% probability level.

**Inclusion complex 5•21 (first fraction)**

crystallographic data (before the SQUEEZE treatment):  
 $C_{72}H_{48}N_{24}Zn_6I_{12} \cdot 0.9(C_{20}H_{18}N_4) \cdot 0.6(C_6H_{12})$ ,  $M = 3497.80$ , colorless block,  $0.14 \times 0.07 \times 0.07 \text{ mm}^3$ , monoclinic, space group  $C2$ ,  $a = 35.4151(19) \text{ \AA}$ ,  $b = 14.6842(5) \text{ \AA}$ ,  $c = 31.7864(16) \text{ \AA}$ ,  $\beta = 102.068(2)^\circ$ ,  $V = 16165.0(13) \text{ \AA}^3$ ,  $Z = 4$ ,  $D_c = 1.437 \text{ g/cm}^3$ ,  $F000 = 6569$ ,  $\mu = 3.206 \text{ mm}^{-1}$ ,  $T = 93(2) \text{ K}$ ,  $1.310 < \theta < 25.358^\circ$ , 17484 unique reflections out of 29028 with  $I > 2\sigma(I)$ ,  $R_{\text{int}} = 0.0641$ , 1286 parameters, 283 restraints,  $\text{GoF} = 1.022$ , final  $R$  factors  $R_1 = 0.0765$ , and  $wR_2 = 0.2432$  for all data, Flack parameter = 0.070(15).

crystallographic data (after the SQUEEZE treatment):  
 $C_{72}H_{48}N_{24}Zn_6I_{12} \cdot 0.9(C_{20}H_{18}N_4) \cdot 0.6(C_6H_{12})$ ,  $M = 3497.80$ , colorless block,  $0.14 \times 0.07 \times 0.07 \text{ mm}^3$ , monoclinic, space group  $C2$ ,  $a = 35.4151(19) \text{ \AA}$ ,  $b = 14.6842(5) \text{ \AA}$ ,  $c = 31.7864(16) \text{ \AA}$ ,  $\beta = 102.068(2)^\circ$ ,  $V = 16165.0(13) \text{ \AA}^3$ ,  $Z = 4$ ,  $D_c = 1.437 \text{ g/cm}^3$ ,  $F000 = 6569$ ,  $\mu = 3.206 \text{ mm}^{-1}$ ,  $T = 93(2) \text{ K}$ ,  $1.310 < \theta < 25.358^\circ$ , 17484 unique reflections out of 29028 with  $I > 2\sigma(I)$ ,  $R_{\text{int}} = 0.0637$ , 1286 parameters, 283 restraints,  $\text{GoF} = 0.990$ , final  $R$  factors  $R_1 = 0.0655$ , and  $wR_2 = 0.1914$  for all data, Flack parameter = 0.06(4).

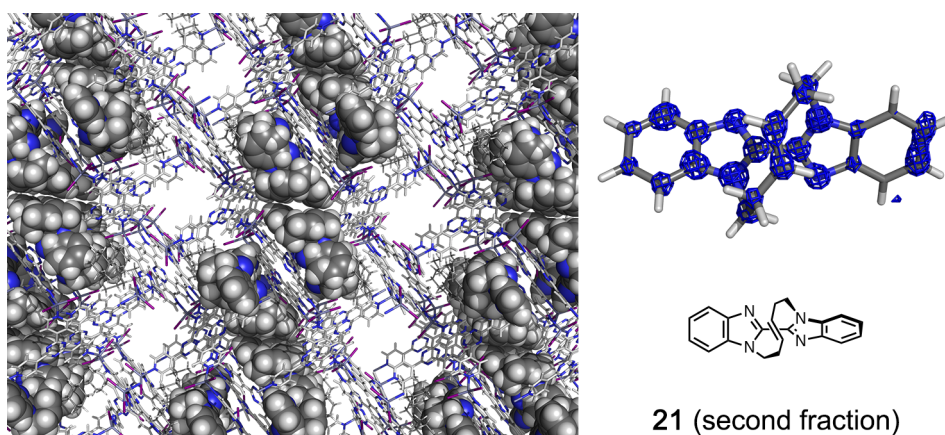


**Figure S6.6.** The X-ray crystal structure of **5•21** (first fraction) and the observed electron density map ( $F_o$ , contour:  $0.8\sigma$ ). Guest molecules were drawn in CPK model in the packing structure.

**Inclusion complex 5•21 (second fraction)**

crystallographic data (before the SQUEEZE treatment):  
 $C_{72}H_{48}N_{24}Zn_6I_{12} \cdot 0.89(C_{20}H_{18}N_4) \cdot 1.41(C_6H_{12})$ ,  $M = 3563.04$ , colorless block,  $0.14 \times 0.07 \times 0.07 \text{ mm}^3$ , monoclinic, space group  $C2$ ,  $a = 35.268(2) \text{ \AA}$ ,  $b = 14.6819(10) \text{ \AA}$ ,  $c = 31.513(2) \text{ \AA}$ ,  $\beta = 101.729(3)^\circ$ ,  $V = 15976.8(17) \text{ \AA}^3$ ,  $Z = 4$ ,  $D_c = 1.481 \text{ g/cm}^3$ ,  $F000 = 6718$ ,  $\mu = 3.246 \text{ mm}^{-1}$ ,  $T = 93(2) \text{ K}$ ,  $1.320 < \theta < 25.356^\circ$ , 18676 unique reflections out of 28685 with  $I > 2\sigma(I)$ ,  $R_{\text{int}} = 0.0482$ , 1281 parameters, 247 restraints,  $\text{GoF} = 0.966$ , final  $R$  factors  $R_1 = 0.0697$ , and  $wR_2 = 0.2265$  for all data, Flack parameter = 0.123(13).

crystallographic data (after the SQUEEZE treatment):  
 $C_{72}H_{48}N_{24}Zn_6I_{12} \cdot 0.89(C_{20}H_{18}N_4) \cdot 1.41(C_6H_{12})$ ,  $M = 3563.04$ , colorless block,  $0.14 \times 0.07 \times 0.07 \text{ mm}^3$ , monoclinic, space group  $C2$ ,  $a = 35.268(2) \text{ \AA}$ ,  $b = 14.6819(10) \text{ \AA}$ ,  $c = 31.513(2) \text{ \AA}$ ,  $\beta = 101.729(3)^\circ$ ,  $V = 15976.8(17) \text{ \AA}^3$ ,  $Z = 4$ ,  $D_c = 1.481 \text{ g/cm}^3$ ,  $F000 = 6718$ ,  $\mu = 3.246 \text{ mm}^{-1}$ ,  $T = 93(2) \text{ K}$ ,  $1.320 < \theta < 25.356^\circ$ , 18502 unique reflections out of 28685 with  $I > 2\sigma(I)$ ,  $R_{\text{int}} = 0.0482$ , 1281 parameters, 249 restraints,  $\text{GoF} = 1.053$ , final  $R$  factors  $R_1 = 0.0601$ , and  $wR_2 = 0.1786$  for all data, Flack parameter = 0.10(3).



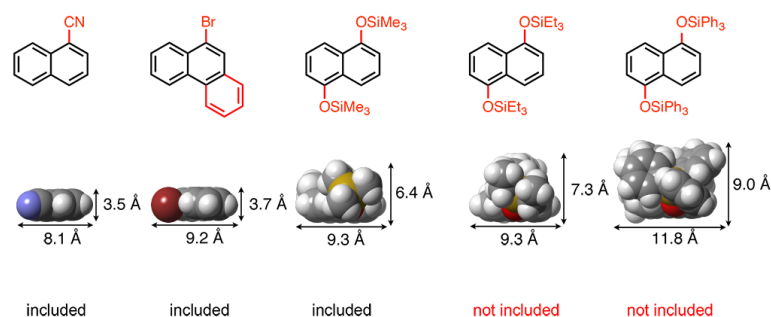
**Figure S6.7.** The X-ray crystal structure of **5•21** (second fraction) and the observed electron density map ( $F_o$ , contour:  $0.8\sigma$ ). Guest molecules were drawn in CPK model in the packing structure.

## References

- 1 H. Ishikawa, T. Suzuki, Y. Hayashi, *Angew. Chem. Int. Ed.* **2009**, *48*, 1304–1307.
- 2 M. Reiter, S. Torssell, S. Lee, D. W. C. Macmillan, *Chem. Sci.* **2010**, *1*, 37–42.
- 3 S. B. Jones, B. Simmons, D. W. C. MacMillan, *J. Am. Chem. Soc.* **2009**, *131*, 13606–13607.
- 4 H. Renata, Q. Zhou, P. S. Baran, *Science* **2013**, *339*, 59–63.
- 5 M. T. Reetz, *Angew. Chemie Int. Ed.* **2001**, *40*, 284–310.
- 6 T. W. Lyons, M. S. Sanford, *Chem. Rev.* **2010**, *110*, 1147–1169.
- 7 A. E. Shilov, G. B. Shul'pin, *Chem. Rev.* **1997**, *97*, 2879–2932.
- 8 T. L. Suyama, W. H. Gerwick, K. L. McPhail, *Bioorg. Med. Chem.* **2011**, *19*, 6675–6701.
- 9 E. V. Vinogradova, P. Müller, S. L. Buchwald, *Angew. Chem. Int. Ed.* **2014**, *53*, 3125–3128.
- 10 A. G. O'Brien, A. Maruyama, Y. Inokuma, M. Fujita, P. S. Baran, D. G. Blackmond, *Angew. Chem. Int. Ed.* **2014**, *53*, 11868–11871.
- 11 D. Kamimura, D. Urabe, M. Nagatomo, M. Inoue, *Org. Lett.* **2013**, *15*, 5122–5125.
- 12 S. Nishio, T. Somete, A. Sugie, T. Kobayashi, T. Yaita, A. Mori, *Org. Lett.* **2012**, *14*, 2476–2479.
- 13 *APEX2*, *SADABS* and *XPREF*, Bruker AXS Inc., Madison, Wisconsin, USA, 2007.
- 14 *CrystalClear-SM Expert 2.1 b32*, Rigaku Corporation, Tokyo, Japan, 2013.
- 15 G. M. Sheldrick, *Acta Cryst.* **2008**, *A64*, 112–122.
- 16 P. van der Sluis, A. L. Spek, *Acta Cryst.* **1990**, *A46*, 194–201.

## Chapter 7

### Scope and Limitations of the Crystalline Sponge Method



#### Abstract

The crystalline sponge method has a wide scope of the target compound, but the method contains intrinsic limitations on the target molecular size, solubility and obtained data quality. The insights about these scope and limitations are obtained by the crystalline sponge analysis of different sized or different functional group attached target molecules. The difference of the obtained data quality with the different guest inclusion conditions was also analyzed. Furthermore, it was revealed that a situation which contained the possibility of missassignment occurs when too flexible target compounds were analyzed.

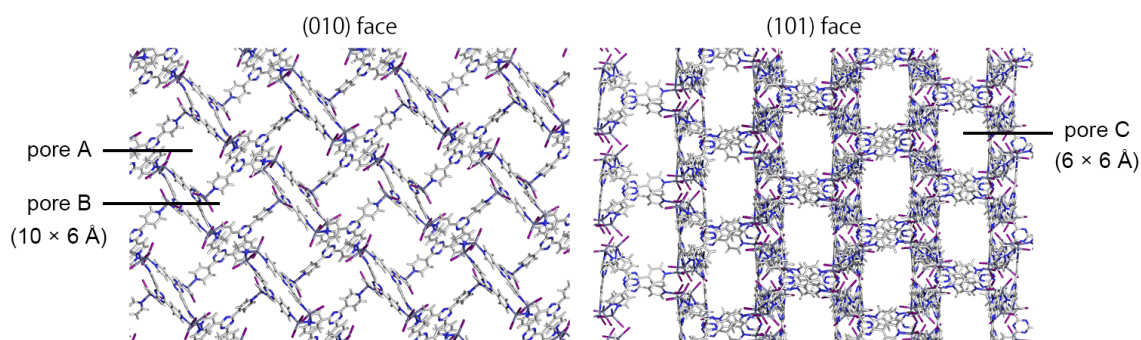


## 7.1 Introduction

Among the hundreds of analysis methods, the perfect analysis method never exists. Any method has advantages and disadvantages, target sample scope, limitations, and obtained information is also different from each other.<sup>1</sup> The important thing is that to get the most out of the analysis method, the above features should be figured out. Furthermore, knowing the available range of the analysis method leads to further improvement of the method or innovation. Considering the crystalline sponge method, the target sample scope was drastically expanded to the non-crystalline compound from the conventional X-ray technique, which was already shown in the previous chapters. The differences also appeared in the analyzing part of the X-ray diffraction measurements.<sup>2</sup> In addition to the target scope and diffraction study difference, the crystalline sponge method has some differences in on the applying conditions and available data quality from the conventional small molecule single crystallography. In this chapter, the scope and limitations of the current crystalline sponge method were shown.

## 7.2 Suitable size of the target compound

The wide target scope of the crystalline sponge analysis is one of the biggest advantages of the method. However, since the target compounds have to be included into the pore of the crystalline sponge **5**, there is an intrinsic limitation on the molecular size of analyzing targets. As previously described, the pore of the crystalline sponge is three dimensionally connected infinite pore, but the sizes from the guest accessible direction are roughly defined by the framework as  $10 \times 6 \text{ \AA}^2$  for larger pore and  $6 \times 6 \text{ \AA}^2$  for smaller one (Figure 7.1). This size limitation was clearly demonstrated by the inclusion experiment of a series of naphthalene derivatives.



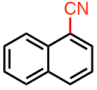
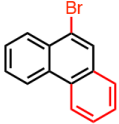

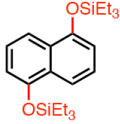
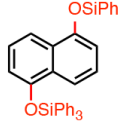
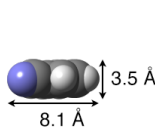
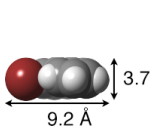
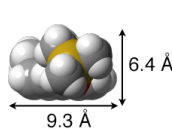
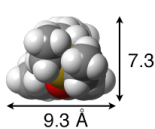
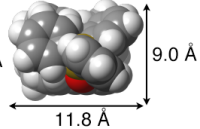
**Figure 7.1.** The size of the three different pores of the crystalline sponge **5**.

The series of naphthalene derivatives with variety of substituents, **22**, **23**, **24**, **25**, and **26** were subjected to the inclusion experiment to the crystalline sponge **5** and X-ray diffraction study. As the result of the crystalline sponge analysis, the smaller **22**, **23** and **24** were included and observed by the X-ray, while the larger **25** and **26** were not included into the crystalline sponge **5** (Table 7.1). The size threshold between included and not included size *i.e.* between the size of **24** and **25**, corresponded to the maximum pore accessible size of the crystalline sponge **5** ( $10 \times 6 \text{ \AA}^2$ ). Though the molecular size is a critical parameter to know whether target molecules can be included or not, the higher refined occupancy or stronger electron density are not always obtained with the smaller molecule as is the case with the guest inclusion in the host-guest chemistry.<sup>3</sup> In fact, among **22**, **23** and **24**, the inclusion crystal **5**•**24** gave the best result in terms of the occupancy. When the target compound is in the range of includable size, the molecular interactions between target molecules and host framework have much effects on the occupancy and observed electron density of the



guest molecule than target molecule size.

**Table 7.1.** Screening of the inclusion size limitation of the crystalline sponge **5**.

entry	1	2	3	4	5
structure	 <b>22</b>	 <b>23</b>	 <b>24</b>	 <b>25</b>	 <b>26</b>
size of the minimum section					
result of the crystalline sponge analysis	included (occupancy 50%)	included (occupancy 68%)	included (occupancy 100%)	not included	not included

### 7.3 Suitable solvent for the guest inclusion

The target compound is included into the crystalline sponge from the supernatant solution based on an equilibrium between the concentration of the target compound in supernatant and in crystalline sponge. Therefore, the target solubility is an important parameter to perform the target inclusion. Based on the extensive screening of the solvent system for inclusion, cyclohexane, dichloromethane, chloroform and 1,2-dichloroethane were found to be suitable solvents for the crystalline sponge method. Thus the inclusion should be carried out with the target compound solution in the solvent listed above or their mixture. When halogenated solvents are employed for the dissolving solvents, the amount of halogenated solvents should be below 10 % (v/v) in the whole solvent system, *i.e.* halogenated solvents should be used as mixed solvents with cyclohexane. Severe crystal damages (decomposition and loss of the crystallinity) were observed by use of higher concentration or pure halogenated solvent. Other solvents such as H<sub>2</sub>O, alcohols (MeOH, EtOH), ethers (Et<sub>2</sub>O, THF, 1,2-dimethoxyethane), toluene, methylcyclohexane, CH<sub>3</sub>CN and DMSO caused the complete deterioration of the crystallinity or dissolution of the crystalline sponge even with a small amount of them.<sup>4</sup> After the decomposition of the crystalline sponge **5** by

the ether, toluene or methylcyclohexane, the supernatant solution turned to be a pink color, which might be come from I<sub>2</sub> derived from oxidation of dissociated free I<sup>-</sup>.

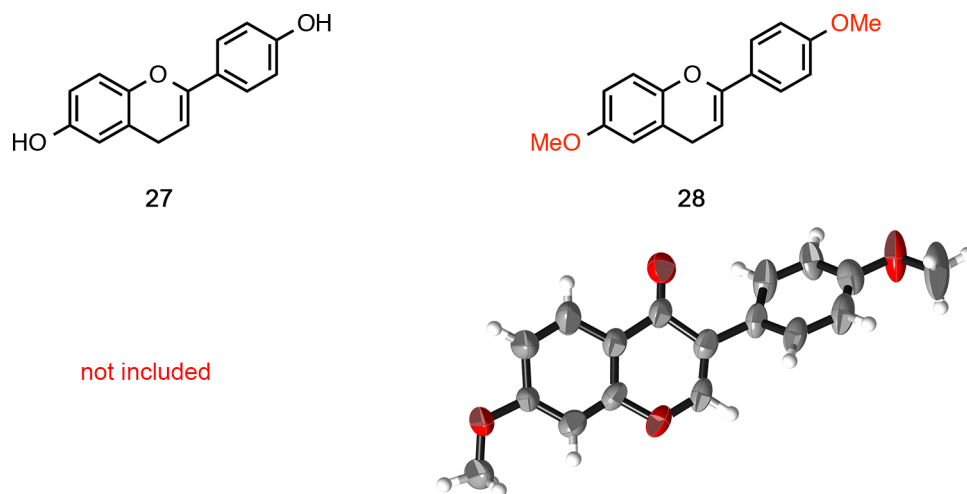
Considering the guest inclusion mechanism, the higher concentration solution of the target compound is better for inclusion (ultimately a neat conditions of liquid sample). However, starting from 5 µg/80 µL concentration is practically acceptable for crystalline sponge analysis due to its small requisite sample amount and sample concentration process by a gradual solvent evaporation.

#### 7.4 Functional group effect on the inclusion

The introduction of the functional groups on the target molecule has both good and bad aspects for the crystalline sponge analysis. The biggest advantage is that the functional group introduction provides the interacting points with the framework. For example hydroxy group provides the hydrogen bond donor for iodine atom in the crystalline sponge. The increased intramolecular polarization is also better for binding by the crystalline sponge.

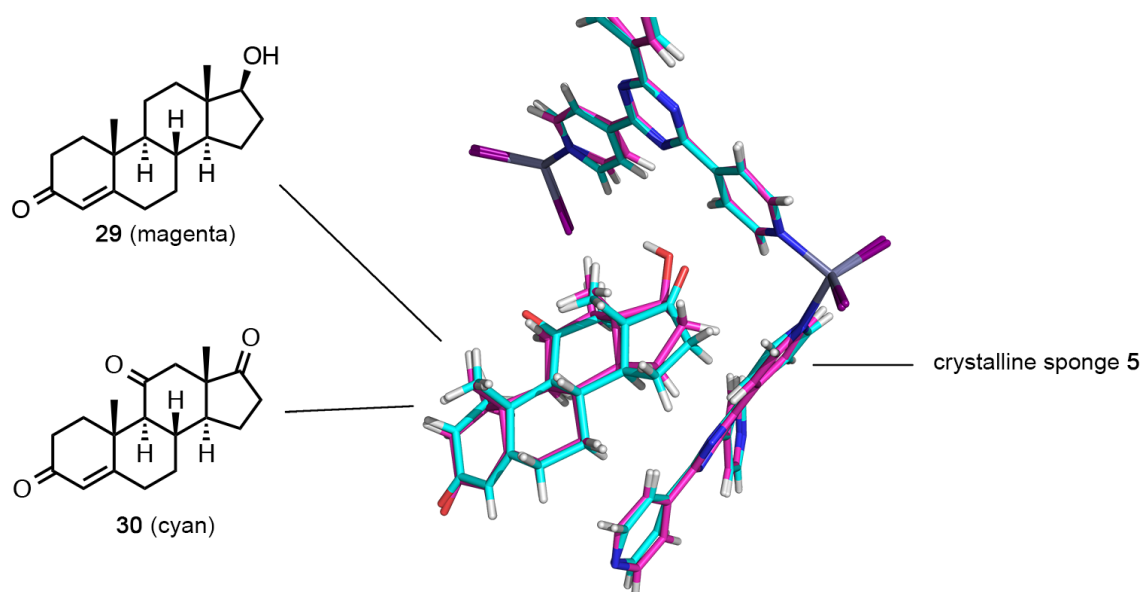
On the other hand, the apparent drawback is that the introduction of functional groups increases the size of the molecule. Additionally, the solubility problem sometimes occurred because of the functional group such as hydroxy group and amide moiety. The compound must be dissolved to the certain solvents (described in *solvent* section), however compounds with too many hydroxy groups cannot be dissolved in the above-mentioned less polar solvents.

Since isoflavone derivative daidzein (**27**) was poorly soluble in cyclohexane or even pure 1,2-dichloroethane, inclusion and crystalline sponge analysis of **27** failed. In this case, methylation of hydroxy group drastically improves the solubility to cyclohexane. Treating **27** with CH<sub>3</sub>I gave dimethylated daidzein derivative (**28**) as white solid, which was soluble in cyclohexane. With cyclohexane solution of **28** (5 µg/5 µL), the crystalline sponge analysis of **28** succeeded and gave excellent quality of the data (Figure 7.3).



**Figure 7.3.** Change of the inclusion result by the difference of the functional group.

The introduction of a functional group sometimes changes the guest bound position in the pore due to the difference of the strength and position of the interaction. However when the target compounds have a same backbone such as steroid, different molecules were bound with similar fashions. Inclusion experiments of steroid derivatives testosterone (**29**) and adrenosterone (**30**) gave the inclusion crystals **5•29**, and **5•30** respectively. The X-ray analysis of respective inclusion crystals revealed included **29** and **30** were trapped at the same place in the pore. Furthermore, superimposing of **5•29** and **5•30** structures well matched and a difference appeared on steroid D ring's hydroxy group and carbonyl group (Figure 7.5). Since the crystalline sponge **5** binds the target compound by multiple molecular interactions at many interaction sites, the difference in small functional group on the steroid backbone structure did not alter their affinity to the crystalline sponge **5**. It indicated that when some compounds were successfully included and analyzed by the crystalline sponge method, its derivatives with the same backbone are expected to be analyzed by the crystalline sponge method as long as they were soluble in appropriate solvents.



**Figure 7.4.** The superimposed image of the X-ray structures of **5•29** (magenta) and **5•30** (cyan). Fitting of the guest orientation was examined based on the orientation of three nitrogen atoms of the pyridine ligand in the host crystalline sponge **5**.

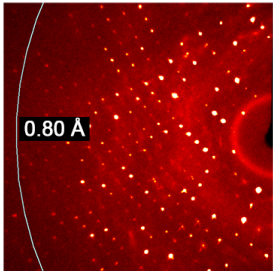
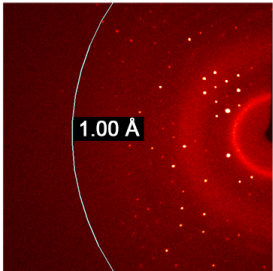
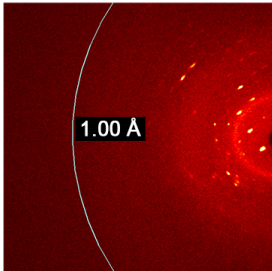
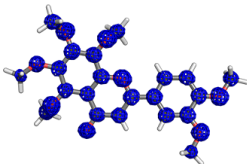
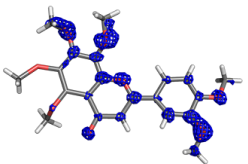
### 7.5 Obtained data quality and structure by the crystalline sponge method

Obtained data quality by the crystalline sponge method vary from excellent (very close to the common single crystal X-ray analysis) to poor (almost no information about the target compound) depending on analyzing compound and inclusion conditions. Typically, the crystalline sponge analysis is much closer to the protein crystallography than small molecular crystallography in terms of the obtained resolution and unit cell size.<sup>5</sup> Therefore, the obtained data should be carefully analyzed without bias. The quality of usual small molecule X-ray diffraction analysis can be evaluated from many aspects, such as resolution, spot shape of the diffraction, the thermal factor and  $R_1$  or  $wR_2$  values. However, it is difficult to evaluate the data quality obtained by the crystalline sponge analysis by the same standard to the small molecule crystallography. For the crystalline sponge analysis, the resolution of the diffraction often becomes low due to the flexible nature and large pore of the host framework. Moreover, the thermal factor of the guest molecules becomes large due to the loose confinement of the guest molecules in the pore by non-covalent weak interactions, and  $R_1$  or  $wR_2$  values do not have much information because these values are almost dominantly determined by the host framework structure.

However, the diffraction pattern gives information about the data quality to certain

extent. Here showed an example for the typical relationship between the data quality and diffraction pattern about inclusion of polymethoxyflavon derivative nobiletin (**31**). Three inclusion crystalline sponges **5•31** were prepared with different guest amount, inclusion time and temperature. For each batch, inclusions were performed: i) using 8 mg of **31** for 9 d at 50 °C; ii) using 5 µg of **31** for 2 d at 50 °C; iii) using 5 µg of **31** for 1 h at 80 °C. When the inclusion was performed with conditions i), **31** was included with 100 % occupancy and the crystallinity of the inclusion crystal was fully maintained *i.e.* the best data quality was obtained. The observed resolution of the diffraction pattern was over 0.8 Å and the structure was converged without any restraints. As decreasing the inclusion amount of **31** with conditions ii), the observed resolution also became lower to ~1.0 Å. Though the data quality was not good as that with conditions i), the structure of **31** was still observable along with the host framework and was able to converge the refinement with some restraints on the structure and decreased occupancy (60%). The Debye-ring like diffraction was the worst case for the structural analysis with conditions iii). The occupancy of the guest **31** in this structure could not be determined, but might be below 20%. From these poor quality data, analyzing the structure was difficult even for the host framework, and guest structure was almost impossible to observe. Nothing should be discussed with these quality data.

**Table 7.1.** Typical diffraction patterns and data quality obtained by the crystalline sponge analysis.

entry	i)	ii)	iii)
guest amount	8 mg	10 $\mu$ g	5 $\mu$ g
soaking time	9 d	2 d	1 h
inclusion temperature	50 $^{\circ}$ C	50 $^{\circ}$ C	80 $^{\circ}$ C
diffraction pattern and resolution	 0.80 Å good diffraction pattern	 1.00 Å low resolution (insufficient guest inclusion)	 1.00 Å Debye-ring like (deterioration of the crystallinity)
observed electron density map (0.8 $\sigma$ )			n/a
refined occupancy	100%	60%	n/a

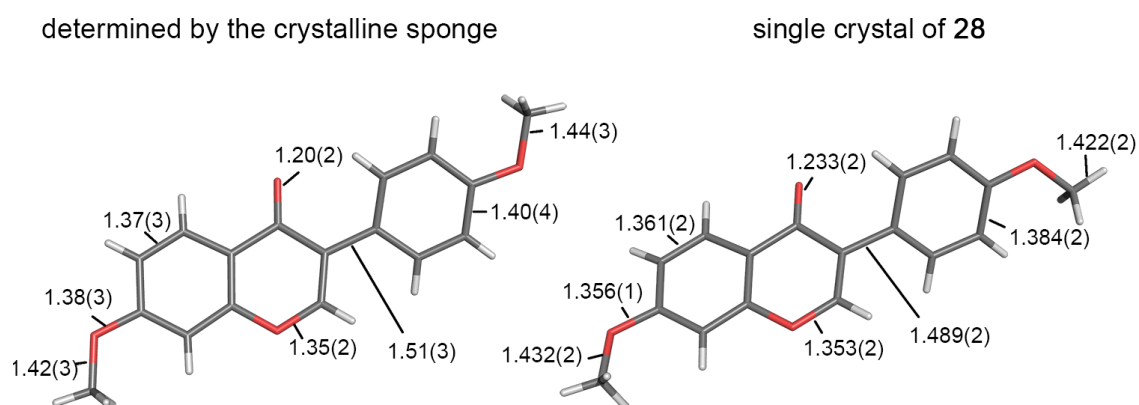
The reasons of poor quality data were mainly categorized into two. i) Low inclusion amount or no inclusion of the target compound. ii) Deterioration of the crystallinity of the crystalline sponge.

For the former problem, guest inclusion amount problem, if the analyzing target is intrinsically not includable into the crystalline sponge due to the size or solubility, the target should be changed. When the target inclusion was observed even with a small amount, optimizing the inclusion conditions may increase the inclusion guest amount and may improve the data quality. For the latter problem, making the inclusion time short sometimes prevents the deterioration of the crystallinity such as compound **18** and **19** (described in chapter 6).

In terms of the determination of the bond length by the crystalline sponge method, the error bar is still larger than that of the conventional small molecule X-ray diffraction analysis even for the best data of the crystalline sponge method.

One of the best quality data was obtained for the crystalline sponge analysis of **28** shown above. The X-ray diffraction analysis was converged at 100% occupancy

without any restraints on the **28**. Also, the thermal factor was reasonably small. However, the error bars on the determined bond lengths were an order of magnitude larger than those of the conventional small molecule single crystal X-ray analysis of **28** (Figure 7.5).<sup>6</sup> To improve the situation, the higher redundancy is required for the X-ray measurement, but it causes the longer measurement time. Furthermore, considering the included guest molecule's nature that the guests are loosely bound by the weak interactions in the crystalline sponge, guests in the crystalline sponge are not as rigid and completely aligned as the single crystal of the target compound. Therefore, determining the bond length in the same order as the conventional crystallography is not practical even for the excellent quality crystalline sponge analysis data. Putting that aside, however, the crystalline sponge method is still highly effective for analyzing atom connectivity, stereochemistry and so on.



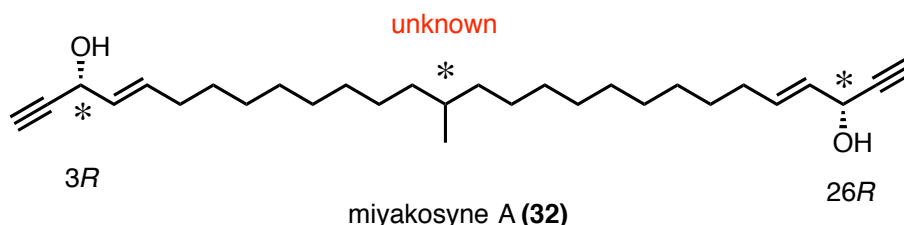
**Figure 7.5.** Observed bond lengths and error bars of **28** by the crystalline sponge method and reported in the literature.

Furthermore, the differences on the obtained data by the crystalline sponge and conventional single crystal X-ray analysis appeared not only in the data quality, but also in the conformation and packing structure of the target compound. Crystal structure of pure target compound is determined only by the molecular interaction or packing structure of the pure target compound. However, in the crystalline sponge method, since the target compound is bound by the molecular interaction with the host crystalline sponge, observed target compound conformation is always affected by the host crystalline sponge and packing structure in the pore. Therefore, sometimes the observed conformation is different from the structure obtained by the single crystal

X-ray analysis of pure target compound. As shown in Figure 7.5, the directions of the methoxy group on the phenyl rings were different between the structure of the crystalline sponge analysis and the structure of pure single crystal.

### 7.6 Missassignment due to the disorder

When a scarce marine natural product miyakosyne A (**32**),<sup>7</sup> which has three stereocenters in the structure. The absolute structures of two of the three stereocenters (C3 and C26) were previously determined to be *R* configuration (Figure 7.6). However, the stereochemistry of C14 still remained unclear. Therefore, the determination of the stereochemistry of the C14 by the crystalline sponge method was performed as a relative stereochemistry to the C3 and C26. By means of the crystalline sponge method, the stereochemistry on C14 was converged in *S* configuration. However, it was revealed that the analyzed *S* configuration was incorrect and the actual stereochemistry of C14 was *R* configuration by HPLC analysis of the sample prepared by total synthesis of all the isomers of miyakosyne A and derivatization with Ohri's reagent.<sup>8,9</sup>

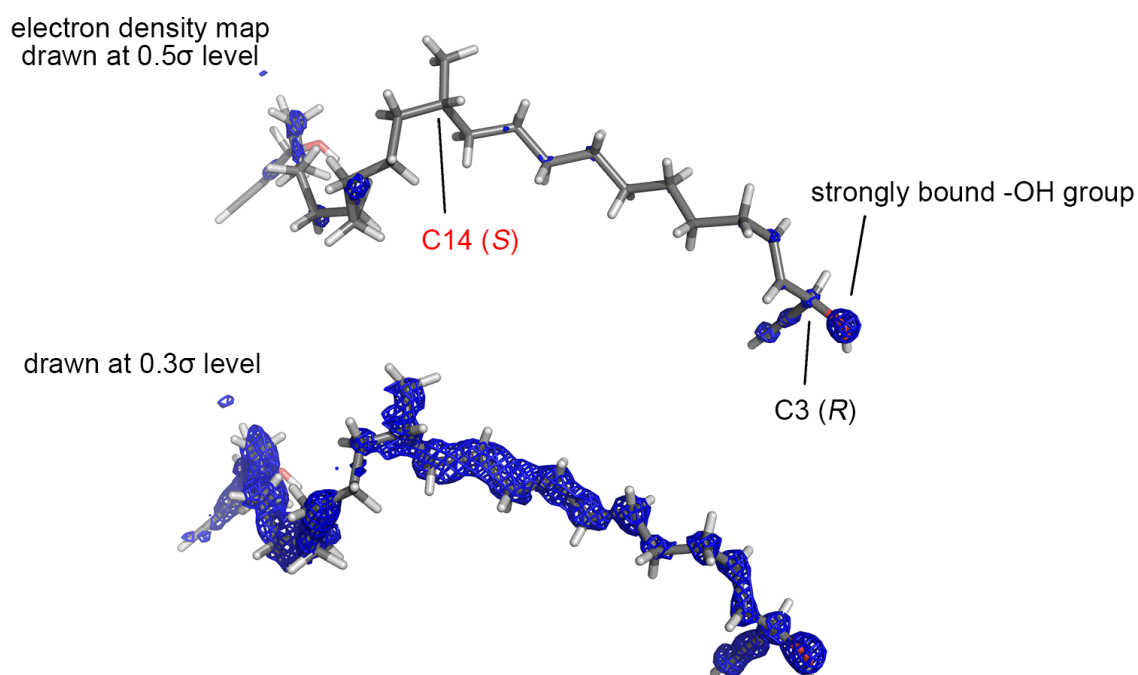


**Figure 7.6.** A chemical structure of miyakosyne A.

An inclusion crystal **5•32** was obtained by soaking a crystal of **5** into cyclohexane solution of **32** (5 μg/80 μL). The X-ray diffraction study of inclusion crystal **5•32** gave an excellent diffraction pattern (~0.8 Å resolution) and the structure was solved in a chiral monoclinic *C2* space group. After an assignment of the host framework, included **32** structure was observed as residual electron density. In particular, hydroxyl groups at C3 and C26 were bound to ZnI<sub>2</sub> by O–H•••I hydrogen bond and clearly observed. Furthermore, the stereochemistries of C3 and C26 were correctly determined as *R* configuration. Thus, structural analysis of **32** started with the hydroxy groups and terminal alkyne part, and the stereochemistry on C14 was analyzed as the relative configuration to C3 and C26. Since the central alkyl chain was too



flexible, the residual electron density assignable to the methylene chain was weaker than that of the hydroxyl group. However, the assignment of alkyl chain based on the reported structure was converged with DFIX command (Figure 7.7). Especially the stereochemistry of C14 was converged with *S* configuration. In order to confirm the *S* configuration, the structural refinement was run with intentionally assigned *R* configuration on C14, the stereochemistry was inverted and converged with *S* configuration by the refinement. Thus, the stereochemistry of miyakosyne A was analyzed as *3R,14S,26R*-configuration by the crystalline sponge method.



**Figure 7.7.** Observed electron density maps ( $F_o$ , contour:  $0.5\sigma$  and  $0.3\sigma$ ) superimposed on the refined **32** structure.

On the other hand, recently the actual stereochemistry of **32** was determined as *3R,14R,26R*-configuration by another synthetic approach. All the diastereomers of **32** were synthesized and analyzed its stereochemistry by HPLC after derivatization with Ohri's reagent. The HPLC analysis revealed the stereochemistry of **32** was *3R,14R,26R*-configuration. The *3R,14R,26R*-configuration was also supported by the NMR measurement of derivatized diastereomers.<sup>7,8</sup>

By the synthetic approach's result, it was revealed the stereochemistry of C14 was missassigned by the crystalline sponge method. The missassignment occurred due to

the disorder on the alkyl chain of **32**. Two hydroxy groups were bound by the hydrogen bond, but the central long alkyl chain part was less interacted with the host framework and loosely trapped. This loose trap caused the disorder and afforded the relatively weak and blurred electron density, which led to the missassignment of C14 configuration. This result indicated that the observed structure by the crystalline sponge method should be carefully analyzed when the blurred weak electron density was obtained.

### 7.7 Summary

In this chapter, the scope and limitations of the crystalline sponge method was studied. The crystalline sponge method has an intrinsic target size limitations around  $9 \times 7 \text{ \AA}$ . In addition to the compound size, the solubility of the target is an important factor to perform the crystalline sponge analysis. The accuracy of the obtained data are not the same as that of obtained by the small molecule crystallography. Therefore, as might be expected, the obtained data by the crystalline sponge method should be carefully analyzed when the target compound is flexible or the observed electron density is blurred.

## 7.9 Experimental section

Materials and Methods	145-148
Crystallographic data	149-157
<b>Figure S7.1-S7.9. X-ray crystallographic data</b>	149-157

## Materials and method

### Reagents and equipment

Solvents and reagents were purchased from TCI Co., Ltd., WAKO Pure Chemical Industries Ltd., and Sigma-Aldrich Corporation and used without further purification. Microscopic FT-IR spectra were recorded on a Varian DIGILAB Scimitar instrument and are reported in frequency of absorption ( $\text{cm}^{-1}$ ). Single crystal X-ray diffraction data were collected on a BRUKER APEX-II CCD diffractometer equipped with a focusing mirror ( $\text{MoK}_\alpha$  radiation  $\lambda = 0.71073 \text{ \AA}$ ) and a  $\text{N}_2$  generator (Japan Thermal Eng. Co., Ltd.) or Rigaku XtaLAB P200 diffractometer equipped with a PILATUS-200K detector with multi-layer mirror monochromator ( $\text{MoK}_\alpha$  radiation  $\lambda = 0.71073 \text{ \AA}$ ). For single crystal X-ray diffraction analysis and microscopic IR measurement, fluorolube® and mineral oil were used as a protectant for the single crystals.

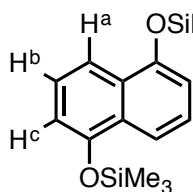
### X-ray crystallographic analysis

Single crystal X-ray diffraction data were processed with Bruker APEX2 software and CrystalClear program.<sup>10,11</sup> For Bruker data, absorption correction was performed by multi-scan method in SADABS and space groups were determined by XPREP program.<sup>1</sup> The structures were solved by direct methods and refined by full-matrix least-squares calculations on  $F^2$  using SHELXL-97 and SHELXL-2013 program.<sup>12</sup> In the determination of space group, the XPREP program suggested space group was employed for analyzing the structure.

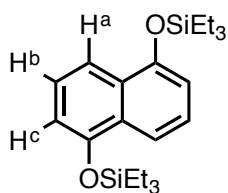
After the initial phase determination, all the atoms for the host framework (*i.e.* ZnI<sub>2</sub> and tpt ligands) were assigned and the structure was refined anisotropically except for hydrogen atoms. Since the host framework was in some cases highly disordered, atoms were partially restrained with DFIX, FLAT, SIMU and ISOR commands. Atoms for the guest molecules (including solvent molecules) were then assigned to the residual Q-peaks. The guest structures were first refined isotropically with a suitable occupancy that is estimated by refinement using FVAR. If available, the guest structures were subsequently refined anisotropically. The final crystal structures leave large solvent-accessible voids where only weak Q-peaks were observed because that solvent or guest molecules are highly disordered. Such Q-peaks have been treated with PLATON SQUEEZE program, resulting in reasonable  $R_1$  and  $wR_2$  values as compared with  $R_{\text{int}}$ .<sup>13</sup> For inclusion crystal **5•32**, the absolute configuration of the two hydroxy groups were already known, thus MERG 4 command was applied to improve the redundancy and data quality. Therefore, Flack parameter was not employed to evaluate the accuracy of determined absolute structure.

**General procedure of syntheses of naphthalene derivatives**

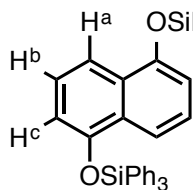
To a solution of 1,5-dihydroxynaphthalene (500 mg, 3.12 mmol) and  $\text{NEt}_3$  (4.3 mL, 31.2 mmol) in acetone (40 mL) was added monochlorosilane (7.80 mmol) under Ar atmosphere. The reaction mixture was stirred at room temperature for overnight. After removal of the solvent in vacuo, the reaction mixture was extracted with  $\text{CH}_2\text{Cl}_2$  and washed with brine and dried over  $\text{Na}_2\text{SO}_4$  and concentrated to dryness in vacuo. The residue was purified by column chromatography on silica gel to afford naphthalene derivatives.

**1,5-bis((trimethylsilyl)oxy)naphthalene (24)**

Starting from 1,5-dihydroxynaphthalene (500 mg, 3.12 mmol) and chlorotrimethylsilane (1.0 mL, 7.80 mmol), to give **24** (741 mg, 78%) as white solid.  $^1\text{H}$  NMR (500 MHz,  $\text{CDCl}_3$ , 300 K):  $\delta$  7.74 (d,  $J = 8.5$  Hz, 2H,  $H^a$ ), 7.29 (t,  $J = 8.0$  Hz, 2H,  $H^b$ ), 6.86 (d,  $J = 7.5$  Hz, 2H,  $H^c$ ), 0.34 (s, 18H,  $\text{CH}_3$ ).  $^{13}\text{C}$  NMR (125 MHz,  $\text{CDCl}_3$ , 300 K):  $\delta$  151.5, 129.7, 125.2, 116.0, 113.4, 0.53. IR (ATR, neat): 1590, 1505, 1406, 1268, 1253, 983, 838, 778  $\text{cm}^{-1}$ . Elemental analysis (%); calcd for  $\text{C}_{16}\text{H}_{24}\text{O}_2\text{Si}_2$ : C 63.10, H 7.94. found: C 62.92 H 8.03. MS (EI-MS) for  $\text{C}_{16}\text{H}_{24}\text{O}_2\text{Si}_2$  calcd for  $[\text{M}]^+$   $m/z$  304.13, found 304.

**1,5-bis((triethylsilyl)oxy)naphthalene (25)**

Starting from 1,5-dihydroxynaphthalene (500 mg, 3.12 mmol) and chlorotriethylsilane (1.3 mL, 7.80 mmol), to give **25** (1.03 g, 85%) as white solid.  $^1\text{H}$  NMR (500 MHz,  $\text{CDCl}_3$ , 300 K):  $\delta$  7.79 (d,  $J = 8.5$  Hz, 2H,  $H^a$ ), 7.28 (t,  $J = 8.0$  Hz, 2H,  $H^b$ ), 6.86 (d,  $J = 7.5$  Hz, 2H,  $H^c$ ), 1.03 (t,  $J = 8.0$  Hz, 18H,  $\text{CH}_3$ ), 0.84 (q,  $J = 8.0$  Hz, 12H,  $\text{CH}_2$ ).  $^{13}\text{C}$  NMR (125 MHz,  $\text{CDCl}_3$ , 300 K):  $\delta$  151.7, 129.5, 125.1, 115.6, 112.9, 6.9, 5.4. IR (ATR, neat): 2954, 2872, 1590, 1503, 1407, 1268, 1253, 993, 741  $\text{cm}^{-1}$ . Elemental analysis (%); Calcd for  $\text{C}_{22}\text{H}_{36}\text{O}_2\text{Si}_2$ : C 67.98, H 9.34. found C 67.69 H 9.38. MS (EI-MS) for  $\text{C}_{22}\text{H}_{36}\text{O}_2\text{Si}_2$  calcd for  $[\text{M}]^+$   $m/z$  388.23, found 388.

**1,5-bis((triphenylsilyl)oxy)naphthalene (26)**

Starting from 1,5-dihydroxynaphthalene (500 mg, 3.12 mmol) and chlorotriphenylsilane (2.30 g, 7.80 mmol), to give **26** (1.69 g, 80%) as white solid.  $^1\text{H}$  NMR (500 MHz,  $\text{CDCl}_3$ , 300 K):  $\delta$  7.95 (d,  $J = 8.5$  Hz, 2H,  $H^a$ ), 7.72 (d,  $J = 7.0$  Hz, 12H, phenyl *o-H*), 7.45 (t,  $J = 7.5$  Hz, 12H, phenyl *p-H*), 7.38 (t,  $J = 7.5$  Hz, 12H, phenyl *m-H*), 7.10 (t,  $J = 8.0$  Hz, 2H,  $H^b$ ), 6.76 (d,  $J = 7.5$  Hz, 2H,  $H^c$ ).  $^{13}\text{C}$  NMR (125 MHz,  $\text{CDCl}_3$ , 300 K):  $\delta$  151.1, 135.6, 133.7, 130.5, 129.2, 128.2, 125.2, 116.2, 113.6. IR (ATR, neat): 1589, 1500, 1402, 1258, 1118, 992, 778, 735  $\text{cm}^{-1}$ . HRMS (ESI-MS) for  $\text{C}_{46}\text{H}_{37}\text{O}_2\text{Si}_2$  calcd for  $[\text{M}+\text{H}]^+$   $m/z$  677.2327, found 677.2305.

**Inclusion of guest molecules into crystalline sponge 5****General procedure for inclusion of guest molecules into crystalline sponge 5**

To a micro vial containing a cyclohexane exchanged single crystal of  $[(\text{ZnI}_2)_3(\text{tpt})_2]_n$  (**5**; tpt = tri(4-pyridyl)-1,3,5-triazine) and cyclohexane (75  $\mu\text{L}$ ), 5  $\mu\text{L}$  of 1,2-dichloroethane solution of target compounds (1 mg/1 mL) was added. Then, the crystal containing microvial was allowed to stand at 50  $^\circ\text{C}$  and the solvent was gradually evaporated over 2 d.

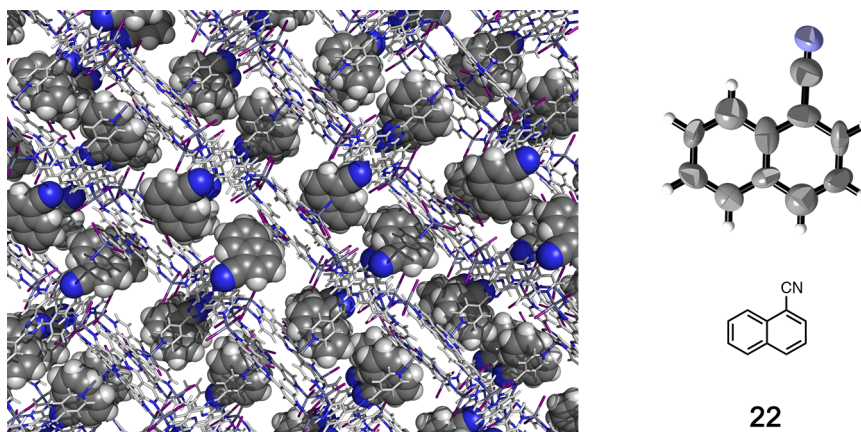
**Inclusion of 32 into crystalline sponge 5**

To a micro vial containing a cyclohexane exchanged single crystal of  $[(\text{ZnI}_2)_3(\text{tpt})_2]_n$  (**5**; tpt = tri(4-pyridyl)-1,3,5-triazine) and cyclohexane (45  $\mu\text{L}$ ), 5  $\mu\text{L}$  of cyclohexane solution of target compounds (1 mg/1 mL) was added. Then, the crystal containing microvial was allowed to stand at room temperature for 2 d.

**Crystallographic data****Inclusion complex 5•22**

Crystallographic data (before the SQUEEZE treatment):  $C_{36}H_{24}N_{12}Zn_3I_6 \cdot 0.5(C_{11}H_7N)$ ,  $M = 1658.77$ , colorless rod,  $0.12 \times 0.06 \times 0.05 \text{ mm}^3$ , monoclinic, space group  $C2/c$ ,  $a = 34.656(4)$ ,  $b = 14.9884(16)$ ,  $c = 30.130(3) \text{ \AA}$ ,  $\beta = 100.352(2)^\circ$ ,  $V = 15396(3) \text{ \AA}^3$ ,  $Z = 8$ ,  $D_c = 1.431 \text{ g/cm}^3$ ,  $F_{000} = 6176$ ,  $\mu = 3.362 \text{ mm}^{-1}$ ,  $T = 90(2) \text{ K}$ ,  $1.19 < \theta < 26.41^\circ$ , 9663 unique reflections out of 15769 with  $I > 2\sigma(I)$ ,  $R_{\text{int}} = 0.0397$ , 623 parameters, 131 restraints,  $\text{GoF} = 1.603$ , final  $R$  factors  $R_1 = 0.1156$  and  $wR_2 = 0.4319$  for all data.

Crystallographic data (after the SQUEEZE treatment):  $C_{36}H_{24}N_{12}Zn_3I_6 \cdot 0.5(C_{11}H_7N)$ ,  $M = 1658.77$ , colorless rod,  $0.12 \times 0.06 \times 0.05 \text{ mm}^3$ , monoclinic, space group  $C2/c$ ,  $a = 34.656(4)$ ,  $b = 14.9884(16)$ ,  $c = 30.130(3) \text{ \AA}$ ,  $\beta = 100.352(2)^\circ$ ,  $V = 15396(3) \text{ \AA}^3$ ,  $Z = 8$ ,  $D_c = 1.431 \text{ g/cm}^3$ ,  $F_{000} = 6176$ ,  $\mu = 3.362 \text{ mm}^{-1}$ ,  $T = 90(2) \text{ K}$ ,  $1.19 < \theta < 26.41^\circ$ , 9663 unique reflections out of 15769 with  $I > 2\sigma(I)$ ,  $R_{\text{int}} = 0.0383$ , 623 parameters, 131 restraints,  $\text{GoF} = 1.603$ , final  $R$  factors  $R_1 = 0.0785$  and  $wR_2 = 0.2904$  for all data.



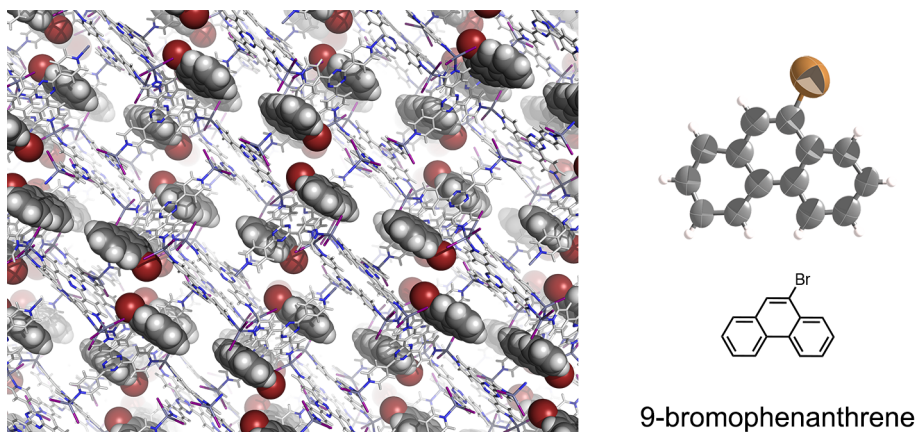
**Figure S7.1.** The X-ray crystal structure of inclusion crystal **5•22**. Guest molecules were drawn in CPK model in the packing structure and the thermal ellipsoid of the guest molecule was drawn at the 50% probability level.



**Inclusion complex 5•23**

Crystallographic data (before the SQUEEZE treatment):  $C_{36}H_{24}N_{12}Zn_3I_6 \cdot 0.68(C_{14}H_9Br)$ ,  $M = 1756.82$ , pale yellow rod,  $0.07 \times 0.05 \times 0.05 \text{ mm}^3$ , monoclinic, space group  $C2/c$ ,  $a = 35.862(5)$ ,  $b = 14.902(2)$ ,  $c = 31.358(5) \text{ \AA}$ ,  $\beta = 102.694(2)^\circ$ ,  $V = 16349(4) \text{ \AA}^3$ ,  $Z = 8$ ,  $D_c = 1.408 \text{ g/cm}^3$ ,  $F_{000} = 6455$ ,  $\mu = 3.453 \text{ mm}^{-1}$ ,  $T = 90(2) \text{ K}$ ,  $1.33 < \theta < 25.00^\circ$ , 9795 unique reflections out of 14400 with  $I > 2\sigma(I)$ ,  $R_{\text{int}} = 0.0705$ , 650 parameters, 213 restraints,  $\text{GoF} = 2.368$ , final  $R$  factors  $R_1 = 0.1830$  and  $wR_2 = 0.5558$  for all data. CCDC deposit number: unpublished data.

Crystallographic data (after the SQUEEZE treatment):  $C_{36}H_{24}N_{12}Zn_3I_6 \cdot 0.68(C_{14}H_9Br)$ ,  $M = 1756.82$ , pale yellow rod,  $0.07 \times 0.05 \times 0.05 \text{ mm}^3$ , monoclinic, space group  $C2/c$ ,  $a = 35.862(5)$ ,  $b = 14.902(2)$ ,  $c = 31.358(5) \text{ \AA}$ ,  $\beta = 102.694(2)^\circ$ ,  $V = 16349(4) \text{ \AA}^3$ ,  $Z = 8$ ,  $D_c = 1.408 \text{ g/cm}^3$ ,  $F_{000} = 6455$ ,  $\mu = 3.453 \text{ mm}^{-1}$ ,  $T = 90(2) \text{ K}$ ,  $1.33 < \theta < 25.00^\circ$ , 9795 unique reflections out of 14400 with  $I > 2\sigma(I)$ ,  $R_{\text{int}} = 0.0705$ , 650 parameters, 213 restraints,  $\text{GoF} = 1.448$ , final  $R$  factors  $R_1 = 0.1162$  and  $wR_2 = 0.3753$  for all data. CCDC deposit number: 910388.



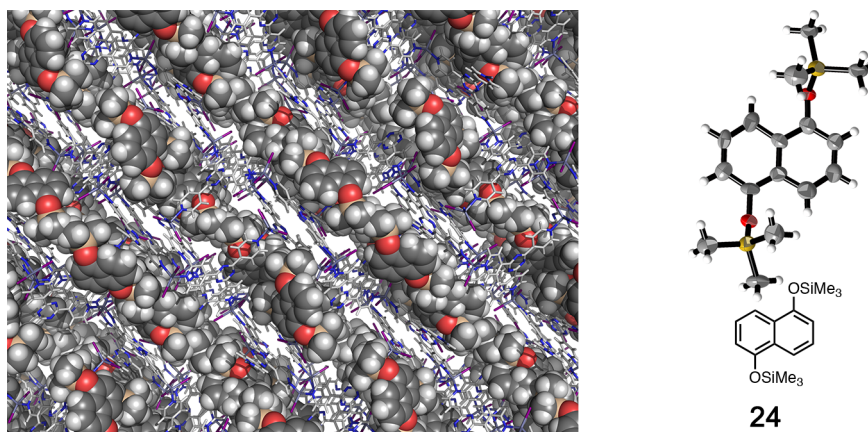
**Figure S7.2.** The X-ray crystal structure of 9-bromophenanthrene inclusion crystalline sponge **5**. Guest molecules were drawn in CPK model in the packing structure and the thermal ellipsoid of the guest molecule was drawn at the 50% probability level.

**Inclusion complex 5•24**

Crystallographic data (before the SQUEEZE treatment):  $C_{36}H_{24}N_{12}Zn_3I_6 \cdot C_{16}H_{24}O_2Si$ ,  $M = 1886.71$ , colorless rod,  $0.12 \times 0.04 \times 0.04 \text{ mm}^3$ , monoclinic, space group  $C2/c$ ,  $a = 35.0001(17)$ ,  $b = 14.7024(7)$ ,  $c = 31.2365(15) \text{ \AA}$ ,  $\beta = 101.6340(10)^\circ$ ,  $V = 15743.6(13) \text{ \AA}^3$ ,  $Z = 8$ ,  $D_c = 1.592 \text{ g/cm}^3$ ,  $F000 = 7168$ ,  $\mu = 3.329 \text{ mm}^{-1}$ ,  $T = 90(2) \text{ K}$ ,  $1.188 < \theta < 28.347^\circ$ , 13698 unique reflections out of 18189 with  $I > 2\sigma(I)$ ,  $R_{\text{int}} = 0.0163$ , 931 parameters, 247 restraints, GoF = 1.709, final  $R$  factors  $R_1 = 0.0643$  and  $wR_2 = 0.2396$  for all data.

Crystallographic data (after the SQUEEZE treatment):  $C_{36}H_{24}N_{12}Zn_3I_6 \cdot C_{16}H_{24}O_2Si$ ,  $M = 1886.71$ , colorless rod,  $0.12 \times 0.04 \times 0.04 \text{ mm}^3$ , monoclinic, space group  $C2/c$ ,  $a = 35.0001(17)$ ,  $b = 14.7024(7)$ ,  $c = 31.2365(15) \text{ \AA}$ ,  $\beta = 101.6340(10)^\circ$ ,  $V = 15743.6(13) \text{ \AA}^3$ ,  $Z = 8$ ,  $D_c = 1.592 \text{ g/cm}^3$ ,  $F000 = 7168$ ,  $\mu = 3.329 \text{ mm}^{-1}$ ,  $T = 90(2) \text{ K}$ ,  $1.188 < \theta < 28.347^\circ$ , 13630 unique reflections out of 18189 with  $I > 2\sigma(I)$ ,  $R_{\text{int}} = 0.0158$ , 931 parameters, 247 restraints, GoF = 1.709, final  $R$  factors  $R_1 = 0.0480$  and  $wR_2 = 0.1770$  for all data.

IR (single crystal, mineral oil) 3054, 2928, 2854, 1662, 1618, 1576, 1516, 1418, 1371  $\text{cm}^{-1}$

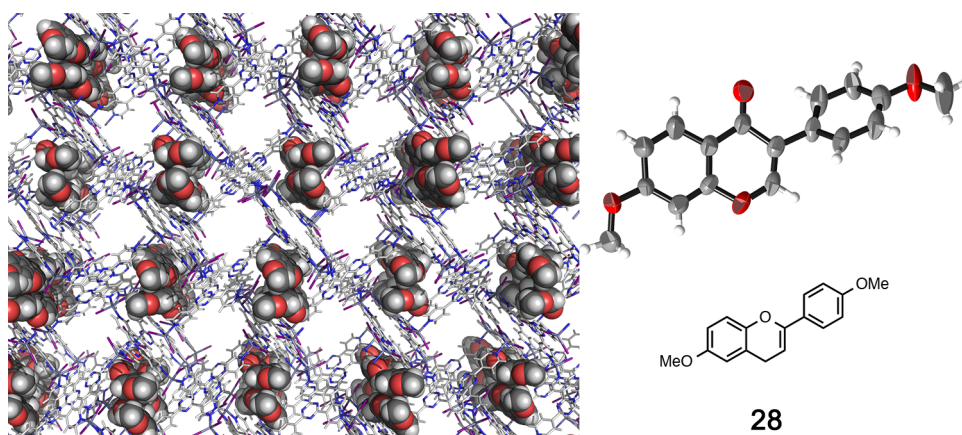


**Figure S7.3.** The X-ray crystal structure of inclusion crystal **5•24**. Guest molecules were drawn in CPK model in the packing structure and the thermal ellipsoid of the guest molecule was drawn at the 50% probability level.

**Inclusion complex 5•28**

Crystallographic data (before the SQUEEZE treatment):  $C_{36}H_{24}N_{12}Zn_3I_6 \cdot (C_{17}H_{14}O_4) \cdot 0.71(C_6H_{12})$ ,  $M = 1924.60$ , colorless rod,  $0.07 \times 0.05 \times 0.04$  mm<sup>3</sup>, monoclinic, space group  $C2/c$ ,  $a = 34.651(5)$ ,  $b = 14.997(2)$ ,  $c = 31.193(5)$  Å,  $\beta = 101.951(2)^\circ$ ,  $V = 15858(4)$  Å<sup>3</sup>,  $Z = 8$ ,  $D_c = 1.612$  g/cm<sup>3</sup>,  $F_{000} = 7314$ ,  $\mu = 3.280$  mm<sup>-1</sup>,  $T = 90(2)$  K,  $1.201 < \theta < 26.399^\circ$ , 12903 unique reflections out of 16135 with  $I > 2\sigma(I)$ ,  $R_{int} = 0.0330$ , 757 parameters, 13 restraints, GoF = 1.127, final  $R$  factors  $R_1 = 0.0837$  and  $wR_2 = 0.2738$  for all data.

Crystallographic data (after the SQUEEZE treatment):  $C_{36}H_{24}N_{12}Zn_3I_6 \cdot (C_{17}H_{14}O_4) \cdot 0.71(C_6H_{12})$ ,  $M = 1924.60$ , colorless rod,  $0.07 \times 0.05 \times 0.04$  mm<sup>3</sup>, monoclinic, space group  $C2/c$ ,  $a = 34.651(5)$ ,  $b = 14.997(2)$ ,  $c = 31.193(5)$  Å,  $\beta = 101.951(2)^\circ$ ,  $V = 15858(4)$  Å<sup>3</sup>,  $Z = 8$ ,  $D_c = 1.562$  g/cm<sup>3</sup>,  $F_{000} = 7040$ ,  $\mu = 3.277$  mm<sup>-1</sup>,  $T = 90(2)$  K,  $1.201 < \theta < 26.399^\circ$ , 12720 unique reflections out of 16135 with  $I > 2\sigma(I)$ ,  $R_{int} = 0.0330$ , 757 parameters, 13 restraints, GoF = 1.038, final  $R$  factors  $R_1 = 0.0707$  and  $wR_2 = 0.2101$  for all data.

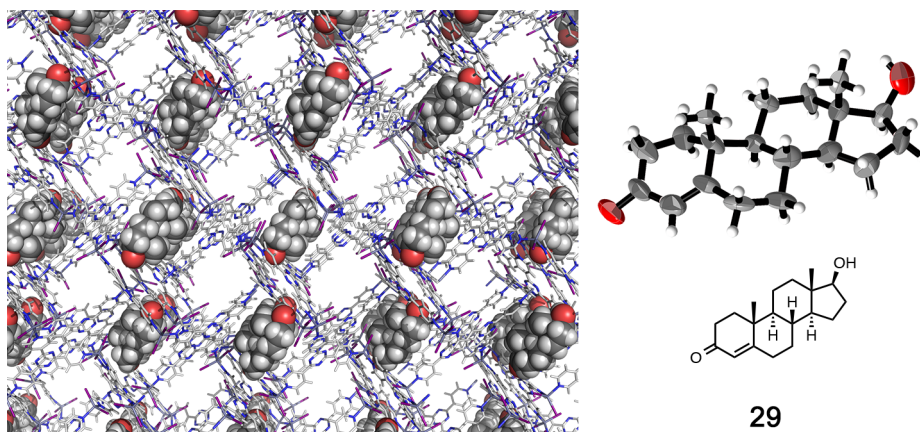


**Figure S7.4.** The X-ray crystal structure of inclusion crystal **5•28**. Guest molecules were drawn in CPK model in the packing structure and the thermal ellipsoid of the guest molecule was drawn at the 50% probability level.

**Inclusion complex 5•29**

Crystallographic data (before the SQUEEZE treatment):  $C_{36}H_{24}N_{12}Zn_3I_6 \cdot 0.76(C_{19}H_{28}O_2)$ ,  $M = 3387.56$ , colorless rod,  $0.08 \times 0.08 \times 0.05 \text{ mm}^3$ , monoclinic, space group  $C2$ ,  $a = 34.980(3)$ ,  $b = 14.8667(14)$ ,  $c = 31.196(3) \text{ \AA}$ ,  $\beta = 102.7940(10)^\circ$ ,  $V = 15820(3) \text{ \AA}^3$ ,  $Z = 4$ ,  $D_c = 1.422 \text{ g/cm}^3$ ,  $F000 = 6345$ ,  $\mu = 3.274 \text{ mm}^{-1}$ ,  $T = 90(2) \text{ K}$ ,  $1.19 < \theta < 26.58^\circ$ , 26470 unique reflections out of 32778 with  $I > 2\sigma(I)$ ,  $R_{\text{int}} = 0.0402$ , 1218 parameters, 128 restraints,  $\text{GoF} = 1.064$ , final  $R$  factors  $R_1 = 0.0644$  and  $wR_2 = 0.2048$  for all data, Flack parameter =  $0.08(3)$ .

Crystallographic data (after the SQUEEZE treatment):  $C_{36}H_{24}N_{12}Zn_3I_6 \cdot 0.76(C_{19}H_{28}O_2)$ ,  $M = 3387.56$ , colorless rod,  $0.08 \times 0.08 \times 0.05 \text{ mm}^3$ , monoclinic, space group  $C2$ ,  $a = 34.980(3)$ ,  $b = 14.8667(14)$ ,  $c = 31.196(3) \text{ \AA}$ ,  $\beta = 102.7940(10)^\circ$ ,  $V = 15820(3) \text{ \AA}^3$ ,  $Z = 4$ ,  $D_c = 1.422 \text{ g/cm}^3$ ,  $F000 = 6345$ ,  $\mu = 3.274 \text{ mm}^{-1}$ ,  $T = 90(2) \text{ K}$ ,  $1.19 < \theta < 26.58^\circ$ , 26068 unique reflections out of 32778 with  $I > 2\sigma(I)$ ,  $R_{\text{int}} = 0.0402$ , 1218 parameters, 176 restraints,  $\text{GoF} = 1.064$ , final  $R$  factors  $R_1 = 0.0424$  and  $wR_2 = 0.1087$  for all data, Flack parameter =  $0.005(13)$ .



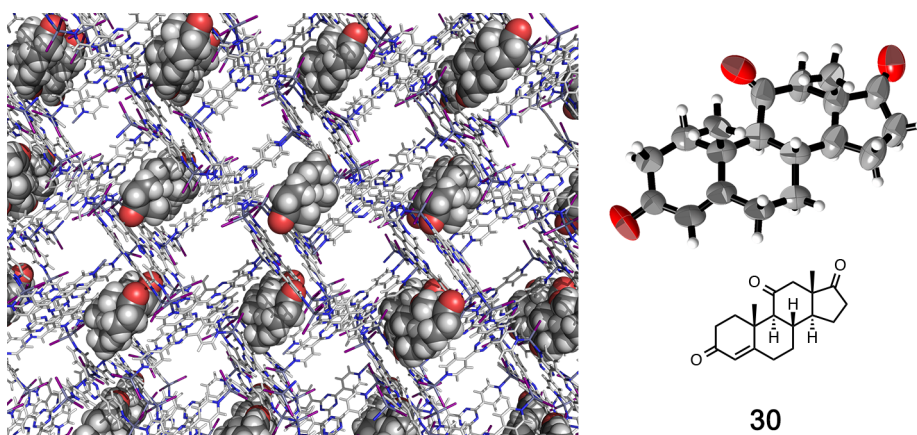
**Figure S7.5.** The X-ray crystal structure of inclusion crystal **5•29**. Guest molecules were drawn in CPK model in the packing structure and the thermal ellipsoid of the guest molecule was drawn at the 50% probability level.



**Inclusion complex 5•30**

Crystallographic data (before the SQUEEZE treatment):  $C_{36}H_{24}N_{12}Zn_3I_6 \cdot (C_{17}H_{14}O_4) \cdot 0.71(C_6H_{12})$ ,  $M = 1924.60$ , colorless rod,  $0.07 \times 0.05 \times 0.04 \text{ mm}^3$ , monoclinic, space group  $C2/c$ ,  $a = 35.263(5)$ ,  $b = 14.853(2)$ ,  $c = 31.016(5) \text{ \AA}$ ,  $\beta = 101.963(2)^\circ$ ,  $V = 15891(4) \text{ \AA}^3$ ,  $Z = 4$ ,  $D_c = 1.385 \text{ g/cm}^3$ ,  $F000 = 6180$ ,  $\mu = 3.257 \text{ mm}^{-1}$ ,  $T = 90(2) \text{ K}$ ,  $0.671 < \theta < 26.371^\circ$ , 26017 unique reflections out of 32354 with  $I > 2\sigma(I)$ ,  $R_{\text{int}} = 0.0398$ , 1227 parameters, 231 restraints, GoF = 1.026, final  $R$  factors  $R_1 = 0.0778$  and  $wR_2 = 0.2488$  for all data, Flack parameter = 0.071(8).

Crystallographic data (after the SQUEEZE treatment):  $C_{36}H_{24}N_{12}Zn_3I_6 \cdot (C_{17}H_{14}O_4) \cdot 0.71(C_6H_{12})$ ,  $M = 1924.60$ , colorless rod,  $0.07 \times 0.05 \times 0.04 \text{ mm}^3$ , monoclinic, space group  $C2/c$ ,  $a = 35.263(5)$ ,  $b = 14.853(2)$ ,  $c = 31.016(5) \text{ \AA}$ ,  $\beta = 101.963(2)^\circ$ ,  $V = 15891(4) \text{ \AA}^3$ ,  $Z = 4$ ,  $D_c = 1.385 \text{ g/cm}^3$ ,  $F000 = 6180$ ,  $\mu = 3.257 \text{ mm}^{-1}$ ,  $T = 90(2) \text{ K}$ ,  $0.671 < \theta < 26.371^\circ$ , 25745 unique reflections out of 32354 with  $I > 2\sigma(I)$ ,  $R_{\text{int}} = 0.0390$ , 1226 parameters, 249 restraints, GoF = 1.098, final  $R$  factors  $R_1 = 0.0554$  and  $wR_2 = 0.1683$  for all data.

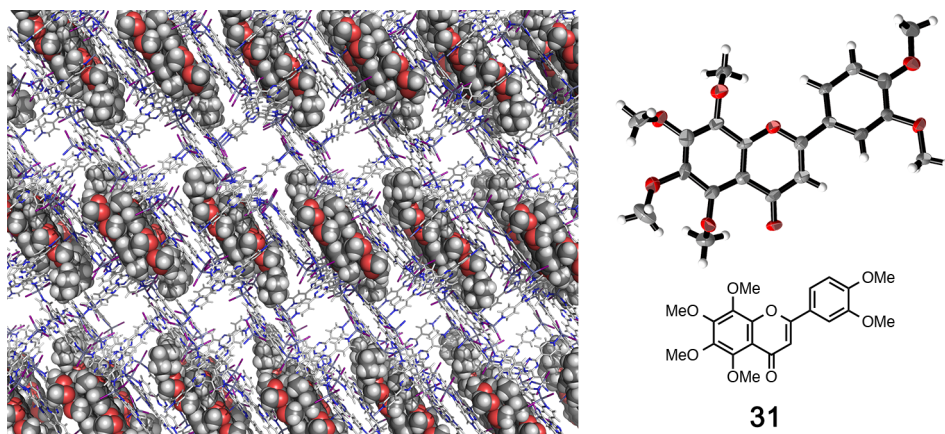


**Figure S7.6.** The X-ray crystal structure of inclusion crystal **5•30**. Guest molecules were drawn in CPK model in the packing structure and the thermal ellipsoid of the guest molecule was drawn at the 50% probability level.

**Inclusion complex 5•31 (8 mg, 9 d inclusion)**

Crystallographic data (before the SQUEEZE treatment):  $C_{72}H_{48}N_{24}Zn_6I_{12} \cdot (C_{21}H_{22}O_8) \cdot (C_6H_{12})$ ,  $M = 3650.90$ , pale yellow rod,  $0.17 \times 0.09 \times 0.05 \text{ mm}^3$ , monoclinic, space group  $C2$ ,  $a = 34.697(4)$ ,  $b = 15.0030(17)$ ,  $c = 30.290(3) \text{ \AA}$ ,  $\beta = 99.9150(10)^\circ$ ,  $V = 15532(3) \text{ \AA}^3$ ,  $Z = 4$ ,  $D_c = 1.561 \text{ g/cm}^3$ ,  $F000 = 6896$ ,  $\mu = 3.344 \text{ mm}^{-1}$ ,  $T = 90(2) \text{ K}$ ,  $0.682 < \theta < 28.467^\circ$ , 30613 unique reflections out of 35679 with  $I > 2\sigma(I)$ ,  $R_{\text{int}} = 0.0217$ , 1367 parameters, 14 restraints,  $\text{GoF} = 1.080$ , final  $R$  factors  $R_1 = 0.0670$  and  $wR_2 = 0.2104$  for all data.

Crystallographic data (after the SQUEEZE treatment):  $C_{72}H_{48}N_{24}Zn_6I_{12} \cdot (C_{21}H_{22}O_8) \cdot (C_6H_{12})$ ,  $M = 3650.90$ , pale yellow rod,  $0.17 \times 0.09 \times 0.05 \text{ mm}^3$ , monoclinic, space group  $C2$ ,  $a = 34.697(4)$ ,  $b = 15.0030(17)$ ,  $c = 30.290(3) \text{ \AA}$ ,  $\beta = 99.9150(10)^\circ$ ,  $V = 15532(3) \text{ \AA}^3$ ,  $Z = 4$ ,  $D_c = 1.561 \text{ g/cm}^3$ ,  $F000 = 6896$ ,  $\mu = 3.344 \text{ mm}^{-1}$ ,  $T = 90(2) \text{ K}$ ,  $0.682 < \theta < 28.467^\circ$ , 30470 unique reflections out of 35679 with  $I > 2\sigma(I)$ ,  $R_{\text{int}} = 0.0213$ , 1367 parameters, 14 restraints,  $\text{GoF} = 1.059$ , final  $R$  factors  $R_1 = 0.0454$  and  $wR_2 = 0.1107$  for all data.

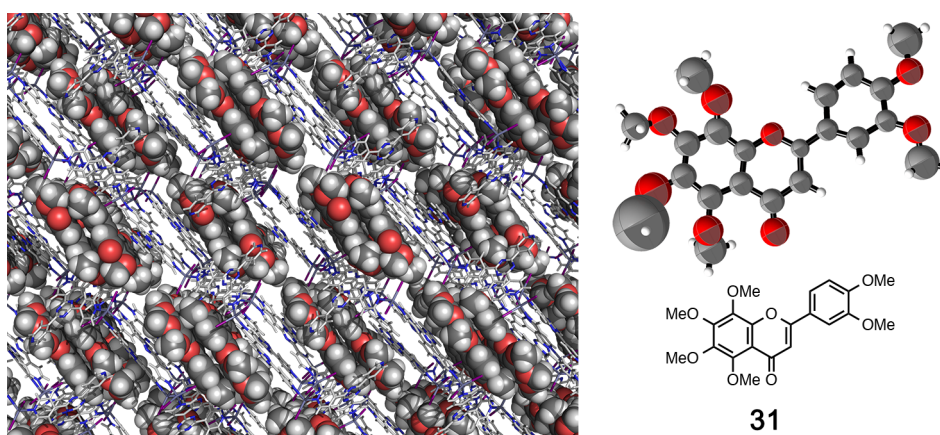


**Figure S7.7.** The X-ray crystal structure of inclusion crystal **5•31** (8  $\mu\text{g}$  of **31**, 9 d). Guest molecules were drawn in CPK model in the packing structure and the thermal ellipsoid of the guest molecule was drawn at the 50% probability level.

**Inclusion complex 5•31 (5  $\mu$ g, 2 d inclusion)**

Crystallographic data (before the SQUEEZE treatment):  $C_{72}H_{48}N_{24}Zn_6I_{12} \cdot 0.6(C_{21}H_{22}O_8)$ ,  $M = 1823.26$ , pale yellow rod,  $0.08 \times 0.08 \times 0.07 \text{ mm}^3$ , monoclinic, space group  $C2/c$ ,  $a = 34.375(7)$ ,  $b = 14.944(3)$ ,  $c = 30.478(6) \text{ \AA}$ ,  $\beta = 99.880(3)^\circ$ ,  $V = 15424(5) \text{ \AA}^3$ ,  $Z = 8$ ,  $D_c = 1.570 \text{ g/cm}^3$ ,  $F_{000} = 6872$ ,  $\mu = 3.368 \text{ mm}^{-1}$ ,  $T = 90(2) \text{ K}$ ,  $3.010 < \theta < 26.387^\circ$ , 7106 unique reflections out of 15285 with  $I > 2\sigma(I)$ ,  $R_{\text{int}} = 0.0940$ , 668 parameters, 51 restraints,  $\text{GoF} = 1.081$ , final  $R$  factors  $R_1 = 0.0682$  and  $wR_2 = 0.2157$  for all data.

Crystallographic data (after the SQUEEZE treatment):  $C_{72}H_{48}N_{24}Zn_6I_{12} \cdot 0.6(C_{21}H_{22}O_8)$ ,  $M = 1823.26$ , pale yellow rod,  $0.08 \times 0.08 \times 0.07 \text{ mm}^3$ , monoclinic, space group  $C2/c$ ,  $a = 34.375(7)$ ,  $b = 14.944(3)$ ,  $c = 30.478(6) \text{ \AA}$ ,  $\beta = 99.880(3)^\circ$ ,  $V = 15424(5) \text{ \AA}^3$ ,  $Z = 8$ ,  $D_c = 1.570 \text{ g/cm}^3$ ,  $F_{000} = 6872$ ,  $\mu = 3.368 \text{ mm}^{-1}$ ,  $T = 90(2) \text{ K}$ ,  $3.010 < \theta < 26.387^\circ$ , 7113 unique reflections out of 15285 with  $I > 2\sigma(I)$ ,  $R_{\text{int}} = 0.0915$ , 668 parameters, 51 restraints,  $\text{GoF} = 0.939$ , final  $R$  factors  $R_1 = 0.0621$  and  $wR_2 = 0.1878$  for all data.

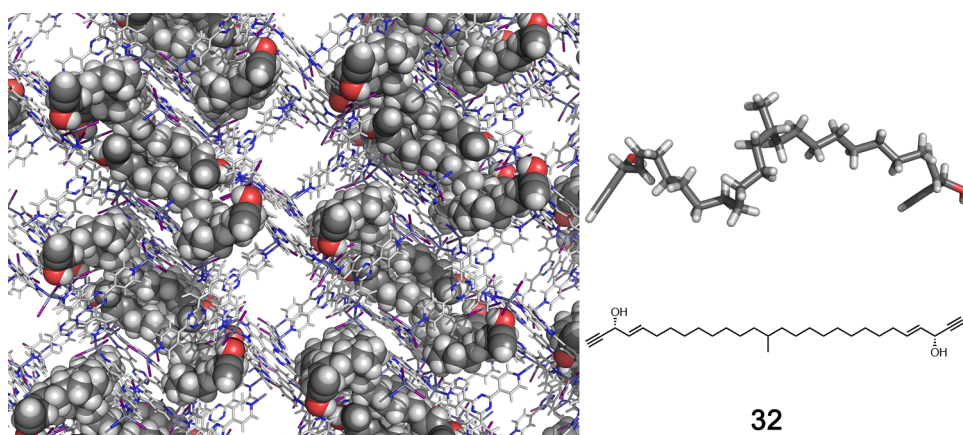


**Figure S7.8.** The X-ray crystal structure of inclusion crystal **5•31** (5  $\mu$ g of **31**, 2 d). Guest molecules were drawn in CPK model in the packing structure and the thermal ellipsoid of the guest molecule was drawn at the 50% probability level.

**Inclusion complex 5•32**

Crystallographic data (before the SQUEEZE treatment):  $C_{72}H_{48}N_{24}Zn_6I_{12} \cdot 0.5(C_{29}H_{48}O_2)$ ,  $M = 3378.70$ , colorless rod,  $0.11 \times 0.09 \times 0.08 \text{ mm}^3$ , monoclinic, space group  $C2$ ,  $a = 34.804(3)$ ,  $b = 14.8607(11)$ ,  $c = 31.624(2) \text{ \AA}$ ,  $\beta = 102.0830(10)^\circ$ ,  $V = 15994(2) \text{ \AA}^3$ ,  $Z = 4$ ,  $D_c = 1.403 \text{ g/cm}^3$ ,  $F_{000} = 6332$ ,  $\mu = 3.238 \text{ mm}^{-1}$ ,  $T = 90(2) \text{ K}$ ,  $1.20 < \theta < 25.00^\circ$ , 20221 unique reflections out of 28203 with  $I > 2\sigma(I)$ ,  $R_{\text{int}} = 0.0258$ , 1350 parameters, 656 restraints,  $\text{GoF} = 1.038$ , final  $R$  factors  $R_1 = 0.0845$  and  $wR_2 = 0.2958$  for all data.

Crystallographic data (after the SQUEEZE treatment):  $C_{72}H_{48}N_{24}Zn_6I_{12} \cdot 0.5(C_{29}H_{48}O_2)$ ,  $M = 3378.70$ , colorless rod,  $0.11 \times 0.09 \times 0.08 \text{ mm}^3$ , monoclinic, space group  $C2$ ,  $a = 34.804(3)$ ,  $b = 14.8607(11)$ ,  $c = 31.624(2) \text{ \AA}$ ,  $\beta = 102.0830(10)^\circ$ ,  $V = 15994(2) \text{ \AA}^3$ ,  $Z = 4$ ,  $D_c = 1.403 \text{ g/cm}^3$ ,  $F_{000} = 6332$ ,  $\mu = 3.238 \text{ mm}^{-1}$ ,  $T = 90(2) \text{ K}$ ,  $1.20 < \theta < 25.00^\circ$ , 20221 unique reflections out of 28203 with  $I > 2\sigma(I)$ ,  $R_{\text{int}} = 0.0258$ , 1350 parameters, 733 restraints,  $\text{GoF} = 1.128$ , final  $R$  factors  $R_1 = 0.0725$  and  $wR_2 = 0.2478$  for all data.



**Figure S7.9.** The X-ray crystal structure of inclusion crystal **5•32**. Guest molecules were drawn in CPK model in the packing structure and the thermal ellipsoid of the guest molecule was drawn at the 50% probability level.



**References**

- 1 G. D. Christian, *Analytical Chemistry 6th edition*, Wiley, New York, **2004**.
- 2 T. R. Ramadhar, S. Zheng, Y. Chen, J. Clardy, *Acta Cryst.* **2015**, **A71**, 46–58.
- 3 S. Mecozzi, J. Rebek, Jr., *Chem. Eur. J.* **1998**, **4**, 1016–1022.
- 4 Almost same result was obtained for the initial washing solvent for nitrobenzene containing crystalline sponge discussed in chapter 2.
- 5 D. E. McRee, P. R. David, *Practical Protein Crystallography 2nd edition*, Academic press, London, **1999**.
- 6 Z.-T. Zhang, X.-B. Wang, Q.-Y. Wang, L.-N. Wu, *J. Chem. Crystallogr.* **2005**, **35**, 923–929.
- 7 Y. Hitora, K. Takada, S. Okada, S. Matsunaga, *Tetrahedron* **2011**, **67**, 4530–4534.
- 8 K. Mori, K. Akasaka, S. Matsunaga, *Tetrahedron* **2014**, **70**, 392–401.
- 9 Y. Hitora, K. Takada, S. Matsunaga, *Tetrahedron* **2013**, **69**, 11070–11073.
- 10 *APEX2, SADABS and XPREP*, Bruker AXS Inc., Madison, Wisconsin, USA, 2007.
- 11 *CrystalClear-SM Expert 2.1 b32*, Rigaku Corporation, Tokyo, Japan, 2013.
- 12 G. M. Sheldrick, *Acta Cryst.* **2008**, **A64**, 112–122.
- 13 P. van der Sluis, A. L. Spek, *Acta Cryst.* **1990**, **A46**, 194–201.



## Chapter 8

### Summary and Future Visions

In this thesis, the method to perform single crystal X-ray diffraction analysis of target compounds without target crystallization was developed using porous complex. The simple strategy of the crystalline sponge method that includes and aligns the target molecule in the porous complex showed huge potential to change the current situation of the structural analysis of molecules. By means of the crystalline sponge method, wide variety of non-crystalline, chiral, dangerous or complicated structure compounds were successfully analyzed.

In chapter 2, the experimental procedure of the inclusion and aligning the target molecules in the crystalline sponge was developed. Solvent exchange from nitrobenzene to cyclohexane gave the suitable crystalline sponge for guest inclusion and alignment in the pore while the crystal maintains its single crystallinity. Also, using stable rod shaped crystalline sponge upon guest inclusion was the key of the success. By means of the established protocol, it was demonstrated that the crystalline sponge method can be performed with a piece of the crystalline sponge and 5  $\mu\text{g}$  of target compound.

In chapter 3, the actual experimental scale of X-ray crystallography was pursued. Conventional X-ray analysis requires a lot of samples not for the measurement, but for the preparing the single crystal of the target. The true one crystal scale X-ray analysis was demonstrated by the nanogram scale crystalline sponge analysis. Moreover, combination of X-ray analysis with HPLC as LC-SCD analysis was also demonstrated. The potential for the GC-SCD was also demonstrated by analysis of the gaseous compound.

In chapter 4, the crystalline sponge method was applied for the absolute structure determination. Due to the strong molecular interactions between the crystalline sponge and included target, the chiral distortion of the whole crystal was induced and

the structure could be analyzed in the chiral space group. Furthermore, since the crystalline sponge contains heavy Zn and I atoms in the host framework, the introduction of the heavy atom to the analyzed target is not necessary.

In chapter 5, applicability of the crystalline sponge method to the risk free X-ray analysis of dangerous compound was demonstrated. Since the crystalline sponge method can be performed with 5  $\mu\text{g}$  of target compound solution, potentially explosive ozonides were analyzed directly from their reaction mixture in microgram scale. For the mixture of the two ozonide diastereomers, these diastereomers were included both together into one crystalline sponge and can be analyzed as different molecules in one crystal structure.

In chapter 6, the potential of the crystalline sponge method as the alternative to 2D NMR or MS analysis in the synthetic chemistry was demonstrated. Though the complete replacement of NMR or MS by the crystalline sponge analysis is nonsense, X-ray analysis by the crystalline sponge analysis is far more effective in certain cases. The substituent positions, regioselectivity and stereochemistry were easily and quickly determined.

In chapter 7, the scope and limitations of the crystalline sponge method were examined. The intrinsic size limitation, target compound scope and difference on the obtained data quality from the small molecule X-ray crystallography were revealed. Consideration of these features may lead to the next generation of the crystalline sponge.

The newborn crystalline sponge method is just at the starting point of the journey. What the author established in this thesis are the basic principle of the method and first generation of the crystalline sponge. The actual experimental method is really simple, easily reproducible and possible to apply to other porous materials. Large pore size and high solvent tolerance are the required features of the new crystalline sponge.

What the author learned from the experiments throughout this thesis is that one of the biggest keys of the crystalline sponge method is the flexibility of the host structure. The author proposes a crystalline polymer as the next generation crystalline sponge with ultimate flexibility. By mixing the target molecules with the crystalline polymer, the target molecule would be loosely bound and aligned between the polymer chain through the interactions and will afford the small crystalline domains observable by the X-ray

analysis. This ultimately flexible crystalline polymer sponge will clear the current crystalline sponge's limitations on target compound size, target solubility to the solvent.

Further development of the crystalline sponge chemistry will contribute to many fields of chemistry suffering from the structural analysis. The author would be delighted from the bottom of the heart if the crystalline sponge method contributes to the progress of natural science.



## Acknowledgment

I would like to express my deepest gratitude to my supervisor, professor, Dr. Makoto Fujita, for his kind guidance, warm encouragement and valuable suggestions throughout this work.

I am deeply grateful to lecturer, Dr. Yasuhide Inokuma for his advice on experiments, presentations and writings. Many breakthroughs in the crystalline sponge chemistry were fruits of numerous luncheon discussions with him.

I also indebted to associate professor, Dr. Sota Sato, associate professor, Dr. Takashi Murase, assistant professor, Dr. Tomohisa Sawada, assistant professor, Dr. Daishi Fujita for their constructive suggestions.

I owe my sincere gratitude to professor, Dr. Kari Rissanen, professor, Dr. Kenichiro Itami, associate professor, Dr. Junichiro Yamaguchi, professor, Dr. Phil S. Baran, professor, Dr. Masayuki Inoue, lecturer, Dr. Daisuke Urabe, professor, Dr. Atsunori Mori, associate professor, Dr. Masamichi Ogasawara, professor, Dr. Shigeki Matsunaga, assistant professor, Dr. Kentaro Takada, and Mr. Yuki Hitora for their kind provisions of their molecules for crystalline sponge analyses and dedicated discussions. I would like to express further gratitude to professor, Dr. Phil S. Baran at The Scripps Research Institute, who welcomed me as a visiting researcher and gave me a wonderful opportunity to study with his brilliant group members.

I would like to express my gratitude to assistant professor, Dr. Kazuaki Ohara, Dr. Takehide Kawamichi, assistant professor, Dr. Koki Ikemoto for their helpful discussions. I am also grateful to my collaborators in Fujita group, Ms. Junko Ariyoshi, Mr. Yuki Takahashi and Mr. Tatsuhiko Arai for their dedicated work on the crystalline sponge method.

I also thank to the financial support from Japan Society for the Promotion of Science, JSPS, Research Fellowships for Young Scientist.

My sincere appreciation goes to my parents and sister, Mr. Shigetomi Yoshioka, Ms. Mari Yoshioka and Ms. Saho Yoshioka, for their continuous support and encouragement. Finally, I wish to express my heartfelt appreciation to my dearest partner, Ms. Asana Yoshioka for her warmth of affection.

Shota Yoshioka